

VOL. 16 NO. 3 MARCH 1968

PUBLISHED MONTHLY

JOURNAL OF

ELECTROANALYTICAL CHEMISTRY

AND INTERFACIAL ELECTROCHEMISTRY

International Journal devoted to all Aspects
of Electroanalytical Chemistry, Double Layer
Studies, Electrokinetics, Colloid Stability, and
Electrode Kinetics.

EDITORIAL BOARD:

J. O'M. BOCKRIS (Philadelphia, Pa.)
G. CHARLOT (Paris)
B. E. CONWAY (Ottawa)
P. DELAHAY (New York)
A. N. FRUMKIN (Moscow)
L. GIERST (Brussels)
M. ISHIBASHI (Kyoto)
W. KEMULA (Warsaw)
H. L. KIES (Delft)
J. J. LINGANE (Cambridge, Mass.)
G. W. C. MILNER (Harwell)
R. H. OTTEWILL (Bristol)
J. E. PAGE (London)
R. PARSONS (Bristol)
C. N. REILLEY (Chapel Hill, N.C.)
G. SEMERANO (Padua)
M. VON STACKELBERG (Bonn)
I. TACHI (Kyoto)
P. ZUMAN (Prague)

E L S E V I E R

GENERAL INFORMATION

See also Suggestions and Instructions to Authors which will be sent free, on request to the Publishers.

Types of contributions

- (a) Original research work not previously published in other periodicals.
- (b) Reviews on recent developments in various fields.
- (c) Short communications.
- (d) Bibliographical notes and book reviews.

Languages

Papers will be published in English, French or German.

Submission of papers

Papers should be sent to one of the following Editors:

Professor J. O'M. BOCKRIS, John Harrison Laboratory of Chemistry,

University of Pennsylvania, Philadelphia 4, Pa. 19104, U.S.A.

Dr. R. H. OTTEWILL, Department of Chemistry, The University, Bristol 8, England.

Dr. R. PARSONS, Department of Chemistry, The University, Bristol 8, England.

Professor C. N. REILLEY, Department of Chemistry,

University of North Carolina, Chapel Hill, N. C. 27515, U.S.A.

Authors should preferably submit two copies in double-spaced typing on pages of uniform size. Legends for figures should be typed on a separate page. The figures should be in a form suitable for reproduction, drawn in Indian ink on drawing paper or tracing paper, with lettering etc. in thin pencil. The sheets of drawing or tracing paper should preferably be of the same dimensions as those on which the article is typed. Photographs should be submitted as clear black and white prints on glossy paper. Standard symbols should be used in line drawings, the following are available to the printers:

▼ ▽ ■ □ ● ◎ ■ □ ◊ ◻ ■ + ×

All references should be given at the end of the paper. They should be numbered and the numbers should appear in the text at the appropriate places.

A summary of 50 to 200 words should be included.

Reprints

Fifty reprints will be supplied free of charge. Additional reprints (minimum 100) can be ordered at quoted prices. They must be ordered on order forms which are sent together with the proofs.

Publication

The *Journal of Electroanalytical Chemistry and Interfacial Electrochemistry* appears monthly and has four issues per volume and three volumes per year.

Subscription price: \$ 52.50 or Sfr. 228.00 per year; \$ 17.50 or Sfr. 76.00 per volume; plus postage. Additional cost for copies by air mail available on request. For advertising rates apply to the publishers.

Subscriptions

Subscriptions should be sent to:

ELSEVIER SEQUOIA S.A., P.O. Box 851, 1001 Lausanne 1, Switzerland

PHOTOCURRENTS AT A METAL-ELECTROLYTE INTERFACE

V. P. SHARMA, P. DELAHAY, G. G. SUSBIELLES AND G. TESSARI*

Department of Chemistry, New York University, New York, N. Y. 10003 (U.S.A.)

(Received June 20th, 1967)

INTRODUCTION

The photoelectric effect at a metal-electrolyte interface has recently been re-investigated¹⁻⁵ and interpreted in various ways. The interpretations are summarized by BARKER *et al.*². The interpretation favoured by this author^{1,2} is based on the following sequence: electron emission, solvation, and subsequent reaction with a scavenger, *e.g.*, hydrogen ion, nitrous oxide. If the electron-scavenger reaction yields a product that does not undergo electrochemical oxidation or reduction at the potential at which the metal is adjusted, a photocurrent is observed, provided the metal is coupled with a reference electrode in a classical potentiometric arrangement (or more sophisticated instrumentation). In the absence of scavenger, according to this interpretation, most emitted electrons are re-trapped by the metal except for those lost by the second-order solvated electron-solvated electron reaction, and the photocurrent is much smaller than in presence of scavenger**. This interpretation seems to account for most observations, and a simple analysis of the coupling of the diffusion of solvated electrons with the electron-scavenger reaction leads to the experimentally-verified limiting law (at low concentrations) predicting proportionality between current and the square root of the scavenger concentration. Photocurrents that are nearly independent of the scavenger concentration, at sufficiently high scavenger concentration, are accounted for by the assumption that practically all emitted electrons react with the scavenger. A limiting photocurrent is then observed.

HEYROVSKÝ's alternative interpretation⁴, based on the formation of a charge-transfer complex at the metal-electrolyte interface, also seems to fit the experimental results. The dependence of the photocurrent on scavenger concentration is also explained but perhaps less uniquely so (at least for the low concentration range) than by BARKER's simple square-root relationship. HEYROVSKÝ has also cited examples of anodic photocurrents (rather than cathodic currents as in most of BARKER's work) to support his interpretation.

Photocurrents observed with a given scavenger concentration strongly depend on the conventional electrode potential. It was suggested⁵ that this dependence might be interpreted by transposition, and possibly modification, of FOWLER's treatment⁶ of the effect on an electric field on photoemission by metals in vacuum. Examination of this suggestion requires experimental values of the photocurrent at

* Present address: Istituto di Chimica Analitica della Università di Bari, Via Amendola 173, Bari, Italy.

** Some impurities act as scavenger, *e.g.*, dissolved oxygen.

different wavelengths for known, at least relatively, photon fluxes. Such data are not available in the literature, to our knowledge, and are reported here. An interpretation is tested, which rests on BARKER's model together with a transposition of FOWLER's treatment. The experimental results reported here could serve in the testing of future improved theoretical models.

EXPERIMENTAL

Photocurrents were measured as follows with a mercury ideal polarized electrode in presence of a scavenger:

The electrode potential was initially set at a known value against a reference electrode by means of a potentiometer. The electrode circuit was open, and the electrode was irradiated by means of a flash-tube fitted with a third-order interference filter having a narrow band-pass. The change of potential at open circuit was measured. The electronic charge lost by emission during the short flash-irradiation was calculated from the change of potential and the differential capacity of the double layer. This capacity was determined in a separate experiment, without flash-irradiation, involving injection of a known charge at open circuit. The change of potential in both types of experiment never exceeded 2.5 mV and was generally smaller. Thus, the dependence of the photocurrent and double-layer capacity on potential could be neglected over this small interval of potential, and results practically pertained to the initially applied potential.

This coulometric method was initially devised for the determination of double layer-capacities in solutions of low conductivity⁷ and was applied in the early work from this laboratory on photocurrents⁵. A mercury pool was used in this work (a hanging mercury drop in capacity measurements) but was abandoned, after extensive testing, because of contamination by traces of adsorbable organic impurities. Electrode contamination was easily detected by the discrepancy between double-layer capacities measured with a mercury pool electrode and reliable published capacities. The technique was modified to allow the use of a dropping mercury electrode (DME) and was described elsewhere⁸ for double-layer capacity measurements. Circuitry of the relays and the timing system was the same as before⁸ except that the cell was directly connected to the oscilloscope (Tektronix 547 with 1A7 plug-in unit) with which the potential-time variations were observed and photographed. Correct values of the double-layer capacity were measured with the DME (within $\pm 3\%$ over the whole range of potentials) but this electrode had the disadvantage, in comparison with the mercury pool, of poor geometry for irradiation by a single source. This disadvantage was only minor because measurements automatically gave the integrated current density over the total electrode area and the duration of irradiation. Other investigators¹⁻⁴ of photocurrents also used a DME with different techniques of measurements than the one applied here.

Practical details were as follows:

Each set of measurements involved the determination of potential-time oscilloscope traces with: (a) flash-irradiation, (b) flash-irradiation with an opaque screen between the flash tube and the DME (blank correction) and (c) charge injection without irradiation for the determination of the double layer capacity (Fig. 1).

The flash tube was a high-energy xenon source (Electro Powerpacs, type

S-13-138), rated at a maximum of 600 J, connected to a 0–3000 V laser power supply (Electro Powerpacs, type 322). This power supply was connected to an a.c. regulated power supply (Sorensen, model ACR 2000) to avoid the effect of line-voltage fluctuations. The output high voltage was monitored with a voltage divider ($1:10^4$) connected to an electrometer voltmeter (Keithley, type 600A). The xenon tube was operated at 2080 V and the energy/flash was 325 J*. Third-order interference filters (Baird Atomic) were used from 2500–3900 Å at 200-Å intervals. The half-intensity width

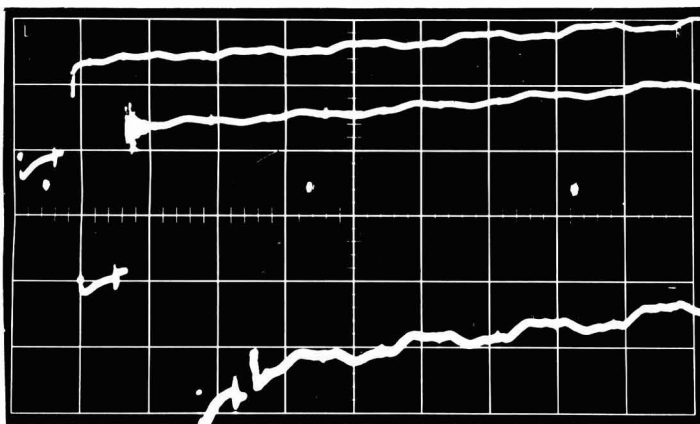


Fig. 1. Potential-time traces at 2900 Å and -1.6 V for 0.1 M sodium fluoride satd. with nitrous oxide. Top, flash-irradiation; middle, coulstatic charge injection without irradiation; bottom, irradiation with opaque screen (blank). The change of potential was measured at the large step in the trace. Horizontal scale: 10 msec/square. Vertical sensitivity: 1 (top and middle) and 0.5 (bottom) mV/square.

was approximately 80 Å, and the peak transmission varied from 5–10% from one filter to another. The tip of the DME was approximately 4 cm away from the flash tube, and the geometry of the system was carefully controlled. The error resulting from displacement of the DME tip with respect to the flash tube was determined, and the arrangement was such that such an error did not exceed $\pm 5\%$.

Photon fluxes at different wavelengths were standardized on a relative basis in a separate experiment with a photomultiplier tube (RCA 6903) as detector (to achieve fast response) operated at 700 V (0–4000 V Harrison, model 6525A, power supply). The phototube was at one end of a 1-m long metal housing cabinet and the flash tube at the other end. Light intensity was attenuated by a factor of 10^7 by neutral density filters (Orion Optics Co.) of known wavelength characteristics (nearly flat from 2900–3900 Å). Wavelength-dependent reflection was minimized by the coating of the housing inside walls with a flat black paint. The current-time curves for flash-irradiation of the phototube, displayed on a Tektronix 547 oscilloscope, were integrated, and a calibration curve was prepared after correction for the phototube wavelength characteristic (as supplied by the manufacturer). The Si13 response of the phototube varied approximately from 50–90% in the 2500–3900 Å range. The third-order interference filter at 2706 Å also exhibited a transmission

* Only 6 out of the 8 25- μ F capacitors in the laser power supply were connected.

band with a peak at 3900 Å, and the phototube readings were corrected accordingly*. This problem did not arise with the other filters. The calibration curve of the flash tube was quite flat from 2700–3300 Å; it dropped by 50% at 2500 Å, and increased rapidly from 3300–3900 Å (by 400% in that range). The flash tube was aged by repeated flashing before calibration, and its characteristic was stable over the whole experiment, as it was operated with a relatively high inductance (flash duration of approximately 0.5 msec).

A quartz cell with ground joint and a Pyrex head was used. Correction for adsorption by quartz at the lower wavelengths was made. Solutions were prepared from analytical-grade reagents and double-distilled water. The high-purity nitrous oxide was of surgical grade (S.S. White, New York, N.Y.). Treatment of the solution with activated charcoal, as recommended by BARKER¹⁰, was tested but found unnecessary. The solution was carefully de-aerated with nitrogen according to standard practice. Temperature: 24–27°.

RESULTS

Sodium fluoride solution with nitrous oxide as scavenger

Results for 0.1 *M* fluoride are plotted in Fig. 2. Sodium fluoride was selected because of the absence of anion specific adsorption in the range of potentials covered. Photocurrents were not corrected for the variation of reflectivity with wavelength because an equation for correction was not available for a metal–electrolyte interface. The correction for a metal in vacuum is certainly not applicable. The resulting uncertainty is probably not of major importance.

It is not certain *a priori* that the photocurrents in Fig. 2a are limiting values because of the limited solubility of nitrous oxide. However, the scavenger concentration was practically the same in all experiments since the solution was saturated with nitrous oxide at nearly constant temperature. Moreover, experiments without third-order interference filter and with the flash tube at 7 cm (instead of 4 cm) yielded changes of potential as high as 30–40 mV (instead of 2.5 mV or less), thus indicating that depletion of nitrous oxide in experiments with a filter was not severe. Finally, the dependence of Q on potential and wavelength, as displayed in Fig. 2a, can be assumed to be the same as for limiting Q -values, provided the ratio of Q to its corresponding limiting value, at given wavelength and potential, is a constant. This assumption is nearly valid, at least according to BARKER's model**. The Q -values plotted in Fig. 2a should be, on the basis of the results obtained without filter, nearly equal to the corresponding limiting values and they should be, at any rate, nearly proportional to the limiting values.

The effect of the potential, E , at constant wavelength is first interpreted, and the wavelength-dependence will be examined after the theoretical discussion. Photocurrents for $E < -1.6$ V are slightly lowered by the decrease of the scavenger concentration at the electrode caused by the increasingly faster scavenger direct reduction. Figure 2b shows that plots of $Q^{1/2}$ vs. E are quite linear and apparently

* A nickel sulfate solution was not used to remove the 3900 Å band, as recommended by the manufacturer, because the transmittancy of this solution varies somewhat upon irradiation⁹.

** This is only true in the BARKER model provided the distance of penetration of electrons before solvation takes place, is supposed to be independent of wavelength and potential. Actually there seems to be a minor variation^{1,2,5}.

parallel, or at least nearly parallel, except for 3700 Å. This abnormal set of data is very likely to be in error, particularly because the blank correction was significant at that wavelength*. $Q^{1/2}$ vs. E plots were reported in our previous work⁵ but it should be emphasized that they do *not* represent a simple analytical relationship. Moreover,

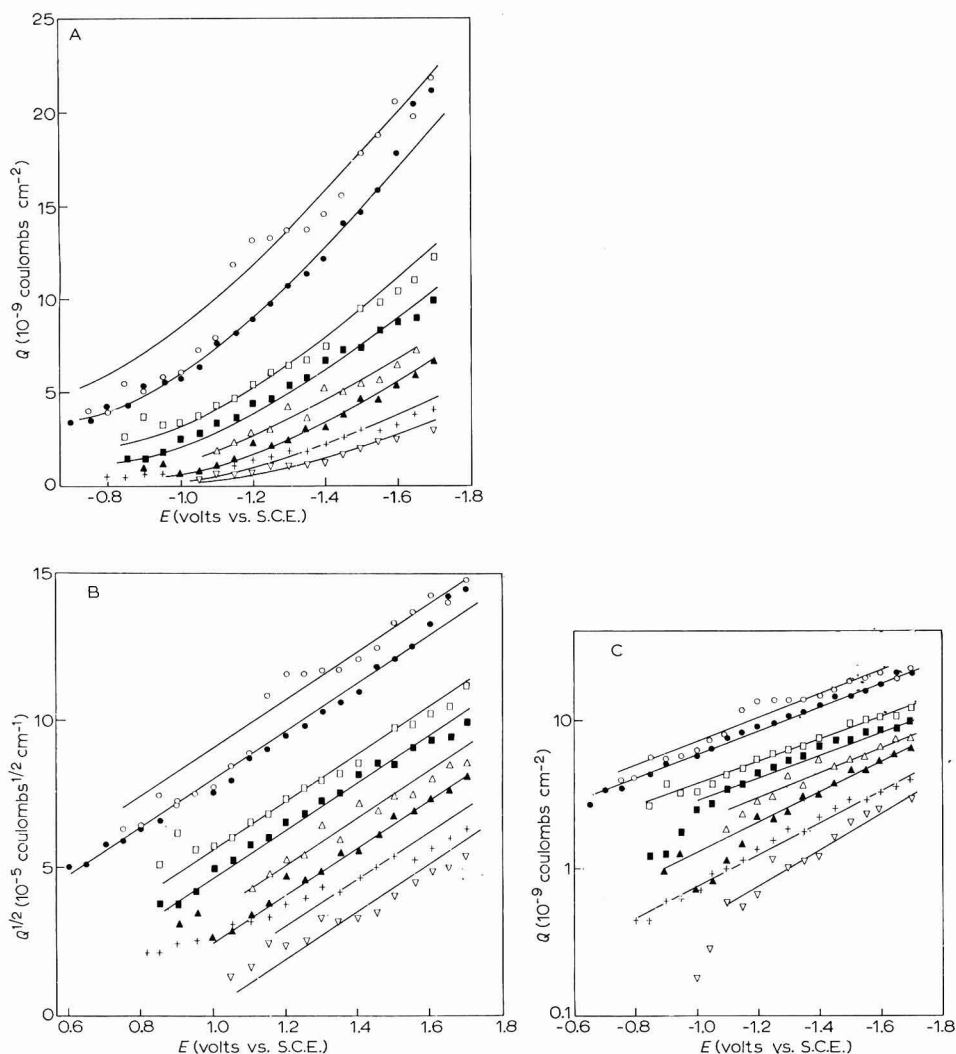


Fig. 2(a). Quantity of electricity lost by electron emission, vs. potential for different wavelengths and for nitrous oxide-satd. 0.1 *M* sodium fluoride. Results corrected for blank. Only values of Q exceeding one-half of the blank correction are plotted. (○), 2506 (●) 2706, (□) 2900, (■) 3100, (△) 3300, (▲) 3500, (+) 3700, (▽) 3900 Å.

(b). Plot of $Q^{1/2}$ vs. potential.

(c). Plot of $\log Q$ vs. potential at constant wavelength.

* Abnormal results could not readily be spotted during experiments because photographed oscilloscope traces (Polaroid camera) had to be enlarged before examination.

there is no obvious theoretical reason why these plots should be parallel. It transpires that transposition of the Fowler treatment, which is discussed below, leads to nearly linear and parallel $Q^{\frac{1}{2}}$ vs. E plots over fairly limited field and wavelength ranges.

The dependence of the photocurrent on potential was also examined on the basis of HEYROVSKÝ's ideas⁴ which lead to proportionality to an exponential function of potential and wavenumber. The plots of $\log Q$ vs. E at constant wavelength are quite linear but do not appear to be parallel over the whole potential range (Fig. 2c). The plots of $\log Q$ vs. wavenumber at constant E are not linear over the whole wavenumber range (Fig. 3).

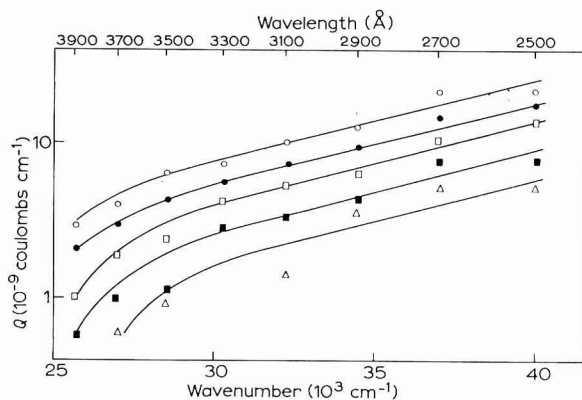


Fig. 3. Plot of $\log Q$ vs. wavenumber at constant potential for the data of Fig. 2. (\circ) -1.7 , (\bullet) -1.5 , (\square) -1.3 , (\blacksquare) -1.1 , (\triangle) -0.7 V.

Sodium halide solution saturated with nitrous oxide

The effect of the shift of the point of zero charge, resulting from a change in the nature of the anion, was investigated for 0.1 M sodium halide solutions at 2900 and 3700 Å. Plots of $Q^{\frac{1}{2}}$ vs. E were essentially linear and parallel at each wavelength. Such plots, prepared by using the rational potentials corresponding to each solution, exhibited a negative shift, at constant $Q^{\frac{1}{2}}$, from iodide to fluoride. The shifts* with respect to iodide were at 2900 Å: -0.05 (Cl⁻), -0.06 (Br⁻), -0.12 V (F⁻). At 3700 Å, the shifts were: -0.17 (Cl⁻), -0.2 (Br⁻), -0.3 V (F⁻). Thus, plots of $Q^{\frac{1}{2}}$ vs. the rational potential corresponding to each solution showed, at a given rational potential, a higher $Q^{\frac{1}{2}}$ for iodide than for fluoride, chloride and bromide being in intermediate positions. The shifts of rational potential were not the same at 2900 and 3700 Å**. It is noted that the shifts at 3700 Å were of the same magnitude and sign as those (at constant charge density on the electrode) for plots of the charge density on the metal vs. the rational potential for a mercury electrode in 0.1 M solution of each of the sodium halides.

Perchloric acid as scavenger

A detailed study was made also with 1 M perchloric acid as scavenger. The

* The bromide-chloride inversion is probably due to experimental errors.

** Photochemical complications, especially with iodide and bromide, cannot be excluded at 2900 Å. No correction was made for the absorbancy of the solutions.

results did not prove conclusive and will not be described in detail. The main difficulty with this scavenger arises from the limited range of potential (if any) over which interpretation is not complicated by secondary effects. At not too negative potentials, hydrogen, which is the primary product of the H^+ -solvated electron reaction, is presumably oxidized^{1,2}, and the measured photocurrent is lowered accordingly. At more negative potentials, electrochemical discharge of H^+ markedly decreases the local concentration of H^+ at the electrode. This faradaic process also interferes with the determination of potential-time traces because it causes a rapid decay of potential at open circuit.

TRANSPPOSITION OF FOWLER'S TREATMENT

We now attempt to compare some of the previous results with the predictions of a transposition of FOWLER's treatment⁶ from a metal-vacuum interface to a metal-electrolyte interface. If we tentatively adopt BARKER's model, the experimental photocurrent results from: (a) emission of electrons for which the sum of the kinetic energy, normal to the electrode-electrolyte interface, and the energy of the incident photon is at least as high as the barrier at the interface and (b) tunnelling of electrons having a lower energy than those in the first process. FOWLER limited his treatment to the first process and did not calculate the transmission coefficient. This coefficient was subsequently calculated for a metal-vacuum interface^{11,12}. These calculations cannot be used directly here because the field strength at a metal-electrolyte interface is too high (up to $3 \cdot 10^7$ V cm⁻¹) to allow the previously used WKB approximation at much lower field ($< 10^5$ V cm⁻¹). The barrier was replaced by adjacent rectangular barriers the combination of which was quite equivalent to the barrier described below. The total photocurrent for the metal-electrolyte interface is the sum of two components calculated by integrating the product of the number of electrons involved in each of the above processes by the corresponding transmission coefficient over the proper energy range. The transmission coefficient* for emission was not strongly dependent on wavelength between 2500 and 3900 Å (0.5-0.7 approximately). The tunnelling contribution to the total current was quite negligible ($< 5\%$) except for field exceeding $4 \cdot 10^7$ V cm⁻¹, *i.e.*, for larger fields than those prevailing in the compact double layer for the electrode potentials covered in the experiment. Since the above improvements are quite minor in this case and since the application of FOWLER's treatment to this problem is only tentative, the calculations will be outlined in their simplest form without tunnelling contribution and for a constant transmission coefficient.

The barrier is given approximately by:

$$W = W_a - eE_1x + \frac{e^2}{4\varepsilon_1x} - \frac{e^2}{4\varepsilon_1(x_d - x)} \frac{\varepsilon_2 - \varepsilon_1}{\varepsilon_2 + \varepsilon_1} \quad (I)$$

where W is the energy, W_a the sum of the Fermi level energy and the work function, e the electron charge, E_1 the field, x the distance from the metal-electrolyte interface,

* The transmission coefficient was also calculated by assuming that the electron is solvated in the compact double layer (1.7 eV-deep well) and was found nearly equal to unity. This model is different from that of BARKER who considered that solvation occurs at greater distances (≥ 30 Å) from the interface.

x_d the distance between the metal-electrolyte interface and the plane of closest approach and ϵ_1 and ϵ_2 the dielectric constants in the compact and diffuse double layer, respectively.

The second term on the r.h.s. of eqn. (1) accounts for the effect of the field in the compact double layer. The third term accounts for imaging by the metal. This term, as written, approaches infinity for $x=0$ and is not valid very near the metal surface. It is cut off¹³ for $W=0^*$. The last term on the r.h.s. of eqn. (1) corresponds to imaging on the plane of closest approach. The form of this term in eqn. (1) is only approximate because rigorous treatment would be much more elaborate. This term represents a contribution to W which varies linearly with x (used between 3.5 and 5 Å). The quantity, $(\epsilon_2 - \epsilon_1)/(\epsilon_2 + \epsilon_1)$, corrects approximately for the variation of the dielectric constant from the compact to the diffuse double layer on the simplifying assumption of a stepwise variation of dielectric constant¹⁴.

The energy corresponding to the top of the barrier of eqn. (1) was computed**, and the number, N , of electrons having an energy exceeding that of the barrier top was then calculated according to FOWLER by means of his general*** equation (see equation just above his eqn. (5) in ref. 6). The photocurrent is proportional to N ,

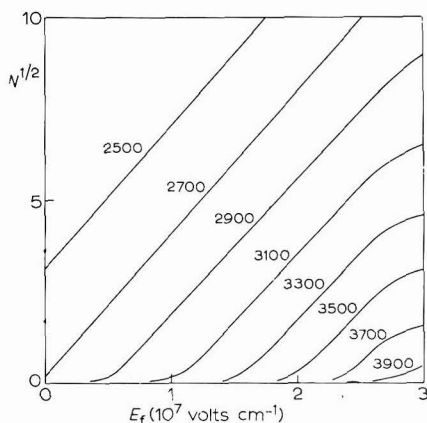


Fig. 4. Plot of the square root of the calculated photocurrent (arbitrary scale) vs. potential.

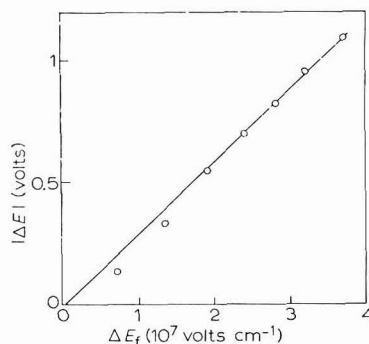


Fig. 5. Plot of the shift of potential, ΔE , from Fig. 2b, at constant current, vs. the shift of field, ΔE_f , from Fig. 4. Shifts were measured with reference to the 2506-Å lines in Figs. 2b and 4.

but the proportionality constant is now known. Its calculation would require a detailed treatment of photon-electron interactions which is not embodied in FOWLER's simpler treatment****. Results are shown in Fig. 4 as plots of $N^{1/2}$ vs. the field, E_f . These plots are nearly linear and parallel, but these features can be regarded as

* Ref. 13 pertains to a metal in vacuum.

** The value $\epsilon_1=3$ was selected since the calculation pertains to the motion of an electron in a polarizable medium. Calculations were also performed with $\epsilon_1=6$, which is the value often adopted in double-layer studies, and results were similar. ϵ_2 was equal to 20; work function, 4.53 eV. Calculations were also performed with a work function of 4.03 and 5.03 eV and results were similar.

*** The approximate equation, which is generally applied in studies of the field effect in vacuum, was not applied here because it holds only near the threshold.

**** Such treatments are more tentative, in any case, because of the complexity of the problem.

empirical as they do not correspond to any analytical relationship in the theoretical treatment.

Since plots in Figs. 2b and 4 are essentially linear and parallel, we can compare, at constant current, the shift of the potential E in Fig. 2b with the shift of the field E_f in Fig. 4 from one wavelength to another*. The resulting correlation yields a rather linear plot (Fig. 5) and indicates that the field in the compact double layer varies quite linearly with potential**. This conclusion is reasonable since the potentials considered here are quite far from the point of zero charge and negative with respect to this point***. However the thickness (≈ 3 Å) of the compact double layer that can be computed from the slope of the line in Fig. 5 is somewhat low, and the calculation is not wholly convincing. It appears that transposition of the Fowler treatment is not entirely justified, at least in the simple manner adopted here. A better approximation could possibly be obtained by consideration of electron scattering by water molecules. Analysis of the correction, however, does not appear to be simple****. Further complications are not to be excluded. It should be added that the foregoing calculations implicitly pre-suppose the essential features of the Barker model, and, consequently, the lack of validity of this model would of course invalidate the theoretical analysis.

The effect of wavelength can also be analyzed, without introduction of theoretical consideration, simply by plotting, at constant current, the shift, ΔE , in Fig. 2b against the energy in electron volts corresponding to the frequency. A reasonably straight line is then obtained, but this matter is not discussed further as the significance of such a plot is not clear to us.

ACKNOWLEDGEMENT

This work was supported by the National Aeronautics and Space Administration under the sustaining Grant No. NGR-33-016-067 to New York University (for V. P. S.), the Office of Naval Research and the National Science Foundation.

SUMMARY

Photocurrents were measured by means of a coulostatic method with a DME, for 0.1 *M* sodium fluoride saturated with nitrous oxide from 2506–3900 Å at 200-Å intervals. The DME was irradiated with a xenon flash tube (325 J/flash) fitted with third-order interference filters having a half-intensity band width of approximately 80 Å. Irradiation intensities were standardized, and results are reported for the same flux of photons at each wavelength. Plots of the square root of the photocurrent against potential were essentially linear and parallel at each wavelength. The possibili-

* Such a comparison could be made, even if the $Q^{\frac{1}{2}}$ -plots were not linear and parallel, because the comparison is made at constant current. However, the comparison would then not be unique.

** The same conclusion holds for calculations performed with a work function of 4.03 and 5.03 eV instead of 4.53 eV.

*** The difference of potential across the diffuse double layer can be regarded as constant with respect to the shifts plotted in Fig. 5.

**** The spreading of an electron wave, originating from a point in the plane corresponding to the "centers" of the mercury atoms next to water molecules is about 3-Å wide when it reaches the first water molecules¹⁵. Multiple scattering can then be expected with all the attending complexity. Similar but simpler problems have been treated¹⁶.

ty of exponential dependence of the photocurrent on potential and frequency was also examined. A similar study was carried out for 0.1 *M* solution of sodium halides saturated with nitrous oxide.

FOWLER's treatment of the field effect on photoemission by a metal in vacuum is transposed to the metal-electrolyte interface, and theoretical and experimental results are compared.

REFERENCES

- 1 G. C. BARKER AND A. W. GARDNER, paper presented at the 1963 Moscow meeting of C.I.T.C.E.
- 2 G. C. BARKER, A. W. GARDNER AND D. C. SAMMON, *J. Electrochem. Soc.*, **113** (1966) 1182.
- 3 H. BERG AND H. SCHWEISS, *Electrochim. Acta*, **9** (1964) 425; previous papers by H. BERG are listed.
- 4 M. HEYROVSKÝ, Dissertation, University of Cambridge, 1966, see references to earlier investigators.
- 5 P. DELAHAY AND V. S. SRINIVASAN, *J. Phys. Chem.*, **70** (1966) 420.
- 6 R. H. FOWLER, *Phys. Rev.*, **38** (1931) 45.
- 7 P. DELAHAY, R. DE LEVIE AND A. M. GIULIANI, *Electrochim. Acta*, **11** (1966) 1141.
- 8 P. DELAHAY AND D. J. KELSH, *J. Electroanal. Chem.*, **16** (1968) 116.
- 9 J. G. CALVERT AND J. N. PITTS, JR., *Photochemistry*, John Wiley and Sons, Inc., New York, 1966, p. 729.
- 10 G. C. BARKER, *Transactions of the Symposium on Electrode Processes*, edited by E. YEAGER, John Wiley and Sons, Inc., New York, 1961, pp. 325-365.
- 11 E. GUTH AND C. J. MULLIN, *Phys. Rev.*, **59** (1941) 575.
- 12 D. W. JUNKER, *ibid.*, **99** (1955) 1155.
- 13 P. H. CUTLER AND J. J. GIBBONS, *ibid.*, **111** (1958) 394.
- 14 L. D. LANDAU AND E. M. LIFSHITZ, *Electrodynamics of Continuous Media*, English translation by J. B. SYKES AND J. S. BELL, Pergamon Press, Oxford, 1960, p. 40.
- 15 R. L. PLATZMAN, *Basic Mechanisms in Radiobiology*, Publication No. 305, U.S. National Research Council, 1953, pp. 22-50.
- 16 A. MESSIAH, *Quantum Mechanics*, Vol. 2, English translation by J. POTTER, North-Holland Publishing Co., Amsterdam, 1963, pp. 848, 854.

J. Electroanal. Chem., **16** (1968) 285-294

POTENTIAL-STEP ELECTROLYSIS FOLLOWED BY LINEAR-SWEEP VOLTAMMETRY AT A PLANE MERCURY-FILM ELECTRODE

W. T. DE VRIES*

Department of Chemistry, Free University, Amsterdam (The Netherlands)

(Received April 27th, 1967)

INTRODUCTION

In a previous paper¹ we described a theoretical investigation on the current-potential curve obtained when potential-step electrolysis is followed by linear potential-sweep voltammetry. This method has been used for analytical purposes by YARNITSKY AND ARIEL in the field of anodic stripping voltammetry². Thus, after the usual preliminary steps of pre-electrolysis (during which the metal to be determined is reduced at and collected into a mercury electrode at a constant negative potential with stirring of the aqueous solution) and rest period (in which convection in the solution and the mercury is allowed to decay), the potential of the electrode is stepped towards a positive potential. After a suitable waiting period, a linear sweep back towards negative potentials is applied and a re-reduction current peak is obtained.

For the case of semi-infinite linear diffusion the result is strikingly simple: the re-reduction current peak, obtained during the linear potential sweep after the potential-step oxidation and the waiting period, and measured from the extrapolated oxidation current, is the same as that obtained when the metal is oxidized directly by a linear potential-sweep towards positive values, except for a reversal of direction with respect to the potential axis. In the first case, the peak potential is $57/n$ mV more cathodic than in the latter case.

An important assumption in our previous calculations¹ is that conditions of semi-infinite diffusion prevail. This assumption is probably not valid for the experiments described by YARNITSKY AND ARIEL². Apart from the eventual influences of spherical diffusion, depletion of the mercury-drop electrode used by these workers probably played a noticeable role in these experiments. When the electrode becomes depleted of reduced metal (R) during the oxidation period, the surface concentration of oxidized metal (O) will diminish by diffusion during the remainder of the oxidation period and during a certain period after initiation of the potential sweep and the height of the subsequent re-reduction peak will be diminished. We report here therefore a theoretical investigation of the method of potential-step electrolysis followed by linear-sweep voltammetry at a plane mercury-film electrode, in order to assess the influence of this and other effects and to be able to specify the best experimental conditions for analytical application of the method.

* Temporary address until March 1, 1968: Department of Chemistry, The Israel Institute of Technology, Technion City, Haifa, Israel.

Only the case of potential-step *oxidation* followed by linear-sweep *reduction* has so far been considered in detail, although the results for the case of semi-infinite diffusion can easily be transposed to the case of potential-step reduction followed by linear-sweep oxidation. For an electrode of small volume, this will not be the case because of the accumulation of reduced metal into a limited volume during the reduction period. Thus, the limited volume of the electrode will not only cause the subsequent oxidation (stripping) peak to be higher, but also to have less width^{3,4} and we have, therefore, also considered the case of potential-step reduction followed by oxidation with a linear potential sweep.

POTENTIAL-STEP OXIDATION FOLLOWED BY LINEAR-SWEEP REDUCTION

(a) *The problem; initial and boundary conditions*

It is assumed that the electrode reaction ($M^0 \rightarrow M^{n+} + ne$) is reversible without kinetic complications and that the metal forms an amalgam with the mercury. Thus, Fick's equations for linear diffusion of both oxidized and reduced species must be solved:

$$\frac{\partial}{\partial t} C_R(x, t) = D_R \cdot \frac{\partial^2}{\partial x^2} C_R(x, t) \quad (1)$$

$$\frac{\partial}{\partial t} C_O(y, t) = D_O \cdot \frac{\partial^2}{\partial y^2} C_O(y, t) \quad (2)$$

where x is the distance in the mercury film and y that in the aqueous solution. The thickness of the mercury film is taken as l . The mercury-solution interface is at $x=y=0$.

The initial conditions are:

$$C_R(x, 0) = C^0, \quad 0 < x < l \quad (3)$$

$$C_O(y, 0) = 0, \quad y > 0 \quad (4)$$

and the boundary conditions are:

$$t < \tau: \quad C_O(0, t) = \theta C_R(0, t) \quad (\theta \gg 1) \quad (5)$$

$$\theta = \sqrt{(D_R/D_O)} \exp[(nF/RT)(E_i - E_0)] \quad (6)$$

$$t > \tau: \quad \frac{C_O(0, t)}{C_R(0, t)} = \theta \exp[-\sigma(t - \tau)] \quad (7)$$

with

$$\sigma = \frac{nF}{RT} v$$

$$-D_R \left(\frac{\partial C_R}{\partial x} \right)_{x=0} = D_O \left(\frac{\partial C_O}{\partial y} \right)_{y=0} = q(t) \quad (8)$$

$$D_R \left(\frac{\partial C_R}{\partial x} \right)_{x=l} = 0 \quad (9)$$

$$\lim_{y \rightarrow \infty} C_O(y, t) = 0. \quad (10)$$

Thus, the metal which is initially present at a concentration C^0 , is oxidized by a potential step at time $t=0$, from an infinitely negative potential (see eqn. (4)) to a positive value, E_1 . The electrode is kept at this potential during the waiting period of τ sec. Starting at time $t=\tau$, the potential of the electrode is linearly changed with time towards negative values:

$$E(t) = E_1 - v(t - \tau). \quad (11)$$

The flux of O and R at the electrode surface, $q(t)$, is so defined as to have a positive value for a reduction process. The symbols not defined above have their usual significance.

(b) *Integral equations and dimensionless parameters*

Straightforward application of the Laplace transform technique leads to the following integral equations for the concentrations of O and R at the mercury-solution interface:

$$C_R(0, t) = C^0 + \frac{1}{\sqrt{\pi D_R}} \int_0^t \frac{q(\xi)}{\sqrt{t-\xi}} d\xi + \frac{2}{\sqrt{\pi D_R}} \sum_{i=1}^{\infty} \int_0^t \frac{q(\xi)}{\sqrt{t-\xi}} \exp \left[\frac{-i^2 l^2}{D_R(t-\xi)} \right] d\xi \quad (12)$$

$$C_O(0, t) = \frac{-1}{\sqrt{\pi D_O}} \int_0^t \frac{q(\xi)}{\sqrt{t-\xi}} d\xi. \quad (13)$$

For convenience, the following dimensionless quantities are defined:

$$\gamma = \sqrt{D_O/D_R} \quad (14)$$

$$K = \sigma\tau \quad (15)$$

$$\lambda = t/\tau \quad (16)$$

$$\varphi(\lambda) = q(t)\sqrt{\tau/C^0}\sqrt{D_R K} = q(t)/C^0\sqrt{D_R\sigma} \quad (17)$$

$$G = l^2/D_R\tau. \quad (18)$$

Substitution of the appropriate dimensionless parameters into eqns. (12) and (13) leads to the dimensionless form of these integral equations:

$$\frac{C_R(0, t)}{C^0} = 1 + \sqrt{\frac{K}{\pi}} \int_0^\lambda \frac{\varphi(\xi)}{\sqrt{\lambda-\xi}} d\xi + 2\sqrt{\frac{K}{\pi}} \int_0^\lambda \frac{\varphi(\xi)}{\sqrt{\lambda-\xi}} \exp \left[\frac{-i^2 G}{\lambda-\xi} \right] d\xi \quad (19)$$

$$\frac{C_O(0, t)}{C^0} = -\frac{1}{\gamma} \sqrt{\frac{K}{\pi}} \int_0^\lambda \frac{\varphi(\xi)}{\sqrt{\lambda-\xi}} d\xi. \quad (20)$$

The integral equations (19) and (20) are a convenient starting point for the subsequent mathematical analysis, as will be apparent from the following sections.

(c) *The oxidation current*

The expression for the dimensionless oxidation current can be found most easily by combining eqns. (5), (19), and (20), Laplace-transforming the resulting integral equation and writing the series expansion in closed form; the result is:

$$\varphi(s) = -\frac{\psi}{\sqrt{Ks}} \frac{\exp[2\sqrt{Gs}] - 1}{(\psi + 1) \exp[2\sqrt{Gs}] + \psi - 1}, \quad (21)$$

where s is the Laplace transform variable and ψ is defined by

$$\psi = \gamma\theta = \exp[(nF/RT)(E_i - E_{\frac{1}{2}})]. \quad (22)$$

The second fraction of eqn. (21) can be written as

$$(z-1)/\{(\psi+1)z+\psi-1\} \quad (23)$$

with $z = \exp[2\sqrt{Gs}] > 1$. Normally, the assumption is made that $\psi \gg 1$, and then the following series expansion for expression (23) is obtained:

$$\psi^{-1} \left\{ 1 + 2 \sum_{i=1}^{\infty} (-1)^i z^{-i} \right\}. \quad (24)$$

However, for the purpose of this investigation it is not desirable to introduce this simplification at this stage; if all the terms in expression (23) are retained, the following series expansion is obtained:

$$\frac{1}{\psi+1} \left\{ 1 + \frac{2\psi}{\psi-1} \sum_{i=1}^{\infty} \left(-\frac{\psi-1}{\psi+1} \right)^i z^{-i} \right\}. \quad (25)$$

With the use of expression (25), eqn. (21) can be manipulated into a form suitable for back-transformation to the variable λ ; this back-transformation results in:

$$\varphi(\lambda) = -\frac{\psi}{(\psi+1)\sqrt{\pi K \lambda}} \left\{ 1 + \frac{2\psi}{\psi-1} \sum_{i=1}^{\infty} \left(-\frac{\psi-1}{\psi+1} \right)^i \exp \left[-\frac{i^2 G}{\lambda} \right] \right\}. \quad (26)$$

When eqn. (26) is simplified by assuming $\psi \gg 1$, one obtains:

$$\varphi(\lambda) = -(\lambda/\sqrt{\pi K \lambda}) \left\{ 1 + 2 \sum_{i=1}^{\infty} (-1)^i \exp[-i^2 G/\lambda] \right\}. \quad (27)$$

For small values of G/λ , eqn. (27) converges slowly; for these cases, a more suitable expression for the oxidation current can be found by starting from a formula given by CARSLAW AND JAEGER⁵. The mathematical manipulations are quite straightforward and the result, in terms of the dimensionless parameters defined above, can be written as:

$$\varphi(\lambda) = -(2/\sqrt{GK}) \sum_{i=0}^{\infty} \exp[-\frac{1}{4}(2i+1)^2 \pi^2 (\lambda/G)], \quad (28)$$

which is the equivalent of eqn. (27) because in its derivation it is assumed that $\psi \gg 1$.

Numerical calculations of the oxidation current for various values of G have been carried out using eqns. (27) and (28). It has been found that eqn. (28) converges more rapidly than eqn. (27) for $G/\lambda < 2$.

Figure 1 shows the oxidation current, $\varphi(\lambda) \times \sqrt{K} = q(t)/\tau/C^0\sqrt{D_R}$, for various values of G and $0 < \lambda < 2$. It can be seen that the oxidation current decays to a smaller value at the end of the waiting period ($\lambda = 1$) when the mercury film becomes thinner and/or the waiting period longer.

(d) Integral equation for the re-reduction current-potential curve

The approach used to find the integral equation describing the re-reduction

current-potential curve is almost the same as that used earlier¹. A new current function, $\Phi'(\lambda)$, is defined:

$$\Phi'(\lambda) = \varphi(\lambda) + \frac{\psi}{(\psi+1)\sqrt{\pi K \lambda}} \left\{ 1 + \frac{2\psi}{\psi-1} \sum_{i=1}^{\infty} \left(-\frac{\psi-1}{\psi+1} \right)^i \exp \left[-i^2 \frac{G}{\lambda} \right] \right\}. \quad (29)$$

The re-reduction current peak is not measured from the zero-current axis, but from the base-line formed by the oxidation current extrapolated beyond the waiting period. Of course, $\Phi'(\lambda) = 0$ for $0 < \lambda < 1$.

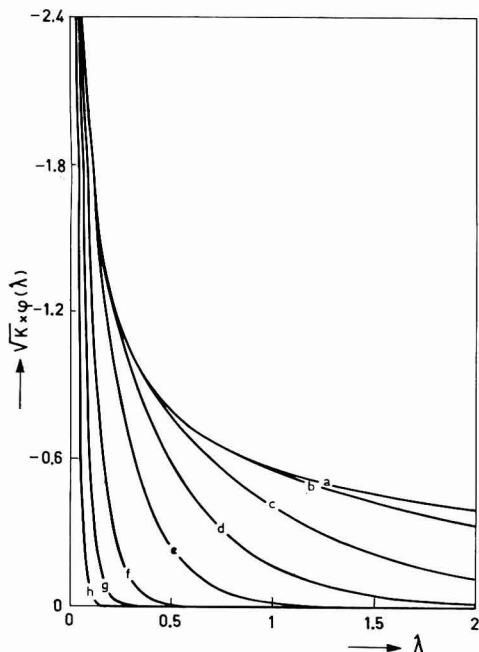


Fig. 1. Oxidation current, as a function of time, at a mercury-film electrode following a potential step. The corresponding G -values are: (a), ∞ ; (b), 5; (c), 2; (d), 1; (e), 0.5; (f), 0.2; (g), 0.1; (h), 0.05.

In order to find the desired integral equation the procedure is as follows. First, eqns. (19) and (20) are Laplace-transformed, while the series expansion resulting from eqn. (19) is written in closed form. Equation (29) is also Laplace-transformed and the resulting series expansion reduced to its closed form (see eqns. (23) and (25)). From the latter equation an expression for $\varphi(s)$ is obtained by algebraic rearrangement, and this is substituted into the Laplace transforms of eqns. (19) and (20). The appropriate fractions are again expanded in series form to permit back-transformation, giving finally:

$$\begin{aligned} \frac{C_R(0,t)}{C^0} = & \frac{1}{\psi+1} + \sqrt{\frac{K}{\pi}} \int_1^\lambda \frac{\Phi'(\xi)}{\sqrt{\lambda-\xi}} d\xi + 2\sqrt{\frac{K}{\pi}} \sum_{i=1}^{\infty} \int_1^\lambda \frac{\Phi'(\xi)}{\sqrt{\lambda-\xi}} \exp \left[-\frac{i^2 G}{\lambda-\xi} \right] d\xi \\ & + \frac{2\psi}{\psi^2-1} \sum_{i=1}^{\infty} \left(-\frac{\psi-1}{\psi+1} \right)^i \operatorname{erfc} i \sqrt{\frac{G}{\lambda}}; \end{aligned} \quad (30)$$

$$\frac{C_o(0,t)}{C^0} = \frac{\psi}{\gamma(\psi+1)} - \frac{1}{\gamma} \sqrt{\frac{K}{\pi}} \int_1^\lambda \frac{\Phi'(\xi)}{\sqrt{\lambda-\xi}} d\xi + \frac{2\psi^2}{\gamma(\psi^2-1)} \sum_{i=1}^{\infty} \left(-\frac{\psi-1}{\psi+1}\right)^i \operatorname{erfc} i \sqrt{\frac{G}{\lambda}}. \quad (31)$$

(The integration from $\xi=0$ to $\xi=1$ is omitted as it contributes nothing since $\Phi'(\lambda)=0$ for $0 < \lambda < 1$.) Equations (7), (30), and (31) are now combined and the following substitutions made:

$$x = K(\lambda-1) = \sigma(t-\tau); \quad (32)$$

$$\Phi(x) = \Phi'(\lambda); \quad (33)$$

$$H = GK = l^2 \sigma / D_R. \quad (34)$$

At this stage, the simplifying assumption that $\psi \gg 1$ is introduced; algebraic rearrangements lead to:

$$\begin{aligned} \frac{1}{\psi} (e^x - 1) \left(1 + 2 \sum_{i=1}^{\infty} (-1)^i \operatorname{erfc} i \sqrt{\frac{H}{x+K}} \right) - \frac{e^x}{\psi/\pi} \int_0^x \frac{\Phi(\xi)}{\sqrt{x-\xi}} d\xi = \\ \frac{1}{\sqrt{\pi}} \int_0^x \frac{\Phi(\xi)}{\sqrt{x-\xi}} d\xi + \frac{2}{\sqrt{\pi}} \sum_{i=1}^{\infty} \int_0^x \frac{\Phi(\xi)}{\sqrt{x-\xi}} \exp \left[-\frac{i^2 H}{x-\xi} \right] d\xi. \end{aligned} \quad (35)$$

A comparison of this equation with eqn. (26) of ref. 6 shows that they are of identical form except for the factor

$$Q\sqrt{H/(x+K)} = 1 + 2 \sum_{i=1}^{\infty} (-1)^i \operatorname{erfc} i \sqrt{G/\lambda} \quad (36)$$

in the first left-hand side term of eqn. (35) (note that $G/\lambda = H/(x+K)$). Combination of eqn. (35) with eqn. (13) of ref. 6 gives an approximate form useful for small values of H .

(e) *The continuity of the current-potential curve at the start of the potential sweep*

At this point it seems appropriate to make some remarks about the effect of the initial and boundary conditions on the continuity of the current-potential curve at the start of the potential sweep. In the theory of normal linear-sweep voltammetry^{7,8} it is customary, in the treatment of a reduction process, to assume the concentration of R to be zero at time $t=0$: $C_R(x,0)=0$. This mathematical assumption causes a discontinuity in the current response at time zero, as the application of the potential sweep starting at E_i is then equivalent to a potential step from an infinitely positive potential to the (also positive) initial potential, E_i . Thus, at time $t=0$, the concentration of R at the electrode surface has to adjust to a small but finite value, θC_o^0 , where C_o^0 is the initial concentration of O and θ is defined by eqn. (6).

The above formulation of initial conditions leads to the following integral equation representation of the well-known Ševčík-Randles P -function:

$$(1/\pi) \int_0^x \{P(\xi)/\sqrt{x-\xi}\} d\xi = 1/(\psi e^{-x} + 1). \quad (37)$$

When, however, the initial concentration of R is assumed to be $C_R(x,0) = \theta C_o^0$ instead of zero,

$$(1/\pi) \int_0^x \{P(\xi)/\sqrt{x-\xi}\} d\xi = (1 - e^{-x})/(\psi e^{-x} + 1), \quad (38)$$

and it is seen that in this case, for $x=0$ both sides of the equation are zero, which is not the case with eqn. (37). Although this does not affect the shape of the P -function near $E_{\frac{1}{2}}$ and beyond, the use of eqn. (37) caused difficulties in the work of PERONE AND MUELLER on derivative linear-sweep voltammetry⁹. The discontinuity at time $t=0$ attains significant values at the first peaks of the second and third derivative curves (d^2P/dx^2 and d^3P/dx^3). These authors apparently did not take into account the fact that this effect stems from their use of eqn. (37), and they failed to draw a clear distinction between the theoretical and experimental aspects of this phenomenon. Use of eqn. (38) would have prevented this difficulty.

In order to avoid this discontinuity, we preferred to use eqn. (26) for the oxidation current, and not the more simple equation (27). The use of this latter equation causes the term (e^x-1) in eqn. (35) to become e^x , thus giving rise to a discontinuity at time $t=0$.

(f) The function $Q(\sqrt{G/\lambda})$, defined by eqn. (36)

The function $Q(\sqrt{G/\lambda})$, defined by eqn. (36) converges slowly for small values of G/λ . An approximation for small values of G/λ can be found as follows. The Laplace-transform (from λ to s), in closed form, of this function is:

$$\mathcal{L}\left\{Q\left(\sqrt{\frac{G}{\lambda}}\right)\right\} = \frac{1}{s} \frac{\exp[2\sqrt{Gs}] - 1}{\exp[2\sqrt{Gs}] + 1}. \quad (39)$$

It is easy to derive the following relationship:

$$\frac{e^u - 1}{e^u + 1} = 1 - 2e^{-u} \left(1 - \frac{1}{e^u + 1}\right) = 1 - e^{-u} \left(1 + \frac{u}{2} - \frac{u^3}{24} + \frac{u^5}{240} - \frac{17u^7}{40320} \dots\right). \quad (40)$$

The expression between brackets is obtained by expansion of e^u in powers of u and carrying out the indicated division. Substituting $2\sqrt{Gs}$ for u in eqn. (40) results in:

$$\mathcal{L}\left\{Q\left(\sqrt{\frac{G}{\lambda}}\right)\right\} = \frac{1}{s} - \exp[-2\sqrt{Gs}] \left(\frac{1}{s} + \frac{G^{1/2}}{s^{1/2}} - \frac{G^{3/2}}{3} s^{1/2} + \frac{2G^{5/2}}{15} s^{3/2} - \frac{17G^{7/2}}{315} s^{5/2}\right) \quad (41)$$

and back-transformation gives¹⁰:

$$Q(z) = 1 - \operatorname{erfc} z - \frac{\exp(-z^2)}{\sqrt{\pi}} \left(z + \frac{z^3}{6} - \frac{7}{30} z^5 - \frac{251}{840} z^7\right) \quad (42)$$

with $z = \sqrt{G/\lambda}$.

For very small values of z , one can put $1 - \operatorname{erfc} z = \operatorname{erf} z \approx 2z/\sqrt{\pi}$, and assume that $\exp(-z^2) \approx 1$ and that higher powers of z are negligible compared to z . The result is a still simpler approximation:

$$Q(z) = z/\sqrt{\pi}. \quad (43)$$

In Table 1, the approximations (42) and (43) for $Q(z)$ are compared to the exact equation (36), and it is seen that eqn. (42) especially, is a useful approximation for small values of z . In Fig. 2, $Q(z)$ is shown for $0 < z < 2.4$.

(g) Elimination of parameter $K = \sigma\tau$

From eqn. (35) it can be ascertained that the re-reduction current-potential

curve depends on ψ (*i.e.*, the initial potential with respect to the polarographic half-wave potential, see eqn. (22)), $H = l^2\sigma/D_R$ (combining influences of mercury-film thickness and rate of potential change), and $K = \sigma\tau$ (*i.e.*, duration of oxidation period). Unlike the case of normal linear-sweep voltammetry, the re-reduction current function, $\Phi(x)$, will depend strongly on the value of ψ . A larger value of ψ (more positive potential E_i) will allow more time for the mercury electrode to become depleted during the initial part of the potential sweep. Thus, the height of the re-reduction curve will decrease with increasing ψ . The same considerations lead to the conclusion that peak height will also decrease with increasing K .

TABLE 1

COMPARISON OF THE APPROXIMATIONS (42) AND (43) FOR $Q(z)$ WITH THE EXACT EQUATION (36); $z = \sqrt{G/\lambda}$

z	$\Delta Q(\%)$ eqn. (42)	$\Delta Q(\%)$ eqn. (43)
0.05		-0.04
0.1	-0.9×10^{-4}	-0.17
0.2	-1.6×10^{-4}	-0.68
0.4	-2.5×10^{-2}	-2.89

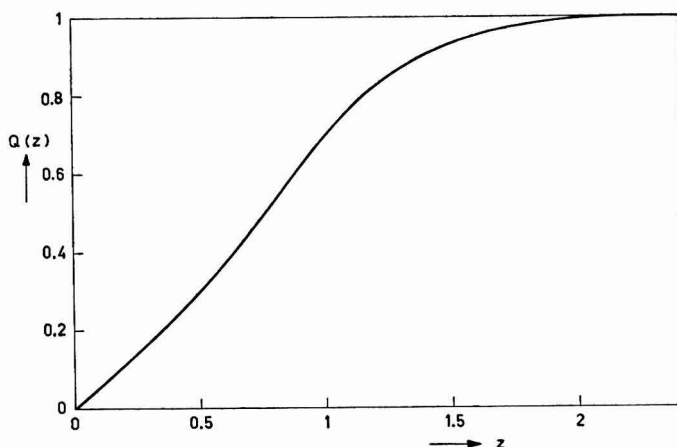


Fig. 2. The function $Q(z)$, with $z = \sqrt{G/\lambda}$, as defined by eqn. (36).

When it is tentatively assumed that the decrease of the re-reduction current peak is largely governed by the time elapsed when the electrode reaches the potential E_i , counted from the application of the potential step, it might be supposed that this decrease remains the same when this time is constant:

$$n(E_i - E_{\frac{1}{2}})/v = \text{constant},$$

or

$$K + \ln \psi = \text{constant}. \quad (44)$$

This assumption proved to be true when the appropriate numerical calculations were carried out. This result enables us to put K equal to zero and thus to eliminate this parameter from eqn. (35). This amounts to starting the sweep at once after

application of the potential step. Thus, the re-reduction current peak depends only on H and ψ .

For a certain value of ψ , one can find pairs of values of K and ψ' according to eqn. (44). The value of ψ' must, however, not be chosen too small, as then the shape of the re-reduction current peak will depend on ψ' , although $K + \ln \psi'$ remains constant¹¹. Thus,

$$\tau = (\ln \psi - \ln \psi')/\sigma = \{(\ln \psi - \ln \psi')/H\} l^2/D_R \quad (45)$$

and it is seen that with $\ln \psi - \ln \psi'$ remaining the same, the waiting period increases with decreasing sweep rate. When H is also kept constant, τ decreases sharply with decreasing film thickness.

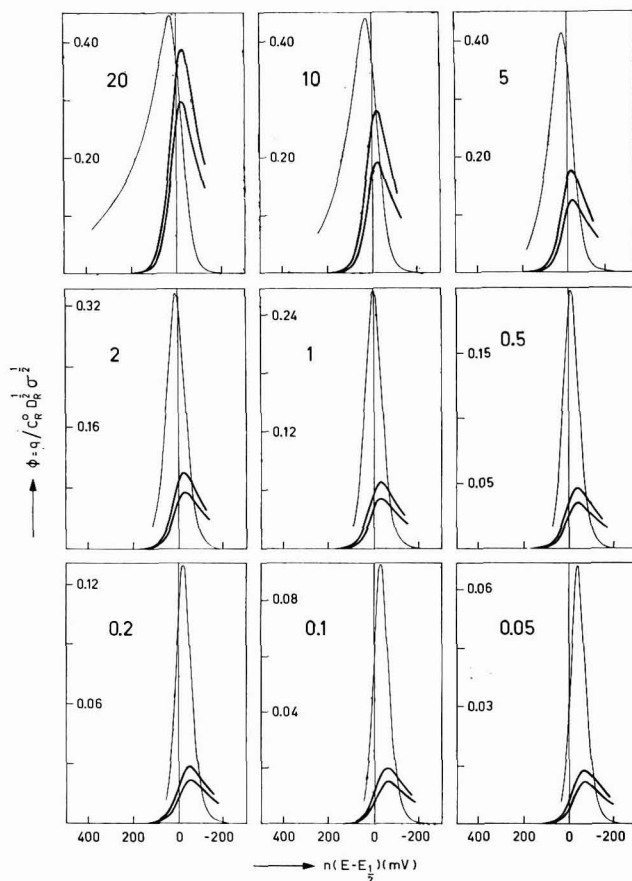


Fig. 3. Re-reduction current-potential curves obtained during a reducing linear potential sweep, for several values of $H = l^2 \sigma / D_R$. For explanation see text.

(h) Numerical calculations and results

The numerical calculations of re-reduction current-potential curves have been carried out using the method of HUBER^{4,6}. The Algol-60 digital computer pro-

gram (available from the author on request) calculates $Q(z)$ by eqn. (42) for $z < 0.250$, and by eqn. (36) for larger values of z .

We have not carried out a comprehensive parameter study; instead, the most important properties of the re-reduction current peaks are summarized in Fig. 3. In each of the nine figures (the large number not belonging to the vertical axis denotes the value of $H = l^2\sigma/D_R$) the thinly-drawn highest curve is obtained on *direct stripping* of the metal from the mercury film, starting the potential sweep at a negative potential. The middle curve is obtained on re-reduction following a potential step towards $n(E_i - E_{\frac{1}{2}}) = 250$ mV (at 25°). For the lowest curve, $n(E_i - E_{\frac{1}{2}}) = 500$ mV.

The height of the re-reduction current peak is strongly dependent on the values of H and $n(E_i - E_{\frac{1}{2}})$, especially for $5 < H < 20$, while the proportion of heights between the direct stripping curve and the re-reduction peaks attains a constant value for small values of H . For semi-infinite linear diffusion, the heights of all three curves would be the same¹. It is estimated that for H -values between 40 and 60, the lower curves will become identical with the Ševčík-Randles P -function. The considerable loss in sensitivity for low values of H is caused by the rapid removal of the metal from the thin mercury film after the potential step, and subsequent diffusion into the solution, which rapidly diminishes the surface concentration of oxidized metal.

(i) *Limiting case for $H \rightarrow 0$*

The constant proportion between the heights of the direct stripping curve and the re-reduction peaks for small values of H suggests a simplification of eqn. (35) analogous to that of the integral equation describing the direct stripping curves⁶. Thus, a function $\Theta(x)$ is defined:

$$\Theta(x) = \Phi(x)/\sqrt{H}, \quad (46)$$

$Q(\sqrt{H/(x+K)})$ (with K put equal to zero) is approximated by eqn. (43), and the right-hand side of eqn. (35) is written as⁶

$$(1/\sqrt{H}) \int_0^x \Phi(\xi) d\xi.$$

The final result is:

$$\frac{e^x - 1}{x^{\frac{1}{2}}} - e^x \int_0^x \frac{\Theta(\xi)}{\sqrt{x - \xi}} d\xi = \frac{\psi\pi^{\frac{1}{2}}}{H^{\frac{1}{2}}} \int_0^x \Theta(\xi) d\xi. \quad (47)$$

Equation (47) defines a function $\Theta(x)$ which depends only on the value of $\psi/H^{\frac{1}{2}}$. We have calculated $\Theta(x)$ -curves for a number of values of $\psi/H^{\frac{1}{2}}$. The maximum value of $\Theta(x)$, Θ_{\max} , is plotted in Fig. 4 vs. $\log(\psi/H^{\frac{1}{2}})$. It is seen that Θ_{\max} decreases with increasing $\psi/H^{\frac{1}{2}}$, reflecting the loss in sensitivity that occurs when the re-reduction is started from more positive potentials and when a thinner mercury film or a lower sweep rate is employed. From the definition of $\Theta(x)$ it follows that at 25° :

$$i_p = 3.7547 \times 10^6 \Theta_{\max} n^2 A C_R^0 l v \text{ amp}, \quad (48)$$

where i_p is the peak current (A), n the number of electrons in the electrode reaction equation, A the electrode area (cm²), C_R^0 the initial concentration of R in the thin layer (mole cm⁻³), l the thickness of the solution layer (cm), and v the sweep rate (V sec⁻¹).

By analogy with the case of direct reduction at a mercury-film electrode⁶, one would expect a relationship of the form

$$n(E_p - E_{\frac{1}{2}}) = c + 29.580 \log H \text{ mV.} \quad (49)$$

This relationship is indeed nearly fulfilled. The constant, c , does not change much when $\psi/H^{\frac{1}{2}}$ is varied over a wide range. In Table 2 the values of Θ_{\max} , the constant c of eqn. (49), and the width at half height, are given for several values of $\psi/H^{\frac{1}{2}}$.

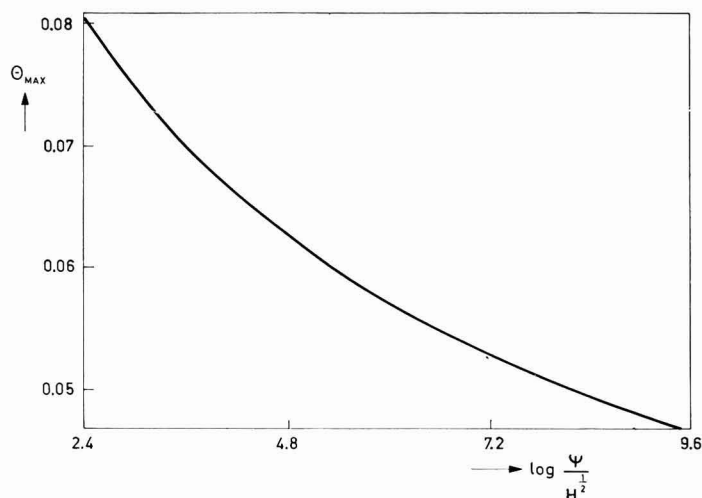


Fig. 4. Maximum value of $\Theta(x)$, Θ_{\max} , as defined by eqn. (47), plotted vs. $\log(\psi/H^{\frac{1}{2}})$.

TABLE 2

PARAMETERS OF $\Theta(x)$, AS DEFINED BY EQN. (47), FOR SEVERAL VALUES OF $\psi/H^{\frac{1}{2}}$; c IS THE CONSTANT OCCURRING IN EQN. (49)

$\psi/H^{\frac{1}{2}}$	Θ_{\max}	c (mV)	$nb_{\frac{1}{2}}$ (mV)
250	0.08058	-25.5	158.5
4,000	0.06991	-28.5	166.6
64,000	0.06259	-30.4	173.1
1,024,000	0.05716	-31.7	178.5
16,384,000	0.05294	-32.6	183.0
262,144,000	0.04954	-33.3	186.7

(j) Discussion

From an analytical viewpoint, the results of the theoretical investigation are somewhat disappointing. The properties of the current-potential curves do not permit a high sensitivity or a good resolution of adjacent peaks to be achieved compared to direct stripping with a thin mercury-film electrode. In the latter case, z_{\max} (which is analogous to Θ_{\max} in eqn. (48), see ref. 6) has the value 0.2971, and the height of the re-reduction curve is decreased by a factor 3.7–5.7. However, base-line difficulties caused by interfering electrode reactions and the presence of other depolarizers introduce other factors and in these cases the method of YARNITSKY

AND ARIEL can give better results². It is advantageous to choose experimental conditions so that conditions of semi-infinite diffusion are approached as closely as possible. The use of a thin mercury-film electrode can therefore not be recommended in this method. The necessity of having a large value of H dictates the use of high sweep rates and short (perhaps even zero) oxidation periods (see eqn. (45)). This will cause the re-reduction current-potential curve to be superimposed on a very steep base-line (formed by the extrapolated oxidation current), and will make the recording and evaluation of the peak difficult. Thus, the approach of PERONE AND BIRK¹², consisting of measuring the time-derivative of the direct stripping curve, seems to hold more promise than the method of potential-step oxidation followed by linear-sweep re-reduction, when a thin mercury-film electrode is employed.

When a mercury-drop electrode is used, application of the method of YARNITSKY AND ARIEL does not entail a serious loss of sensitivity as long as conditions of semi-infinite diffusion are adhered to as closely as possible (short oxidation periods and high sweep rates). Conditions of semi-infinite diffusion are less difficult to achieve with a mercury-drop electrode than with a thin-film electrode owing to the generally large radius of the mercury drop. The drop radius, which is of the order of 0.5 mm = 500 μ , is analogous to the mercury-film thickness, which seldom exceeds 50 μ .

POTENTIAL-STEP REDUCTION FOLLOWED BY LINEAR-SWEEP OXIDATION

(a) Initial and boundary conditions; integral equations

Equations (1) and (2) must be solved with the following initial conditions:

$$C_R(x,0) = 0, \quad 0 < x < l, \quad (50)$$

$$C_O(y,0) = C^0, \quad y > 0, \quad (51)$$

where C^0 now denotes the initial concentration of oxidized metal in the aqueous solution. The boundary conditions are given by:

$$t < \tau: C_O(0,t) = \theta C_R(0,t), \quad \text{with } \theta \ll 1 \quad (52)$$

$$t > \tau: C_O(0,t)/C_R(0,t) = \theta \exp[-\sigma(t-\tau)] \quad (53)$$

$$D_R \left(\frac{\partial C_R}{\partial x} \right)_{x=0} = -D_O \left(\frac{\partial C_O}{\partial y} \right)_{y=0} = q(t) \quad (54)$$

$$\lim_{y \rightarrow \infty} C_O(y,t) = C^0. \quad (55)$$

The boundary condition at $x=l$ is given by eqn. (9). The flux, $q(t)$, is so defined as to have a positive value for the oxidation process. The metal, present in the aqueous solution in its oxidized form, is thus reduced by a potential step applied at time $t=0$ from an infinitely positive potential towards a negative potential, E_i (see eqn. (6)). At the end of the reduction period of τ sec, the potential is linearly changed with time towards more positive values:

$$E(t) = E_i + v(t-\tau). \quad (56)$$

We use the same dimensionless quantities as defined earlier, except for $\varphi(\lambda)$, which is now defined by

$$\varphi(\lambda) = q(t)/\tau/C^0\sqrt{D_0K} = q(t)/C^0\sqrt{D_0\sigma} \quad (57)$$

It is easily verified that the eqns. (1) and (2) with the initial and boundary conditions formulated above can be summarized in the following integral equations:

$$\frac{C_R(0,t)}{C^0} = -\gamma \sqrt{\frac{K}{\pi}} \int_0^\lambda \frac{\varphi(\xi)}{\sqrt{\lambda-\xi}} d\xi - 2\gamma \sqrt{\frac{K}{\pi}} \sum_{i=1}^{\infty} \int_0^\lambda \frac{\varphi(\xi)}{\sqrt{\lambda-\xi}} \exp\left[\frac{-i^2G}{\lambda-\xi}\right] d\xi \quad (58)$$

$$\frac{C_O(0,t)}{C^0} = 1 + \sqrt{\frac{K}{\pi}} \int_0^\lambda \frac{\varphi(\xi)}{\sqrt{\lambda-\xi}} d\xi. \quad (59)$$

(b) *Reduction current and integral equation for the re-oxidation current peak*

The expression for the reduction current can be derived in the same way as for the oxidation current by combining eqns. (52), (58), and (59); this derivation results in:

$$\varphi(\lambda) = -\frac{1}{(1+\psi)\sqrt{\pi K\lambda}} \left\{ 1 - \frac{2\psi}{1-\psi} \sum_{i=1}^{\infty} \left(\frac{1-\psi}{1+\psi} \right)^i \exp\left[-i^2 \frac{G}{\lambda}\right] \right\}, \quad (60)$$

which reduces to the familiar form for semi-infinite diffusion when ψ is assumed to be zero and/or G infinitely large.

Equation (60) is now used to define a new current function, $\Phi'(\lambda)$, strictly analogous to the procedure used in the previous case (see eqn. (29)). The derivation of the desired integral equation also follows the same lines, using the same parameters in the transformation (eqns. (32)–(34)). The final result is:

$$\begin{aligned} (1-e^{-x}) \left(1 + 2 \sum_{i=1}^{\infty} \operatorname{erfc} i \sqrt{\frac{H}{x+K}} \right) - \frac{e^{-x}}{\psi\sqrt{\pi}} \int_0^x \frac{\Phi(\xi)}{\sqrt{x-\xi}} d\xi = \\ \frac{1}{\sqrt{\pi}} \int_0^x \frac{\Phi(\xi)}{\sqrt{x-\xi}} d\xi + \frac{2}{\sqrt{\pi}} \sum_{i=1}^{\infty} \int_0^x \frac{\Phi(\xi)}{\sqrt{x-\xi}} \exp\left[\frac{-i^2H}{x-\xi}\right] d\xi. \end{aligned} \quad (61)$$

This equation has the same form as eqn. (6) of ref. 6, except for the factor $Q(\sqrt{G/\lambda})$ in the first left-hand side term:

$$Q(\sqrt{G/\lambda}) = 1 + 2 \sum_{i=1}^{\infty} \operatorname{erfc} i \sqrt{G/\lambda}. \quad (62)$$

The parameter $K=\sigma\tau$ can be eliminated from eqn. (61) by an analogous reasoning to that in the previous case; then

$$K - \ln \psi = \text{constant}. \quad (63)$$

(c) *The function $Q(\sqrt{G/\lambda})$, defined by eqn. (62)*

The Laplace-transform of $Q(\sqrt{G/\lambda})$ is

$$\mathcal{L}\left\{Q\left(\sqrt{\frac{G}{\lambda}}\right)\right\} = \frac{1}{s} \frac{\exp[2\sqrt{Gs}] + 1}{\exp[2\sqrt{Gs}] - 1}, \quad (64)$$

and the second fraction in the right-hand side of eqn. (64) is written as

$$\frac{e^u + 1}{e^u - 1} = 1 + 2e^{-u} \frac{e^u}{e^u - 1} = 1 + e^{-u} \left(\frac{2}{u} + 1 + \frac{u}{6} - \frac{u^3}{360} + \frac{u^5}{15120} \right). \quad (65)$$

Putting $u = 2\sqrt{G}z$, combining eqns. (64) and (65), and back-transforming the resulting expression gives an approximation for small values of $z = \sqrt{G/\lambda}$:

$$Q(z) = 1 - \operatorname{erfc} z + \frac{\exp(-z^2)}{\sqrt{\pi}} \left(\frac{2}{z} + \frac{z}{3} + \frac{z^3}{90} - \frac{13}{630} z^5 \right) \quad (66)$$

For very small values of z :

$$Q(z) = 2/z\sqrt{\pi}. \quad (67)$$

In Table 3, the approximations (66) and (67) are compared to the exact equation (62). Figure 5 shows $Q(z)$ for $0 < z < 1.6$.

TABLE 3

COMPARISON OF THE APPROXIMATIONS (66) AND (67) FOR $Q(z)$ WITH THE EXACT EQUATION (62); $z = \sqrt{G/\lambda}$

z	ΔQ (%) <i>eqn. (66)</i>	ΔQ (%) <i>eqn. (67)</i>
0.05		-0.04
0.1	-0.12×10^{-4}	-0.19
0.2	-0.18×10^{-4}	-0.66
0.4	1.5×10^{-4}	-2.61

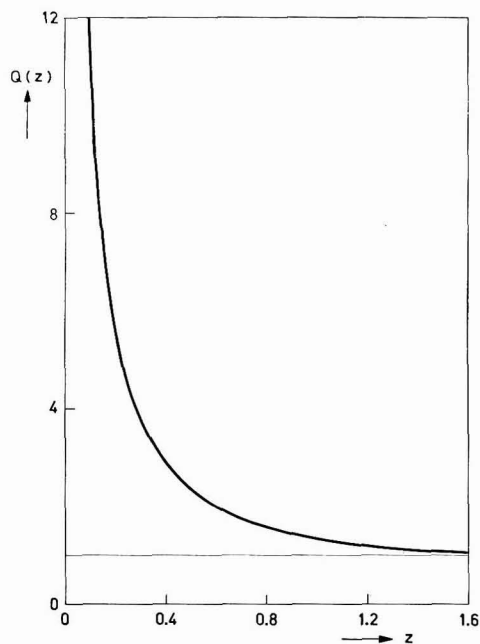


Fig. 5. The function $Q(z)$, with $z = \sqrt{G/\lambda}$, as defined by eqn. (62).

(d) Numerical calculations and results

The numerical calculations of the re-reduction current-potential curves have been carried out by the method of HUBER. $Q(z)$ was calculated by eqn. (66) for $z < 0.4$, while eqn. (62) was used for larger values of z .

The results have been summarized in Fig. 6. In each of the nine figures, the thinly-drawn lowest curve is obtained on direct reduction of O, starting the linear potential sweep at a positive potential. The middle curve is obtained on application of a potential step towards $n(E_1 - E_2) = -250$ mV and immediately starting the linear potential sweep back towards positive potentials. For the highest curve, $n(E_1 - E_2) = -500$ mV. The large number in the figures again denotes the value of $H = l^2\sigma/D_R$. With decreasing H , the re-oxidation peaks become higher and their width decreases.

It might be expected that decreasing the value of H , which can be interpreted as decreasing the value of σ and thus allowing more time for the reduction of metal (leading to a higher concentration in the mercury film), would result in an increase

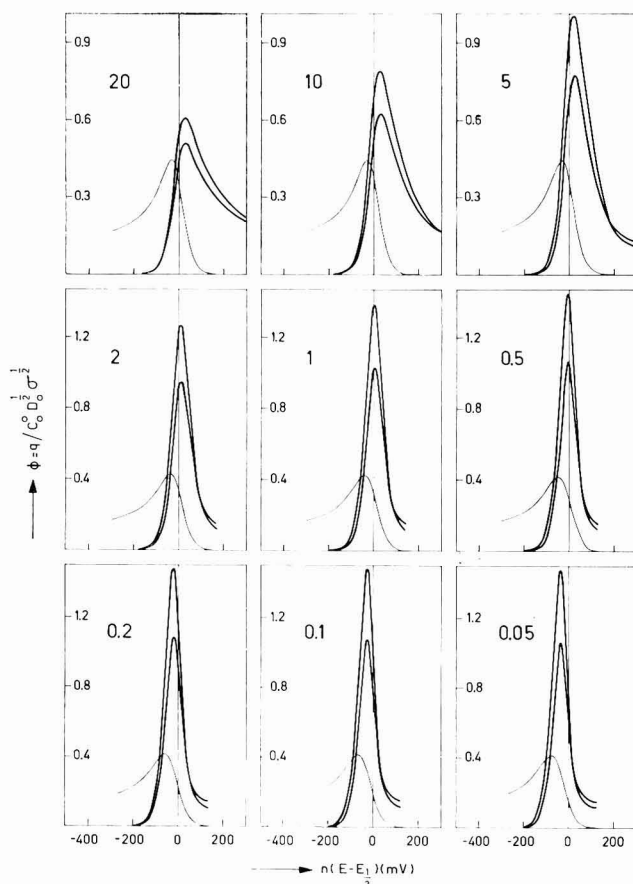


Fig. 6. Re-oxidation current-potential curves obtained during an oxidizing linear potential sweep, for several values of $H = l^2\sigma/D_R$. For explanation see text.

of the height of the (dimensionless) re-oxidation current peak. This is not the case for smaller values of H , as can be seen from Fig. 6. The explanation of this behaviour can be found in the properties of the oxidation current peak obtained with a very thin mercury-film electrode⁶. The height of the peak is proportional to the total amount of metal in the film, lC_R , and to the rate of potential change, σ . Thus, changing H by altering the film thickness leaves lC_R unaltered. When σ is changed, the amount of metal reduced after application of the potential step also changes, being proportional to $\sigma^{-\frac{1}{2}}$ (current is proportional to $t^{-\frac{1}{2}}$). The flux is thus proportional to $\sigma \cdot \sigma^{-\frac{1}{2}} = \sigma^{\frac{1}{2}}$, and the dimensionless flux is independent of σ . Thus, for low values of H , an increase in the dimensionless re-oxidation peak can only be achieved by decreasing the value of ψ .

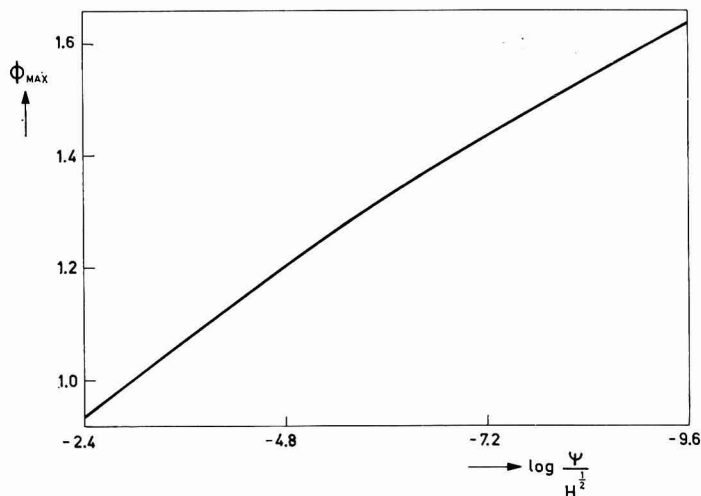


Fig. 7. Maximum value of $\Phi(x)$ for $H \rightarrow 0$, Φ_{max} , as defined by eqn. (68), plotted vs. $\log(\psi/H^{\frac{1}{2}})$.

TABLE 4

PARAMETERS OF $\Phi(x)$, FOR $H \rightarrow 0$, AS DEFINED BY EQN. (68), FOR SEVERAL VALUES OF $H^{\frac{1}{2}}/\psi$; c IS THE CONSTANT OCCURRING IN EQN. (70)

$H^{\frac{1}{2}}/\psi$	Φ_{max}	c (mV)	nb_1 (mV)
250	0.933	5.3	81.9
4,000	1.074	3.3	80.6
64,000	1.206	2.1	78.9
1,024,000	1.326	1.5	78.2
16,384,000	1.437	1.0	77.8
262,144,000	1.541	0.7	77.4

(e) Limiting case for $H \rightarrow 0$

The integral equation describing the re-oxidation current peak for very small values of H can readily be found by simplifying the right-hand side of eqn. (61) in the usual way, and using eqn. (67):

$$2\left(\frac{x}{\pi}\right)^{\frac{1}{2}}(1 - e^{-x}) - \frac{H^{\frac{1}{2}}}{\psi} \frac{e^{-x}}{\pi^{\frac{1}{2}}} \int_0^x \frac{\Phi(\xi)}{\sqrt{x-\xi}} d\xi = \int_0^x \Phi(\xi) d\xi, \quad (68)$$

$\Phi(x)$ depends only on the value of $H^{1/2}/\psi$ when H approaches zero. The maximum value of $\Phi(x)$, Φ_{\max} , is plotted *vs.* $\log(\psi/H^{1/2})$ in Fig. 7. The gradual increase of Φ_{\max} with decreasing $\psi/H^{1/2}$ reflects the influence of a longer time during which reduction takes place. At 25°:

$$i_p = 6.020 \times 10^5 \Phi_{\max} n^{3/2} A C_0^{1/2} D_0^{1/2} v^{1/2} \text{ amp}, \quad (69)$$

while the relationship

$$n(E_p - E_{1/2}) = c + 29.580 \log H \text{ mV} \quad (70)$$

is also nearly fulfilled, as can be seen from Table 4, where several parameters of $\Phi(x)$ are given for some values of $\psi/H^{1/2}$.

(f) Discussion

The method described has not yet found analytical application. Although a (modest) increase in sensitivity is obtained, and adjacent peaks can be better resolved, any practical application would be very limited in scope (*e.g.*, the determination of Cd, Tl, Pb, Cu). This technique could, however, be useful for elucidating the nature of the electrode reactions occurring at a mercury-film electrode. The linear-sweep voltammetric experiments reported by DE VRIES¹³, PERONE AND DAVENPORT¹⁴ and PERONE AND BRUMFIELD¹⁵, show a poor quantitative agreement between theory and experiment, and this shows that many reactions regarded as reversible do not take place as such at a mercury-film electrode. In the case of a metal-based mercury-film electrode (*e.g.*, on Ni, Ag, Au, Pt), formation of intermetallic compounds could come into play, although this is certainly not the only factor causing deviations from reversibility¹³. If the formation of an intermetallic compound is a slow process, its presence or absence could be easily detected using the technique of a reducing potential step followed by an oxidizing linear potential sweep, by varying the time-scale over which the experiment is carried out.

ACKNOWLEDGEMENTS

The greater part of this work was supported financially by The Netherlands Organization for the Advancement of Pure Research (Z.W.O.). The Mathematical Centre, Amsterdam, donated computer time for the numerical calculations and the co-operation of the staff of the Computational Department proved most helpful. Finally, the author wishes to acknowledge the active interest in this work of Prof. M. ARIEL and Prof. E. VAN DALEN.

SUMMARY

A theoretical treatment is given of constant-potential electrolysis followed by linear potential-sweep voltammetry at a mercury-film electrode. The case of an oxidizing potential step followed by reduction with a linear sweep is considered, as well as that of a reducing potential step followed by oxidation with a linear sweep. The analytical aspects of the results are discussed. The effect of initial and boundary conditions on the continuity of the current-potential curve at the start of the potential sweep is considered.

REFERENCES

- 1 W. T. DE VRIES, *J. Electroanal. Chem.*, 14 (1967) 75.
- 2 CH. YARNITSKY AND M. ARIEL, *ibid.*, 10 (1965) 110.
- 3 W. T. DE VRIES AND E. VAN DALEN, *ibid.*, 8 (1964) 366.
- 4 W. T. DE VRIES, *ibid.*, 9 (1965) 448.
- 5 H. S. CARSLAW AND J. C. JAEGER, *Conduction of Heat in Solids*, Clarendon Press, Oxford, 2nd ed., 1959, pp. 100, 101.
- 6 W. T. DE VRIES AND E. VAN DALEN, *J. Electroanal. Chem.*, 14 (1967) 315.
- 7 P. DELAHAY, *New Instrumental Methods in Electrochemistry*, Interscience, New York, 1954, p. 116.
- 8 R. S. NICHOLSON AND I. SHAIN, *Anal. Chem.*, 36 (1964) 706.
- 9 S. P. PERONE AND T. R. MUELLER, *ibid.*, 37 (1965) 2.
- 10 *Tables of Integral Transforms*, edited by A. ERDÉLYI, Vol. I, McGraw Hill, New York, 1954, pp. 246, 369.
- 11 W. H. REINMUTH, *J. Am. Chem. Soc.*, 79 (1957) 6358.
- 12 S. P. PERONE AND J. R. BIRK, *Anal. Chem.*, 37 (1965) 9.
- 13 W. T. DE VRIES, Dissertation, Free University, Amsterdam, 1967.
- 14 S. P. PERONE AND K. K. DAVENPORT, *J. Electroanal. Chem.*, 12 (1966) 269.
- 15 S. P. PERONE AND A. BRUMFIELD, *ibid.*, 13 (1967) 124.

J. Electroanal. Chem., 16 (1968) 295-312

INTERACTION OF POLYPHOSPHATE WITH THE MERCURY ELECTRODE SURFACE

VLADIMÍR VETTERL AND JIŘÍ BOHÁČEK

Institute of Biophysics, Czechoslovak Academy of Sciences, Brno (Czechoslovakia)

(Received May 15th, 1967; in revised form; July 20th, 1967)

INTRODUCTION

During a study of the behaviour of polyphosphates on the mercury dropping electrode by the method of oscillographic polarography with alternating current¹, it has been found that, in an acidic medium, an indentation of a capacitive character is produced on the oscillogram. The capacitive indentations correspond approximately to the desorption maxima on the differential capacity curves^{2,3}. In the present paper the capacity curves of polyphosphate solutions and their changes after the addition of neutral salts are discussed. Measurement of the differential capacity is tedious, but analogous results can be obtained with the aid of a.c. polarography⁴. The a.c. polarograms follow the same trend as the capacity curves^{5,6}. A.c. polarography was used for indicating the changes taking place in polyphosphate solution, caused through spontaneous hydrolytic degradation of the polyphosphate macromolecule.

EXPERIMENTAL

The polyphosphate solution was prepared by dissolving sodium polyphosphates (from Dr. U. P. STRAUSS, U.S.A.) having a mean molecular weight of 14,500, in distilled water and diluting with the respective electrolyte.

The differential capacity was measured by the classical bridge method⁷ with the aid of a low-frequency Schering bridge Tesla TM 351^{8,9}, using a frequency of 1000 c/sec and an alternating voltage amplitude of 10 mV. The measurements were performed with a mercury dropping electrode, flow rate $m = 0.262$ mg/sec, drop-time $t = 6.0$ sec, unless otherwise stated.

The a.c. polarograms were obtained with a GWP 563 polarograph (Akademie-Werkstätten für Forschungsbedarf der DAW, Berlin-Adlershof, Germany)¹⁰ working with a frequency of 78 c/sec and an amplitude of 10 mV. D.c. polarograms were also obtained with the same instrument. The a.c. polarograms were obtained at a sensitivity of 10 μ A and damping 7, and the d.c. polarograms at a sensitivity of 2.5 μ A and damping 2. A mercury dropping electrode having a flow rate of $m = 3.31$ mg/sec and a drop-time $t = 4.0$ sec was used for polarographic measurements.

A Novák's vessel¹¹ with a nitrogen atmosphere was used for differential capacity and polarographic measurements. The potential of the mercury electrode was measured with reference to the mercury pool at 25°.

RESULTS AND DISCUSSION

The capacity curves of solutions containing 5 mg/ml polyphosphate in 0.5 *M* sodium acetate, 1.0 *M* sodium acetate, and 0.5 *M* citric acid were established. A maximum appeared on the curves at a potential of approximately -0.6 V. This maximum was most pronounced when 0.5 *M* citric acid, pH 2.4, was used as supporting electrolyte, with drop-time 6 sec (Fig. 1).

The a.c. polarograms of a solution containing 1 mg/ml polyphosphate in 0.5 *M* citric acid (Fig. 2) follow a similar course to the capacity curves.

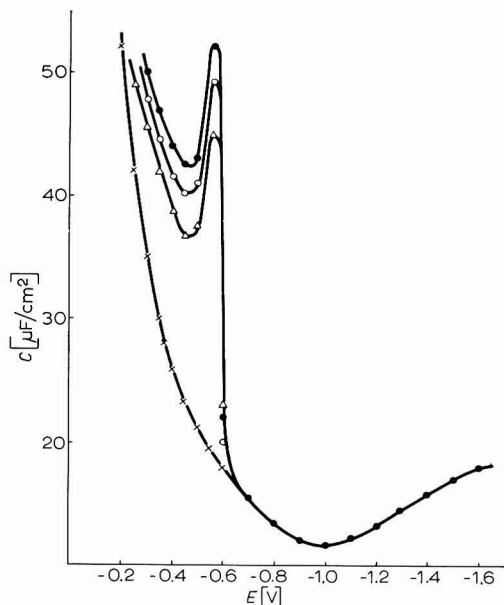


Fig. 1. Capacity curves of soln. of 5 mg/ml polyphosphate in 0.5 *M* citric acid, $m = 0.262$ mg/sec. (x), supporting electrolyte; (Δ), $t = 3.7$ sec; (\bullet), $t = 6.0$ sec; (\circ), $t = 9.7$ sec; 13.4 sec.

No polarographic waves appeared on the d.c. polarograms of 0.5 *M* citric acid and of a solution of polyphosphate in 0.5 *M* citric acid (Fig. 3) in the potential range -0.2 to -1.2 V. The polarograms were almost linear, a break appearing on the polyphosphate polarogram only at a potential of -0.6 V. Under the given conditions, the solutions tested are thus polarographically inactive and the maximum arising on the capacity curves and a.c. polarograms at a potential of -0.6 V is apparently of a capacitive character and arises through an adsorption-desorption process. Polyphosphate is adsorbed on the electrode surface at potentials more positive than -0.6 V and at potentials more negative than -0.6 V is desorbed from the electrode surface (the a.c. polarograms and capacity curves of polyphosphate merge with the curves of pure supporting electrolyte). In the adsorption of polyphosphate, electrostatic forces act between the positive charge of the electrode and the negative charge of the polyphosphate (irrespective of the acidic medium, polyphosphate is at least partly dissociated and/or dissociation takes place on the positively charged electrode surface by induced ionization¹²).

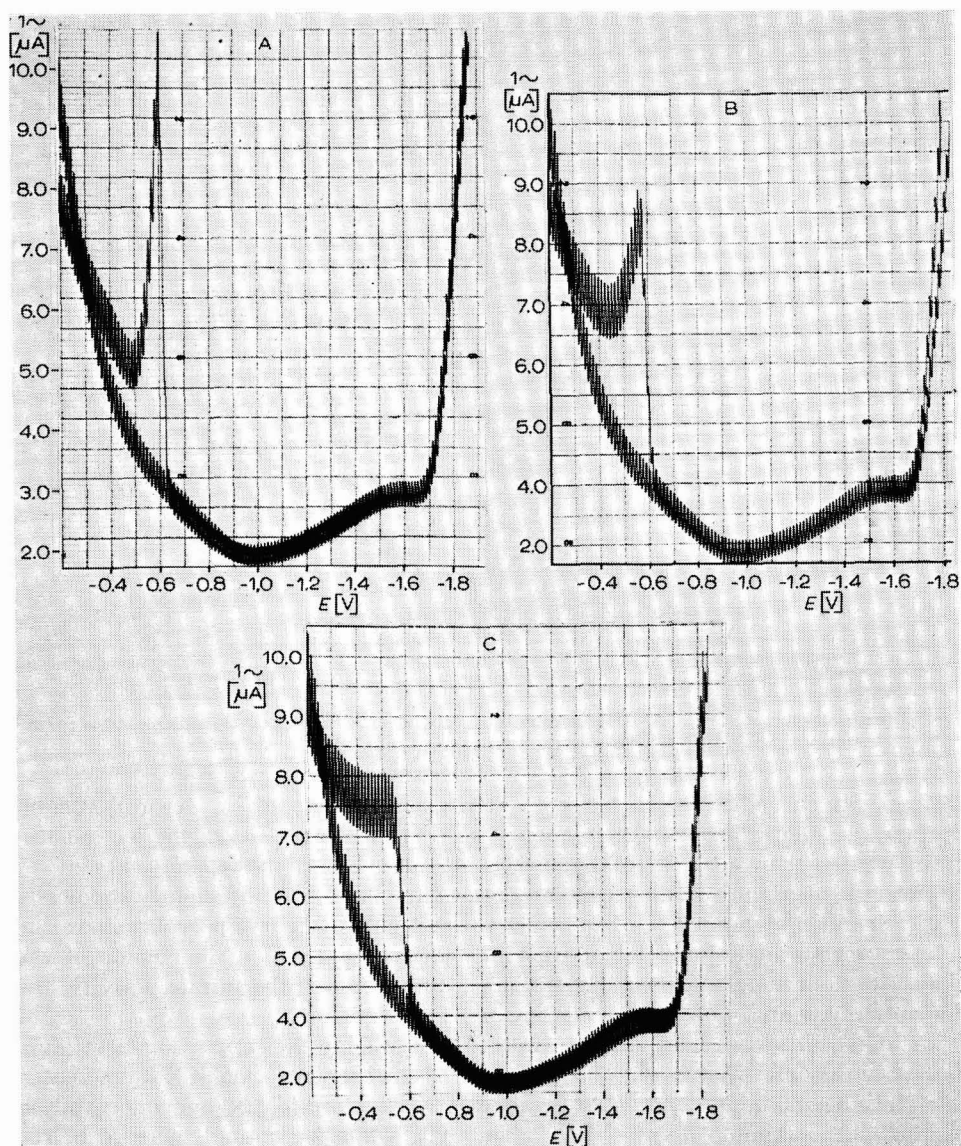


Fig. 2. A.c. polarogram for 0.5 *M* citric acid and 0.5 *M* citric acid containing 1 mg/ml polyphosphate. Sensitivity, 10 μ A; damping, 7; amplitude, 10 mV; frequency, 78 c/sec, sweep rate of potential, 0.2 V/min. After (a) 0 h, (b) 24 h, (c) 48 h.

The potential of the maximum corresponds to the potential of the indentation observed on the oscillograms of polyphosphate solutions¹. Our results support the conclusion that this indentation is of a capacitive character. The maximum of the a.c. polarogram (Fig. 2) is essentially higher than that of the capacity curve (Fig. 1), although the concentration of polyphosphate was one-fifth of that used for

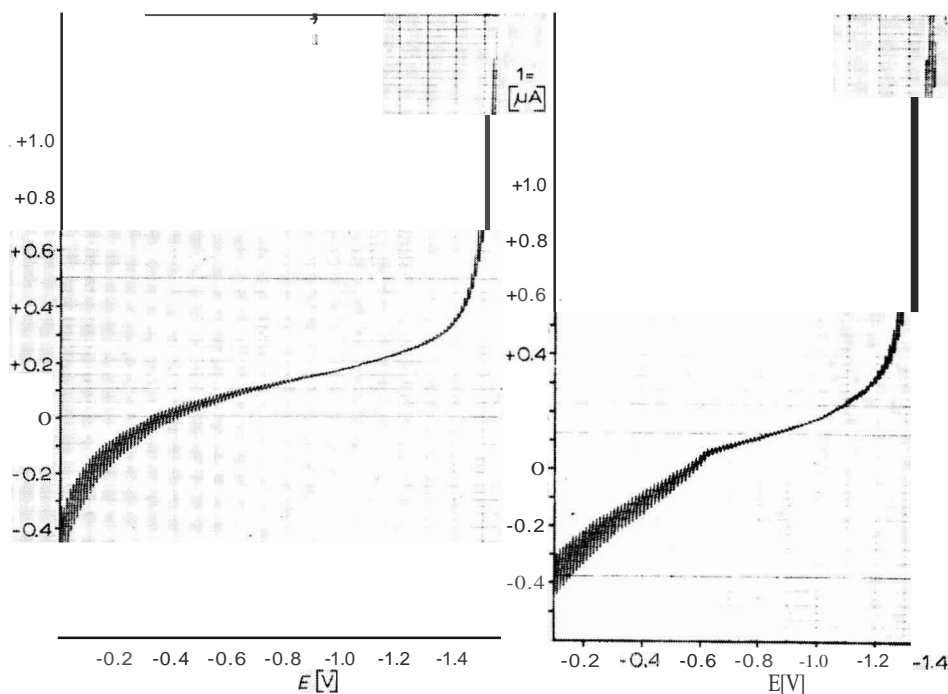


Fig. 3. D.c. polarogram for 0.5 *M* citric acid. Sensitivity, 2.5 μA ; clamping, 2; sweep rate of potential, 0.2 V/min. (a) without, (b) with 1 mg/ml polyphosphate.

the capacity curve because in order to attain a better adsorption-desorption equilibrium, the alternating voltage frequency used in measurements of the a.c. polarograms was less than one-tenth of that used in measurements of the capacity curves^{12,13}. In time, the maximum on the a.c. polarograms diminishes, shifting slightly anodically (Figs. 2b and c) because of the decrease of the molecular weight of polyphosphate due to spontaneous hydrolytic degradation of the macromolecules. Shortening of the chain-length of molecules usually results in a diminution of the surface activity, the desorption maxima subsequently decreasing^{4,14,15}.

The addition of neutral salts, NaCl, KCl, CaCl_2 , to the supporting electrolyte decreased the desorption maximum, Figs. 4-6. If the concentration of NaCl increased five-fold, the maximum diminished by about 5%. At a five-fold higher concentration of KCl, the maximum decreased by about 9%, while a two-fold increase in the concentration of CaCl_2 lowered the maximum by about 23%. This shows that the ability of ions to suppress the maximum increases in the order $\text{Na}^+ < \text{K}^+ < \text{Ca}^{2+}$. The cations form a counter-ion atmosphere around the central polyanion, screen the charges of the dissociated phosphate groups of polyphosphate and thus reduce the ability of polyphosphate to adsorb electrostatically. Na^+ ions seem to be most loosely bound to the polyphosphate; the electric field in the neighbourhood of the electrode may easily repel Na^+ ions from the phosphate groups. Ca^{2+} ions are most strongly bound and are thus the most efficient in hindering the adsorption of polyphosphate. The intensity of the interaction of Na^+ , K^+ , and Ca^{2+} ions with poly-

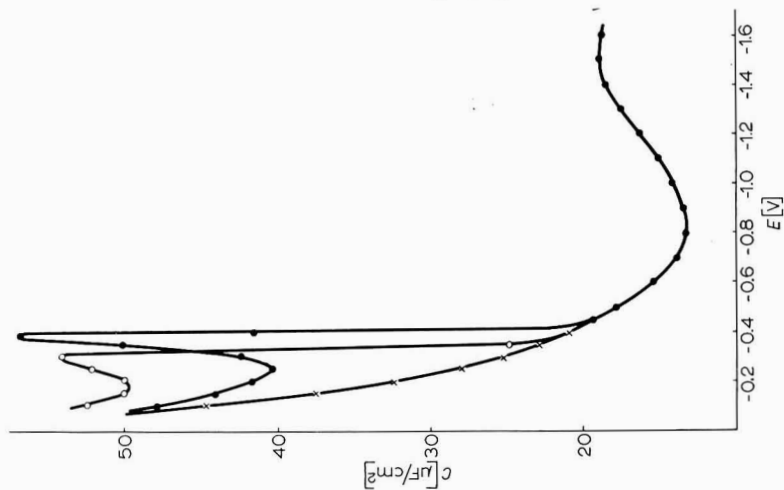


Fig. 4. Effect of addition of NaCl on polyphosphate capacity curve, $t = 6.0$ sec, $m = 0.262$ mg/sec. (×), supporting electrolyte $0.5 M$ citric acid + $0.01 M$ NaCl; (○), 5 mg/ml polyphosphate + $0.5 M$ citric acid + $0.01 M$ NaCl.

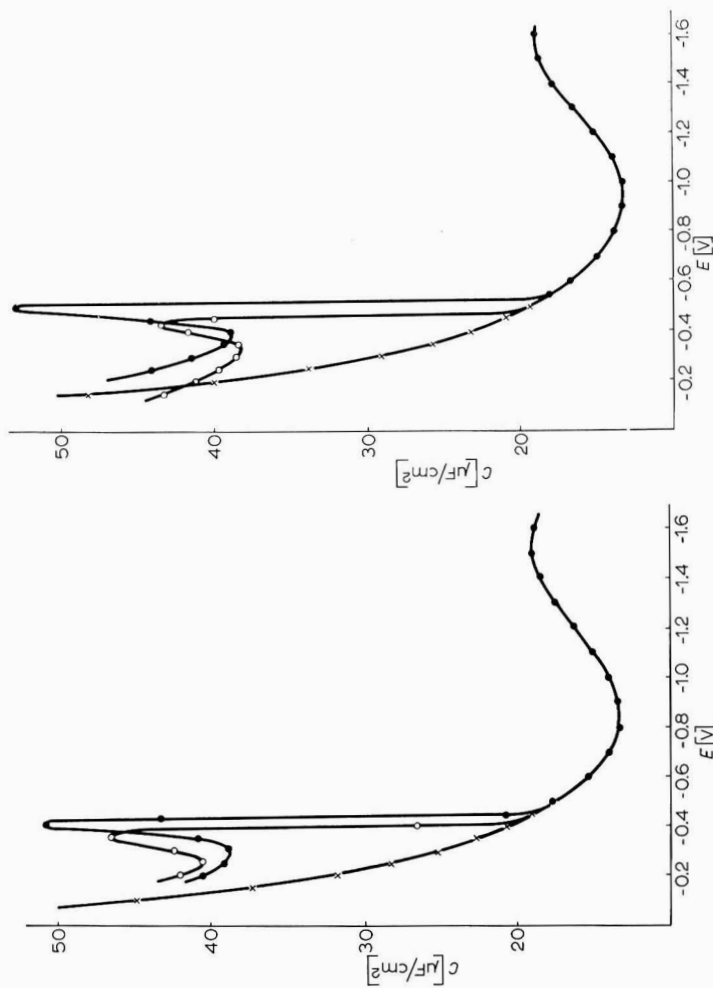


Fig. 5. Effect of KCl ions on polyphosphate capacity curve, $t = 6.0$ sec, $m = 0.262$ mg/sec. (×), supporting electrolyte $0.5 M$ citric acid + $0.005 M$ KCl; (○), 5 mg/ml polyphosphate + $0.5 M$ citric acid + $0.025 M$ KCl.

Fig. 6. Effect of CaCl_2 ions on polyphosphate capacity curve, $t = 6.0$ sec, $m = 0.262$ mg/sec. (×), supporting electrolyte $0.5 M$ citric acid + $0.0005 M$ CaCl_2 ; (●), 5 mg/ml polyphosphate + $0.5 M$ citric acid + $0.0005 M$ CaCl_2 ; (○), 5 mg/ml polyphosphate + $0.5 M$ citric acid + $0.001 M$ CaCl_2 .

phosphate increases in the same order as the intensity of the interaction of these ions with alginic acid^{16,18}. The differences in the coupling of Na⁺ and K⁺ ions to the polyanion are explained by the different radii of the hydrated Na⁺ and K⁺ ions¹⁹. The strong coupling of bivalent ions to the polyions is explained by the specific association of ions with the polymeric chain and with formation of neutral ion pairs^{16,17}.

A similar effect to that produced by the cations of neutral salts is obtained with the cations of bases, and the adsorption of polyphosphate in an alkaline medium is therefore, suppressed (no indentations appear on the oscillogram of polyphosphate solutions in an alkaline medium¹).

ACKNOWLEDGEMENTS

The helpful and critical interest of Professor J. KORYTA and Dr. L. NĚMEC of the Heyrovský Institute of Polarography is gratefully acknowledged. Thanks are also due to Dr. V. KLEINWÄCHTER and Dr. E. PALEČEK for their many pertinent comments and review of the manuscript before its submission for publication.

SUMMARY

Measurements of the differential capacity of the mercury dropping electrode and d.c. and a.c. polarograms of polyphosphate solutions in an acidic medium have been recorded. A comparison of the capacity curves with the a.c. and d.c. polarograms shows that the maximum arising on the capacity curves and the a.c. polarograms at a potential of -0.6 V is of a capacitive character and is due to desorption of polyphosphate from the negatively-charged electrode surface. Polyphosphate is adsorbed on the electrode primarily through electrostatic forces. The cations of the neutral salts, NaCl, KCl, CaCl₂ screen the charges of the phosphate groups of polyphosphate and suppress adsorption with subsequent decrease of the desorption maximum. The ability of cations to suppress the maximum increases in the order Na⁺ < K⁺ < Ca²⁺. In time, degradation of the macromolecules takes place in the phosphate solution in an acidic medium, and the desorption maximum decreases.

REFERENCES

- 1 J. BOHÁČEK AND CH. SINGH, *J. Electroanal. Chem.*, 7 (1964) 222.
- 2 R. KALVODA, *Z. Anal. Chem.*, 224 (1967) 143.
- 3 R. KALVODA AND A. VAŠKELIS, *Collection Czech. Chem. Commun.*, 32 (1967) 2206.
- 4 B. BREYER AND H. H. BAUER, *Alternating Current Polarography and Tensammetry*, Interscience Publishers, John Wiley, New York, 1963.
- 5 H. JEHRING, *Chem. Zvesti*, 18 (1964) 313.
- 6 V. VETTERL, *Abhandl. Deut. Akad. Wiss. (Berlin) Ser. Kl. Med.*, (1966) 493.
- 7 D. C. GRAHAME, *J. Am. Chem. Soc.*, 63 (1941) 1207.
- 8 V. VETTERL, *Slaboproudý Obzor*, 25 (1964) 346.
- 9 V. VETTERL, *Collection Czech. Chem. Commun.*, 31 (1966) 2105.
- 10 W. SKALWEIT AND H. JEHRING, *Chem. Tech. (Berlin)*, 16 (1964) 290.
- 11 J. V. A. NOVÁK, *Collection Czech. Chem. Commun.*, 12 (1947) 237.
- 12 I. R. MILLER AND D. C. GRAHAME, *J. Am. Chem. Soc.*, 78 (1956) 3577.
- 13 I. R. MILLER AND D. C. GRAHAME, *J. Am. Chem. Soc.*, 79 (1957) 3006.
- 14 V. I. MELIK-GAIKAZYAN, *Zh. Fiz. Khim.*, 26 (1952) 560.
- 15 V. D. BEZUGLYI AND E. K. SALICHUK, *Dokl. Akad. Nauk SSSR*, 158 (1964) 1390.
- 16 A. KATCHALSKY, *Biophys. J.*, 4 (1964) No. 1, part 2, 9.
- 17 F. E. HARRIS AND S. A. RICE, *J. Phys. Chem.*, 58 (1954) 725, 733.
- 18 A. KATCHALSKY, R. E. COOPER, J. UPADHAY AND A. WASSERMAN, *J. Chem. Soc.*, (1961) 5198.
- 19 I. KAGAWA AND H. P. GREGOR, *J. Polymer. Sci.*, 23 (1956) 477.

UNDERVOLTAGE EFFECTS IN THE DETERMINATION OF SILVER BY SCANNING COULOMETRY

R. C. PROBST

Savannah River Laboratory, E. I. du Pont de Nemours and Co., Aiken, S. C. 29801 (U.S.A.)

(Received May 23rd, 1967)

INTRODUCTION

The electrodeposition behaviour of a metal ion at an inert electrode in quantities insufficient to form a monolayer at the electrode surface cannot be described by the abridged form of the Nernst equation¹. In most instances, curves relating the amount of the ion deposited to the potential of the electrode, exhibit one or more steps which are considerably more anodic than the step described by the abridged form of the Nernst equation. This phenomenon, referred to as an undervoltage effect, has been extensively investigated by ROGERS and co-workers²⁻⁷, and has been attributed to:

- (i) variations in the activity of the deposit with fractional surface coverage⁷;
- (ii) the nature of the inert electrode and the state of its surface including adsorption effects³;
- (iii) intermetallic bonding⁶.

Undervoltage effects have largely been ignored in controlled-potential coulometric titration procedures involving the deposition and stripping of metals at inert electrodes. This action is justified when the amount of metal ion involved in the formation of a surface monolayer at the inert electrode is a negligible fraction of the total amount titrated. However, when microgram quantities are deposited at, or stripped from an inert electrode, the amount involved in monolayer formation is significant and the deposition and stripping potentials must be selected with care. Almost no quantitative information is available on this effect, and the correct potentials for titrating microgram quantities of a particular metal ion must be determined by experiment.

The technique of scanning coulometry⁸ should be ideally suited for the determination of trace metals in solution. The recorded coulogram is essentially a pictorial display of the reactions at the working electrode; the deposition potentials and the amount of substance deposited can be obtained directly from the coulogram. In view of the importance of primary coulometric methods, a study was made of the quantitative deposition of trace metals at the gold electrode by scanning coulometry. Silver was selected for study because this metal is known to exhibit undervoltage effects, and radioactive ¹¹⁰Ag is readily available for tracer studies.

EXPERIMENTAL

Apparatus

The scanning coulometer is described in an earlier paper⁸. The instrument was used in both the controlled potential and scanning modes. For electrolysis at controlled potential, the titration was initiated at the equilibrium potential of the electrode with respect to the solution. The potential was then advanced manually to the desired electrolysis potential to prevent amplifier overload. The background compensation circuits were not used.

In tracer experiments, radioactive gamma activity was monitored with a 4-in. NaI(Tl) crystal detector and conventional counting equipment.

Cell and electrodes

The cells described in an earlier paper⁸ were fitted with side arms to permit the addition of aliquots of the silver solution. The 1-in.-diameter, cylindrical gold electrodes were fabricated from 20 mil 99.95% gold foil (Handy and Harman, Inc.) with a total surface area of approximately 36 cm²; an $\sim \frac{1}{4}$ -in. gap was left in the side of the cylinder. The edges of the gap were offset $\sim \frac{1}{8}$ in. along the diameter (in the direction of rotation of the stirring bar) to provide for free circulation of the solution on both sides of the foil.

The mercury-mercurous sulfate (1 M sulfuric acid) electrode, MSE, used in this study had a potential of $+0.418 \pm 0.003$ V *vs.* the saturated calomel electrode.

Reagents

All chemicals were reagent-grade and were used without further purification. The distilled water was deionized to remove copper.

Stock solutions of silver were prepared by dissolving weighed amounts of silver nitrate in 1 M nitric acid. Standard solutions, 100–150 μ g of silver/ml, were prepared by diluting the stock solution with 1 M perchloric acid. The resulting solutions were sufficiently concentrated, $\sim 10^{-3}$ M, so that adsorption on the walls of the container was minimal. However, to minimize further loss with time, the solutions were stored in polyethylene bottles and fresh dilutions were prepared periodically.

The ^{110m}Ag solution for the tracer studies was purchased from the Isotopes Division of the Oak Ridge National Laboratory. This solution contained 0.4 mg of carrier silver/ml in 0.6 M nitric acid; the specific activity was 3.95 ± 0.4 mcuries/ml.

All solutions were sparged continuously throughout the titration with helium. The helium had previously been bubbled through distilled water to minimize evaporation from the cell.

Background coulograms and electrode conditioning

Scans of the electrolyte solution were recorded before each titration to provide a convenient means of correcting for the background quantity of electricity and to ensure that no residual silver remained from previous titrations. The cell and electrodes were thoroughly rinsed with deionized water, 10 ml of 1 M perchloric acid was added to the cell, and the solution was then electrolyzed at controlled potential at +0.6, -0.65 and +0.6 V. The electrolysis was continued at each potential until the current had decayed to a steady value. In this study, the current at +0.6 V reached a

steady value of $\sim 1.5 \mu\text{A}$ after about 10 min. The current at -0.65 V was quite high due to the evolution of hydrogen; however, an electrolysis time of 10 min was usually sufficient for complete removal of silver. A background scan was then recorded from $+0.6$ to -0.4 V ; if traces of silver were evident, the solution was again electrolyzed at -0.65 V and then at $+0.6 \text{ V}$ to remove the silver completely from the electrode⁹. The solution was then discarded, and the procedure repeated with a fresh aliquot of 1 M perchloric acid.

Titration by automatic scanning

Upon completion of a background scan, the electrolyte solution was electrolyzed at controlled potential at $+0.6 \text{ V}$ until the background current decayed to a steady value, as before. An aliquot of the silver solution was added, and the coulomb-potential curve was recorded automatically from the equilibrium potential of the electrode to -0.4 V . After the titration, the solution was electrolyzed at -0.65 V and $+0.6 \text{ V}$ and discarded.

The cell was filled with 1 M nitric acid when not in use.

Titration by manual scanning

The procedure for stepwise titrations at a series of potentials was identical with that described above except that the scan rate control was turned to "zero" and the electrolysis potential was advanced manually in 20-mV increments. The electrolysis current was allowed to decay to a steady value at each potential. Thus these titrations were effected under nearly equilibrium conditions.

For stepwise titrations of $^{110\text{m}}\text{Ag}$ solutions, the potential was advanced in 50-mV increments and $25\text{-}\mu\text{l}$ aliquots of the solution were removed at each step and counted for gamma activity. The amount of silver deposited was then calculated as the difference between the gamma activity of the aliquot added to the titration cell, and the gamma activity of the solution at the potential corresponding to each step.

RESULTS

In the initial phase of this study, coulograms (coulomb-potential curves) for the electrodeposition of silver at the gold electrode from 0.1 M perchloric acid were recorded for comparison with similar curves published by GRIESS *et al.*² for the electrodeposition of silver at hammer-forged gold and gold-foil electrodes. The observed electrodeposition behaviour followed a pattern similar to that reported by these authors.

Coulograms recorded in this study (Fig. 1) for the electrodeposition of silver show three waves due to undervoltage effects. The fourth wave ($E_{\frac{1}{2}} = -0.2 \text{ V}$) corresponds to the reduction of silver at its standard potential. The half-wave potentials for the first three waves ($E_{\frac{1}{2}} = +0.55, +0.4$ and $+0.05 \text{ V}$) were essentially independent of concentration, while GRIESS's curves were concentration dependent. Almost identical deposition curves were obtained in 1 M solutions of nitric, sulfuric and perchloric acids. The individual curves were reproducible to $\pm 10^{-4} \text{ C}$. The exclusion of light from the titration cell had no apparent effect.

The reversibility of the deposition process was demonstrated by recording a coulogram for the stripping process under nearly equilibrium conditions. This

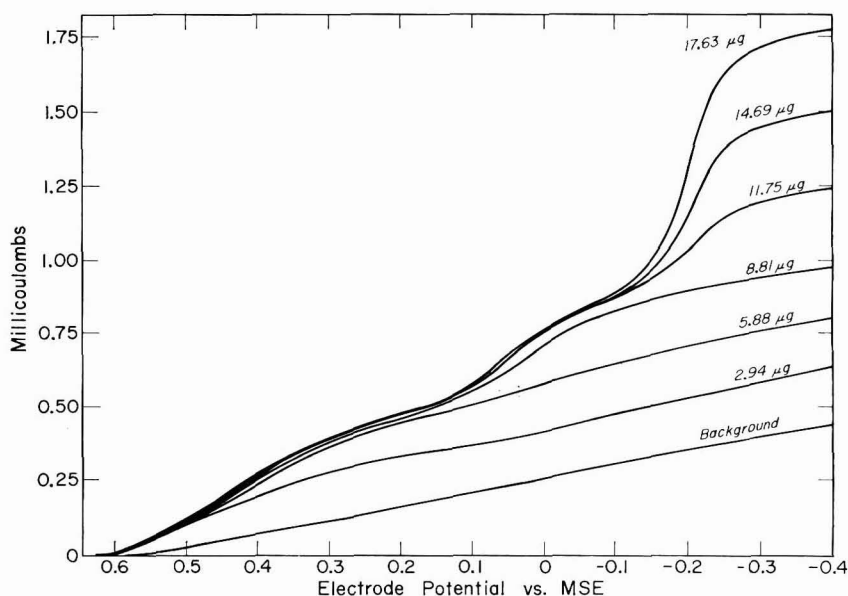


Fig. 1. Coulograms showing the electrodeposition behaviour of silver. 36 cm^2 Au-electrode; $M \text{ HClO}_4$ electrolyte.

coulogram exhibited three well-defined waves with half-wave potentials of $+0.4$, $+0.05$ and -0.2 V . The wave, $E_{\frac{1}{2}} = +0.55 \text{ V}$, was not detected since this small wave merged with the wave produced by the dissolution of gold at $+0.6 \text{ V}$. In similar experiments, in which curves for the stripping process were recorded by scanning coulometry, three waves were also produced; however, the waves corresponding to undervoltage effects were not well defined, and the half-wave potentials for these waves were dependent on the scan rate of the instrument. Coulograms of the dissolution process are, therefore, not useful for quantitative analysis.

Confirmatory evidence for the deposition of silver from $+0.6$ to -0.5 V was obtained by titrating the $^{110\text{m}}\text{Ag}$ solution under nearly equilibrium conditions and by scanning coulometry. Curves for the percentage of radioactivity deposited *vs.* potential exhibited waves at potentials identical with those shown in Fig. 1.

The half-wave potentials and slopes for the waves attributed to undervoltage effects were calculated by means of the modified form of the Nernst equation derived by ROGERS AND STEHNEY⁷, and the wave, $E_{\frac{1}{2}} = -0.2 \text{ V}$, was analyzed by means of the Nernst equation for the deposition of a metal ion at a surface of similar atoms.

The first undervoltage process for the deposition of silver occurs in the potential range from $+0.6$ to $+0.5 \text{ V}$ and involves the deposition of silver in amounts of $\leq 0.025 \mu\text{g}/\text{cm}^2$ of electrode area. Thus, when silver in the titration cell was $< 10^{-6} M$, this was the only wave produced by the deposition of silver. The half-wave potential and corresponding value of the slopes for this process are given in Table 1. The apparent current efficiency for this process varied from 90–160%.

We tried to determine the current efficiency for this process as the ratio of the amount of silver deposited at $+0.5 \text{ V}$ (determined by gamma counting) to the amount

deposited at +0.5 V determined by coulometric measurements. These attempts were only partly successful due in part to the inability to distinguish precisely between the amount of silver adsorbed on the glass components of the cell and that deposited on the electrode, together with the poor reproducibility for coulograms recorded in this range. Also, traces of gold produce a wave on the coulogram that cannot be distinguished from the first silver deposition wave.

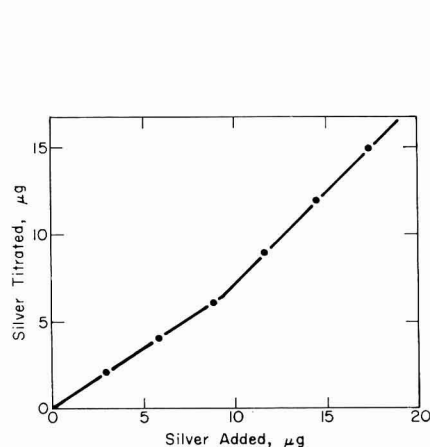
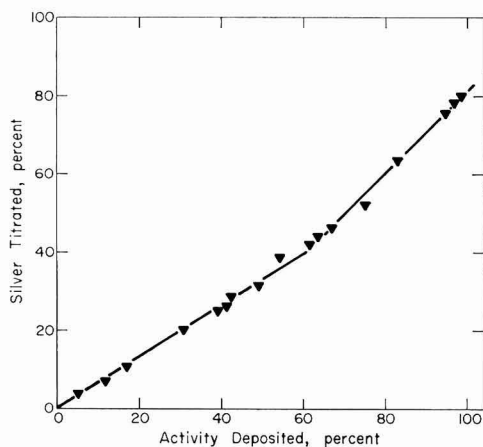
TABLE 1

HALF-WAVE POTENTIALS AND VALUES OF THE SLOPE FOR UNDERVOLTAGE PROCESSES

Wave	$E_{\frac{1}{2}}$ (V)	Slope (V)	Sources
1st	0.56	0.05	Coulogram
2nd	0.41	0.161	% Activity deposited <i>vs.</i> potential
	0.395	0.118	Coulogram
	0.395	0.122	Stepwise titration in 20-mV increments
3rd	+0.06	0.118	% Activity deposited <i>vs.</i> potential
	+0.055	0.103	Coulogram
	+0.04	0.074	Stepwise titration in 20-mV increments.
4th	+0.11	0.06	Coulogram
	+0.14	0.06	% Activity deposited <i>vs.</i> potential

The second wave produced by the deposition of silver appeared whenever the amount of silver in the titration cell was greater than the amount required to produce a deposit of $>0.025 \mu\text{g}/\text{cm}^2$ of electrode area. This process involves the deposition of silver in amounts from 0.025 – $0.130 \mu\text{g}/\text{cm}^2$ of electrode area with a current efficiency of $\sim 150\%$. The half-wave potential and value of the slope for this wave are given in Table 1.

The third silver wave involves the deposition of silver from 0.130 – $0.250 \mu\text{g}/\text{cm}^2$ of electrode area. The maximum amount of silver required to complete the

Fig. 2. Typical electrode calibration curve. Au working electrode; $M \text{ HClO}_4$ electrolyte.Fig. 3. Titrated *vs.* deposited silver. $13 \mu\text{g}$ carrier silver with $^{110\text{m}}\text{Ag}$ tracer; 36 cm^2 Au-electrode; $10 \text{ ml } M \text{ HClO}_4$ electrolyte.

development of this wave is in reasonable agreement with the calculated amount, $0.275 \mu\text{g}/\text{cm}^2$, required to form a monolayer at the gold electrode. Thus, the first three waves are attributed to the monolayer formation process. The half-wave potential and corresponding value of the slope for the third wave are given in Table 1.

The standard potential and slopes for the fourth wave (Table 1) agree well with published values for the $\text{Ag}-\text{Ag}^+$ couple. This wave therefore corresponds to the reversible reduction of the silver ion at the silver electrode.

Curves illustrating the current efficiency obtained for the monolayer formation process (first three waves) are shown in Figs. 2 and 3. The data for Fig. 2 were taken from the curves shown in Fig. 1; the curve is a plot of the amount of silver titrated *vs.* the amount of silver added to the titration cell. The data for the curve in Fig. 3 were obtained by titrating an aliquot of the ORNL ^{110}Ag solution by scanning coulometry. The percentage of silver titrated for the wave was obtained from an electrode calibration curve constructed in the manner of Fig. 2. The break in the curves of Figs. 2 and 3 occurs at the point representing the maximum height of the third wave and the completion of the monolayer formation process. The current efficiency for the monolayer formation as represented by the slope of the curve before the break, is nearly 150%. The slope of unity following the break shows that the deposition of silver at its standard potential proceeds with 100% current efficiency.

Further evidence that the observed undervoltage effects are produced by the monolayer formation process was obtained by recording a family of curves showing the development of the first three silver waves as a function of electrode area. The ratio of the heights of the second and third waves was approximately unity for all electrode areas, and the amount of silver in $\mu\text{g}/\text{cm}^2$ required to completely develop the second silver wave was also approximately constant for all areas. This result is given in Table 2.

TABLE 2

MAXIMUM HEIGHT OF COULOGRAM AT $+0.2 \text{ V}$ *versus* ELECTRODE AREA

Electrode area (geometric) (cm^2)	Max. curve height, (C)	μg Silver corr. for 150% CE	Silver deposited ($\mu\text{g}/\text{cm}^2$)
36.3	3.0	5.2	0.145
27.4	2.2	3.7	0.137
18.3	1.6	2.7	0.147
9.7	0.71	1.2	0.127
			Av. 0.14 ± 0.01

In view of the undervoltage effects as described above, two alternative approaches to the quantitative titration of silver at the gold electrode were evaluated. One approach was to construct a calibration curve for each individual electrode similar to the curve shown in Fig. 2. The amount of silver titrated was then corrected on the basis of the calibration curve to give the actual amount of silver in the titration cell. The second approach was to correct the height of the coulomb-potential curve as measured at -0.3 V for the 150% current efficiency of the monolayer formation process as measured at -0.05 V . Typical results for both approaches are given in Table 3. These data show that the first approach is more precise. The relatively poor

TABLE 3

Electrolyte	Cl ⁻ (μ g)	No. of titrations	Ag (μ g)	Av. recovery and coef. var.	
				By curve	By calcn.
1 M HClO ₄	0	9	2.9-17.6	101 \pm 3.8%	100 \pm 2.7%
0.1 M HClO ₄	0	7	2.9-17.6	99 \pm 2.0%	104 \pm 11.0%
0.1 M HClO ₄	19-46	10	5.9-17.7	98 \pm 3.6%	104 \pm 7.0%
1 M HNO ₃	0	7	2.4-16.8	a	100 \pm 5.6%
0.1 M HNO ₃	0	6	2.9-17.6	a	103 \pm 9.0%
0.1 M HNO ₃	94	6	2.9-17.6	a	102 \pm 7.6%
				99 \pm 3.3%	102 \pm 7.4%

^a No calibration curve prepared.

precision obtained by direct calculation is attributed to the use of the height of the coulogram at -0.05 V as a measure of the amount of electricity consumed by the undervoltage processes. Theoretically, the height of the wave at -0.05 V can be corrected on the basis of the Nernst equations for the undervoltage and primary deposition processes, to show only the amount of electricity consumed by the undervoltage process; however, the calculation is lengthy and only a small increase in precision results.

The effects of pH, chloride ion and nitric and sulfuric acids on the quantitative titration of silver were also studied. Essentially identical results (Table 3) were obtained for the deposition of silver from 0.1 and 1 M solutions of nitric and perchloric acids. Above pH 1, removal of silver from the titration cell becomes increasingly difficult, and the titration results are erratic. However, in spite of this erratic behaviour, the half-wave potentials for the four waves were essentially independent of pH in the range studied.

Trace amounts of chloride ion had a negligible effect on the titration results even when the product of the concentrations exceeded the solubility product for silver chloride by a factor of 25. However, excessive chloride produces low results and must be avoided.

Attempts to use sulfuric acid for this titration were unsuccessful probably because of the limited solubility of silver sulfate. The stoichiometry for the undervoltage processes was essentially the same as that observed in nitric and perchloric acids but the results became progressively lower with increasing concentrations of silver.

DISCUSSION

The electrodeposition behaviour of silver in this study generally agreed with the theory of GRIESS *et al.*² although the reproducibility was better than expected in view of the stated importance of the nature of the electrode surface. Several different gold electrodes were used in these studies; some of these electrodes had been in service for more than two years. The gold foil thus represented more than one order from the vendor. Also, one of these electrodes had a rough and pitted surface resulting from an unsuccessful electro-polishing attempt. No differences in the electrodeposition behaviour of silver other than the amount required for monolayer formation was observed at any of these electrodes. On this basis, the procedure involved in obtaining a

low titration blank may be largely responsible for the reproducible surface conditions at the electrode.

During the initial phase of this study, the first wave for silver, $E_{\frac{1}{2}}=0.55$, was attributed to the deposition of traces of gold because an identical wave appeared on the coulogram whenever traces of gold were added to the titration cell, or when the electrode was scanned into the region 10–20 mV more positive than +0.6 V. Since later experiments with the ^{110}Ag solution indicated that silver was indeed deposited in this potential range, an attempt was made to determine the precise contribution of gold to the height of the coulogram at +0.5 V. The average gold content of the solution at +0.6 V and +0.5 V, both before and after the addition of silver, was determined by activation analysis. The results indicate that the deposition of gold accounted for only, approximately, 15–25% of the wave height at 0.5 V. In view of the variable amounts of gold present in solution at +0.6 V, analytical results based on the height of the first silver wave, $E_{\frac{1}{2}}=0.55$ V, can be expected to be high and the precision to be poor.

We have no explanation for the observed 150% current efficiency of the under-voltage processes for silver. Undervoltage processes for the electrodeposition of bismuth and polonium at the gold electrode proceed at 100% current efficiency. BYRNE AND ROGERS³ have commented on the effect of complex reactions; perhaps the deposition of a polymeric ion is involved here.

ACKNOWLEDGEMENT

The work reported in this paper was developed during investigations under contract AT(07-2)-1 with the U.S. Atomic Energy Commission.

SUMMARY

The effects of the monolayer formation process on the coulometric titration of silver at the gold electrode are described. The electrodeposition of silver in less than monolayer amounts occurred in three distinct steps. These steps were from 0.25 to 0.75 V more positive than predicted by the abridged form of the Nernst equation, and the corresponding current efficiencies were 150%. The standard deviation of the coulometric method in the concentration range that includes monolayer formation was 3.3%.

REFERENCES

- 1 P. DELAHAY, *New Instrumental Methods in Electrochemistry*, Interscience Publishers, New York, 1954, p. 278.
- 2 J. C. GRIESS, JR., J. T. BYRNE AND L. B. ROGERS, *J. Electrochem. Soc.*, 98 (1951) 452.
- 3 J. T. BYRNE AND L. B. ROGERS, *J. Electrochem. Soc.*, 98 (1951) 457.
- 4 J. C. GRIESS, JR., J. T. BYRNE AND L. B. ROGERS, *J. Electrochem. Soc.*, 98 (1951) 98.
- 5 J. C. GRIESS, JR. AND L. B. ROGERS, *J. Electrochem. Soc.*, 95 (1949) 129.
- 6 L. B. ROGERS, D. P. KRAUSE, J. C. GRIESS, JR. AND D. B. EHRLINGER, *J. Electrochem. Soc.*, 95 (1949) 33.
- 7 L. B. ROGERS AND A. F. STEHNEY, *J. Electrochem. Soc.*, 95 (1949) 25.
- 8 R. C. PROPST, *Anal. Chem.*, 35 (1963) 958.
- 9 A. R. NISBET AND A. J. BARD, *J. Electroanal. Chem.*, 6 (1963) 332.

CHRONOCOULOMETRIC MEASUREMENT OF INDIUM(III) ADSORPTION FROM THIOCYANATE MEDIUM

GEORGE W. O'DOM¹ AND ROYCE W. MURRAY

Department of Chemistry, University of North Carolina, Chapel Hill, N.C. 27514 (U.S.A.)

(Received June 2nd, 1967)

The electrochemical reduction of indium(III) is interesting in that it is irreversible for the *quo* ion but is strongly catalyzed by certain anions. Previous references to this effect have been summarized in a recent report by MOORHEAD¹. Like the Ni(II) reductive catalysis^{2,3}, the In(III) catalysis can be utilized for concentration determinations of the activating species at rather low levels⁴. Factors of apparent importance in the catalysis are the surface adsorption properties of the activating species and its labilization of the *quo* coordination shell of the metal ion by an interfacial coordination reaction⁵.

Thiocyanate ion is an example of an activating anion in In(III) reductive catalysis; when added in low concentrations, it produces a catalytic wave near the reversible In(III) potential. At *high* concentrations, thiocyanate permits an In(III) diffusion-controlled reduction in the potential interval -0.5 to -0.9 V *vs.* S.C.E.⁶. The report by MOORHEAD¹ describes an a.c. admittance study of the reduction under this condition. Qualitative evidence for adsorption of an In-SCN complex was derived from observation of a double admittance peak. This finding raises the possibility of involvement of metal complex adsorption in the In(III) reductive catalysis, and it seemed of interest to examine more quantitatively the In(III) adsorption from thiocyanate medium, and from other halide media (iodide and bromide) which also exhibit reductive catalytic activity toward the In(III) ion. This report presents the results of this examination, and the findings of a study of a potentially analogous case, the Ni(II) reduction from thiocyanate medium.

Quantitative data on In(III) adsorption at a hanging mercury drop electrode (HMDE) in thiocyanate medium were derived with the chronocoulometric technique⁷, in which a charge-time transient is recorded following a potential step from an E_{init} , allowing no faradaic reaction, to an E_{final} exhausting the reactant surface concentration. The appropriate relation is

$$Q = 2nFC^0D^{\frac{1}{2}}t^{\frac{1}{2}}/\pi^{\frac{1}{2}} + Q_{ads.} + (Q_{blank} - Q_{\Delta dl}) \quad (1)$$

where $(Q_{blank} - Q_{\Delta dl})$ represents the double-layer contribution to the intercept of a $Q-t^{\frac{1}{2}}$ plot. This plot can be displayed directly on an oscilloscope screen with a recently described chronocoulometric functional readout apparatus⁸. The double-layer correction term, Q_{blank} , is obtained from a potential step in the absence of the metal ion. The term $Q_{\Delta dl}$, which represents the modification of double-layer charge at E_{init} , by

¹ Present address: TRW Systems, One Space Park, Redondo Beach, Calif. 90278.

TABLE I
DOUBLE-LAYER CHARGE CORRECTION DATA FOR INDIUM ADSORPTION FROM THIOCYANATE MEDIUM

$[\text{NaSCN}] \text{ (M)}$	$[\text{NaClO}_4]^a \text{ (M)}$	$Q_{\text{blank}}, (Q_{\Delta at}) \text{ (}\mu\text{C cm}^{-2}\text{)}$	$E_{\text{int.}} = -0.15$	-0.20	-0.30	-0.40	-0.45	-0.50
1.0	0	—	—	24.9, (2.8)	17.9, (1.8)	14.3, (-1.6)	—	9.4, (-1.9)
0.5	0	—	—	22.8, (1.0)	17.6, (-0.7)	12.9, (-1.7)	10.3, (-2.0)	8.3, (-2.0)
0.5	0.4	—	—	24.5, (0.4)	19.1, (-1.2)	13.8, (-2.1)	—	—
0.2	0.7	24.4, (1.6)	—	21.8, (0.2)	16.6, (-1.5)	11.6, (-2.5)	8.7, (-2.7)	—
0.1	0.8	23.2, (1.8)	—	20.2, (-0.3)	15.0, (-1.7)	11.4, (-2.0)	—	—
0.05	0.85	—	—	17.7, (-1.0)	12.1, (-2.0)	9.0, (-2.7)	—	—

^a $[\text{HClO}_4] = 0.1 \text{ M}$

the adsorbed metal complex, is determined⁸ from the difference in integrated current flowing (at $E_{\text{init.}}$) at a DME in the presence and absence of metal ion.

EXPERIMENTAL

Chemicals

Reagent-grade chemicals were used without further purification, except that sodium perchlorate stock solutions were prepared by $\text{Na}_2\text{CO}_3\text{--HClO}_4$ neutralization. Water was ion-exchange and carbon-column purified. Stock NaSCN solutions were prepared just prior to use to avoid any adverse decompositions. The NaSCN electrolyte solutions contained 0.1 M HClO_4 to prevent indium hydrolysis and sufficient NaClO_4 to maintain a constant ionic strength of 1 M to minimize solution resistance. Stock In(III) solutions were prepared from the trinitrate salt (Alfa Inorganics, Inc.) in 0.2 M HClO_4 . The electrolyte solutions displayed no detectable impurity waves by chronopotentiometry.

Cell

The jacketed cell (25°), Pt auxiliary electrode, S.C.E. reference electrode, and hanging mercury drop electrode assembly were of a previously reported design⁹. The calibrated HMDE areas ranged from 0.025 to 0.03 cm^2 . Solutions were degassed with pre-purified nitrogen, and a 1-min pre-equilibration period proved adequate for adsorption equilibrium.

Instrumentation

The chronocoulometric apparatus with automatic $Q\text{--}t^{\frac{1}{2}}$ readout has been previously described⁸. Fairchild diodes FD300 were used instead of 1N485A for D_1 and D_2 and appreciably decreased the circuit switching time. Operation of the functional readout apparatus was verified as satisfactory by spot-check comparisons of recorded $Q\text{--}t$ and $Q\text{--}t^{\frac{1}{2}}$ curves.

RESULTS AND DISCUSSION

Polarograms were obtained for the indium reduction over a 0.05–1 M thiocyanate concentration range and the diffusion-limited character of the wave over the potential interval reported by TANAKA *et al.*⁶ was verified. Qualitative indication of In(III) adsorption from this medium was obtained from chronopotentiometric experiments, which exhibited $i\tau^{\frac{1}{2}}$ -values that increased with increasing current. Chronocoulometric experiments were then performed over the above range of thiocyanate concentrations using equilibration $E_{\text{init.}}$ values from -0.15 to -0.5 V and an $E_{\text{final.}}$ -0.75 V, known from the polarographic data to be in the diffusion-limited potential region. $Q\text{--}t^{\frac{1}{2}}$ displays were linear, and exhibited zero-time intercepts exceeding those obtained in the absence of In(III) (Q_{blank}), confirming the existence of an In(III) surface excess.

Table I gives the Q_{blank} and $Q_{\Delta d1}$ data collected to correct the chronocoulometric $Q\text{--}t^{\frac{1}{2}}$ intercept data from the above experiments, for the double-layer contribution to the charge intercept. The $Q_{\Delta d1}$ correction term was essentially invariant over the 0.4–1.2 mM indium concentration range studied. $Q_{\Delta d1}$ was also unchanged

on gently stirring the solution around the DME, further evidence that adsorption equilibrium is sufficiently well attained during drop life to avoid appreciable errors in the Q_{Adl} term. The Q_{Adl} modification of the double-layer charge at $E_{\text{init.}}$ by indium adsorption is somewhat interesting in that its value changes sign (becomes negative) when the thiocyanate concentration is decreased or $E_{\text{init.}}$ is made more negative. The negative sign of Q_{Adl} means that more anodic current flows to charge the double layer at $E_{\text{init.}}$ when adsorbed indium is present. Analogous effects have been previously reported by BARKER AND FAIRCLOTH¹⁰.

TABLE 2

SURFACE EXCESS VALUES FOR INDIUM ADSORPTION FROM THIOCYANATE MEDIUM

[NaSCN] (M)	[NaClO ₄] (M)	[In ³⁺] (mM)	$\Gamma \cdot 10^{10}$ (moles cm ⁻²) at $E_{\text{init.}}$ =					
			-0.15	-0.20	-0.30	-0.40	-0.45	-0.50
1	0	0.4	—	0.96	1.05	0.84	—	0.59
		0.8	—	1.13	1.20	0.96	—	0.76
		1.2	—	1.26	1.32	1.07	—	0.88
0.5	0	0.4	—	1.31	1.22	1.09	1.01	0.95
		0.8	—	1.29	1.17	1.06	1.18	0.98
		1.2	—	1.28	1.24	1.30	1.30	1.14
0.5	0.4	0.4	—	1.19	1.14	1.01	—	—
		0.8	—	1.19	1.10	0.87	—	—
		1.2	—	—	—	—	—	—
0.2	0.7	0.4	1.36	1.38	1.20	0.96	0.98	—
		0.8	1.34	1.39	1.07	1.07	1.09	—
		1.2	—	1.00	1.26	1.26	1.07	—
0.1	0.8	0.4	1.42	1.38	1.26	1.08	—	—
		0.8	1.36	1.38	1.26	1.21	—	—
0.05	0.85	0.4	—	1.21	0.97	0.54	—	—
		0.8	—	1.23	1.00	0.48	—	—
		1.2	—	1.30	0.86	0.44	—	—

Surface excess values for indium adsorption from thiocyanate medium derived from the chronocoulometric data are given in Table 2. These data are reproducible to about 0.1×10^{-10} moles cm⁻². Variations of the surface excess with equilibration potential, $E_{\text{init.}}$, and thiocyanate concentration are not large, but trends can be discerned. The surface excess exhibits a maximum at about 0.1–0.2 M thiocyanate and decreases as $E_{\text{init.}}$ is made more negative. These data confirm the indium adsorption from thiocyanate medium suggested by MOORHEAD¹, who also observed the same thiocyanate concentration-dependency of the second a.c. admittance peak. Our data do not show the strong dependency of surface excess on indium concentration indicated by MOORHEAD, however.

The slopes of the chronocoulometric $Q-t^{\frac{1}{2}}$ curves for indium in thiocyanate are accurately proportional to the indium concentration. The calculated $D = 7.0 \times 10^{-6}$ cm² sec⁻¹ was obtained for all indium and thiocyanate concentrations employed.

An examination for indium adsorption from iodide and bromide media and for Ni(II) adsorption from thiocyanate medium was also conducted. In 0.5 and 0.1 M

bromide ($E_{\text{init.}} = -0.35$ and -0.45 V, $E_{\text{final}} = -0.75$ V, $[\text{In}^{3+}] = 0.5$ mM) and 0.05 and 1 M iodide ($E_{\text{init.}} = -0.4$ and -0.5 V, $E_{\text{final}} = -0.85$ V, $[\text{In}^{3+}] = 0.5$ mM) media, the chronocoulometric $Q-t^{\frac{1}{2}}$ intercepts were, within experimental error, identical with those of a Q_{blank} in these media. Likewise, chronopotentiometry of indium in 0.05–1 M iodide revealed transition time-independent $i\tau^{\frac{1}{2}}$ values, also indicating no detectable adsorption of indium. Previous data by BARKER AND FAIRCLOTH¹⁰ show absence of indium adsorption from chloride medium. Chronopotentiometry of Ni(II) in 1 M thiocyanate also produced no evidence for nickel adsorption in that constant $i\tau^{\frac{1}{2}}$ values are observed.

In view of the fact that iodide catalyzes the reduction of In(III) much more strongly than does thiocyanate in solutions containing low concentrations of these anions⁴ (yet indium adsorption from thiocyanate medium is appreciable whereas no detectable adsorption is found in iodide medium) it would appear that there is no direct correlation between the catalytic reductive activity of such anions and their tendencies to induce adsorption of the metal complex. This remark must, however, be tempered by the recognition that the present adsorption measurements are conducted at much higher anion concentrations than those required to observe the reductive catalytic effect.

Chronocoulometry and its double potential step permutation have proved to be valuable tools in the recent surge of investigations of metal complex adsorption on mercury electrodes^{7–9, 11–13}. The surface excess data which have appeared thus far in the literature are not sufficiently extensive at this early stage of investigation to permit obvious generalizations, or predictions, on the adsorption or non-adsorption of a given metal complex. The data have shown, however, that the concentration of ligand and the electrode potential at which adsorption equilibrium is established can be important variables in determining the extent, and possible detectability, of metal-complex adsorption. The present In–SCN adsorption data reaffirm the ligand concentration and electrode potential effects on metal-complex adsorptions, and, in the interest of initiating some discussion in the literature on these variables, the authors have been prompted to set down in this writing some of their current thoughts on the problems of their interpretation.

Surface excess data taken over a range of ligand concentrations at a given electrode potential have been observed to exhibit maxima at a particular ligand concentration. This effect was found¹¹ in the adsorption of Cd(II) from thiocyanate medium, and the In–SCN adsorption data also show such behavior. The adsorption of Cd(II) from iodide medium was observed to increase at lower iodide concentrations⁸ and must surely exhibit an adsorption maximum, decreasing thereafter, at iodide concentrations lower than those investigated.

It is reasonable to compare plots of such surface excess–ligand concentration data with distribution curves showing the bulk solution concentration of various coordination states of the metal complex as a function of ligand concentration. If the ligand concentration-dependencies of surface excess and solution concentration of a particular coordination state exhibit essentially identical properties, identification of that particular complex as the predominantly adsorbed species is possible. Such a correlation has been achieved for the Hg(II)–SCN system⁹ where the maximally coordinated $\text{Hg}(\text{SCN})_4^{2-}$ complex was identified as the adsorbing species above 0.1 M thiocyanate concentration. Although in all probability this correlation should also

be possible in the systems exhibiting maxima in their surface excess and solution composition curves, interpretation of the data in those cases can become complicated by other effects. One obvious point of caution is the possibility of simultaneous adsorption of other complexes of higher and lower coordination number. A more subtle point is that it may not be entirely proper to compare surface excess data taken over a range of ligand concentrations at a constant electrode potential, as this ignores the possibility that the surface excess–ligand concentration curves should be prepared at electrode potentials for which there is a constant *charge* on the electrode. In the In–SCN adsorption system, for example, the effect of plotting surface excess against ligand concentration at constant charge rather than at constant electrode potential is to shift the position of the surface excess maximum to lower thiocyanate concentrations. Although in the present study this shift is relatively small, it is conceivable that it could be important in other systems and is an effect of obvious relevance in comparisons with solution complex distribution curves. Inasmuch as the influences of electrode potential or charge on surface excess are not well understood, the best mode of comparison is not at present very clear.

If the effect of the equilibration potential, $E_{\text{init.}}$, on the surface excess is considered, an interesting difference between the adsorption of Cd(II) from iodide medium⁸ and the adsorptions of Cd(II), Zn(II), and In(III) from thiocyanate medium^{11,13} can be discerned. The latter systems exhibit a surface excess which decreases at more negative electrode potentials. At low iodide concentrations, Cd(II) also exhibits a barely detectable trend in this direction but at the higher iodide concentrations clearly shows an *increased* surface excess with increasingly negative $E_{\text{init.}}$ (a limited study of Pb(II) in thiocyanate⁹ suggests that this system also is more strongly adsorbed at more negative potentials). These observations are indicative of the general operation of at least two factors having opposing potential-dependencies, with the dominance of one over the other producing the observed overall trend of adsorption with potential in a given case.

If it can be assumed in a metal-complex adsorption system that the ligand is interposed between the electrode and the metal ion, a useful approach to imagining an adsorption potential-dependency, we suggest, may be to think in terms of the relative tendencies toward adsorption of “free” ligand and (metal) “bound” ligand. The potential-dependency of “free” anionic ligands common in current metal-complex adsorption studies (halides, thiocyanate) is a steadily increasing adsorption at more positive electrode potentials. Thus, if the form of the electrode–ligand interaction in “bound” ligands is substantially similar to that for a “free” ligand, the metal-complex adsorption can also be expected to increase at more positive electrode potentials. If, however, the positive metal ion weakens the electrode–ligand interaction for a “bound” anionic ligand, the enhancement of “bound” ligand adsorption by a more positive electrode potential will probably not be as great as in the “free” ligand adsorption. Such a difference in adsorbability can enhance competition effects, of either an electrical or physical nature, between “bound” and “free” ligand for residence space on the electrode surface. Because of the different degrees of potential-dependence of “free” and “bound” ligand, this competition will be more intense at more positive electrode potentials and, thus, can ultimately bring about a trend toward *decreased* metal-complex adsorption at more positive electrode potentials, or a reduction of the extent of metal-complex adsorption to an undetectable level.

These arguments on "free" and "bound" ligand adsorptions, while reasonable in themselves, are obviously of a speculative nature and ignore the possible effects of variables such as the concurrent adsorptions of different kinds of "bound" ligand (adsorptions of metal complexes bearing different numbers of ligands). They result in the interesting prediction, however, that, at an intermediate level of "free"–"bound" ligand competition, maxima may occur in surface excess–electrode potential curves. Such maxima have not yet been clearly detected in published experimental studies on metal-complex adsorptions, and the worthiness, or unworthiness, of the above arguments will depend on their future detection and careful characterization.

ACKNOWLEDGEMENT

Work supported by the Directorate of Chemical Sciences, Air Force Office of Scientific Research, Grant AF-AFOSR-584-66.

SUMMARY

The adsorption of indium(III) at a mercury electrode from acidified thiocyanate medium has been quantitatively characterized using the chronocoulometric technique. The indium(III) surface excess increases at more positive electrode potentials and passes through a maximum at 0.1–0.2 M thiocyanate concentration. Indium(III) gave no detectable adsorption from iodide or bromide media, nor did nickel(II) adsorb from thiocyanate medium. There appears to be no obvious correlation between the catalysis of indium(III) reduction by thiocyanate, iodide, and bromide ions and the tendencies of these anions to cause indium(III) adsorption. Some discussion of the problems of interpretation of the electrode potential and ligand concentration effect on metal complex adsorption is given.

REFERENCES

- 1 E. D. MOORHEAD, *Anal. Chem.*, **38** (1966) 1796.
- 2 H. B. MARK, JR. AND C. N. REILLEY, *J. Electroanal. Chem.*, **4** (1962) 189.
- 3 H. B. MARK, JR. AND C. N. REILLEY, *Anal. Chem.*, **35** (1963) 195.
- 4 A. ENGLE, J. LAWSON AND D. A. AIKENS, *ibid.*, **37** (1965) 203.
- 5 H. B. MARK, JR., *J. Electroanal. Chem.*, **7** (1964) 276.
- 6 N. TANAKA, T. TAKEUCHI AND R. TAMAMUSHI, *J. Chem. Soc. Japan*, **37** (1964) 1435.
- 7 F. C. ANSON, *Anal. Chem.*, **38** (1966) 54.
- 8 G. W. O'DOM AND R. W. MURRAY, *ibid.*, **39** (1967) 51.
- 9 R. W. MURRAY AND D. J. GROSS, *ibid.*, **38** (1966) 392.
- 10 G. C. BARKER AND R. L. FAIRCLOTH, *Advances in Polarography, Proc. Sec. Intern. Congr., Cambridge, 1959*, Vol. 1, edited by I. S. LONGMUIR, Pergamon Press, 1960, p. 313.
- 11 F. C. ANSON, J. H. CHRISTIE AND R. A. OSTERYOUNG, *J. Electroanal. Chem.*, **13** (1967) 343.
- 12 F. C. ANSON AND D. A. PAYNE, *ibid.*, **13** (1967) 35.
- 13 R. A. OSTERYOUNG AND J. H. CHRISTIE, *Anal. Chem.*, **38** (1966) 1620.

J. Electroanal. Chem., **16** (1968) 327–333

CHRONOPOTENTIOMETRIC DETERMINATION OF U(III), U(IV), UO_2 (VI) AND Np(IV) IN MOLTEN LiCl–KCl EUTECTIC*

F. CALIGARA**, L. MARTINOT AND G. DUYCKAERTS

Laboratory of Nuclear Chemistry of the University of Liège, Liège (Belgium)

(Received February 13th, 1967)

INTRODUCTION

Analytical chemistry in molten salts is still largely unexplored: the unusual experimental conditions make difficult the simple transposition of analytical methods from aqueous solutions to molten salts, and so far the most valuable results have been obtained by electroanalytical methods.

HILL *et al.*¹ describe a voltammetric determination of U(III), in LiCl–KCl, by oxidation on a Pt microelectrode. Attempts to determine U(III) in the presence of U(IV) by the same method were unsuccessful but good results were obtained by coulometric titration of U(III) in KCl–NaCl– MgCl_2 , by means of Pt(II) anodically generated *in situ*.

Uranium(IV) has been investigated by SMIRNOV² and THALMAYER *et al.*³, who used chronopotentiometry for the determination of its diffusion coefficient. MAMANTOV AND MANNING⁴ have shown that tetravalent uranium can be quantitatively determined in molten fluorides by voltammetry, chronopotentiometry or chronoamperometry.

SMIRNOV² and STROMATT⁵ studied chronopotentiometrically the reduction of UO_2 (VI) in NaCl–KCl, and determined its diffusion coefficient at various temperatures.

From a strictly analytical viewpoint, HILL *et al.*¹ and FONDANAICHE AND KIKIMDAL⁶ have made quantitative determinations of UO_2 (VI) in LiCl–KCl eutectic in the temperature range 400–450°. They used classical voltammetry and platinum and graphite indicator electrodes, respectively.

This paper describes a systematic application of chronopotentiometry to the quantitative determination of uranium in its various oxidation states and of Np(IV), in the LiCl–KCl eutectic between 400 and 550°.

EXPERIMENTAL

The preparation of the LiCl–KCl eutectic and of trivalent or tetravalent uranium solutions have already been described⁷. $\text{Cs}_2\text{UO}_2\text{Cl}_4$, used for the preparation of the UO_2 (VI) solution, was prepared according to the method described by Koor *et al.*⁸. Cs_2NpCl_6 used for preparing the solution of Np(IV) has been described elsewhere⁹.

We employed a classical chronopotentiometric circuit with three electrodes. The constant current was supplied by a rapid-response galvanostat ($\approx 2 \mu\text{sec}$,

* Research carried out in the frame of the Euratom contract 011-64-6-TPUB.

** Present address: Institut of Transuranic Elements Euratom, Karlsruhe (West Germany).

Tacussel PRT). The potential difference between the indicator and the reference electrode was measured by a high impedance millivoltmeter ($10^{14} \Omega$, Tacussel S6E), coupled with a fast pen recorder (1/8 sec for full-scale deflection, Speed-Servo Angus Esterline).

The reference electrode consisted of an $\text{Ag}|\text{Ag}(\text{I})||\text{LiCl-KCl}||\text{Pyrex}$ electrode. The concentration of AgCl in the reference electrode was $2.03 \times 10^{-3} \text{ mF}$.

Three types of indicator electrode were used:

a bright platinum foil ($s=0.22 \text{ cm}^2$)

platinum wires: diameter 1 mm ($s=0.1 \text{ cm}^2$)

diameter 0.4 mm ($s=0.046 \text{ cm}^2$).

The auxiliary electrode consisted of a large platinum foil ($s=4 \text{ cm}^2$).

The experiments were carried out in dry glove-boxes. Further experimental details are given in our previous publication⁷.

RESULTS

Figure 1 (a, b, c, d) shows typical chronopotentiograms of the following reactions:

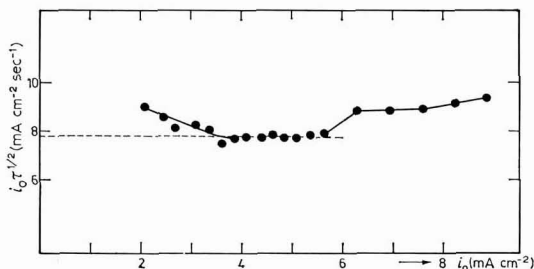
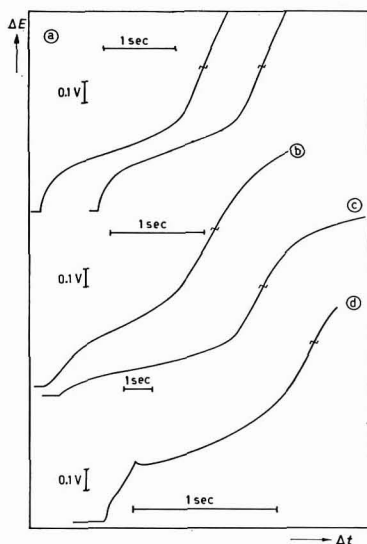
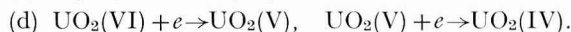
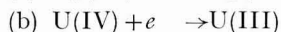
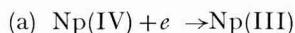


Fig. 1. Chronopotentiograms of the reaction: (a), $\text{Np}(\text{IV}) + e \rightarrow \text{Np}(\text{III})$; $[\text{Np}(\text{IV})] = 5.7 \times 10^{-2} \text{ M}$, $t^0 = 400^\circ$, $i_0 = 4.32 \text{ mA cm}^{-2}$; electrode, platinum wire, diam. 1 mm. (b), $\text{U}(\text{IV}) + e \rightarrow \text{U}(\text{III})$; $[\text{U}(\text{IV})] = 2.26 \times 10^{-1} \text{ M}$, $t^0 = 450^\circ$, $i_0 = 54.8 \text{ mA cm}^{-2}$. (c), $\text{U}(\text{III}) \rightarrow \text{U}(\text{IV}) + e$; $[\text{U}(\text{III})] = 8.65 \times 10^{-2} \text{ M}$, $t^0 = 400^\circ$, $i_0 = 5.64 \text{ mA cm}^{-2}$. (d), $\text{UO}_2(\text{VI}) + e \rightarrow \text{UO}_2(\text{V})$; $[\text{UO}_2(\text{VI})] = 1.08 \times 10^{-2} \text{ M}$, $t^0 = 400^\circ$, $i_0 = 1.1 \text{ mA cm}^{-2}$; electrode, platinum foil.

Fig. 2. Plot of the function $i_0 t^{1/2}$ vs. i_0 . $[\text{U}(\text{III})] = 4.02 \times 10^{-2} \text{ M}$, $t^0 = 400^\circ$.

Figure 2 shows the variation of the product $i_0\tau^{1/2}$ with the current density, i_0 , for the oxidation of U(III) where i_0 is the current density at the indicator electrode, and τ the transition time.

The relationship between $i_0\tau^{1/2}$ and concentration for the various ions is given in Figs. 3 and 4.

Table 1 gives the diffusion coefficients, D , calculated from the data of Figs. 3 and 4.

The curve $i_0\tau^{1/2}$ vs. C for $\text{UO}_2(\text{VI})$ is given only for 400° , because at higher temperatures UO_2Cl_2 is unstable, decomposing according to the reaction:

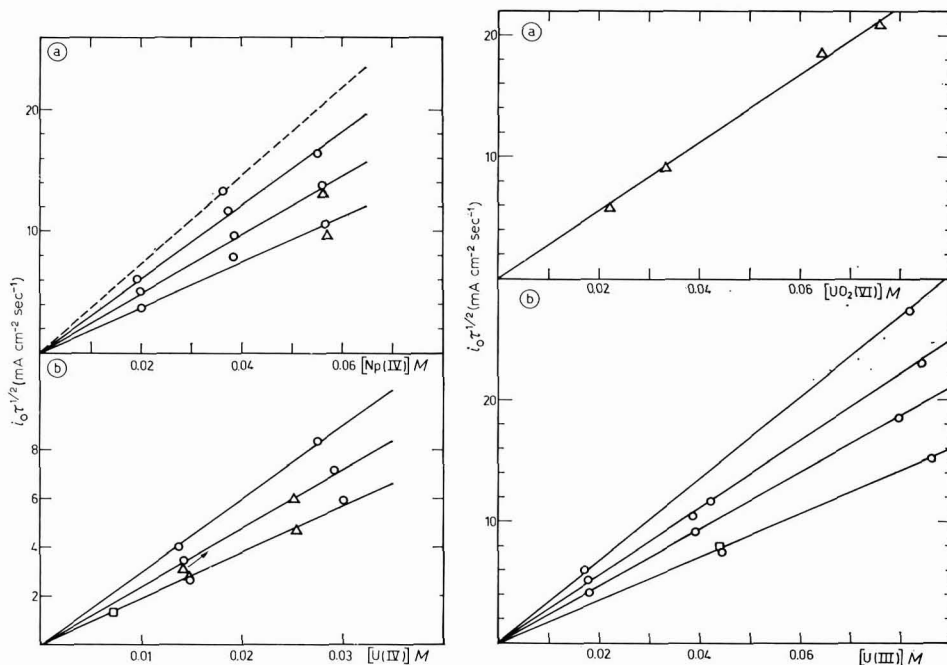


Fig. 3. Plot of $i_0\tau^{1/2}$ vs.: (a), [Np(IV)] at various temps., $1.5 \leq i_0 \leq 20$ mA cm⁻²; (b) U(IV), $0.59 \leq i_0 \leq 13.65$ mA cm⁻². (○) Pt wire \varnothing 1 mm; (□) Pt wire \varnothing 0.4 mm; (△) Pt foil.

Fig. 4. Plot of $i_0\tau^{1/2}$ vs.: (a), [UO₂(VI)] at various temps., $0.82 \leq i_0 \leq 2.74$ mA cm⁻²; (b), U(III), $0.22 \leq i_0 \leq 16.35$ mA cm⁻². (△) Pt foil; (○) Pt wire \varnothing 1 mm; (□) Pt wire \varnothing 0.4 mm.

TABLE 1

$t^\circ\text{C}$	D (cm ² sec ⁻¹ · 10 ⁶)	U(III)	U(IV)	UO ₂ (VI)	Np(IV)
400		4.1 ± 0.10	4.5 ± 0.20	2.3 ± 0.15	4.7 ± 0.20
450		6.8 ± 0.20	8.0 ± 0.15		8.1 ± 0.12
500		10.3 ± 0.30	12.1 ± 0.20		11.7 ± 0.20
550		13.6 ± 0.30			15.7 ± 0.25

The chronopotentiograms for the reduction of $\text{UO}_2(\text{VI})$ in LiCl-KCl are similar to those reported by STROMATT⁵ for NaCl-KCl . As observed by STROMATT, the value of the ratio, $\tau_2/\tau_1=3$, where τ_1 is the transition time for the reaction $\text{UO}_2(\text{VI}) + e^- \rightarrow \text{UO}_2(\text{V})$ and τ_2 the transition time for the reduction $\text{UO}_2(\text{V}) + e^- \rightarrow \text{UO}_2(\text{IV})$, is difficult to determine.

For reactions involving soluble species, the cylindrical electrode, 1 mm in diameter, has proved to be the most satisfactory. It can be used both for cathodic and anodic reactions, over the whole temperature range, whereas other electrodes are limited regarding the temperature or type of electrode reaction. With all types of electrodes, the most reproducible results were obtained at lower temperatures.

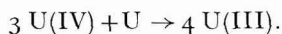
For the cathodic reduction of $\text{UO}_2(\text{VI})$, the foil electrode has given the best results.

The statistical analysis of the results obtained has, however, shown that, where different electrodes have been used for the determination of $D^{1/2}$, they give slightly different results. These discrepancies are attributed to the difficulty of a precise measurement of the electrode surface.

The concentration of U(IV) and Np(IV) may be determined with an accuracy of $\pm 4\%$, for U(III) and $\text{UO}_2(\text{VI})$ an accuracy of 6% is obtained since the precision of D is about half these values.

The analysis of U(IV) and U(III) together in the same solution would seem to be possible. As the reduction of U(IV) takes place at less negative potentials than the reduction of U(III) , the first transition time in a chronopotentiogram of such a mixture should give the concentration of U(IV) .

The second transition time (for the reaction $\text{U(III)} + 3e^- \rightarrow \text{U(O)}$) cannot be recorded without large discrepancies which arise when metallic uranium plates the cathode. In fact, metallic uranium does not form a superficial alloy with Pt or with W. To overcome this difficulty, U(IV) was reduced to U(III) and then an anodic chronopotentiogram was run to determine the total amount of U(III) . If the concentration of U(IV) previously determined by cathodic chronopotentiometry on the mixture, is subtracted from this value, the initial amount of U(III) is obtained. In this method U(IV) is reduced with metallic uranium wire so that the overall reaction is



This method was not used for analytical determinations of U(III) and U(IV) but we have shown that the values of $D_{\text{U(IV)}}$ obtained at 400° from two solutions containing $[\text{U(III)}]=0.0248 \text{ M}$; $[\text{U(IV)}]=0.0106 \text{ M}$ and $[\text{U(III)}]=0.0135 \text{ M}$; $[\text{U(IV)}]=0.0219 \text{ M}$ fall within the limits of $D_{\text{U(IV)}}$ -values measured with solutions containing only U(IV) .

The same holds true for the $D_{\text{U(III)}}$ -values obtained after the reduction of U(IV) .

The similarity of the polarisation curve of Np(IV) on a platinum electrode suggested that the same procedure could be adopted for analyzing a mixture of Np(IV) and Np(III) , but this would necessitate the use of a metallic neptunium electrode.

It is of interest to note that the transition times that give satisfactory results range from 0.5 to 7 sec, which means that a rapid pen recorder may be used and there is no need for oscillographic equipment.

DISCUSSION

The transition time, τ , in chronopotentiometry is given by Sand's formula:

$$i_0\tau^{\frac{1}{2}} = 0.5 \pi^{\frac{1}{2}} nFD^{\frac{1}{2}}C \quad (1)$$

where: F = Faraday, C = concentration (mole cm^{-3}), i_0 = current density, D = diffusion coefficient, n = number of electrons involved in the electrochemical reaction.

This formula holds true for semi-infinite linear diffusion. The mass transport towards the indicator electrode must be diffusion-controlled, and any convective movement excluded.

At the transition time, as defined by eqn. (1), the diffusion layer is depleted of reactive species, and $\delta E/\delta t$ is maximum (E is the potential of the indicator electrode *versus* a reference electrode).

The potential-time curve for a reversible process involving two soluble species is given by:

$$E = E_{\tau/4} + (RT/nF) \log \{(\tau^{\frac{1}{2}} - t^{\frac{1}{2}})/t^{\frac{1}{2}}\} \quad (2)$$

Figure 1 shows that our experimental curves differ from the ideal shape: the inflection point is less sharp and cannot be determined accurately for several reasons, some of which are inherent in molten-salt systems and some typical of the systems investigated here.

First, molten-salt systems, and especially the LiCl-KCl eutectic employed in our experiments, are difficult to obtain in a very pure state. Traces of electrochemically-active impurities interfere with the electrode process and cause the experimental curve to depart from its ideal shape. Also, it is impossible to devise a cell geometry that gives a perfectly homogeneous distribution of the current density on the surface of the indicator electrode. This inhomogeneity causes local overpotentials, which differ from the average electrode potential.

Finally owing to the high temperature at which the measurements are made, the temperature control becomes rather difficult and, especially with large electrodes, micro-convective movements may arise from temperature gradients.

When the reduction of $\text{UO}_2(\text{VI})$ is involved, the formation of the solid product, UO_2 (which adheres to the electrode) changes its surface. This explains the hump in Fig. 1 (d).

From Sand's formula, the product $i_0\tau^{\frac{1}{2}}$ should be independent of the current density, i_0 . As shown in Fig. 2, this is true only within a limited range of current densities.

If i_0 becomes too small, τ becomes exceedingly large and convective movements disturb the diffusion layer: the mass transport towards the electrode exceeds the merely diffusive process and the product, $i_0\tau^{\frac{1}{2}}$, increases.

According to the theory of chronopotentiometry¹⁰, at the transition time the thickness of the diffusion layer is greater the smaller i_0 .

When a cylindrical electrode is employed, the conditions of linear diffusion required by Sand's formula are reasonably approximated only when the diffusion layer is thin compared to the electrode diameter. Sand's formula does not hold true for very small values of i_0 and the product, $i_0\tau^{\frac{1}{2}}$ increases. PETERS AND LINGANE¹¹ have proposed a formula which corrects the experimental results by taking into

account the non-linear diffusion, but our experience has shown that this formula is applicable only if the correction does not exceed 10–15% of the measured τ .

On the other hand, if i_0 becomes too large, both with cylindrical or plane electrodes the diffusion layer becomes too thin. In this case, the roughness of the electrode surface becomes important, the real i_0 becomes smaller than that calculated from the geometrical surface of the electrode, and τ again increases abnormally.

Also, when i_0 is very high and τ very small, a considerable fraction of the current is used to charge the double layer. This also contributes to an increase above the value calculated from Sand's formula.

ACKNOWLEDGEMENTS

We wish to thank Dr. KOOI of Euratom and M. FRESON, General Secretary of the I.I.S.N. for their encouragement and the financial support.

SUMMARY

The use of chronopotentiometry for the quantitative analysis of uranium and neptunium in a molten LiCl–KCl eutectic has been investigated: U(IV) or Np(IV) may be determined with an accuracy of $\pm 4\%$ and U(III) or UO₂(VI) with an accuracy of $\pm 6\%$ in the temperature range 400–550°.

U(III) and U(IV) may be determined in the same solution with the accuracies given above.

REFERENCES

- 1 D. L. HILL, J. PERANO AND R. A. OSTERYOUNG, *J. Electrochem. Soc.*, 107 (1960) 698.
- 2 M. V. SMIRNOV, *Electrochemistry of Molten and Solid Electrolytes*, authorised translation from Russian, Consultants Bureau, New York, 1964.
- 3 C. E. THALMAYER, S. BRUCKENSTEIN AND D. M. GRUEN, *J. Inorg. Nucl. Chem.*, 26 (1964) 347.
- 4 G. MAMANTOV AND D. L. MANNING, *Anal. Chem.*, 38 (1966) 1494.
- 5 R. W. STROMATT, *J. Electrochem. Soc.*, 110 (1963) 1277.
- 6 J. C. FONDANAICHE AND T. KIKIMDAL, *Bull. Soc. Chim. France*, (1966) 875.
- 7 F. CALIGARA, L. MARTINOT AND G. DUYNCKAERTS, *Bull. Soc. Chim. Belges*, 76 (1967) 15.
- 8 J. KOOI, E. WEISSKOPF AND D. M. GRUEN, *J. Inorg. Nucl. Chem.*, 13 (1960) 310.
- 9 F. CALIGARA, L. MARTINOT AND G. DUYNCKAERTS, *J. Chim. Phys.*, in press, 1967.
- 10 P. DELAHAY, *New Instrumental Methods in Electrochemistry*, Interscience Publishers, New York, 1954, p. 179.
- 11 D. H. PETERS AND J. J. LINGANE, *J. Electroanal. Chem.*, 2 (1961) 1.

J. Electroanal. Chem., 16 (1968) 335–340

I. POLAROGRAPHIC BEHAVIOUR OF *cis*- AND *trans*-CINNAMIC ACID AND SUBSTITUTED CINNAMIC ACIDS

(Received June 24th, 1967)

J. Electroanal. Chem., 16 (1968) 341-350

for the number of electrons transferred, n , lying between 1 and 2. The dimerisation would be promoted by increasing the concentration of depolariser; it would also be more likely to occur with decreasing dielectric constant of the medium, *i.e.*, with increasing stabilisation of the free radical intermediate.

ONO AND UEHARA⁶ have studied the problem and suggest a 2-electron reduction to the dihydro derivative. Their attempts to prove this by isolating the products of the controlled-potential electroreduction of cinnamic acid at a mercury pool cathode, were unsuccessful as a mixture of dihydrocinnamic acid and dimer (24% and 53%, respectively) was obtained. It is clear that in this case controlled-potential electrolysis at a mercury pool cathode cannot be used to confirm the course of the electrode process at a dropping mercury electrode as the increased concentration of depolariser required facilitates the dimerisation of the intermediate at the expense of the competing monomeric reaction.

An earlier study⁵ in aqueous unbuffered media had shown the presence of two waves which had been correctly attributed, by MARKMAN AND ZINKOVA⁷, to reduction of undissociated acid and its conjugate base. The wave for the reduction of the anion occurred at negative potentials *i.e.*, -2.0 V. No valid conclusions could be drawn from the relative heights of the two waves since the recombination reaction seriously alters the pH in the vicinity of the electrode.

In the present investigation, the polarographic reduction of a range of substituted cinnamic acids and three esters of cinnamic acid have been studied. A comparison has also been made of the polarographic behaviour of the *cis*- and *trans*-isomers of cinnamic acid and 3-chlorocinnamic acid.

EXPERIMENTAL

Reagents

Compounds I–IV, VI, VII (Table 1) and IX–XI (Table 2) were obtained commercially. Compounds V and VIII were prepared from the corresponding aldehydes by a modified Doebner reaction¹⁰. The purity of these compounds was checked by melting-point determination, and by elemental analysis.

A 10^{-2} M stock solution of each compound was prepared in absolute ethanol,

TABLE 1
COMPOUNDS OF TYPE $X-C_6H_4CH=CHCOOH$

	<i>X</i>	<i>pK'</i>	$\alpha^{a,b}$	dE_1/dpH (mV/pH) ^c
I	H	7.6	0.57	75
II	4-CH ₃	7.3	0.52	87
III	3-Cl	7.6	0.60	88
IV	4-Cl	7.25	0.53	85
V	4-Br	7.65	0.57	91
VI	3-OCH ₃	7.65	0.57	83
VII	4-OCH ₃	7.6 ^d	0.43 ^d	60 ^d
VIII	4-CN	7.8		

^a Measured at pH 6.1.

^b Mean $\alpha = 0.54 \pm 0.02$

^c Mean $dE_1/dpH = 81 \pm 4$ mV/pH unit.

^d A very poorly defined wave makes these results approximate only.

with the exception of 4-cyanocinnamic acid for which a $5 \cdot 10^{-3} M$ stock solution was prepared because of the low solubility. Buffer solutions were prepared from AnalaR reagents using glass-distilled water.

Apparatus

A Radelkis polarograph type OH-102 (Metrimpex, Hungary) was used to record polarograms by the conventional 2-electrode system. The polarographic vessel was a Kalousek cell with a separated saturated calomel reference electrode (SCE). Capillary constants measured at the potential of the SCE in 0.1 *M* potassium chloride solution were $t = 4.0$ sec, $m = 1.61$ mg sec⁻¹, at $h = 60$ cm.

TABLE 2

COMPOUNDS OF THE TYPE $C_6H_5CH=CH-COOR$

	<i>R</i>	α^a	E_1^b (<i>V</i> vs. SCE)
IX	CH ₃ -	0.508	-1.666
X	C ₂ H ₅ -	0.476	-1.651
XI	C ₆ H ₅ -CH ₂ -	0.495	-1.638

^a Measured at pH 6.7.

^b E_1 pH-independent above pH 7.5.

TABLE 3

MICROCOULOMETRICALLY-DETERMINED NUMBER OF ELECTRONS CONSUMED IN THE REDUCTION OF CINNAMIC ACID OR SUBSTITUTED CINNAMIC ACID

Compound	Medium	<i>n</i>
I	50% ethanolic acetate buffer, pH 6.1	1.90; 2.01
III	50% ethanolic acetate buffer, pH 6.1	1.97; 1.91; 1.94

Half-wave potential measurements, and accurate measurements of the potential of the dropping mercury electrode (DME) required for logarithmic analysis of the wave shape, were made using a 3-electrode system. The potential of the DME was measured potentiometrically against a reference SCE in an auxiliary circuit using a Precision potentiometer 7565 (Pye, Cambridge). A modified Kalousek vessel was used, in which the junction of an auxiliary SCE was immersed in the solution studied.

Controlled-potential electrolysis for microcoulometric measurements and identification of the electrolysis products was carried out using the Radelkis polarograph as a potentiostat, and a modified H cell¹¹ for a volume of 0.5 ml.

The relative pH-values of buffer solutions containing 50% ethanol were measured with a Vibron pH-meter model 39A (E.I.L. Ltd., Surrey).

Ultraviolet spectra were measured with an Ultrascan spectrophotometer (Hilger and Watts Ltd., London). The *trans-cis* isomerism of cinnamic acid was achieved by irradiating a solution in a quartz cell with a 500-W xenon lamp.

Procedure

Solutions for polarography were prepared by mixing measured volumes of

ethanol, stock solution of depolariser, water and aqueous buffer solution in a 10-ml graduated flask. The volume contraction on mixing ethanol and water was corrected by dilution to volume with aqueous ethanol. The solution was transferred to the Kalousek cell, deoxygenated with a stream of nitrogen for 3 min, and the polarographic wave measured. Possible hydrolysis of the depolariser in the cell was detected by repeating the recording 10 min after the start of the first recording.

For the controlled-potential electrolysis, the solution was prepared as for polarography, and a 0.5-ml aliquot transferred to the electrolysis cell. After the solution had been deoxygenated by passing a stream of nitrogen for 20 min, the electrolysis was carried out, over a period of 3 h, at the potential at which the polarographic wave reached its limiting value. Polarograms were recorded at intervals of 1 h during the electrolysis. It was shown that the limiting current measured at any time during the electrolysis showed no change after mixing the solution briefly with a stream of nitrogen. This confirmed that, for the electrolysis cell used, the homogeneity of the solution was maintained by the stirring effect of the falling mercury drops. The number of electrons, n , was calculated from the equation¹²,

$$n = k_1 t / 2.3 k_2 V F \log(i_0/i_e)$$

The conversion of *trans*-cinnamic acid to its *cis*-isomer was followed spectrophotometrically. A $5 \cdot 10^{-5} M$ cinnamic acid solution in 50% ethanol was pumped from the quartz cell in which it was irradiated, through a flow-through cell in the spectrophotometer, and then returned to the quartz cell for further irradiation. This arrangement allowed the change in absorption spectrum to be measured continuously during irradiation. The overall change in the spectrum showed a decrease in absorbance characteristic of the *trans*-*cis* isomerism; the wavelength of maximum absorption shifted from 273 m μ to 264 m μ , confirming the formation of *cis*-cinnamic acid. A kinetic study showed that the conversion was complete after 30 min. A $10^{-2} M$ solution was irradiated for a similar period, and absorption spectra were measured on diluted aliquots before and after irradiation, to confirm that the conversion time was concentration-independent. Solutions of *cis*-cinnamic acid prepared in this way showed no change in absorption after standing for 2 h.

RESULTS AND DISCUSSION

The $>C=C<$ bond in cinnamic and substituted cinnamic acids is reduced in

TABLE 4
CURRENTS IN μA

Compound	pH						
	4.4	5.1	5.6	6.1	6.7	7.3	7.8
I			1.97	1.90	1.78	1.22	0.75
II				1.60	1.68	0.90	0.67
III	1.34	1.52	1.84	1.82	1.79	1.15	0.82
IV	1.38	1.57	1.70	1.70	1.55	0.77	0.50
V	1.26	1.47	1.45	1.47	1.47	0.94	0.67
VI			1.71	1.62	1.60	1.07	0.72
VII				1.74	1.82	1.23	

a single wave, the height of which is independent of pH over a limited range (Table 4). Above pH 6.5, the height of the wave decreases in the form of a dissociation curve (Fig. 1). With the exception of 4-cyanocinnamic acid*, all the compounds studied were reduced in a not-too-well defined wave because the reduction occurs at very negative potentials where the wave is obscured by the wave due to the reduction of the cation of the supporting electrolyte. Below pH 4.0, the reduction of the >C=C<

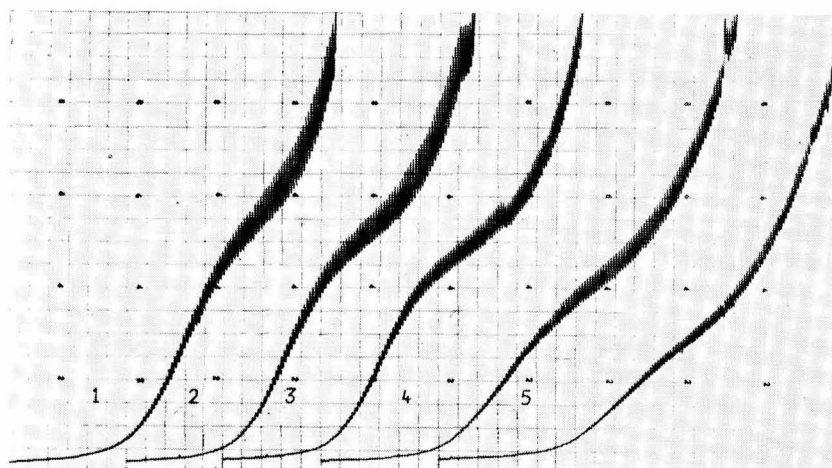


Fig. 1. pH-dependence of waves of $5 \cdot 10^{-4} M$ cinnamic acid in 50% ethanol. pH: (1), 5.6; (2), 6.1; (3), 6.7; (4), 7.3; (5), 7.8. Starting potentials: (1 and 2), -1.3 ; (3), -1.35 ; (4), -1.4 ; (5), -1.45 V *vs.* SCE. Sensitivity, $4 \mu A$ f.s.d.; 25 mV/absc.

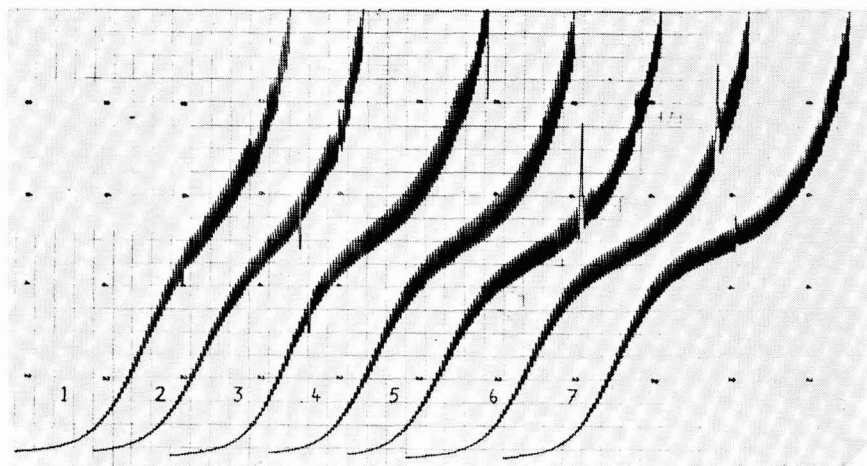


Fig. 2. Polarographic waves of $5 \cdot 10^{-4} M$ substituted cinnamic acids in 50% ethanolic acetate buffer, pH 6.7. Substituents: (1), $4\text{-CH}_3\text{O}$; (2), 4-CH_3 ; (3), H; (4), $3\text{-CH}_3\text{O}$; (5), 4-Cl ; (6), 4-Br ; (7), 3-Cl . Starting potentials: (1 and 2), -1.5 ; (3 and 4), -1.475 ; (5), -1.45 ; (6 and 7), -1.4 V. Sensitivity, $4 \mu A$ f.s.d.; 25 mV/absc.

* The behaviour of this compound differed markedly from the general pattern; a detailed study will be reported later.

bond is completely masked by the reduction of hydrogen ions. The presence of substituents on the benzene ring had a marked effect on the definition of the wave (Fig. 2). Substituents with a $+I$ -effect caused the wave to be shifted to more positive potentials and hence improved the shape of the wave. On the other hand, $-I$ substituents caused $E_{\frac{1}{2}}$ to be shifted to more negative values with the result that the wave became less clearly defined and the pH-range over which the wave was measurable became even more limited.

The effect of varying the composition of the supporting electrolyte was studied, in an attempt to improve the shape of the wave.

(i) The effect of varying the ethanol concentration was studied. No significant improvement in the shape of the wave was observed.

(ii) The concentration of the acetate buffer (with respect to acetate anion) was varied over the range 0.1–0.5 M . With decreasing buffer concentration, the reduction of the cation of the supporting electrolyte was shifted to more negative potentials and hence the wave became better defined.

(iii) The influence of several cations was next studied. Potassium, lithium, and ammonium ions (0.1 M as chlorides) had no effect, but in the presence of magnesium and lanthanum, no wave was observed. Cations of the tetra-alkylammonium type (Et_4N^+ , Bu_4N^+) caused a marked improvement in the shape as $E_{\frac{1}{2}}$ was shifted some 50 mV more positive.

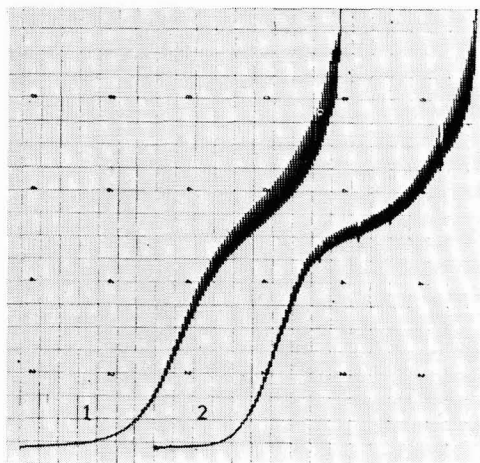


Fig. 3. Effect of cations on polarographic wave of $5 \cdot 10^{-4} M$ cinnamic acid in 50% ethanolic acetate buffer pH 6.1. Cations: (1), 0.01 M Na^+ ; (2), 0.01 M Et_4N^+ . Starting potentials -1.35 V vs. SCE. Sensitivity, $4 \mu\text{A}$ f.s.d.; 25 mV/absc.

The optimum conditions were found to be 50% ethanol together with 0.1 M buffer. Although the presence of tetra-alkylammonium ions had been shown to improve the shape of the wave, its general use is not recommended owing to its strongly surface-active properties. For purely analytical work, however, the use of a 0.1 M acetate buffer containing tetra-ethylammonium chloride is suggested (Fig. 3).

The number of electrons transferred in the electrode process was estimated

by comparing the wave-height of cinnamic acid with the wave for equimolar solutions of:

- (a) benzaldehyde semicarbazone ($n=4$)
- (b) 1,4-naphthoquinone ($n=2$)
- (c) benzaldehyde ($n=1$)

the three standards being measured in an acetate buffer, pH 4.2, containing 50% ethanol. The results indicated that $n=2$.

This was confirmed by microcoulometric determination of the number of electrons transferred. The values obtained for X = H, and 3-Cl are shown in Table 3, the precision being better with the more well defined 3-Cl wave.

The isolation of the products obtained from the microcoulometric analysis was attempted as a further check. The object was to prove that the residual solution after constant potential electrolysis at the DME contains only dihydrocinnamic acid together with residual cinnamic acid. After extraction with ether the products were separated by thin-layer chromatography. Owing to the difference in R_F -values, the separation was difficult and it was found that using a range of solvents recommended¹³ for the chromatographic separation of carboxylic acids, no spots corresponding to the presence of dimer were observed.

An attempt to detect the molecular ion corresponding to the dimer by mass spectroscopy of the electrolysis product was unsuccessful as the product was found to decarboxylate. Different spectra were obtained with high and low inlet temperatures, corresponding to the different volatilities of cinnamic acid and its reduction product.

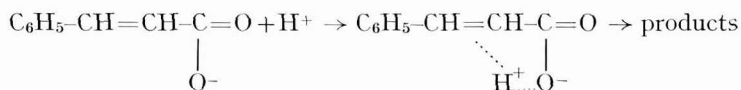
Mechanism of the electrode process

The polarographic reduction of cinnamic acid can, in principle, occur through one or more of three electroactive species:

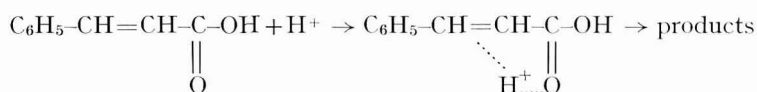
- (i) the protonated complex $\text{C}_6\text{H}_5-\overbrace{\text{CH}=\text{CH}-\text{COOH}}^{\text{H}^+}$,
- (ii) the undissociated acid,
- (iii) the cinnamate anion.

The overall diffusion control of the electrode process at pH-values below 6.5, was shown by the dependence of the wave-height on the height of the mercury reservoir. The dependence of the current on depolariser concentration was found to be rectilinear over the range $1 \cdot 10^{-4}$ – $1 \cdot 10^{-3}$ M.

A linear dependence of half-wave potential on pH (Fig. 4) indicated that protonation was the first, rate-determining step in the reaction. Over the pH-range (4–8) in which a polarographic wave was observed, the anion predominates in solution. The electroactive species is therefore a protonated form of the anion:



It is not possible to say with certainty whether one or two protons are involved in the pre-protonation. Thus a second protonation, following the recombination of the anion with a proton, is not precluded:



The behaviour of the acid was compared with that of a series of cinnamic acid esters, IX, X, and XI (Table 2) in which ionisation of the carboxyl group is impossible. In each case a single wave was observed the height of which remained practically constant over the pH-range 6–13 (Table 5). Above pH 8, the half-wave potential was independent of pH, indicating reduction of the ester without pre-protonation.

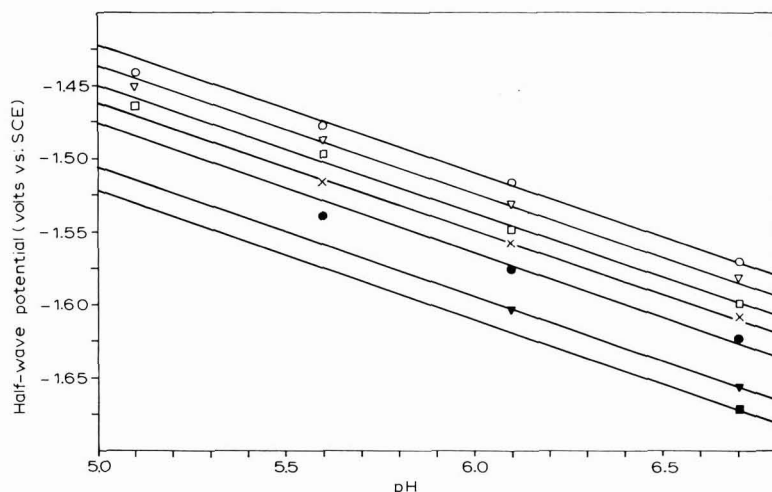
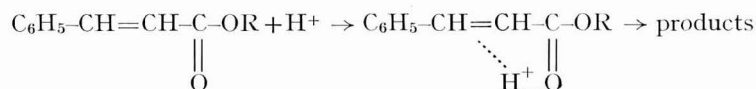


Fig. 4. Dependence of half-wave potentials of substituted cinnamic acids on pH. Substituents: (○), 3-Cl; (▽), 4-Br; (□), 4-Cl; (×), 3-CH₃O; (●), H; (▼), 4-CH₃; (■), 4-CH₃O.

TABLE 5
CURRENTS IN μA

Compound	pH								
	5.6	6.1	6.7	7.3	7.8	8.2	8.7	10.7	13
IX		1.87	1.81	1.57	1.49	1.46	1.36	1.36	1.23
X		1.94	2.05	1.84	1.73	1.57	1.57	1.57	1.47
XI	1.68	1.68	1.66	1.50	1.45	1.40	1.32	1.25	1.25

In the pH-range 6–8, the half-wave potential was linearly dependent on pH and the electroactive species was thus a protonated form of the ester:



The analogy between the overall behaviour of the acid and esters suggests that the acid is reduced in the form of the mono-protonated anion.

Structural effects

A linear relationship between half-wave potential and the Hammett substituent constant was obtained from compounds I–VII (Fig. 5) and confirmed that cinnamic acids mono-substituted in the 3- or 4-position obey the modified Hammett equation¹⁴:

$$\Delta E_{\frac{1}{2}} = \sigma \varrho'$$

The observed value of the reaction constant, $\varrho' = 0.16$ V, was based on the measurements of seven half-wave potentials at four different pH-values. The value of the Hammett reaction constant, ϱ , in dimensionless form is given by

$$\varrho = (\alpha n F / RT) \varrho' = +2.8$$

The half-wave potential of 4-cyanocinnamic acid was found to differ significantly from that predicted by the Hammett equation for a substituent constant,

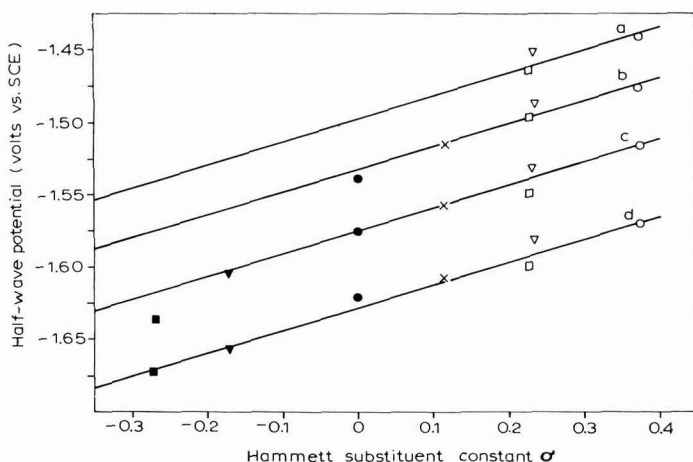


Fig. 5. Dependence of half-wave potentials on Hammett substituent constant, σ , for substituted cinnamic acids. Symbols as in Fig. 4. pH: (a) 5.1; (b) 5.6; (c) 6.1; (d) 6.7.

$\sigma = 0.628$; in this case a mixed electrode process operated in the pH-range concerned. The low value of the reaction constant, ϱ' , is a consequence of the fact that a protonated form of the depolariser is the electroactive species.

A plot of the polarographic dissociation constant, pK' , against the substituent constant, σ , showed little correlation, whereas the $E_{\frac{1}{2}}-\sigma$ plot was linear. This indicates that the substituent exerts a greater effect on the β -carbon atom than on the ionisation of the carboxyl group.

MARKMAN AND ZINKOVA⁷ have studied the *cis*- and *trans*-isomers of cinnamic acid and found a wide variation in the values of the limiting diffusion current and the transfer coefficient, α , for the two isomers. In view of the structural similarity, these results are surprising; one possible explanation could be the non-quantitative chemical synthesis of the *cis*-isomer.

Polarograms of *cis*-cinnamic acid prepared as described previously by irradiation of the *trans*-isomer, were measured at pH 4.4 and pH 6.1, and compared with

those of the corresponding *trans*-isomer measured under identical conditions. A very slight shift towards more positive potentials was observed for the *cis*-isomer, but owing to the poor definition of the waves, accurate measurement of $\Delta E_{\frac{1}{2}}$ was not possible. The wave-heights for the isomers, however, were the same.

The *cis* isomer of 3-chlorocinnamic acid was next studied as this derivative showed a well defined wave. Comparison of this wave with that of the corresponding *trans*-acid showed that the diffusion coefficients of the isomers were the same. The difference in half-wave potentials ($E_{\frac{1}{2}cis} - E_{\frac{1}{2}trans}$) was found to be 21 mV.

ACKNOWLEDGEMENTS

The authors wish to express their thanks to Dr. P. ZUMAN for helpful discussions during the preparation of this paper. One of us (M.J.D.B.) wishes to thank Murex Ltd. for financial support.

SUMMARY

Cinnamic acid and substituted cinnamic acids are polarographically reduced in 50% ethanol in a single 2-electron wave between pH 4 and pH 8. At pH-values above 6.5, the height of the wave decreases in the form of a dissociation curve. The shape of the wave is much improved in the presence of tetra-alkylammonium ions. From the linear dependence of half-wave potential on pH, it is apparent that a protonated anion is the electroactive species. Comparison with the behaviour of cinnamate esters suggests the mono-protonated anion is electroactive. The half-wave potentials of substituted cinnamic acids, except for 4-cyanocinnamic acid, obey the modified HAMMETT equation $\Delta E_{\frac{1}{2}} = \sigma\rho'$. The difference in half-wave potentials of the *cis*- and *trans*-isomers is 21 mV.

REFERENCES

- 1 B. FLEET AND R. BELCHER, *J. Chem. Soc.*, 324 (1965) 1749.
- 2 L. SCHWAER, *Collection Czech. Chem. Commun.*, 7 (1935) 326.
- 3 G. SEMERANO AND A. CHISINI, *Gazz. Chim. Ital.*, 66 (1936) 310.
- 4 S. WAWZONEK, S. C. WANG AND P. LYONS, *J. Org. Chem.*, 15 (1950) 593.
- 5 S. ONO AND T. HAYASHI, *Bull. Chem. Soc. Japan*, 26 (1953) 268.
- 6 S. ONO AND M. UEHARA, *Bull. Univ. Osaka Prefect.*, Ser. A, 5 (1957) 139.
- 7 A. L. MARKMAN AND E. V. ZINKOVA, *Zh. Obshch. Khim.*, 27 (1957) 1438.
- 8 J. SEVCIK AND J. MOLLIN, *Acta Univ. Palackianae Olomuc.*, Fac. Rerum Nat., 9 (1962) 231.
- 9 O. H. WHEELER AND C. B. COVARRUBIAS, *J. Org. Chem.*, 28 (1963) 2015.
- 10 *Organic Synthesis*, edited by N. RABJOHN, Wiley, New York, Collected Volume 4 (1963) 732.
- 11 B. FLEET AND P. ZUMAN, *Collection Czech. Chem. Commun.*, in press.
- 12 G. A. GILBERT AND E. K. RIDEAL, *Trans. Faraday Soc.*, 47 (1951) 396.
- 13 H. GANSHIRT, D. WALDI AND E. STAHL, *Thin Layer Chromatography*, edited by E. STAHL, Academic Press, London, 1965, p. 357.
- 14 P. ZUMAN, *Collection Czech. Chem. Commun.*, 25 (1960) 3225.

J. Electroanal. Chem., 16 (1968) 341-350

ELECTROCHEMICAL OXIDATION OF FORMATE IN DIMETHYLSULFOXIDE AT GOLD AND PLATINUM ELECTRODES

EINAR JACOBSEN*, JULIAN L. ROBERTS, Jr.** AND DONALD T. SAWYER

Department of Chemistry, University of California, Riverside, Calif. 92502 (U.S.A.)

(Received June 7th, 1967)

There has been considerable work in recent years on the mechanism of electro-oxidation of formic acid in aqueous solutions. The overall oxidation products for acidic conditions are carbon dioxide and hydrogen. However, the oxidation mechanism is complicated and involves adsorption of formic acid and a slow pre-electrochemical step in which formic acid decomposes to form atomic hydrogen and an adsorbed formate ($\cdot\text{COOH}$) radical¹⁻⁸.

Formate ions in aqueous alkaline solutions are not oxidized at platinum electrodes^{2,3}. However, in anhydrous formic acid, formate ions are electroactive and the oxidation of formate on platinum, gold and palladium electrodes has been studied in detail⁹. The overall oxidation products are carbon dioxide and hydrogen ions, but adsorbed $\text{HCOO}\cdot$ intermediates are involved in the electrode reaction.

During a recent electrochemical study of dissolved carbon dioxide and its reduction products in dimethylsulfoxide¹⁰, it was observed that formate ion is oxidized at a gold electrode. The present investigation has been undertaken to study the electrochemical oxidation of formate in dimethylsulfoxide and to determine whether the oxidation mechanism in this non-aqueous medium is similar to that in anhydrous formic acid.

EXPERIMENTAL

Apparatus

All electrochemical measurements were made with a versatile electronic instrument previously described by DEFORD¹¹. It is based on the use of Philbrick operational amplifiers and is capable of performing chronopotentiometry, controlled-voltage coulometry and cyclic voltammetry by appropriate interconnection of the operational modules. Potential-time curves were recorded with a Sargent model SR strip-chart recorder, and cyclic voltammograms were obtained with a Moseley X-Y recorder, model 7030A.

The electrochemical cell, the reference electrode, and the platinum and gold electrode have been described previously¹². The areas of the platinum and gold electrodes were determined using ferricyanide in 0.5 *F* potassium chloride, assuming that the diffusion coefficient of ferricyanide is $7.67 \times 10^{-6} \text{ cm}^2 \text{ sec}^{-1}$.

A gas chromatographic system similar to that described by KYRYACOS AND

* On leave from the University of Oslo, Norway.

** On leave from the University of Redlands, Redlands, California.

Boord¹³ was used to attempt the detection of carbon monoxide in the reaction products. The apparatus was calibrated with a mixture of 10% carbon monoxide in nitrogen. The amounts of dissolved carbon dioxide and formic acid in the sample after electrochemical oxidation at controlled potential were determined by pH titration using conventional apparatus.

Reagents

A 0.1 *F* solution of tetraethylammonium perchlorate was used as supporting electrolyte. The salt, obtained from Eastman Organic Chemical Co., was recrystallized from doubly-distilled water, dried and stored in a vacuum desiccator. Dimethylsulfoxide (DMSO), obtained from J. T. Baker Co., was reagent-grade with a lot analysis of 0.05% water. Stock solutions of tetraethylammonium formate were prepared by adding an equivalent amount of 10% aqueous tetraethylammonium hydroxide to formic acid, removing the water by vacuum evaporation, and dissolving the residue in DMSO. The solution was standardized by titration with perchloric acid in DMSO¹⁰.

Tetraethylammonium formate is hygroscopic and the water could not be completely removed by vacuum evaporation. To investigate the effect of water and of excess hydroxide (which is rapidly decomposed in DMSO) on the oxidation of formate, a few solutions were prepared by adding known amounts of concentrated (25% w/w, aqueous) tetraethylammonium hydroxide and formic acid to de-aerated supporting electrolyte in the cell.

RESULTS

Chronopotentiometry

The oxidation of tetraethylammonium formate in DMSO gives well-defined one-step chronopotentiograms. The quarter-wave potential is +0.33 and -0.07 V vs. S.C.E. at a gold and a platinum electrode, respectively. As indicated in Table 1, the value of $i\tau^{1/2}/AC^0$ is practically constant which implies a diffusion-controlled process.

The reverse (cathodic) chronopotentiogram shows two small waves the sum of which is less than 1/3 of the forward anodic wave. The reverse waves appear at high

TABLE 1

CHRONOPOTENTIOMETRIC DATA FOR THE OXIDATION OF FORMATE IN DIMETHYLSULFOXIDE

Gold electrode ^a			Platinum electrode ^b		
<i>i</i> (μA)	τ (sec)	$i\tau^{1/2}/C^0A$ ($A\text{ cm sec}^{1/2}\text{ mole}^{-1}$)	<i>i</i> (μA)	τ (sec)	$i\tau^{1/2}/C^0A$ ($A\text{ cm sec}^{1/2}\text{ mole}^{-1}$)
120	3.35	213	120	3.15	212
100	4.92	215	100	4.46	214
70	10.1	216	70	9.45	214
50	20.2	217	50	18.9	216
40	32.3	220	40	30.2	219
		Av. 216			Av. 215

^a Area, 0.185 cm²; C^0 , 5.58×10^{-6} moles cm⁻³

^b Area, 0.226 cm²; C^0 , 4.44×10^{-6} moles cm⁻³

negative potentials (-1.2 and -1.9 V *vs.* S.C.E. at a gold electrode) and indicate an irreversible process. The potential-time relationship for such irreversible systems with mass transfer controlled by linear diffusion is given by¹⁴

$$E = -\frac{0.059}{(1-\alpha)n_a} \log \frac{nFC^0k_{b,h}^0}{i_0} - \frac{0.059}{(1-\alpha)n_a} \log \left[1 - \left(\frac{t}{\tau} \right)^{\frac{1}{2}} \right] \quad (1)$$

where E is the potential of the working electrode *vs.* the normal hydrogen electrode, $(1-\alpha)$ the anodic transfer coefficient, n_a the number of electrons in the rate-controlling step of the oxidation process, F the faraday, $k_{b,h}^0$ the heterogeneous rate constant for the oxidation (backward) reaction, i_0 the current density, C^0 the concentration of the electroactive species in the bulk of the solution in moles cm^{-3} , τ the transition time for oxidation in an unstirred solution and t the time after the electrolysis is started.

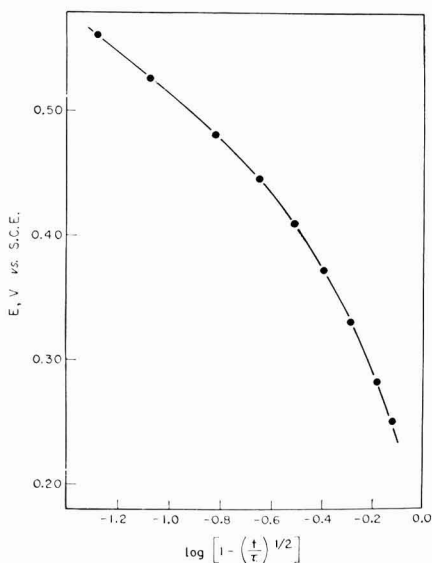


Fig. 1. Analysis of chronopotentiogram for oxidation of 5.58×10^{-3} F tetraethylammonium formate in dimethylsulfoxide at a gold electrode.

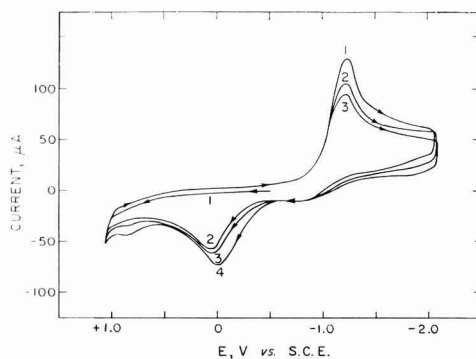


Fig. 2. Cyclic voltammograms of 3.44×10^{-3} F formic acid in dimethylsulfoxide. (1, 2 and 3), first, second and third cyclic potential sweeps, respectively; (4), obtained after electrolysis at -2.0 V for 30 sec. Scan rate, 0.2 V/sec.

This expression indicates that a plot of E *vs.* $\log [1 - (t/\tau)^{\frac{1}{2}}]$ should give a straight line. However, at a gold electrode (Fig. 1) the line is curved, which implies that the oxidation of formate is not a simple irreversible electrode reaction and that the value of $(1-\alpha)n_a$ is not constant during the electrolysis. Hence, a chemical reaction, an adsorption process, or more than one electroactive species, must be involved in the electrode process.

The reversed (cathodic) chronopotentiometric waves of formate in DMSO at a gold electrode occur at the potentials for reduction of formic acid ($E_{\tau/4} = -1.3$ V *vs.*

S.C.E.) and dissolved carbon dioxide ($E_{\tau/4} = -1.9$ V *vs.* S.C.E.) in the same medium, indicating that formic acid and carbon dioxide may be the overall oxidation products of formate.

Coulometry

Coulometric oxidations of formate at controlled potential have been performed to determine the number of electrons involved in the overall oxidation reaction. These experiments have been carried out using a small electrolysis cell with a Teflon stirring bar, and a gold foil (area, 35 cm²) as the anode, with the potential of the anode controlled at +0.60 V *vs.* S.C.E. The number of coulombs consumed in the oxidation of 42.1 ml of 6.40×10^{-3} *F* tetraethylammonium formate in DMSO is 28.1. The theoretical value for a one-electron oxidation is 26.0, which indicates that the overall oxidation of formate involves only one electron.

The oxidation products of formate have been determined by pH titrations of samples from the coulometric cell. Dissolved carbon dioxide has been determined by adding the sample to a solution containing an excess of sodium hydroxide and titrating with 0.01 *F* perchloric acid. The difference between the two pH breaks is equivalent to the amount of dissolved carbon dioxide in the sample. Additional samples, stripped with nitrogen to remove carbon dioxide (the loss of formic acid under these conditions is negligible), have been used to determine the formic acid and free hydrogen ions by titration with 0.01 *F* sodium hydroxide.

The pH titrations establish that 3.9×10^{-3} *F* carbon dioxide and 3.40×10^{-3} *F* formic acid are formed upon oxidation of 6.40×10^{-3} *F* formate.

Samples have been analyzed for carbon monoxide by gas chromatography, but no carbon monoxide was detected. Hence, the final oxidation products of one mole of formate in DMSO are $\frac{1}{2}$ mole of carbon dioxide and $\frac{1}{2}$ mole of formic acid.

Cyclic voltammetry

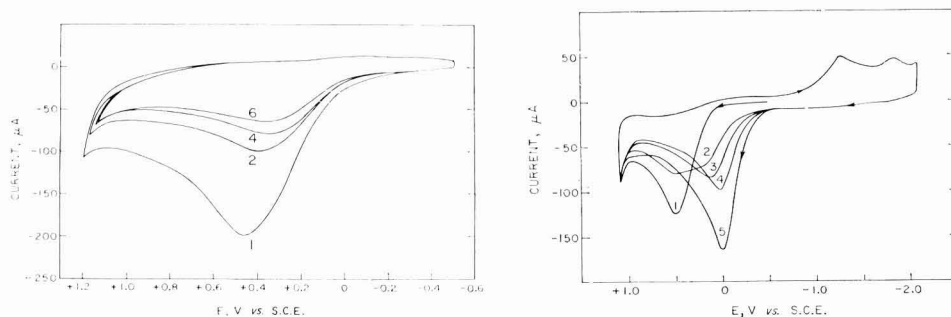
Voltammetric experiments have been performed using the same gold electrode and the same electrolysis cell as in chronopotentiometry.

Formic acid. Because the coulometric and chronopotentiometric data indicate that formic acid is formed upon oxidation of formate, experiments have been performed to determine the voltammetric behaviour of formic acid in DMSO. The residual current does not change during an anodic scan in the range -0.5 V to $+1.0$ V *vs.* S.C.E. upon addition of $2 \cdot 10^{-3}$ *F* formic acid to the supporting electrolyte (Curve 1, Fig. 2). However, a well-defined cathodic wave is observed at the reversed scan. The peak potential of this wave is -1.25 V *vs.* S.C.E. and the value, $i/\nu^{\frac{1}{2}}C^0A$, is essentially constant and independent of the scan rate, indicating a diffusion-controlled process. If the anodic scan is started at a potential more negative than the cathodic wave, a new anodic wave with peak potential close to 0 V *vs.* S.C.E. is observed (Curve 2, Fig. 2). When the cyclic scan is repeated between $+1.0$ V and -2.0 V *vs.* S.C.E. (without stirring the solution), the peak current of the cathodic wave decreases whereas that of the anodic wave increases. The anodic wave is never observed if the anodic scan is started at a potential more positive than the cathodic wave. However, the height of the anodic wave increases and the peak potential is shifted to less positive potentials with the time the electrode has been kept at potentials more negative than the cathodic wave (Curve 4, Fig. 2). Apparently, the anodic wave is due to oxidation

of the products formed by reduction of formic acid, whereas the acid itself is not electroactive in the potential range from -0.5 V to $+1.0$ V *vs.* S.C.E.

Hydroxide ion. Tetraethylammonium hydroxide in DMSO is oxidized at a gold electrode at potentials above $+0.8$ V *vs.* S.C.E. The peak current decreases with the time elapsed after mixing the solution, indicating that hydroxide ions are decomposed in DMSO. The peak potential is dependent on the scan rate and shifts from $+0.8$ V at $\nu=0.01$ V/sec to $+1.0$ V at $\nu=1.0$ V/sec. Hence, the second anodic peak observed on Curve 4, Fig. 2 is probably the oxidation wave of hydroxide ions formed during the reduction at -2.0 V.

Formate ion. Voltammograms of the tetraethylammonium formate stock solution exhibit a drawn-out oxidation wave with a peak potential of about $+0.4$ V *vs.* S.C.E. No cathodic wave is observed upon reversing the scan, indicating a completely irreversible reaction. When the cyclic scan is repeated between -0.5 V and $+1.0$ V without stirring the solution, the peak current decreases (Fig. 3) which indicates that the electrode reaction is partly inhibited by the oxidation products. When the anodic scan is followed by a cathodic sweep to more negative values, two small peaks appear at -1.25 V and -1.90 V *vs.* S.C.E., respectively, which are close to the potentials for the reverse chronopotentiometric waves.



Figs. 3-4. Cyclic voltammograms of 3.44×10^{-3} *F* tetraethylammonium formate in dimethylsulfoxide. (1, 2, 3, 4 and 6), first, second, third, fourth and sixth cyclic potential sweeps, respectively, (5), recorded after electrolysis at -2.0 V for 60 sec. Scan rate: (3) 0.5 V sec^{-1} ; (4) 0.2 V sec^{-1} .

If the cyclic scan is repeated between -2.0 V and $+1.0$ V, a new anodic peak is observed at potentials close to 0 V *vs.* S.C.E. (Fig. 4). This wave is probably identical with that one obtained upon oxidation of the reduction product of formic acid. To avoid complications from these products, voltammograms have been recorded by cyclic scans between -0.5 and $+1.0$ V *vs.* S.C.E.

A number of voltammograms have been recorded at different scan rates for different concentrations of tetraethylammonium formate solutions. At fast scan rates, a well-defined peak is observed. At low concentrations of formate, the anodic peak potential is shifted only slightly to more positive values with increasing scan rate. The peak potential, however, is shifted to more positive values and becomes increasingly dependent on the scan rate at higher concentrations of formate (Fig. 5). Voltammograms recorded at slower scan rates (less than 0.05 V/sec) are less well defined because the curve is divided into two poorly-developed peaks (Fig. 6). This implies that two oxidation processes occur at the electrode.

For irreversible anodic reactions the currents of which are limited by diffusion, DELAHAY¹⁵ has derived an expression for the peak current, i_p ,

$$i_p = 3.01 \times 10^5 n [n_a (1 - \alpha)]^{1/2} A D C^0 \nu^{1/2} \quad (2)$$

where n_a is the number of electrons on the rate-controlling step, $(1 - \alpha)$ the anodic transfer coefficient, A the area of the electrode, D the diffusion coefficient, and ν the scan rate.

According to this equation, the value of $i_p/\nu^{1/2} C^0$ should be constant, and independent of concentration and scan rate for a diffusion-controlled reaction. Figure 7

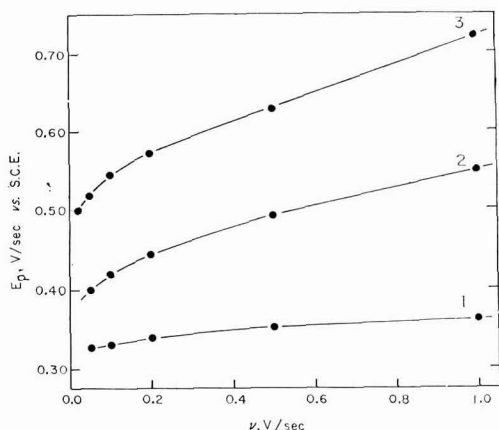


Fig. 5. Variation of peak potential with scan rate for tetraethylammonium formate. Concn. of formate: (1), 7.0×10^{-4} ; (2), 2.6×10^{-3} ; (3), 5.2×10^{-3} F.

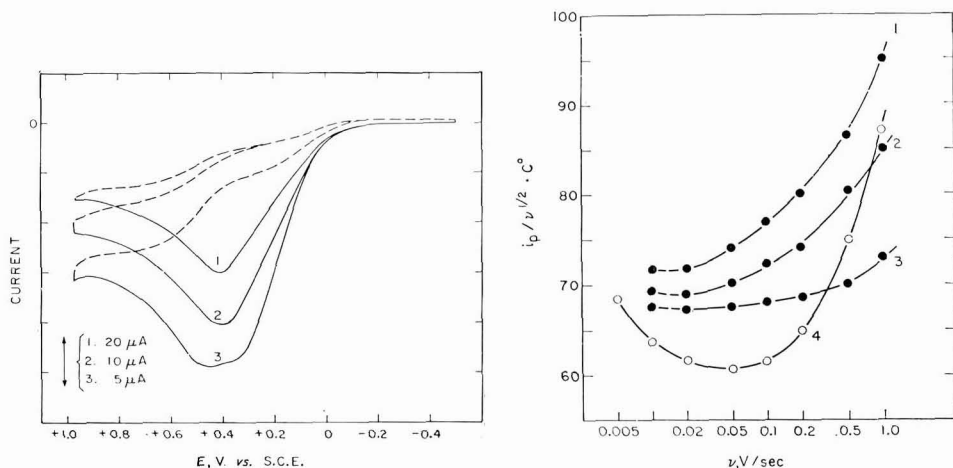


Fig. 6. Cyclic voltammograms of 2.6×10^{-3} F tetraethylammonium formate at different scan rates (ν): (1), 0.1; (2), 0.05; (3), 0.02 V/sec. (---), reverse (cathodic) potential sweeps.

Fig. 7. Variation of anodic peak current function ($i_p/\nu^{1/2} C^0$) with scan rate. Concn. of formate: (1), 7.0×10^{-4} ; (2), 1.35×10^{-3} ; (3), 5.2×10^{-3} F; (4), values for the first wave of a 1.72×10^{-3} F formate soln. which contains $< 0.1\%$ H₂O.

shows this quantity appears to approach a constant value at low scan rates. At faster scan rates, however, the current function increases and becomes increasingly dependent on the scan rate with decreasing concentrations of formate.

Because tetraethylammonium formate is hygroscopic, the variation of the peak potential and of the current function with increasing concentration of formate may be due to an increasing concentration of water in the solutions. To investigate the effect of water on the oxidation wave of formate, a few solutions have been prepared by mixing concentrated (25% w/w, aqueous) tetraethylammonium hydroxide with an

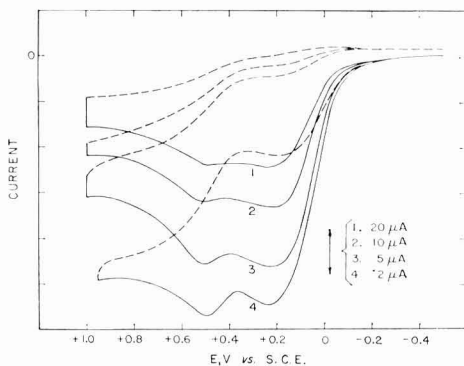


Fig. 8. Cyclic voltammograms of $1.72 \times 10^{-3} F$ formate in dimethylsulfoxide containing $< 0.1\%$ H_2O . (---), reverse (cathodic) potential sweep. Scan rates: (1), 0.2; (2), 0.1; (3), 0.05; (4), 0.01 V/sec.

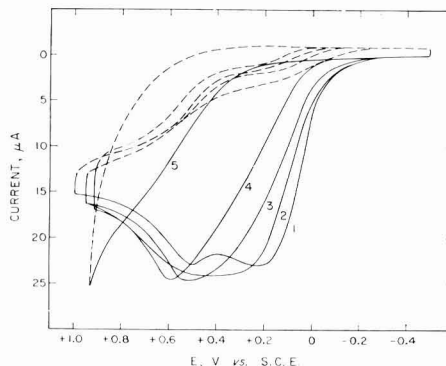


Fig. 9. Effect of water on cyclic voltammograms of $1.72 \times 10^{-3} F$ formate in dimethylsulfoxide. Concn. of water: (1), 0.1; (2), 0.2; (3), 1.0; (4), 4; (5), 40%, (---), reverse (cathodic) sweep. Scan rate 0.05 V/sec. Currents not corrected for dilution.

TABLE 2

EFFECT OF WATER ON THE VOLTAMMETRIC OXIDATION OF FORMATE IN DIMETHYLSULFOXIDE AT A GOLD ELECTRODE

Scan rate ($V \text{ sec}^{-1}$)	E_{p1} ($V \text{ vs. S.C.E.}$)	E_{p2}	i_t (μA)	$i_t/v^{\frac{1}{2}}C^0$ ($A \text{ sec}^{\frac{1}{2}} \text{ cm}^3 V^{-\frac{1}{2}} \text{ mole}^{-1}$)
A. (H_2O), 0.1%				
1.00	0.30		150	87.0
0.50	0.25 to 0.35		91	75.0
0.20	0.22	0.50	50	65.0
0.10	0.22	0.50	33.5	61.5
0.05	0.21	0.51	23.5	60.5
0.02	0.22	0.50	15.0	61.5
0.01	0.23	0.50	11.0	64.0
0.005	0.23	0.50	8.3	68.5
B. (H_2O), 0.2%				
1.00	0.42		138	80.0
0.50	0.42		91	75.0
0.20	0.41		54	70.5
0.10	0.40		36	66.5
0.05	0.34 to 0.46		23.5	60.5
0.02	0.26	0.54	15.0	61.5
0.01	0.25	0.60	10.5	61.0
0.005	0.24	0.62	7.5	61.5

equivalent amount of formic acid in dimethylsulfoxide containing 0.027% water. Voltammograms of these solutions (in which the total concentration of water is less than 0.1%) exhibit two peaks at all scan rates below 0.5 V/sec, indicating that two oxidation processes occur at the electrode even at fast sweep rates (Fig. 8). In addition to the absence of cathodic waves, both waves are drawn out indicating that a chemical reaction is coupled between two irreversible charge transfers¹⁵. As indicated in Table 2, the peak potential of both waves is constant at scan rates below 0.2 V/sec. The value of $i/p^{1/2}C^0$ for the first wave is approximately the same as that for the single wave obtained for the formate stock solution (Fig. 7). The current function increases, however, at low scan rates, indicating that kinetic effects are involved in the electrode reaction and become more important as the scan rate decreases.

The addition of small amounts of water to the solution has no immediate effect on the voltammograms. After 10–20 min stirring, however, the peak height of the first wave decreases and only one drawn-out wave is obtained at fast scan rates (Table 2). The current function of the first wave for this solution does not increase at slow scan rates, indicating that the kinetic effects are suppressed by the presence of water.

With a further increase in the water concentration only one wave is obtained at all sweep rates and the peak potential is shifted to more positive values with increasing concentration of water. In the presence of 40% water the entire wave is obliterated (Fig. 9).

The addition of a 100% excess of formic acid to a formate solution has no significant effect on the voltammograms. However, upon addition of excess tetraethylammonium hydroxide, a new oxidation wave appears at potentials close to 0 V *vs.* S.C.E. The peak current of this wave increases and the peak potential is shifted to less positive potentials with increasing amounts of hydroxide. This wave is probably identical with the anodic wave obtained after electrolyzing formic acid or formate at –2.0 V (which generates hydroxide ions in the solution). The peak current of this wave decreases upon addition of water to the solution, indicating that the electrode reaction is inhibited by the presence of water.

DISCUSSION AND CONCLUSIONS

The coulometric experiments establish that the electrochemical oxidation of formate in dimethylsulfoxide is a one-electron process and that $\frac{1}{2}$ mole of carbon dioxide and $\frac{1}{2}$ mole of formic acid are formed/mole of formate electrolyzed. The formation of these products has also been confirmed by reverse chronopotentiometry and by cyclic voltammetry. Hence, the overall oxidation of formate is represented by



Cyclic voltammetry indicates, however, that two oxidation reactions take place at the electrode and that a slow chemical or adsorption process is coupled between the two charge transfers. An intermediate adsorbed radical probably is thus involved in the electrode reaction. A mechanism is proposed which accounts for this and which has been suggested previously for the oxidation of formate in anhydrous formic acid⁹,





If these reactions go to completion, the overall process is represented by eqn. (3). Reaction (5a) is probably slow such that reaction (6) is favoured at fast scan rates. Only one drawn-out wave is observed for fast scan rates which implies that reactions (4) and (6) occur at almost the same potential. When the voltammograms are recorded at very fast scan rates, reactions (4) and (6) may occur before reaction (7) is complete. This would cause the peak current to increase with increasing scan rate and the value of $i/v^{1/2}C^0$ to become greater than expected for an overall one-electron reaction.

Voltammograms recorded at slow scan rates exhibit two well-defined peaks at +0.2 V and +0.5 V *vs.* S.C.E., corresponding to reactions (4) and (5b), respectively. The free radical, $\cdot\text{HCOO}$, is apparently adsorbed on the electrode during the first charge transfer. This adsorbed species probably inhibits further electron transfer at +0.2 V and causes the peak current to decrease. At extremely slow scan rates, reaction (5a) appears to go to completion such that $\cdot\text{HCOO}$ is decomposed and the peak current can increase (Curve 4, Fig. 7).

In the presence of small amounts of water, the two peaks are observed only at slower scan rates and the current function of the first wave does not increase at the slowest scan rates (Table 2). This implies that $\text{H}\cdot$ is not stable and that reaction (6) is favored in the presence of small amounts of water. Upon the addition of an increasing amount of water the peak potential is shifted to more positive values (Fig. 9) which implies that the hydrated formate ion $[\text{HCOO}(\text{H}_2\text{O})^-]$ is more stable and not as easily oxidized as the simple formate ion. The shift in the peak potential as well as the variation of $i/v^{1/2}C^0$ with increasing concentration of formate (Figs. 5 and 7) is probably the result of an increasing amount of water.

Chronopotentiometric experiments indicate a diffusion-controlled reaction. However, these experiments have been performed in the presence of small amounts of water. Cyclic voltammetry of a similar solution (Curve 3, Fig. 7) gives a fairly constant "diffusion-controlled" value for $i/v^{1/2}C^0$ at scan rates from 0.02–0.2 V/sec (a time-scale comparable to the chronopotentiometric transition times).

In the presence of excess hydroxide ion, the oxidation of formate occurs at potentials close to 0 V *vs.* S.C.E. When the hydroxide is produced electrolytically (*i.e.*, without introduction of water) the peak current is greater than for formate alone (Fig. 4), which implies an overall 2-electron oxidation.



The peak current decreases in the presence of water, which may indicate that an unstable free radical intermediate also is involved in this electrode reaction. The mechanism is probably represented by reactions (4), (5a), (5b) and (6), but the presence of excess hydroxide ion prevents reaction (7) and thereby gives an overall two-electron process with one mole of formate giving one mole of carbon dioxide.

ACKNOWLEDGEMENT

This work was supported by the National Science Foundation under Grant No. GP 4303.

SUMMARY

The electrochemical oxidation of formate in dimethylsulfoxide has been studied by chronopotentiometry, controlled-potential coulometry, and cyclic voltammetry at gold electrodes. The oxidation products are carbon dioxide and hydrogen ions, which react with formate ion. Thus, the overall reaction is a one-electron oxidation in which one-half mole of carbon dioxide and one-half mole of formic acid are formed for each mole of formate ion electrolyzed. Cyclic voltammetry indicates that adsorbed free radical intermediates are involved in the oxidation process and that these are coupled between two irreversible charge transfers. Oxidation mechanisms are proposed which are consistent with the data.

REFERENCES

- 1 M. W. BREITER, *Electrochim. Acta*, **8** (1963) 447, 457.
- 2 R. A. MUNSON, *J. Electrochem. Soc.*, **111** (1964) 372.
- 3 C. LIANG AND T. C. FRANKLIN, *Electrochim. Acta*, **9** (1964) 517.
- 4 W. VIELSTICH AND V. VOGEL, *Ber. Bunsenges. Physik. Chem.*, **68** (1964) 688.
- 5 M. W. BREITER, *J. Electrochem. Soc.*, **111** (1964) 1298.
- 6 D. R. RHODES AND E. F. STEIGELMANN, *J. Electrochem. Soc.*, **112** (1965) 16.
- 7 S. B. BRUMMER, *J. Phys. Chem.*, **69** (1965) 1363.
- 8 V. S. BAGOTZKY AND YU. B. VASSILIEV, *Electrochim. Acta*, **11** (1966) 1439.
- 9 B. E. CONWAY AND M. DZIECIUCH, *Can. J. Chem.*, **41** (1963) 21, 38, 55.
- 10 L. V. HAYNES AND D. T. SAWYER, *Anal. Chem.*, **39** (1967) 411.
- 11 D. D. DEFORD, private communication, presented at the 133rd American Chemical Society Meeting, San Francisco, California, 1958.
- 12 J. L. ROBERTS, JR. AND D. T. SAWYER, *J. Electroanal. Chem.*, **12** (1966) 90.
- 13 G. KYRYACOS AND C. E. BOORD, *Anal. Chem.*, **29** (1957) 787.
- 14 P. DELAHAY, *New Instrumental Methods in Electrochemistry*, Interscience, New York, 1954.
- 15 R. S. NICHOLSON AND I. SHAIN, *Anal. Chem.*, **37** (1965) 178.

J. Electroanal. Chem., **16** (1968) 351-360

ELECTROCHEMICAL OXIDATION OF OXALATE ION IN DIMETHYLSULFOXIDE AT A GOLD ELECTRODE

EINAR JACOBSEN* AND DONALD T. SAWYER

Department of Chemistry, University of California, Riverside, Calif. 92502 (U.S.A.)

(Received July 31st, 1967)

Oxalic acid is oxidized readily in aqueous solutions with platinum and gold electrodes at a potential above $+0.8$ V *vs.* S.C.E. by a mechanism which involves adsorption of oxalic acid prior to electron transfer¹⁻⁵. The oxidation is a two-electron process which gives carbon dioxide and hydrogen ions as products. The undissociated acid is probably the reacting species with the second charge transfer the rate-determining step⁴. When the pH of the supporting electrolyte is increased above pH 3, the electrode reaction is inhibited; oxidation of oxalic acid does not occur in alkaline media²⁻⁴.

The electrochemical oxidation of oxalic acid in non-aqueous media has not been investigated to the best of our knowledge. However, during a recent electrochemical study of dissolved carbon dioxide and its reduction products in dimethylsulfoxide⁶, oxalate ion was observed to give a chronopotentiometric oxidation wave at a gold electrode. The present discussion summarizes the results of a detailed investigation of the electrochemical oxidation of oxalate ion in dimethylsulfoxide at a gold electrode.

EXPERIMENTAL

Apparatus

All electrochemical measurements were made with a versatile electronic instrument based on the use of Philbrick operational amplifiers⁷. This instrument was capable of performing chronopotentiometry and cyclic voltammetry by appropriate interconnection of the operational modules. Potential-time curves were recorded with a Sargent model SR strip-chart recorder and cyclic voltammograms were obtained with a Moseley Model 7030A X-Y recorder.

The reference electrode, the electrochemical cell and the gold electrode have been described previously⁶. The area of the gold electrode was determined by chronopotentiometry to be 0.185 cm² using ferricyanide ion in 0.5 *F* potassium chloride; the diffusion coefficient of ferricyanide ion was assumed to be 7.67×10^{-6} cm² sec⁻¹⁸. All potentials are reported *versus* the aqueous saturated calomel electrode (S.C.E.).

Reagents

A 0.1 *F* solution of tetraethylammonium perchlorate in dimethylsulfoxide was used as supporting electrolyte. The salt, obtained from Eastman Organic Chemical

* On leave from the University of Oslo, Norway

Co., was recrystallized from doubly-distilled water, dried and stored in a vacuum desiccator. Dimethylsulfoxide (DMSO), obtained from J. T. Baker Co., was reagent-grade with a lot analysis of 0.05% water.

Sodium, lithium and ammonium oxalate are insoluble in DMSO at the $5 \cdot 10^{-3}$ *F* level. Tetraethylammonium oxalate was prepared by adding equivalent amounts of tetraethylammonium hydroxide to oxalic acid and removing the water by vacuum evaporation. The residue, however, was very hygroscopic and did not dissolve completely in DMSO. Hence, the drying was omitted and all oxalate solutions were prepared by adding known amounts of tetraethylammonium hydroxide and oxalic acid to the supporting electrolyte.

A 0.1 *F* stock solution of oxalic acid (which dissolved readily in DMSO) was prepared by dissolving the appropriate amount of oxalic acid (Baker and Adamson) in 100 ml of DMSO. Tetraethylammonium hydroxide (25% w/w aqueous solution obtained from Matheson, Coleman and Bell) was standardized against oxalic acid in DMSO by potentiometric titration⁶. As indicated by curve A of Fig. 1, two sharp

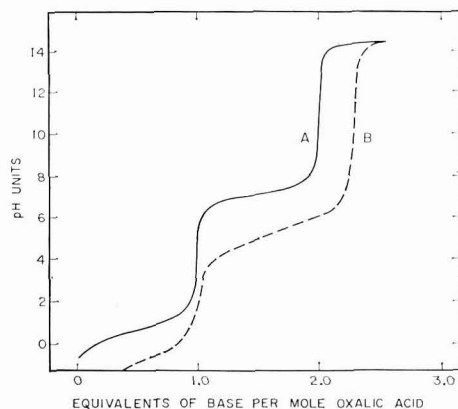


Fig. 1. (A), Potentiometric titration of $2 \cdot 10^{-2}$ *F* oxalic acid in DMSO (containing 0.1 *F* tetraethylammonium perchlorate and 1% water) with tetraethylammonium hydroxide; (B), back-titration with perchloric acid after exposure of soln. to air for 2 h.

breaks in the titration curve were obtained after addition of one and two equivalents of base, respectively. The same curve was obtained when the solution was back-titrated with perchloric acid in DMSO, provided that an atmosphere of purified nitrogen was maintained over the solution and that the titration was completed within one hour. However, if the oxalate solutions were exposed to air the oxalate began to decompose to give curve B in Fig. 1. The latter curve indicates that a weak base was formed at the expense of the strong base when the oxalate solution was exposed to air. The decomposition product may have been bicarbonate ion formed by the reaction



To avoid decomposition of oxalate ion and to keep the total amount of water as

low as possible, known amounts of the oxalic acid stock solution and of concentrated (25% w/w, 1.718 *F*) tetraethylammonium hydroxide were added to de-aerated supporting electrolyte in the cell, by means of micropipettes, just prior to the measurements. The total amount of water in the solution after addition of the reagents was approximately 0.1%.

RESULTS

Chronopotentiometry

Oxalic acid in DMSO is not oxidized at potentials below +1.2 V *vs.* S.C.E. At higher potentials, a chronopotentiometric wave with an E_4 -value of +1.25 V is observed. This wave may be due to the oxidation of oxalic acid but the transition time is highly dependent on the pre-conditioning of the electrode. Therefore, the wave is probably due, at least in part, to the oxidation of the gold electrode.

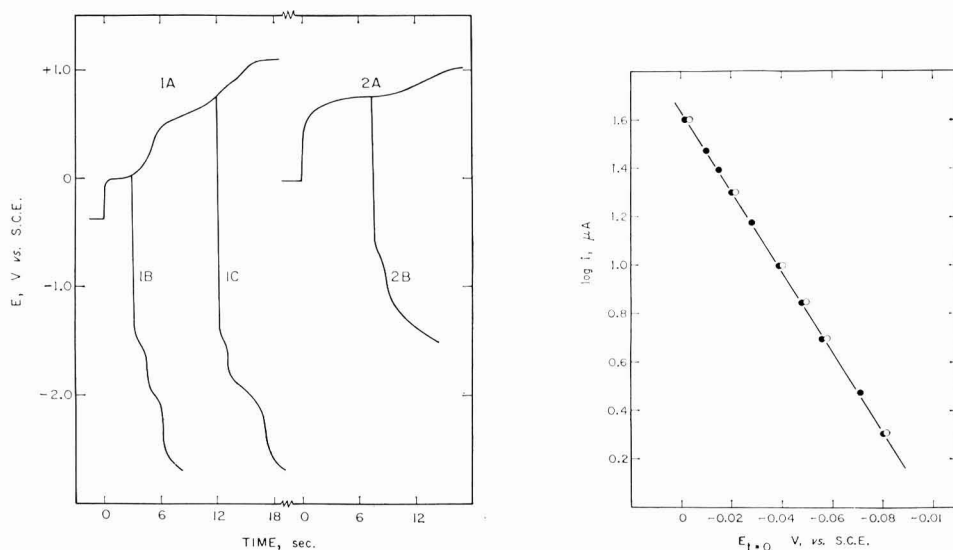


Fig. 2. Chronopotentiograms for oxidation of 1.8×10^{-3} *F* oxalic acid in the presence of 1 (curve 1) and 2 (curve 2) equiv. tetraethylammonium hydroxide/mole oxalic acid in DMSO. Curves B and C, waves for current reversal. Current, 30 μ A (curve 1) and 20 μ A (curve 2).

Fig. 3. (●), Plot of $E_{t=0}$ *vs.* $\log i$ for galvanostatic oxidation of 1.72×10^{-3} *F* oxalate ion in DMSO at a gold electrode; (○), values after addition of 100% excess hydroxide (4 equiv. hydroxide ion/mole oxalic acid).

Upon the addition of tetraethylammonium hydroxide to oxalic acid in DMSO, an oxidation wave is observed with an E_4 -value of +0.72 V *vs.* S.C.E. (curve 2, Fig. 2). The transition time of this wave (at constant current density) increases with increasing amounts of hydroxide ion and reaches a limiting value at a concentration of one equivalent of hydroxide ion/mole of oxalic acid. For a solution containing 1.8×10^{-3} *F* oxalic acid plus 1.8×10^{-3} *F* tetraethylammonium hydroxide, the chronopotentiometric constant, $i\tau^{1/2}/AC^0$, has an average value of 198 ± 6 A cm sec^{1/2} mole⁻¹ for tran-

sition times from 1–20 sec (see eqn.(1)). A small reverse chronopotentiometric wave (cathodic) is observed with an $E_{0.22}$ -value of -0.75 V which is close to the potential for reduction of oxygen in DMSO⁹. Another interesting point is that tetraethylammonium hydroxide in the absence of oxalic acid gives an independent chronopotentiometric oxidation wave with an E_4 -value of approximately $+0.8$ V *vs.* S.C.E.

On the addition of more than one equivalent of tetraethylammonium hydroxide/mole of oxalic acid, a new oxidation wave appears on the chronopotentiogram at a less positive potential. A typical chronopotentiogram of oxalate ion (two equivalents of tetraethylammonium hydroxide/mole of oxalic acid) is illustrated by curve 1, Fig. 2. A well-defined oxidation wave with an E_4 -value of 0.0 V *vs.* S.C.E. is followed by two poorly-defined waves which appear at potentials close to that for the oxidation wave of hydroxide ion.

If mass transfer is controlled by linear diffusion in an unstirred solution, then the Sand equation is applicable¹⁰

$$i\tau^{\frac{1}{2}} = \frac{1}{2}nF\pi^{\frac{1}{2}}D^{\frac{1}{2}}AC^0 \quad (2)$$

where i is the current, τ the transition time, n the number of electrons involved in the overall reaction, F the faraday, D the diffusion coefficient, A the electrode area and C^0 the bulk concentration. The chronopotentiometric data summarized in Table 1 establish that the value of $i\tau^{\frac{1}{2}}/AC^0$ for the first oxidation wave of oxalate ion decreases with decreasing current density, whereas the corresponding value for the sum of the three waves is constant. In the presence of a large excess of tetraethylammonium

TABLE 1

CHRONOPOTENTIOMETRIC DATA FOR THE OXIDATION OF OXALATE ION IN DMSO AT A GOLD ELECTRODE

i (μA)	τ_1 (sec)	$(\tau_1 + \tau_2 + \tau_3)$ (sec)	$i\tau_1^{\frac{1}{2}}/AC^0$ ($A \text{ cm sec}^{\frac{1}{2}} \text{ mole}^{-1}$)	$i(\tau_1 + \tau_2 + \tau_3)^{\frac{1}{2}}/AC^0$ ($A \text{ cm sec}^{\frac{1}{2}} \text{ mole}^{-1}$)
A. 1.72×10^{-3} <i>F</i> oxalic acid plus 3.44×10^{-3} <i>F</i> tetraethylammonium hydroxide				
80	1.00	1.85	252	342
70	1.14	2.36	236	339
60	1.43	3.30	226	342
50	1.90	4.85	217	346
40	2.70	7.30	207	339
35	3.40	9.65	203	342
30	4.40	13.0	198	339
25	5.80	19.1	189	342
20	8.10	28.6	178	336
15	12.9	—	169	—
10	26.4	—	161	—
B. 1.72×10^{-3} <i>F</i> oxalic acid plus 6.88×10^{-3} <i>F</i> tetraethylammonium hydroxide				
90	0.94		274	
80	1.18		274	
70	1.56		274	
60	2.10		274	
50	2.60		254	
40	3.78		245	
30	5.80		228	
20	10.6		205	
15	16.5		192	

hydroxide, the transition time of the first wave increases and a constant value for $i\tau^{1/2}/AC^0$ is obtained at high current densities (section B, Table 1). The effect of excess hydroxide ion on the second and third oxidation waves of oxalate ion cannot be studied because they are masked by the oxidation wave for hydroxide ion.

Curves 1B and 1C in Fig. 2 represent the chronopotentiometric waves obtained by current reversal. Two reverse waves with $E_{0.22}$ -values of -1.5 and -1.95 V, respectively, are observed even if the current is reversed before the transition time of the first wave (curve C, Fig. 2). The transition time of the second reverse wave increases with increasing time of electrolysis before current reversal, whereas that of the first decreases slightly. However, the sum of the two transition times appears to be much greater than $\frac{1}{3}$ of the electrolysis time in the forward reaction, indicating that the oxidation products are adsorbed on the electrode.

When the current is reversed just before the transition time of the third oxidation wave, a small prewave at about -0.7 V is observed on the reverse chronopotentiogram. This wave is probably from the oxidation product of the third oxidation wave for oxalate ion.

The chronopotentiogram in Fig. 2 indicates that the oxidation of oxalate ion in DMSO is a highly irreversible process. For such constant-current processes the potential-time relationship has been derived for an electrode reaction in unstirred solution where mass transfer is controlled by linear diffusion¹⁰. For an oxidation process at 25° this may be expressed as

$$E = \frac{-0.0592}{(1-\alpha)n_a} \log \frac{nFAC^0 k_{b,h}^0}{i} - \frac{0.0592}{(1-\alpha)n_a} \log [1 - (t/\tau)^{1/2}] \quad (3)$$

where E is the potential of the working electrode *vs.* NHE, α the transfer coefficient, n_a the number of electrons in the rate-determining step, A the electrode area, F the faraday, $k_{b,h}^0$ the heterogeneous rate constant for the oxidation reaction, C^0 the concentration of the electroactive species in the bulk of the solution, τ the transition time, and t the time of electrolysis. When t is zero, eqn. (3) reduces to

$$E_{t=0} = \{-0.0592/(1-\alpha)n_a\} \log(nFAC^0 k_{b,h}^0/i) \quad (4)$$

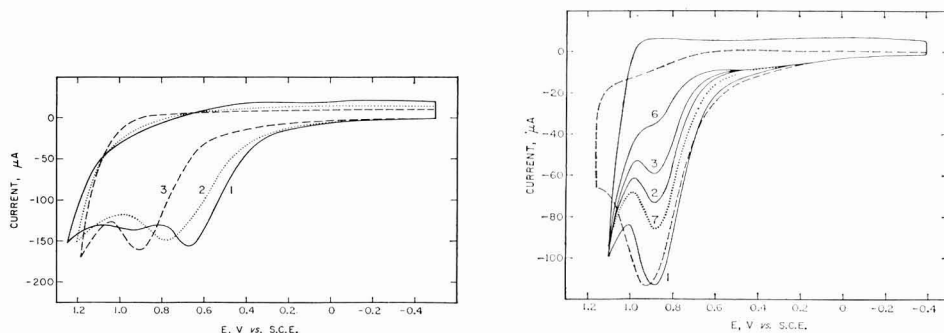
Equation (3) indicates that $(1-\alpha)n_a$ can be evaluated from the slope of a plot of E *vs.* $\log(\tau^{1/2} - t^{1/2})$ for the chronopotentiometric wave. The value of $(1-\alpha)n_a$ can also be evaluated from the slope of a plot of $E_{t=0}$ *vs.* $\log i$ through the use of eqn. (4).

By applying a constant current and recording the potential of the working electrode as a function of time, the value of $E_{t=0}$ can be obtained by extrapolation of the potential-time curve to zero-time. A plot based on eqn. (4) for the first oxidation wave of oxalate ion is illustrated in Fig. 3. The slope of the line gives a value for $(1-\alpha)n_a$ of 0.98 which implies a two-electron oxidation. A plot of E_t *vs.* $\log(\tau^{1/2} - t^{1/2})$ for the chronopotentiometric wave gives a curved line which indicates that the initial two-electron reaction is probably followed by a complicating slow adsorption or chemical process. Identical plots of $E_{t=0}$ *vs.* $\log i$ are obtained for oxalate ion in the absence and in the presence of a large excess of hydroxide ion. Hence, the electrode reaction must be the same for both solutions and the decrease in $i\tau^{1/2}/AC^0$ with decreasing current density for the first oxidation wave of oxalate ion (Table 1) is probably the result of a secondary chemical process which is hindered by excess hydroxide ion.

The potential-time curves of oxalic acid in the presence of one equivalent of hydroxide ion/oxalic acid are curved and do not allow even an approximate value for $E_{t=0}$ to be obtained. A plot of E_t vs. $\log(\tau^{\frac{1}{2}} - t^{\frac{1}{2}})$ for this solution also gives a curved line. The shape of the chronopotentiometric potential-time curve (curve 2, Fig. 2) indicates that two electrode reactions occur at almost the same potential and that the value of $(1-\alpha)n_a$ cannot be determined for these solution conditions.

Cyclic voltammetry

Cyclic voltammograms of supporting electrolyte for the voltage range -0.5 to $+1.0$ V do not change upon addition of oxalic acid, which establishes that oxalic acid in DMSO is not oxidized at a gold electrode for this potential range. When tetraethylammonium hydroxide is added to the oxalic acid solution, a well-defined anodic wave appears on the voltammograms. The peak current increases with increasing concentration of hydroxide ion and reaches a limiting value when one equivalent of hydroxide ion is added/mole of oxalic acid. As indicated by Fig. 4, the recorded peak potential is highly dependent on the time elapsed after mixing the solution. Immediately after mixing, the peak potential is $+0.68$ V, but it shifts rapidly to more positive values. Ten minutes after the addition of hydroxide ion, the peak potential becomes constant ($+0.9$ V at a scan rate of 1 V/sec) and no further shift in the peak potential is observed during the next 2 h.



Figs. 4-5. Cyclic voltammograms of 1.72×10^{-3} F oxalic acid plus 1.72×10^{-3} F tetraethylammonium hydroxide in DMSO. Fig. 4: (1), 1; (2), 4; (3), 10 min after addition of hydroxide ion recorded. Scan rate, 1 V sec $^{-1}$. Fig. 5: recorded 15 min after soln. preparation. (1, 2, 3, 6), 1st, 2nd, 3rd, 6th cyclic scans, respectively; (7), recorded after electrode held at -0.4 V in unstirred soln. for 30 sec (following 6th scan). (---), voltammogram of 1.72×10^{-3} F tetraethylammonium hydroxide in DMSO in absence of oxalic acid. Scan rate, 0.5 V sec $^{-1}$.

The voltammetric data for aged one-to-one oxalic acid-tetraethylammonium hydroxide solutions are summarized in Table 2. The value of $i_p/v^{\frac{1}{2}}C^0$ decreases with decreasing scan rate which indicates that the electrode reaction is not diffusion-controlled. The peak current also decreases upon repeating the cyclic scan between -0.4 and $+1.0$ V (Fig. 5); this indicates that the oxidation product is adsorbed on the electrode and probably inhibits further oxidation. However, the peak current again increases if the electrode is kept in the unstirred solution at -0.4 V for a short time before repeating the anodic potential sweep (curve 7, Fig. 5). This implies that the adsorbed oxidation product is rapidly decomposed. Voltammograms recorded at slow scan rates (less than 0.01 V/sec) do not exhibit a significant decrease in peak

TABLE 2

VOLTAMMETRIC DATA FOR THE OXIDATION OF TETRAETHYLAMMONIUM HYDROXIDE IN DMSO AT A GOLD ELECTRODE

All data obtained 10–60 min after solution preparation

Scan rate (V/sec)	E_p (V. vs. S.C.E.)	i_p (μA)	$i_p/v^{1/2}C^0$ ($A \text{ sec}^{1/2} \text{ cm}^3 \text{ V}^{-1/2} \text{ mole}^{-1}$)
A. $1.72 \times 10^{-3} F$ hydroxide ion in the presence of $1.72 \times 10^{-3} F$ oxalic acid			
1.0	0.92	160	93.0
0.5	0.89	113	93.0
0.2	0.87	71	92.5
0.1	0.84	49.0	90.2
0.05	0.83	34.5	89.5
0.02	0.82	21.5	88.5
0.01	0.82	15.2	88.5
0.005	0.81	10.7	88.0
B. $1.72 \times 10^{-3} F$ hydroxide ion in the absence of oxalic acid			
1.0	0.95	170	99.0
0.5	0.92	113	93.0
0.2	0.90	65	84.7
0.1	0.87	42	77.2
0.05	0.86	29.2	75.6
0.02	0.83	18.0	74.0
0.01	0.82	12.6	73.5
0.005	0.80	8.9	73.0

current at the second and following cyclic scans; this also indicates a rapid decomposition of the adsorbed products. Reproducible peak currents are obtained at all scan rates by stirring the solution for one minute between each cyclic potential sweep. The peak current decreases slowly (a few %/hour) with the time elapsed after mixing the solution and is probably due to a slow decomposition of the electroactive species.

Voltammetric data for the oxidation of tetraethylammonium hydroxide in DMSO in the absence of oxalic acid are also included in Table 2 and Fig. 5. A peak at +0.65 V is not observed immediately after mixing the solution. However, the peak potential as well as the peak current are essentially the same as those obtained for the one-to-one oxalic acid–tetraethylammonium hydroxide solutions 10 min after preparation. The voltammograms of tetraethylammonium hydroxide do not change upon addition of excess oxalic acid.

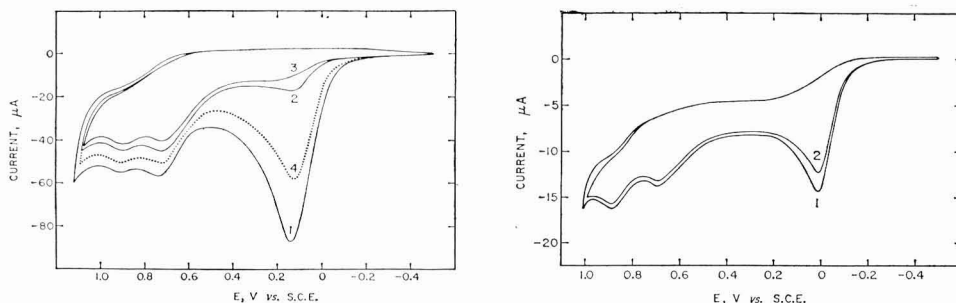
Apparently, when aqueous hydroxide is added to oxalic acid in DMSO, the first reaction product is the acid oxalate ion ($H(COO)_2^-$) which is oxidized at +0.68 V to give curve 1 in Fig. 4. After a few minutes, however, the acid oxalate ion hydrolyzes to oxalic acid (which is not oxidized) and DMSO solvated hydroxide ions; the latter are oxidized at +0.8 to +0.9 V. If tetraethylammonium hydroxide is dissolved in DMSO before the addition of oxalic acid, the hydroxide ions are so strongly solvated that essentially no acid oxalate ion is formed and only the oxidation wave for hydroxide ion is observed. Upon the addition of more than one equivalent of tetraethylammonium hydroxide/mole of oxalic acid a new well-defined peak appears on the voltammograms at a less positive potential. A typical voltammogram recorded for a solution of oxalic acid in the presence of two equivalents of hydroxide ion is illustrated in Fig. 6. Voltammograms recorded at fast scan rates exhibit two anodic peaks at

TABLE 3
VOLTAMMETRIC DATA FOR THE OXIDATION OF OXALATE ION IN DMSO AT A GOLD ELECTRODE
1.72 $\times 10^{-3}$ F oxalic acid and 3.44 $\times 10^{-3}$ F tetraethylammonium hydroxide

Scan rate (V sec ⁻¹)	$\frac{(E_p)_1}{(V \text{ vs. S.C.E.})}$	$\frac{(E_p)_2}{(E_p)_3}$	$\frac{(i_p)_1}{(\mu A)}$	$\frac{(i_p)_2}{(i_p)_3}$	$\frac{(i_p)_1/\nu^{\frac{1}{2}}}{(\mu A \text{ sec}^{\frac{1}{2}} V^{-\frac{1}{2}})}$	$\frac{(i_p)_2/\nu^{\frac{1}{2}}}{(i_p)_3/\nu^{\frac{1}{2}}}$	$\frac{[(i_p)_1 + (i_p)_2]/\nu^{\frac{1}{2}} C^0}{(A \text{ cm}^2 \text{ sec}^{\frac{1}{2}} V^{-\frac{1}{2}} \text{ mole}^{-1})}$
1.0	0.25	0.75	215	27	215	27	141
0.5	0.18	0.75	150	22	212	31	141
0.2	0.14	0.73	87	20	195	45	139
0.1	0.10	0.72	58	17.5	183	55	138
0.05	0.07	0.71	38	15.0	170	67	138
0.02	0.04	0.70	22.0	9.0	155	63	127
0.01	0.02	0.70	14.5	5.5	145	55	116
0.005	0.01	0.70	9.5	3.5	134	50	107

+0.1 and +0.7 V, respectively. However, at slower scan rates, a third peak at +0.9 V (probably due to oxidation of hydroxide ions) appears on the voltammograms.

Solutions containing two equivalents of tetraethylammonium hydroxide/mole of oxalic acid appear to be more stable than acid oxalate ion solutions. The peak potentials do not shift with time and only a slight decrease in the peak currents is observed 3 h after mixing the solution.



Figs. 6-7. Voltammograms of $1.72 \times 10^{-3} F$ oxalic acid plus $3.44 \times 10^{-3} F$ tetraethylammonium hydroxide in DMSO. (1-3), 1st, 2nd, 3rd cyclic scans, respectively; (4), recorded after electrode held at -0.4 V for 30 sec (following 3rd scan). Fig. 6, scan rate 0.2 V sec^{-1} . Fig. 7, scan rate 0.01 V sec^{-1} .

When cyclic scans are repeated between -0.4 and $+1.0$ V, the peak current of the first wave decreases (Fig. 6). A decrease in the peak current is also observed if the potential sweep is reversed at $+0.4$ V, which indicates that the oxidation product from the first electrode reaction is also adsorbed on the electrode. The adsorbed products, however, are decomposed fairly rapidly. Voltammograms recorded at slow scan rates show only a slight decrease in the peak current at the second and the following scan (Fig. 7) and the peak current (recorded at fast scan rates) increases again if the electrode is kept at -0.4 V a short time before the next anodic potential sweep (curve 4, Fig. 6). If the solution is stirred for one minute between each experiment the peak currents are perfectly reproducible.

Voltammetric data for a one-to-two oxalic acid-tetraethylammonium hydroxide solution in DMSO are given in Table 3. The peak currents of the second and third waves have been measured from the extension of the preceding wave. The third wave is not completely separated from the second wave and only approximate values for its peak current can be measured. As indicated in Table 3, the values of $i_p/\nu^{1/2}$ for all three waves are dependent on the scan rate. The electrode reactions are thus not diffusion-controlled.

On the addition of a large excess of tetraethylammonium hydroxide to the oxalate solution, the voltammetric peak at $+0.7$ V disappears and only the first wave at $+0.1$ V and the oxidation wave of excess hydroxide ion at $+0.9$ V are observed on the voltammograms (Fig. 8). The data summarized in Table 4 give a constant value for $(i_p)_1/\nu^{1/2}C^0$ (with the exception of the lowest scan rates) for the first wave in the presence of excess hydroxide ion. This value is almost identical with the corresponding value for the sum of the first and second waves tabulated in the last column of Table 3.

Figures 4-8 establish that a wave is not observed for the reverse cathodic scan. However, if the cathodic potential sweep is extended to more negative values two

peaks are observed at -1.5 and -2.0 V, respectively (curve 2, Fig. 9). These waves are not observed on voltammograms of the supporting electrolyte or for solutions that are reduced without previous oxidation. Hence, these two waves must be due to reduction of the oxidation products formed by the anodic reaction. As shown in Fig. 9, the same cathodic peaks are observed whether or not the cyclic sweep is reversed at $+0.45$ or at $+1.1$ V vs. S.C.E. Only the peak currents are dependent on

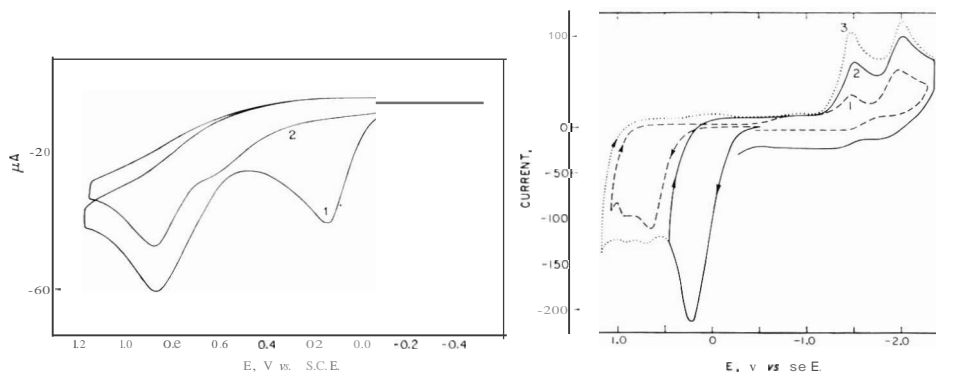


Fig. 8. (1), Voltammogram of $0.82 \times 10^{-3} F$ oxalic acid plus $3.4 \times 10^{-3} F$ tetraethylammonium hydroxide in DMSO; (2) 2nd cyclic scan. Scan rate, 0.2 V sec^{-1} .

Fig. 9. Cyclic voltammograms of $1.72 \times 10^{-3} F$ oxalic acid in presence of: (1), I; (2 and 3), 2 equiv. of tetraethylammonium hydroxide/mole oxalic acid in DMSO. Curve 1, recorded immediately after soln. preparation. Scan rate, 1 V sec^{-1} .

TABLE 4

VOLTAMMETRIC DATA FOR THE OXIDATION OF OXALATE ION IN DMSO IN THE PRESENCE OF EXCESS HYDROXIDE ION AT A GOLD ELECTRODE

$0.82 \times 10^{-3} F$ oxalic acid and $3.4 \times 10^{-3} F$ tetraethylammonium hydroxide

Scan rate (V/sec)	$(E_p)_1$ (V vs. S.C.E.)	$(E_p)_2$	$(i_p)_1$ (μA)	$(ip)_2/vICo$ ($A \text{ cm}^2 \text{ sec}^{-1} \text{ V}^{-1} \text{ mole}^{-1}$)
1.0	0.24	0.90	115	140
0.5	0.18	0.90	81	140
0.2	0.14	0.88	57	139
0.1	0.10	0.86	35.5	137
0.05	0.08	0.85	35.0	136
0.02	0.04	0.82	12.8	110
0.01	0.01	0.80	8.2	100

the potential at which the potential sweep is reversed, indicating that the same oxidation products are formed by the electrode reactions at $+0.2$ and $+0.7$ V, respectively. Cyclic voltammograms of acid oxalate ion solutions (measured immediately after mixing the solution) also exhibit the same cathodic peaks (curve 1, Fig. 9). This confirms that the same oxidation products are formed by the electrode reaction for oxalate ion (at $+0.2$ V) and for acid oxalate ion (at $+0.7$ V).

The peak current at -1.5 V decreases rapidly with decreasing scan rate and the peak is not observed at scan rates below 0.02 V/sec . The oxidation product is, therefore, decomposed rapidly (Table 5). The second cathodic peak has the same

potential as that for reduction of carbon dioxide (-2.0 V *vs.* S.C.E.)⁶. This implies that the final product from the oxidation of oxalate ion is probably carbon dioxide. The second cathodic peak is poorly developed at slower scan rates but its peak current appears to increase at the expense of the first peak (at -1.5 V) with decreasing scan rates.

TABLE 5

EFFECT OF SCAN RATE ON THE PEAK CURRENTS OF THE FORWARD AND REVERSE WAVES FOR 1.72×10^{-3} F TETRAMETHYLAMMONIUM OXALATE

Cyclic scan reversed at $+1.1$ V; reverse peak at -1.5 V *vs.* S.C.E.

Scan rate ($V \text{ sec}^{-1}$)	$(i_p)_a$ (μA)	$(i_p)_c$ (μA)	$(i_p)_c/(i_p)_a$
1.0	215	110	0.51
0.5	150	63	0.42
0.2	87	28	0.32
0.1	58	15	0.26
0.05	38	6	0.16
0.02	22	2	0.09

TABLE 6

VOLTAMMETRIC DATA FOR THE OXIDATION OF 1.55×10^{-3} F TETRAETHYLAMMONIUM OXALATE IN DMSO-WATER MIXTURES AT A GOLD ELECTRODE

Scan rate ($V \text{ sec}^{-1}$)	$(E_p)_1$ (V <i>vs.</i> S.C.E.)	$(E_p)_2$ (V <i>vs.</i> S.C.E.)	$(i_p)_1$ (μA)	$(i_p)_1/v^{1/2}C^0$ ($A \text{ cm}^3 \text{ sec}^{1/2} V^{-1/2} \text{ mole}^{-1}$)
A. 10% H ₂ O in DMSO				
1.0	0.46	0.72	200	129
0.5	0.38	0.72	140	128
0.2	0.34	0.71	90	130
0.1	0.30	0.71	61	125
0.05	0.28	0.70	42	121
0.02	0.25		25.0	114
0.01	0.20		16.3	105
B. 25% H ₂ O in DMSO				
1.0	0.66		214	138
0.5	0.62		150	137
0.2	0.54		95	137
0.1	0.50		67	137
0.05	0.48		46	133
0.02	0.46		28	127
0.01	0.46		19	123

On the addition of water to tetraethylammonium oxalate in DMSO the peak potential of the first oxidation wave is shifted to more positive values and the peak current of the hydroxide ion wave at $+0.9$ V decreases. In the presence of 10% water, only the two first waves are observed on the voltammograms (Table 6). With further increase in the water concentration, the first wave is shifted almost to the same potential as the second wave, and in the presence of 25% water only one wave is observed. The value of $(i_p)_1/v^{1/2}C^0$ for this wave is constant at fast scan rates which implies a diffusion-controlled process (Table 6).

CONCLUSIONS

The experimental results indicate that oxalate ion in DMSO (containing 0.1% water) is in slow equilibrium with acid oxalate ion and hydroxide ion



The galvanostatic experiments establish that oxalate ion undergoes a two-electron oxidation at a gold electrode. Furthermore, the chronopotentiometric and the cyclic voltammetric data indicate that an unstable intermediate is produced by the oxidation process, probably an adsorbed radical species



The radical is reduced at -1.5 V to give the first of the reverse waves in Figs. 2 and 9. However, it is unstable (Table 5) and is decomposed to carbon dioxide



which is responsible for the second reverse wave in Figs. 2 and 9.

The second oxidation wave of oxalate ion, which occurs at the same potential as the oxidation wave of a freshly prepared acid oxalate ion solution ($E_p, +0.7$ V), can be represented by



This reaction also represents the electrode process for the chronopotentiometric oxidation of the acid oxalate ion (curve 2A, Fig. 2). Carbon dioxide and hydrogen ions formed by reactions (7) and (8) react with hydroxide ions



Consequently, reaction (5) is shifted to the right and the concentration of $(\text{COO})_2^{2-}$ (and hence the value of $(i_p)/\nu^{1/2}C^0$) decreases whereas the concentration of $\text{H}(\text{COO})_2^-$ (and the value of $(i_p)/\nu^{1/2}C^0$) increases with decreasing scan rate (Table 3).

In the presence of excess hydroxide ion, reaction (5) is shifted to the left and only the first oxidation wave (reaction (6)) is observed. However, in the presence of water, reaction (5) is shifted to the right and only the second oxidation wave (reaction (8)) is observed on the voltammograms. The value of $i_p/\nu^{1/2}C^0$ for the single wave obtained in the presence of excess hydroxide ion as well as the value obtained in the presence of 25% water is close to the sum of the corresponding values for the first and second waves obtained from solutions in which both oxalate ion and acid oxalate ion are present according to reaction (5) (Tables 3, 4, and 6).

Chronopotentiometric and voltammetric experiments indicate that acid oxalate ion is not stable in DMSO and that it is decomposed to form oxalic acid and DMSO solvated hydroxide ion (Fig. 2). Furthermore, when hydroxide ions are removed from the solution by reactions (9) and (10), the acid oxalate ion decomposition will be accelerated



Consequently, for slow scan rates where reactions (9) and (10) are brought to completion, the peak current for acid oxalate ion (at +0.7 V) decreases and that of hydroxide ion (at +0.9 V) increases with decreasing scan rate (Table 3). Reaction (11) is favoured at slow scan rates and causes the value of $[(i_p)_1 + (i_p)_2]/v^{1/2}C^0$ to decrease at scan rates below 0.05 V/sec.

Tetraethylammonium hydroxide in DMSO is oxidized at a gold electrode with a peak potential of +0.8 to +0.9 V (Table 2 and Fig. 5). The wave is probably due to a one-electron oxidation of hydroxide ion to a radical intermediate which is adsorbed on the electrode



The radical species may decompose to water and oxygen, the latter being responsible for the reverse chronopotentiogram of curve 2B, Fig. 2⁹.

The peak current for hydroxide ion decreases in the presence of water and the wave is completely obliterated in a 10% water-DMSO mixture. Apparently, hydroxide ions are not oxidized at potentials below +1.0 V in water-DMSO mixtures. Further work on the electrochemical oxidation of hydroxide ion in DMSO is in progress.

ACKNOWLEDGEMENT

This work was supported by the National Science Foundation under Grant No. GP-7201.

SUMMARY

The electrochemical oxidation of oxalate ion in dimethylsulfoxide at a gold electrode has been studied by chronopotentiometry and cyclic voltammetry. The final oxidation product is carbon dioxide but an unstable intermediate is formed during the oxidation process. In the absence of excess hydroxide ion, oxalate ion is partly hydrolyzed to acid oxalate ion which is oxidized to carbon dioxide and hydrogen ions. Oxidation mechanisms are proposed that are consistent with the data.

REFERENCES

- 1 J. J. LINGANE, *J. Electroanal. Chem.*, **1** (1960) 379.
- 2 J. GINER, *Electrochim. Acta*, **4** (1961) 42.
- 3 F. C. ANSON AND F. A. SCHULTZ, *Anal. Chem.*, **35** (1963) 1114.

- 4 J. W. JOHNSON, H. WROBLOWA AND J. O'M. BOCKRIS, *Electrochim. Acta*, 9 (1964) 639.
- 5 M. D. MORRIS, *J. Electroanal. Chem.*, 8 (1964) 350.
- 6 L. V. HAYNES AND D. T. SAWYER, *Anal. Chem.*, 39 (1967) 411.
- 7 D. D. DEFORD, private communication, presented at the 133rd American Chemical Society Meeting, San Francisco, California, 1958.
- 8 M. VON STACKELBERG, M. PILGRAM AND V. TOOME, *Z. Electrochem.*, 57 (1953) 342.
- 9 D. T. SAWYER AND J. L. ROBERTS, JR., *J. Electroanal. Chem.*, 12 (1966) 90.
- 10 P. DELAHAY, *New Instrumental Methods in Electrochemistry*, Interscience Publishers, Inc., New York, 1954.

J. Electroanal. Chem., 16 (1968) 361-374

BIAMPEROMETRIC INDICATION IN CHELOMETRIC TITRATIONS IN ACIDIC SOLUTIONS

F. VYDRA AND K. ŠTULÍK

Czechoslovak Academy of Sciences, J. Heyrovský Polarographic Institute, Analytical Laboratory, Prague (Czechoslovakia)

(Received May 15th, 1967)

Biamperometric and bipotentiometric titrations are often used in analysis because of their simplicity and versatility. Biamperometric and bipotentiometric indications are used mainly in redox titrations, especially in the determination of water with Karl Fischer reagent, and in precipitation and complexometric titrations. Biamperometric EDTA titrations of various substances, using two mercury electrodes or electrodes of the same metal as that to be determined (*e.g.*, copper electrodes for the determination of copper) have been described in the literature¹⁻⁶.

Recently, a series of papers reported on biamperometric titrations with EDTA and related compounds for the determination of various metals using two platinum electrodes⁷⁻²¹. In these titrations, relatively high applied voltages are used (400-1100 mV) and the titration curves obtained are of the V-type for the electroactive metals titrated (*e.g.*, Fe³⁺, Tl³⁺, Cu²⁺) and of the reversed L-type for electroinactive metals (*e.g.*, Al³⁺, Th⁴⁺, Bi³⁺). Because in these titrations two oxidation forms are not present in the solution, as in other biamperometric titrations (only one oxidation state of the titrated metal and its chelate is present in the solution up to the equivalence, and only the metal chelate and excess titrant after the equivalence), we followed the course of the titration curves, recording the potentials of the indicating electrodes during the titration and the polarization curves of the titration systems in an attempt to find the mechanism of indication.

EXPERIMENTAL

The shape of the titration curves, and electrode potentials during the course of titration were followed using an apparatus (Fig. 1) consisting of two rotating platinum wire electrodes with area 0.15 cm², rotating in the range 600-1400 rev./min. Two saturated calomel electrodes were located close to these electrodes (about 1 mm distance). The voltage was applied to the electrodes from a Kohlrausch drum and the current was measured by means of a mirror galvanometer with maximum sensitivity 3.5×10^{-9} A mm⁻¹. The exact values of applied voltage and the potentials of the platinum electrodes *vs.* S.C.E. were measured by an electron-tube compensation pH-meter, PHK-1 (Mikrotechna, Czechoslovakia).

The polarization curves were recorded using a rotating wire platinum electrode with area 0.12 cm² rotating at 1000 rev./min, an S.C.E. reference electrode and a PO4d polarograph (Radiometer, Copenhagen, Denmark).

The pH-values of the solutions were measured with a glass electrode (pH-meters PHK-1 and PHM-25, Radiometer, Copenhagen, Denmark).

Before each measurement, for titrations as well as polarization curve recordings, the adsorbed substances were removed electrolytically from electrode surfaces. The auxiliary platinum electrode was immersed in the solution and first oxygen (30 sec) and then hydrogen (1 min) was evolved on each indicating electrode in 0.1 *N* H₂SO₄ solution or in distilled water, using an applied voltage of 4.0 V.

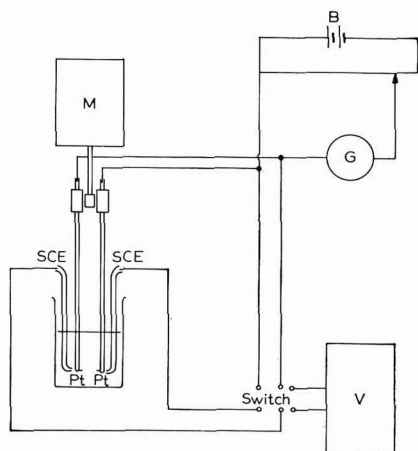


Fig. 1. Apparatus for biamperometric titration with measurement of electrode potentials. (M), motor; (B), battery; (G), galvanometer; (V), voltmeter.

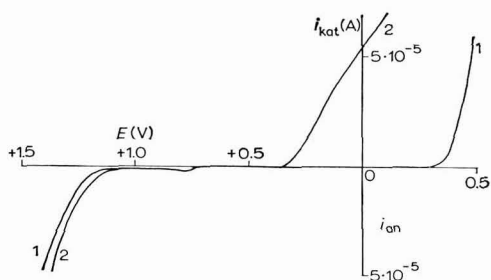


Fig. 2. Polarization curves of base electrolyte (monochloroacetic acid–ammonia, pH 2.3; ionic strength 0.1). (1), dissolved oxygen removed by bubbling with nitrogen; (2), in the presence of dissolved oxygen.

The 0.05 *M* solutions of metal salts were prepared by dissolving the solid substances in water; they were standardized by EDTA visual titrations or gravimetrically. 0.05 *M* EDTA solution was prepared by dissolving the solid material (Lachema, Czechoslovakia) in water and adjusting the pH to 5.0 with NaOH solution. The buffer solutions were prepared from trichloroacetic acid (pH 1–2), chloroacetic acid (pH 2–3), acetic acid (pH 4–7) and ammonia using potentiometric control. The resulting ionic strength was approximately $\mu = 1.0$.

RESULTS

Titrations of Fe³⁺ and Al³⁺ ions with EDTA solution were studied, Fe³⁺ representing the electroactive metal and Al³⁺ the electroinactive metal. The total volume of solution titrated was 100 ml and the concentration of titrated metal, 10^{−3} *M*. Solutions were buffered in most cases, the total ionic strength of the solutions being 0.1 (for buffers see EXPERIMENTAL). In some cases titrations were carried out in unbuffered solutions. The titrant was 0.05 *M* EDTA.

The polarization curves were recorded in solutions of the same composition

using a rate of polarization of 200 mV/min. All potential values are measured against S.C.E.

The polarization curve of the base electrolyte (buffer, monochloroacetic acid-ammonia, pH 2.3; $\mu=0.1$) is shown in Fig. 2. If the dissolved oxygen was removed by bubbling with nitrogen, the cathodic liberation of hydrogen began at about -0.35 V and anodic oxygen was liberated at about $+1.2$ V. At a potential value of about $+0.8$ V there was an anodic pre-wave due to the formation of platinum oxides (curve 1). If dissolved oxygen was present in the solution (concentration about 10^{-3} M), its reduction wave appeared at a potential of about $+0.35$ V (curve 2). These potential values were obtained when polarizing from negative to positive potentials. If polarization is from positive to negative, the polarization curve is shifted by 20–100 mV in the positive direction. In this case, the "dissolution pattern" due to the anodic dissolution of platinum oxides²² does not appear, probably as a result of the reduction effect of the base electrolyte.

The experiments showed that dissolved oxygen influences neither the shape nor the position of the polarographic waves of the titration systems and therefore it was not removed from the solutions.

If two rotating electrodes are immersed in the solution, they reach a potential of about $+0.3$ V. When a voltage is applied to these electrodes, the cathode potential shifts to negative values and that of the anode to positive values. Because cathodic, like anodic, electrode reactions of oxygen are of a kinetic nature, they can be represented by the Tafel equation²³

$$\eta = a + b \log i$$

where η is the overvoltage and a and b are constants.

The shift of electrode potential due to an increasing applied voltage will be given by the slope of the Tafel equation ($b=0.12$ for platinum).

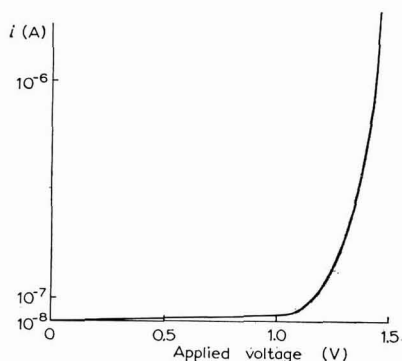


Fig. 3. Dependence of background current upon applied voltage; monochloroacetic acid-ammonia, pH 2.3; ionic strength 0.1.

The dependence of current values upon the applied voltage is given in Fig. 3. These values appear in the course of titration as residual current (background). From Fig. 3 it follows that in a given base electrolyte an applied voltage in the range 0–1.2 V can be used without obtaining too high a background current value. This applied voltage range will shift with the pH of the solution by -0.059 V/pH unit due

to the shift of cathodic and anodic oxygen waves according to the equation²⁴

$$E = E_0 - 0.059 \text{ pH}$$

When the base electrolyte contains, for example, ferric ions ($10^{-3} M$) these give a cathodic wave with a half-wave potential of about $+0.47 \text{ V}$. Two platinum electrodes immersed in this solution have a potential of about $+0.760 \text{ V}$. When an increasing voltage is applied to the electrodes, their potentials shift again according

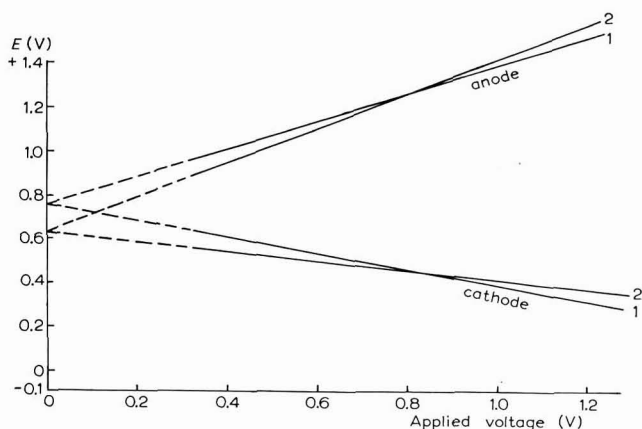


Fig. 4. Dependence of electrode potential at start of Fe^{3+} -EDTA ($10^{-3} N \text{ Fe}^{3+}$) titration upon the applied voltage. (1), $0.1 M$ buffer ammonium monochloroacetate, pH 2.3; (2) unbuffered soln. $10^{-2} M \text{ NaCl}$.

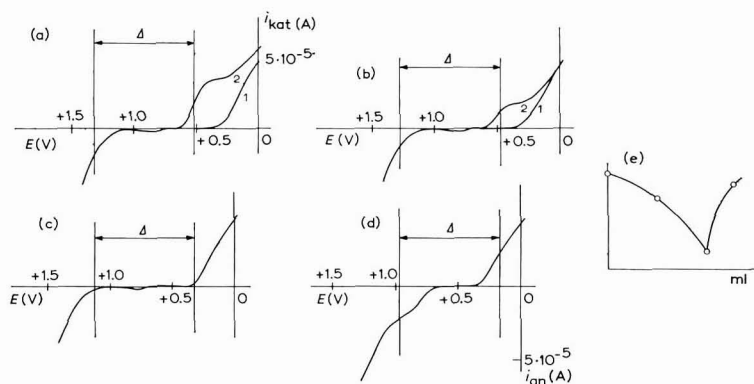


Fig. 5. Polarization curves for various phases of Fe^{3+} -EDTA titration. (a), beginning; (b), one-half of equivalence; (c), equivalence; (d), 50% over-titrated; (e) resulting titration curve. (Δ), applied voltage; (1) base electrolyte; (2) curves of titration systems: (a, b), Fe^{3+} ; (d), EDTA.

to the Tafel slope of the oxygen and ferric ions waves (Fig. 4). The current begins to increase from the background value at an applied voltage of about 0.3 V and then increases exponentially with increasing applied voltage.

During the titration of this solution with EDTA, the ferric ion wave decreases owing to the formation of Fe-EDTA chelate but the wave of this chelate does not appear in all potential ranges. At the equivalence point, the current decreases to the

background level (the dissociation of Fe-EDTA chelate is negligible). After equivalence, the anodic EDTA wave (half-wave potential approximately +0.8 V) appears and the potentials of the electrodes shift to negative values so that anodic oxidation of EDTA and cathodic reduction of dissolved oxygen takes place (Fig. 5). The shift of electrode potentials during the titration up to the equivalence point is a result of the decreasing concentration of ferric ions (according to the Peters equation). At the equivalence point, potentials shift to values at which new electrode reactions begin (EDTA oxidation, dissolved oxygen reduction) (Fig. 6). In general, the electrode potentials reach such values that anodic and cathodic currents are equal, the potential difference between electrodes being constant and equal to the applied voltage.

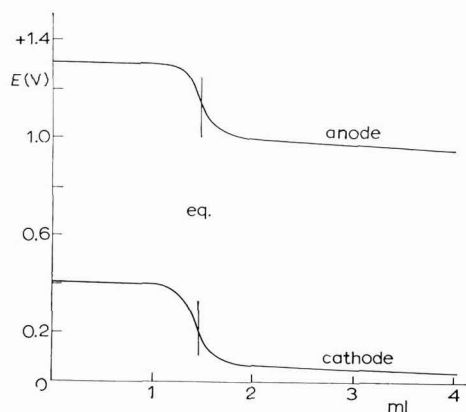


Fig. 6. Dependence of electrode potential upon volume of titrant added. 10^{-3} N Fe^{3+} ; buffer ammonium monochloroacetate, pH 2.3; ionic strength 0.1; titrated with 0.05 N EDTA.

When an electroinactive metal is titrated (*e.g.*, Al^{3+}), up to the equivalence point only background current flows in the circuit; after equivalence, the current increases as a result of the electrode reaction of EDTA and dissolved oxygen. The titration curve has the shape of a reversed L.

It is, therefore, inconvenient to remove dissolved oxygen in these titrations because this would necessitate the use of higher applied voltages for obtaining the current increase after the equivalence (the distance between the hydrogen reduction wave and anodic wave of EDTA is about 0.6 V greater than that between the EDTA anodic wave and oxygen reduction wave).

When voltage is applied to the electrodes, it is necessary to wait about 15 min to obtain a constant current value because the initial current decreases exponentially with time. The currents due to EDTA oxidation are also time-dependent because of the complex character of the electrode reaction of EDTA and related compounds. This problem will be discussed in the following paper.

The dependence of the shape of titration curve upon the ionic strength and pH of the solution

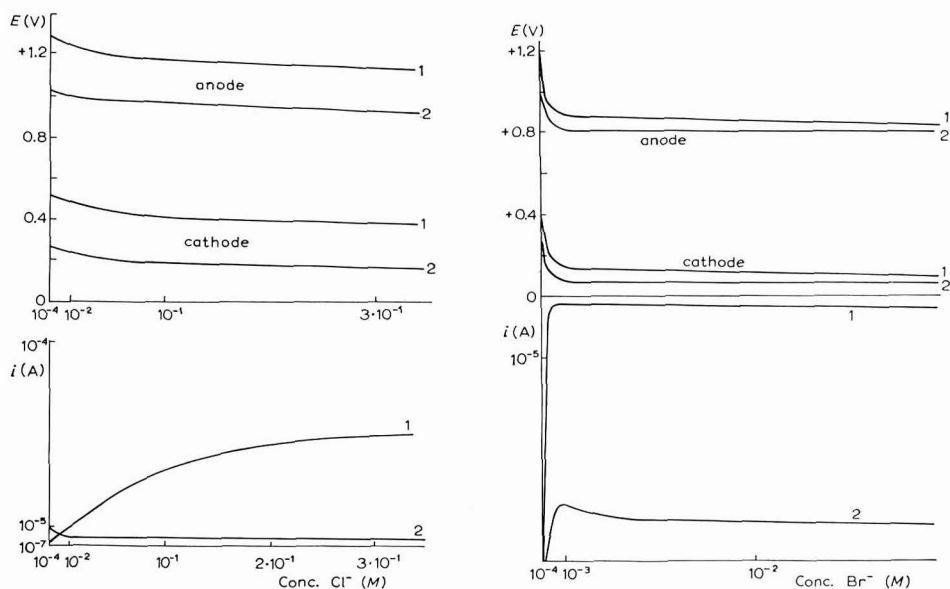
A solution of monochloroacetate-ammonia buffer, pH 2.3, was used and sodium perchlorate solution was added to obtain various values of ionic strength

between 0.1 and 3.0. The electrode potentials are not affected by increasing ionic strength, the current slowly decreases with increasing ionic strength. The decrease of current after the equivalence point is greater than before the equivalence point and at ionic strengths of about 3.0, the current due to EDTA oxidation disappears. This phenomenon will be discussed in the following paper dealing with the voltammetry of EDTA and related compounds.

The pH of the solution affects the shape of the titration curve in very acidic solutions where dissociation of metal chelates takes place and there is curvature of the titration curve in the vicinity of the equivalence point. Above pH 4.0 the current after the equivalence point decreases owing to the decreasing height of the anodic EDTA wave. In neutral and alkaline media, the shape of the titration curves is different from that in acidic solutions owing to the different behaviour of EDTA on the platinum electrode (in alkaline solutions the titration curve rises up to the equivalence point after which the current remains constant). The mechanism of biamperometric indication in this case is more complicated and work on this aspect is now in progress.

The effect of halide ions on the shape of the titration curves

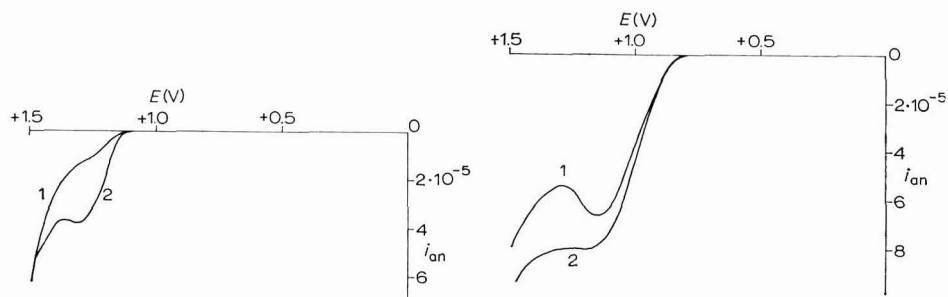
In the presence of fluorides, only the slow decrease of current due to increasing ionic strength takes place (in the case of ferric ions, the current up to the equivalence point decreases due to the formation of iron fluoride complex). The presence of chloride and bromide ions, however, cause an increase of current up to the equivalence point while the potential of the electrodes shifts to more negative values (Figs. 7 and



Figs. 7-8. Dependence of electrode potentials and measured currents of Fe^{3+} -EDTA titration upon concn. of: (7) chloride ions, (8) bromide ions in soln. Buffered soln., pH 2.3; applied voltage 0.8 V. (1), beginning of the titration; (2), end of titration, 50% over-titrated.

8). The current after the equivalence slowly decreases with increasing concentration of Cl^- and Br^- .

Cl^- and Br^- yield anodic waves on the platinum electrode at potentials of +1.15 V and +0.85 V, respectively. The chloride wave appears at chloride concentrations of 10^{-3} – 10^{-2} M and its height very slowly increases with concentration. The bromide wave appears even at a concentration of 10^{-5} M and increases rather quickly with increasing Br^- concentration. In these electrode reactions, there is evidently adsorption of halides and electrode reaction products on the electrode surface (the drop in limiting current occur when adsorbed oxygen displaces these ions from the electrode surface). The presence of ferric ions causes an increase in the height of these anodic waves in a solution of monochloroacetate–ammonia buffer of pH 2.3 (Figs. 9 and 10). This effect was not observed in strongly acidic medium²⁵.



Figs. 9–10. Anodic wave of: (9) $4 \cdot 10^{-2}$ M chloride ions, (10) 10^{-3} M bromide ions. Buffer monochloroacetic acid–ammonia, pH 2.1; (1) without Fe^{3+} ; (2) in the presence of 10^{-3} N Fe^{3+} .

In the presence of chloride or bromide, the overall current value during the titration is given by the cathodic reduction of the metal titrated and anodic oxidation of Cl^- or Br^- . The potential difference between these waves is less than in the case of anodic liberation of oxygen and therefore the indication at a given applied voltage is more sensitive (the current measured is greater). High concentrations of these halides in the solution cause overlapping of the anodic waves of EDTA and halides and a decrease of the current after the equivalence point. If these facts are taken into consideration, the optimum concentration of chloride is 10^{-1} M and that of bromide 10^{-3} M in order to obtain the highest current values and a sufficiently sharp break in equivalence.

CONCLUSION

Chelometric titrations with EDTA and with related compounds that behave similarly in acidic medium, can be carried out using applied voltages in the range 0–1.2 V. When applied voltages greater than 1.2 V are used, the background value of current very quickly increases due to the electrolysis of base electrolyte. By choosing a suitable applied voltage, a desired current value can be obtained. The titrations are possible in buffered as well as unbuffered solutions and the composition of titrated solution does not have any significant effect on the shape of titration curve.

The effect of chloride and bromide ions shows that it is possible to use with advantage other substances that yield anodic polarographic waves at suitable

potentials and react neither with titrant nor with the substance titrated, as an anodic redox system instead of oxygen liberation, to obtain greater sensitivity of indication.

High salt concentrations in solution cause a decrease of current after the equivalence point but the determination of the equivalence point becomes impossible when the ionic strength exceeds 3.0 in the case of the titration of electroinactive metals. When electroactive metals are titrated, the V-shaped titration curve changes at an ionic strength of 3.0 to L-shaped with some decrease of accuracy of determination.

If the polarization curves of the substance to be titrated and of the titrant are known, a suitable applied voltage can be determined and the approximate shape of the titration curve constructed. The intersection of the voltammetric wave of the substance to be titrated and the wave of anodic oxygen liberation (or *e.g.* anodic bromide wave) with the straight lines $E = \text{constant}$ ($E = \text{potential}$) at the desired current values is obtained, and the distance between the intersection of these lines with the potential axis gives the necessary applied voltage. The necessary applied voltage for the part of titration curve after the equivalence where the waves of dissolved oxygen and the anodic wave of the titrant appear, is obtained similarly.

From the series of polarization curves corresponding to the various phases of the titration, it is possible to construct the approximate shape of the titration curve. The applied voltage must be located on the potential axis in such a way that the cathodic current equals the anodic current in each phase of the titration.

The method of indication described is suitable for all chelating agents that yield anodic voltammetric waves. The following paper, discusses the voltammetric behaviour of EDTA and related compounds on a platinum electrode with respect to their use as titrants in biamperometric titrations.

SUMMARY

The mechanism of indication in chelometric titrations with ethylenediaminetetraacetic acid (EDTA) as titrant, using two identical platinum electrodes has been studied. The currents measured in the course of the titration were due to cathodic reduction of the metal titrated and anodic oxygen liberated up to the equivalence point and after this, to anodic oxidation of EDTA and cathodic reduction of oxygen dissolved in the solution. The general conditions for these titrations are given.

REFERENCES

- 1 A. E. MARTIN AND C. N. REILLEY, *Anal. Chem.*, **31** (1959) 992.
- 2 E. R. NIGHTINGALE, *Anal. Chim. Acta*, **19** (1958) 587.
- 3 W. S. KNIGHT AND R. A. OSTERYOUNG, *Anal. Chim. Acta*, **20** (1959) 481.
- 4 G. GUÉRIN, J. DESBARRES AND B. TRÉMILLON, *J. Electroanal. Chem.*, **1** (1960) 226.
- 5 R. C. MONK AND K. C. STEED, *Anal. Chim. Acta*, **26** (1962) 305.
- 6 H. L. KIES, *J. Electroanal. Chem.*, **8** (1964) 325.
- 7 P. N. PALEĚ AND N. I. UDALČOVA, *Tr. Komis. po Analit. Khim. Akad. Nauk SSSR*, **11** (1960) 299.
- 8 P. K. AGASYAN, E. P. NIKOLAEVA AND L. A. DEMINA, *Zavodsk. Lab.*, **30** (1964) 1434.
- 9 F. VYDRA AND J. VORLÍČEK, *Chemist-Analyst*, **53** (1964) 103.
- 10 F. VYDRA AND J. VORLÍČEK, *Talanta*, **11** (1964) 665.
- 11 F. VYDRA AND J. VORLÍČEK, *Talanta*, **12** (1965) 139.

- 12 J. VORLÍČEK AND F. VYDRA, *Talanta*, 12 (1965) 377.
- 13 F. VYDRA AND J. VORLÍČEK, *Talanta*, 12 (1965) 647.
- 14 J. VORLÍČEK AND F. VYDRA, *Microchem. J.*, 9 (1965) 1.
- 15 J. VORLÍČEK AND F. VYDRA, *Talanta*, 12 (1965) 671.
- 16 J. VORLÍČEK AND F. VYDRA, *Chemist-Analyst*, 54 (1965) 87.
- 17 J. VORLÍČEK AND F. VYDRA, *Microchem J.*, 9 (1965) 152.
- 18 J. VORLÍČEK AND F. VYDRA, *Collection Czech. Chem. Commun.*, 30 (1965) 4272.
- 19 F. VYDRA AND J. VORLÍČEK, *Collection Czech. Chem. Commun.*, 31 (1966) 51.
- 20 F. VYDRA AND J. VORLÍČEK, *Talanta*, 13 (1966) 439.
- 21 F. VYDRA AND J. VORLÍČEK, *Talanta*, 13 (1966) 603.
- 22 I. M. KOLTHOFF AND N. TANAKA, *Anal. Chem.*, 26 (1954) 632.
- 23 K. J. VETTER, *Angew. Chem.*, 73 (1961) 277.
- 24 R. N. ADAMS, *Solid electrodes*, in *Progress in Polarography*, Vol. II, Interscience Publishers Inc., New York, 1962, p. 503.
- 25 J. WEBER, personal communication.

J. Electroanal. Chem., 16 (1968) 375-383

THE VOLTAMMETRY OF ETHYLENEDIAMINETETRAACETIC ACID (EDTA) AND RELATED COMPOUNDS ON A ROTATING PLATINUM ELECTRODE

K. ŠTULÍK AND F. VYDRA

Czechoslovak Academy of Sciences, J. Heyrovský Polarographic Institute, Analytical Laboratory, Prague (Czechoslovakia)

(Received May 15th, 1967)

In a previous paper¹ we discussed the mechanism of biamperometric indication of EDTA titrations using two platinum electrodes. Since EDTA-type substances behave in a similar manner to EDTA in biamperometric titration, we have studied their electrode reactions on a rotating platinum electrode because a knowledge of these is necessary for choosing the best titration conditions.

Although the behaviour of organic compounds on platinum electrodes has been the subject of many investigations, these studies have been limited to substances of relatively simple composition. Recently, the oxidation of a number of alcohols, aldehydes and organic acids on platinum electrodes has been studied^{2,3}. The authors show that these organic compounds are adsorbed on the electrode surface and are dehydrogenated; this is followed by the slow reaction of the organic compounds with the radical OH^\cdot adsorbed on the electrode. In certain potential ranges, these reactions are slowed down by the adsorption of oxygen.

The reaction of EDTA on a platinum anode has also been investigated^{4,5}. EDTA was found to give anodic waves of diffusion character, the height of which is dependent upon the pH of the solution and concentration of EDTA. With increasing pH of the solution, the waves shift to more negative potential values. In the pH-range 7.9–12.2, the wave-heights increased with increasing pH. The dependence of height and position of wave upon the pH is a result of variations in the dissociation equilibria of EDTA.

On a graphite electrode impregnated with paraffin, a anodic EDTA wave with half-wave potential +1.2 V has been found, the height of this wave being directly proportional to the concentration of EDTA⁶.

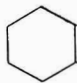
Because very little seems to be known about anodic EDTA oxidation and EDTA analogues have not so far been investigated, we examined the behaviour of some of these compounds on the rotating platinum electrode (Table 1).

EXPERIMENTAL

A platinum rotating wire electrode of area 0.12 cm² with rate of rotation 1000 rev./min, a reference saturated calomel electrode, and a PO4d polarograph (Radiometer, Copenhagen, Denmark) were used for recording polarization curves.

TABLE 1

EDTA-TYPE SUBSTANCES STUDIED

$\text{H}_2\text{N}-\text{CH}_2-\text{CH}_2-\text{NH}_2$	ethylenediamine (en)
$\begin{array}{c} \text{CH}_2\text{COOH} \\ \diagup \\ \text{HN} \\ \diagdown \\ \text{CH}_2\text{COOH} \end{array}$	iminodiacetic acid (imino)
$\begin{array}{c} \text{CH}_2\text{COOH} \\ \\ \text{HOCH}_2\text{C}-\text{N}-\text{CH}_2\text{COOH} \\ \\ \text{HOCH}_2\text{C} \end{array}$	nitrilotriacetic acid (NTA)
$\begin{array}{c} \text{HOCH}_2\text{C} \quad \text{CH}_2\text{COOH} \\ \diagdown \quad \diagup \\ \text{N}-\text{CH}_2-\text{CH}_2-\text{N} \\ \diagup \quad \diagdown \\ \text{HOCH}_2\text{C} \quad \text{CH}_2\text{COOH} \end{array}$	ethylenediaminetetraacetic acid (EDTA)
$\begin{array}{c} \text{CH}_2\text{COOH} \\ \\ \text{N}-\text{CH}_2\text{COOH} \\ \\ \text{N}-\text{CH}_2\text{COOH} \\ \\ \text{CH}_2\text{COOH} \end{array}$ 	1,2-diaminocyclohexanetetraacetic acid (DCTA)
$\begin{array}{c} \text{HOCH}_2\text{C} \quad \text{CH}_2\text{COOH} \\ \diagdown \quad \diagup \\ \text{N}-\text{CH}_2-\text{CH}_2-\text{O}-\text{CH}_2-\text{CH}_2-\text{O}-\text{CH}_2-\text{CH}_2-\text{N} \\ \diagup \quad \diagdown \quad \quad \quad \diagup \quad \diagdown \\ \text{HOCH}_2\text{C} \quad \text{CH}_2\text{COOH} \end{array}$	ethyleneglycol-bis-(2-aminoethylether)tetraacetic acid (EGTA)
$\begin{array}{c} \text{HOCH}_2\text{C} \quad \text{CH}_2\text{COOH} \quad \text{CH}_2\text{COOH} \\ \diagdown \quad \diagup \quad \diagup \\ \text{N}-\text{CH}_2-\text{CH}_2-\text{N}-\text{CH}_2-\text{CH}_2-\text{N} \\ \diagup \quad \diagdown \quad \diagdown \quad \diagup \\ \text{HOCH}_2\text{C} \quad \text{CH}_2\text{COOH} \end{array}$	diethylenetriaminepentaacetic acid (DTPA)
$\begin{array}{c} \text{HOCH}_2\text{C} \quad \text{CH}_2\text{COOH} \quad \text{CH}_2\text{COOH} \\ \diagdown \quad \diagup \quad \diagup \\ \text{N}-\text{CH}_2-\text{CH}_2-\text{N}-\text{CH}_2-\text{CH}_2-\text{N}-\text{CH}_2-\text{CH}_2-\text{N} \\ \diagup \quad \diagdown \quad \diagdown \quad \diagup \quad \diagup \quad \diagdown \\ \text{HOCH}_2\text{C} \quad \text{CH}_2\text{COOH} \quad \text{CH}_2\text{COOH} \end{array}$	triethylenetetraminehexaacetic acid (TTHA)

pH measurements were carried out with a glass electrode using a PHM-25 pH-meter (Radiometer, Copenhagen, Denmark).

Before each measurement, the electrodes were electrolytically cleaned by evolving oxygen and hydrogen, as described in a previous paper¹. Unless otherwise stated, measurements were carried out at room temperature.

The 0.05 *M* solutions of ethylenediamine, imino, NTA, EDTA, DCTA, EGTA, DTPA, and TTHA were prepared by dissolving the solid substances in water and adjusting the pH to 5.0 with NaOH solution. If the purity of the material was below 99.9%, it was purified by dissolving in NaOH and precipitating with H₂SO₄. The products en, imino, NTA, EDTA, TTHA were obtained from Lachema, Czechoslovakia and DCTA, DTPA, EGTA from Geigy, Switzerland.

Buffer solutions were prepared from trichloroacetic acid (pH 1–2), monochloroacetic acid (pH 2–3), acetic acid (pH 4–7) and ammonia with potentiometric control, the resulting ionic strength being approximately 1.0. For pH-ranges above 7.0, buffer solutions consisting of acetic or boric acid and ammonia or potassium hydroxide were used.

RESULTS

The EDTA analogues were used at a concentration of $5 \cdot 10^{-4}$ *M* in 0.02 or 0.1 *M* buffer solutions, the total volume being 100 ml. The speed of polarization was 200 mV/min. Since dissolved oxygen has no effect on the shape and half-wave potentials of waves it was unnecessary to remove it from the solution.

The EDTA-type substances were studied in a wide pH-range (0.5 *M* HNO₃–pH 11.5). The wave-heights and half-wave potentials obtained are given in Table 2.

Neither ethylenediamine nor iminodiacetic acid yield a voltammetric wave in this pH-range, but only shift the anodic oxygen liberation potentials to more positive values by about 20–100 mV. The anodic waves of the other substances studied appeared even in solutions of 0.5 *M* HNO₃, their height increased with decreasing acidity of the solution up to approximately pH 2.0 and then decreased. In the pH-range 3.5–4.0, all waves completely disappeared. The characteristic shape of the waves in acid solution is given in Fig. 1. The height of these waves increases with increasing concentration of EDTA-type substances, but this dependence is not linear and has an asymptotic character (Fig. 2).

In the pH-range 3.5–4.0 to 5.5–6.5 only the potential of anodic oxygen liberation shifts to more negative values in dependence upon the concentration of substances studied (Fig. 3). This dependence has the same asymptotic character as the dependence of wave height on concentration.

In solutions of pH above 5.5 only the waves of EDTA, DCTA and TTHA appear with a slightly lower slope than that of waves in acidic solutions. In some cases double waves appear (Table 2, Fig. 4). The half-wave potentials shift to the more negative values with increasing pH of the solution (Table 2).

All the waves are obtained only when the direction of polarization is from negative to positive potentials. If polarization is in the opposite direction, the currents due to the oxidation of the EDTA-type substances are obtained only for very slow polarization carried out point-by-point in intervals about 30 sec–1 min. The shape of current–potential dependence in this case is very different from the shape

TABLE 2

HALF-WAVE POTENTIALS AND HEIGHTS OF ANODIC WAVES OF EDTA-TYPE SUBSTANCES ON ROTATING PLATINUM ELECTRODE
 $h = 1 \text{ mm} = 8 \cdot 10^{-7} \text{ A}$; potentials vs. S.C.E.; soln. of 0.02 *M* ammonium acetate

<i>pH</i>	<i>en</i> $\frac{h}{E_i}$ (mm)	<i>imino</i>		<i>NTA</i>		<i>EDTA</i>		<i>DCTA</i>		<i>EGTA</i>		<i>DTPA</i>		<i>TTHA</i>		
		$\frac{h}{E_i}$ (mm)	$\frac{h}{E_i}$ (mm)	$\frac{h}{E_i}$ (mm)	$\frac{h}{E_i}$ (mm)	$\frac{h}{E_i}$ (mm)	$\frac{h}{E_i}$ (mm)	$\frac{h}{E_i}$ (mm)	$\frac{h}{E_i}$ (mm)	$\frac{h}{E_i}$ (mm)	$\frac{h}{E_i}$ (mm)	$\frac{h}{E_i}$ (mm)	$\frac{h}{E_i}$ (mm)	$\frac{h}{E_i}$ (mm)	$\frac{h}{E_i}$ (mm)	
0.5 <i>M</i> HNO ₃	—	b	—	a	15.5	+0.93	21.0	+0.89	10.0	+0.88	12.0	+0.90	45.0	+0.88	70.0	+0.85
															16.5	+1.15
0.1 <i>M</i> HNO ₃	—	b	—	a	29.5	+0.89	19.0	+0.87	14.0	+0.88	12.5	+0.87	34.0	+0.86	38.2	+0.83
															6.5	+1.10
1.4	—	b	—	a	8.7	+0.89 ^a	25.5	+0.85	8.0	+0.91	14.0	+0.84	76.5	+0.94	70.5	+0.88 ^a
									38.0	+1.12						
2.4	—	b	—	a	7.2	+0.85	16.2	+0.80	9.5	+0.78	14.0	+0.84	19.0	+0.80	75.5	+0.82 ^a
2.8	—	b	—	a	2.6	+0.80	11.5	+0.77	7.5	+0.74	5.0	+0.77	11.0	+0.76	77.0	+0.81
3.8	—	b	—	a	1.2	+0.71	3.0	+0.73	4.8	+0.68	—	a	1.5	+0.69	5.0	*
4.6	—	b	—	a	—	a	10.0 ⁺	+0.76 ⁺	—	a	—	a	—	a	1.3	+0.63
5.4	—	b	—	a	—	a	—	a	—	a	—	a	—	a	—	a
6.0	—	b	—	a	—	a	50.0 ⁺	+0.77 ⁺	8.0	+0.63	—	a	—	a	10.9	+0.57
															19.5	+0.90
6.8	—	b	—	a	—	a	11.0	+0.79*	47.5	+0.62	—	a	2.0	+0.64	8.5	+0.56
															22.0	+0.87
8.2	—	b	—	a	—	a	—	a	1.5	+0.54	—	a	—	a	—	a
9.0	—	b	—	a	—	a	4.5 ⁺	+0.49 ⁺	—	a	—	a	—	a	—	a
							11.0	+0.88	—	a	—	a	—	a	—	a
11.3	—	a	—	a	—	a	—	a	—	a	—	a	—	a	—	a
0.1 <i>M</i> NaOH	—	b	—	a	—	a	—	a	—	a	—	a	—	a	—	a

* badly shaped wave; + in 0.1 *M* acetate; a shift of anodic oxygen liberation potentials to negative values; b to positive values.

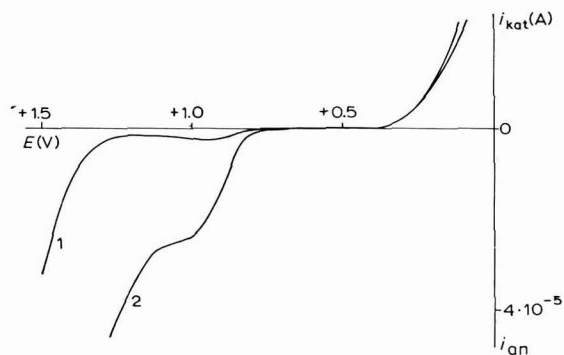


Fig. 1. Anodic EDTA wave in acidic soln.; pH 1.8, 0.02 *M* buffer monochloroacetic acid-ammonia. $5 \cdot 10^{-4}$ *M* EDTA. (1), base electrolyte; (2), base electrolyte + EDTA.

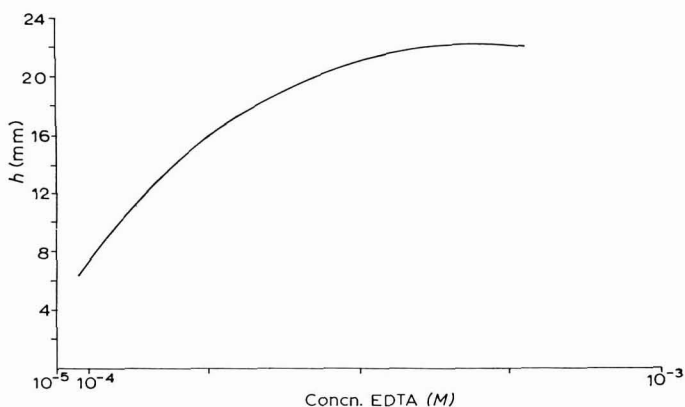


Fig. 2. Dependence of EDTA wave height on concn. pH 2.1, 0.02 *M* buffer monochloroacetic acid-ammonia.

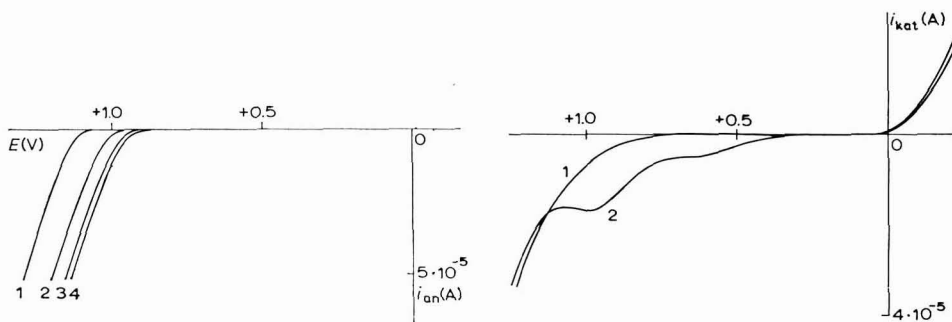


Fig. 3. Dependence of potential shift of anodic oxygen liberation on EDTA concn.; pH 5.0, 0.02 *M* buffer acetic acid-ammonia. (1), base electrolyte; (2), 10^{-4} *M*; (3), $2 \cdot 10^{-4}$ *M*; (4) $3 \cdot 10^{-4}$ *M* EDTA.

Fig. 4. Anodic EDTA wave in alkaline soln., pH 9.0, 0.1 *M* buffer acetic acid-ammonia, $5 \cdot 10^{-4}$ *M* EDTA. (1), base electrolyte; (2) base electrolyte + EDTA.

of waves obtained using continual polarization from negative to positive potentials (Fig. 5).

In many cases there are drops in the limiting currents the extent of which increases with increasing concentration of EDTA-type substances. The value of the slope of the waves is in the range 0.08–0.1. Also, the time-dependence of the current

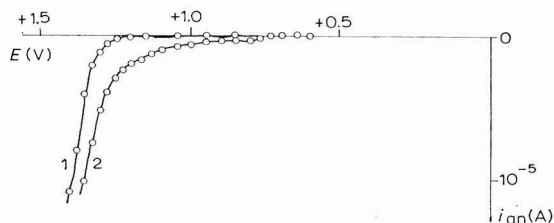


Fig. 5. EDTA anodic wave recorded from + to - potentials, point by point; pH 2.1, 0.02 *M* buffer monochloroacetic acid-ammonia; potential of electrode changed by 20 mV in 30-sec intervals. (1), base electrolyte; (2), $5 \cdot 10^{-4}$ *M* EDTA.

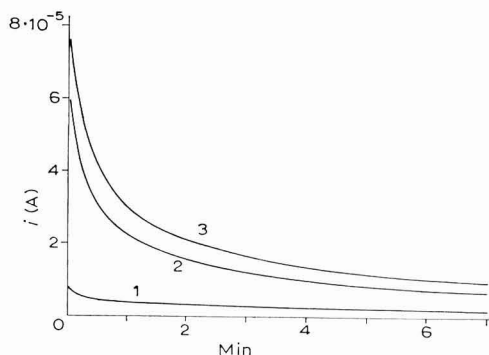


Fig. 6. Dependence of currents due to EDTA oxidation on time; pH 2.1, 0.02 *M* buffer monochloroacetic acid-ammonia, $5 \cdot 10^{-4}$ *M* EDTA. (1), foot of anodic wave; (2), half of the wave; (3), limiting current.

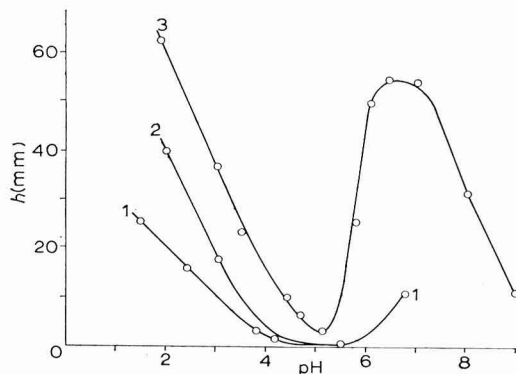


Fig. 7. Dependence of EDTA wave height on soln. composition; pH 2.3, $5 \cdot 10^{-4}$ *M* EDTA. (1) 0.02 *M* buffer monochloroacetic acid-ammonia; (2), unbuffered soln. (HNO_3); (3), 0.1 *M* buffer monochloroacetic acid-ammonia.

values is of interest (Fig. 6). The wave height is depressed by surface-active substances (*e.g.*, amyl alcohol).

In acidic media, the waves are practically independent upon the composition of the solution. The height and the shape of the waves of EDTA, DCTA, and TTHA in alkaline media are, however, dependent upon the solution composition. The highest and the best-shaped waves appear in acetate medium; the height increases with increasing concentration of acetate up to 0.3 *M* and then slowly decreases. In this range of acetate concentrations the region of pH in which no waves are obtained, narrows (Fig. 7).

The dependence of wave shape upon the speed of polarization is given in Fig. 8 and the dependence of half-wave potential and wave height upon the rate of rotation of the electrode, in Fig. 9.

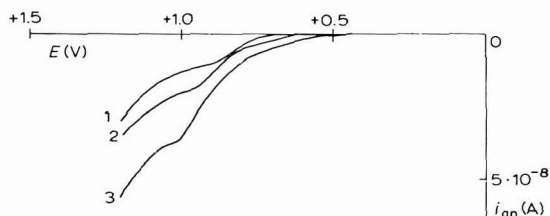


Fig. 8. Dependence of shape and height of EDTA wave on the rate of polarization; pH 2.1, 0.02 *M* buffer monochloroacetic acid–ammonia, $5 \cdot 10^{-4}$ *M* EDTA. (1), 20; (2), 200; (3), 400 mV min⁻¹.

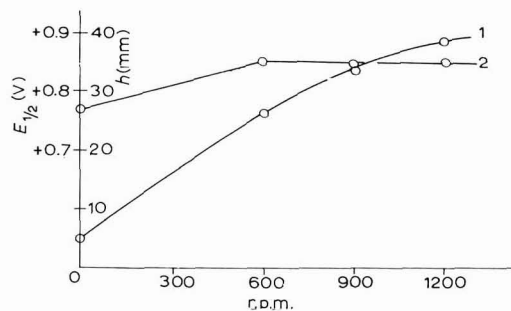


Fig. 9. Dependence of height and half-wave potential of EDTA wave on rate of rotation of electrode; pH 2.1, 0.02 *M* buffer monochloroacetic acid–ammonia, $5 \cdot 10^{-4}$ *M* EDTA. (1), wave-height; (2), half-wave potential.

THE PROBABLE MECHANISM OF ELECTRODE REACTIONS

The dependencies mentioned above indicate that EDTA-type substances are first of all adsorbed on the electrode surface; then anodic oxidation takes place followed by adsorption of the electrode reaction products on the electrode surface which slows down the electrode process. In certain potential ranges (approximately 0.3–0.5, 0.6–0.8, and 1.0–1.3 V) the electrode process is probably slowed down also by adsorption of oxygen^{2,3}. The resulting anodic waves therefore represent currents of complex character from all these effects. In view of this, the use of the term, half-wave potential, is not in the proper sense, but indicates the potential value at

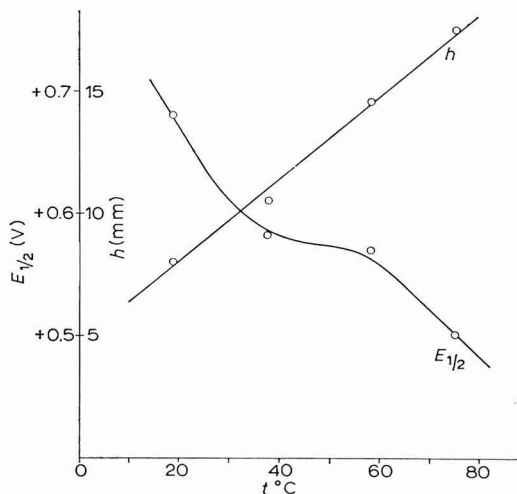


Fig. 10. Dependence of height and half-wave potential of EDTA wave on temperature; pH 2.1, 0.02 *M* buffer monochloroacetic acid–ammonia, $5 \cdot 10^{-4}$ *M* EDTA.

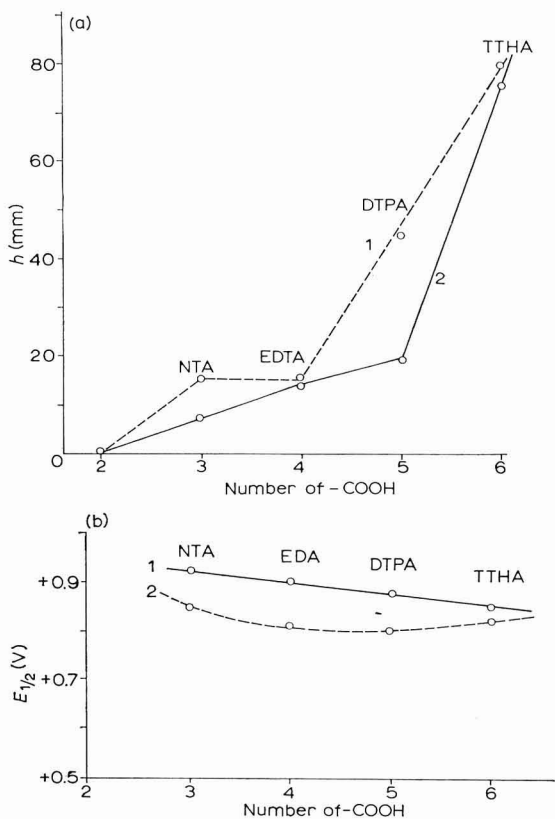


Fig. 11. Dependence of: (a) height of anodic waves, (b) half-wave potential of anodic waves, on the number of carboxylic groups in molecule of substance oxidized. Concn. of substance studied, $5 \cdot 10^{-4}$ *M*. (1) soln. of 0.5 *M* HNO_3 ; (2) pH 2.4, buffer acetic acid–ammonia.

which the waves reach one-half of their height because this is the value most convenient for the determination of wave position on the potential axis.

From the linear temperature-dependence of the wave height given in Fig. 10, it can be concluded that the reaction rate increase due to increase in temperature (which should be of exponential shape) is to a certain degree compensated by partial desorption of the substance studied from the electrode surface.

We assume that at anodic oxidation of EDTA-type substances, decarboxylation takes place as discussed by SCHWARZENBACH⁷ and KOPECKÁ⁸. This supposition is also confirmed by the dependence of wave-heights and half-wave potentials upon the number of carboxylic groups in the molecules of the substances studied (Fig. 11, a and b). With increasing number of carboxylic groups, the anodic wave-height increases and half-wave potentials shift slightly to more negative values. The structure of the chain of EDTA-type acids has no significant effect upon either wave-height or half-wave potential. Only in the case of DCTA, the molecule of which contains the cyclohexane ring, were substantially higher waves than that of EDTA found in alkaline media (Table 2). The assumption of decarboxylation of these substances is also supported by the fact that ethylenediamine does not yield voltammetric waves in the pH-range studied.

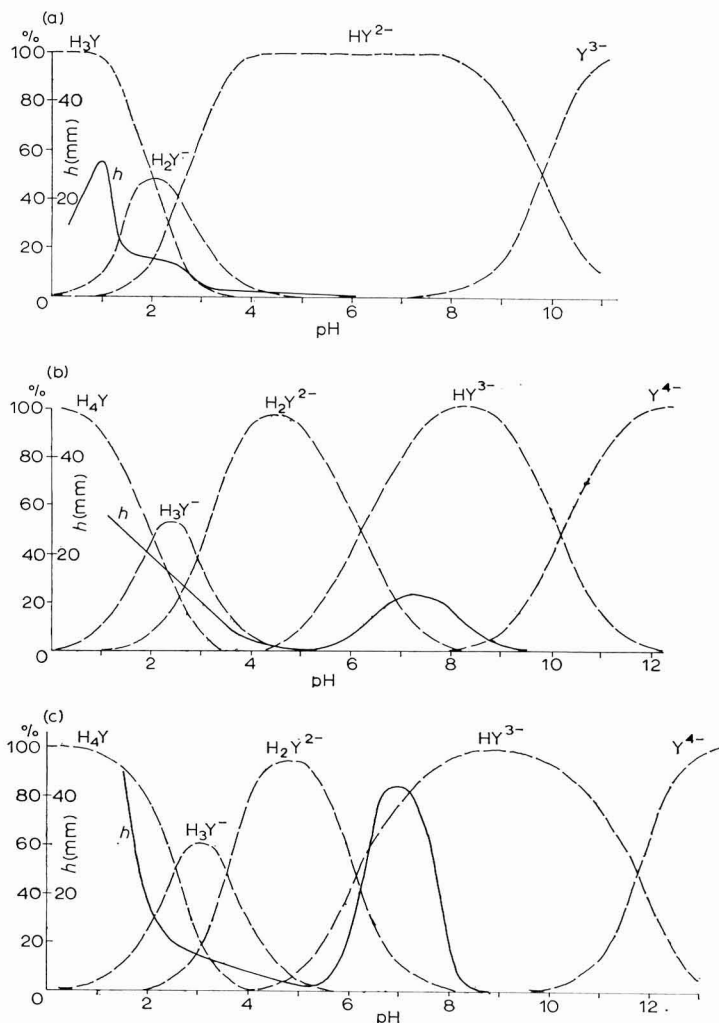
The adsorption and decarboxylation of EDTA-type substances is evidently influenced by their dissociation depending on the pH of the solution. Figure 12 (a)–(f) shows the percentage of various dissociated forms of the substances studied in the solution depending on the pH, and the corresponding heights of their anodic waves. These dependencies show that anodic waves appear in pH-ranges where the non-dissociated acid and once-deprotonized form, exist. In the pH-range of existence of the twice-deprotonized ion, no wave appears only the anodic oxygen liberation shifts to negative values. In the range of pH where the three-times-deprotonized form exists, the waves of EDTA, DCTA, and TTHA appear.

CONCLUSION

From the results obtained and taking into account the discussion in the previous paper¹, it can be concluded that all the substances studied, with the exception of ethylenediamine and iminodiacetic acid, can be used as titrants in biamperometric titration with two platinum electrodes in acidic media. EDTA, DCTA and TTHA can also be used in alkaline media, especially DCTA which yields very high anodic waves in solutions of pH 6.0–9.0. In the pH-region about pH 5.0, it is possible to use the potential shift of anodic oxygen liberation due to the EDTA-type substances present. Some difficulties can arise as a result of the time-dependence of the anodic currents of these substances. Solutions of low ionic strength are preferred for the titration as the anodic current decreases with increasing ionic strength (the maximum permissible ionic strength is about 3.0). From the point of view of anodic oxidation of EDTA-type substances, solutions of acetates are the most suitable titration media.

SUMMARY

The behaviour of EDTA, ethylenediamine, iminodiacetic, 1,2-diaminocyclohexanetetraacetic, nitrilotriacetic, ethyleneglycol-bis-(2-aminoethylether)tetraacetic,



diethylenetriaminepentaacetic, and triethylenetetraminehexaacetic acids was studied on a rotating platinum electrode. These substances, with the exception of ethylenediamine and iminodiacetic acid, yield anodic voltammetric waves on a platinum electrode, the heights and half-wave potentials of which are dependent upon pH and the composition of the solution. The probable mechanism of the electrode reactions is given.

REFERENCES

- 1 F. VYDRA AND K. ŠTULÍK, *J. Electroanal. Chem.*, **16** (1968) 000.
- 2 O. A. CHAZOVA, YU. B. VASILEV AND V. S. BAGOTSKII, *Izv. Akad. Nauk SSSR, Ser. Khim.*, **10** (1965) 1778.

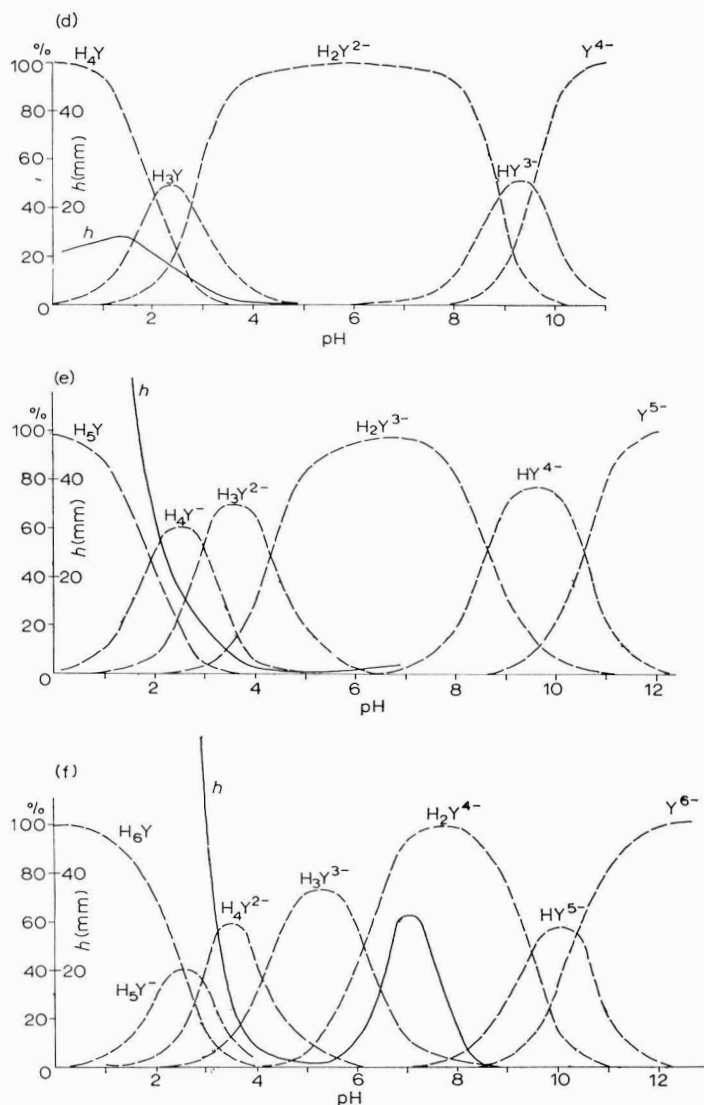


Fig. 12. Percentages of various dissociated forms of EDTA-type substances at various pH-values and the dependence of the wave-heights of these substances on pH. Buffered solns; of EDTA-type substances, $5 \cdot 10^{-4}$ M. (a), NTA; (b), EDTA, (c), DCTA, (d), EGTA; (e), DTPA; (f), TTHA.

- 3 O. A. CHAZOVA, YU. B. VASILEV AND V. S. BAGOTSKII, *Izv. Akad. Nauk SSSR, Ser. Khim.*, 9 (1965) 1531.
- 4 YU. I. USATENKO AND A. M. VITKINA, *Nauch. Dokl. Vyssei shkoly, Khim. i Khim. Tekhnol.*, (1958) 502; *Chem. Abstr.* 53 (1959) 964h.
- 5 L. S. REISHAKHRIT, V. N. MARTYNOVA AND Z. I. TICHONOVA, *Vestn. Leningr. Univ.*, 20 (1965) 146.
- 6 E. A. TERENCEVA AND B. V. BERNACKAYA, *Z. Anal. Chem.*, 21 (1966) 870.
- 7 G. SCHWARZENBACH, *Helv. Chim. Acta*, 32 (1949) 839.
- 8 L. KOPECKÁ, *Chem. Listy*, 50 (1956) 1084.

SENSITIVE AMPEROMETRIC TITRATION OF *o*-PHENYLENEDIAMINE EMPLOYING CATALYTIC ELECTRODE REACTION END-POINT DETECTION

E. KIROWA-EISNER AND HARRY B. MARK, JR.

Department of Chemistry, University of Michigan, Ann Arbor, Mich. 48104 (U.S.A.)

(Received July 17th, 1967)

INTRODUCTION

Certain complexes of metal ions, such as Ni(II), Sn(IV), In(III), Co(II), are reduced at potentials considerably more positive than those observed for the reduction of these metals in non-complexing media¹ (in a *hexaquo* form in non-complexing aqueous media). In some cases, when the concentration of the complexing agent is small compared to the concentration of the metal ion, a polarographic prewave is obtained which is catalytic in nature with respect to the concentration of the complexing agent, as the limiting current is several orders of magnitude greater than the diffusion limiting current for the metal complex. Even so, the limiting prewave current is essentially proportional to the concentration of the complexing agent (provided the prewave limiting current is less than about 15% of the main wave limiting current of the uncomplexed metal ion^{1,2}). Because of the proportionality of prewave limiting current to concentration of complexing agent and the extreme sensitivity resulting from the catalytic or cyclic behavior of the electrochemical reaction with respect to the complexing agent, these types of metal-complex systems have been employed successfully for the polarographic determination of trace concentrations¹ of the complexing agent. A detailed description of the nature of the electrode reaction and some analytical applications using the prewaves are summarized in previous papers^{2,3}. It was thought that the catalytic electrode reactions of these metal-complex systems might be employed as end-point detection (or indicator) reactions for sensitive micro-amperometric titrations using these complexing agents.

The *o*-phenylenediamine (opda)-Ni(II) system was chosen to demonstrate the application of the catalytic prewave as an amperometric end-point indicator, since the catalytic effect of this system is large¹ and the prewave is very well defined (the prewave half-wave potential is over 350 mV more positive than the Ni(II) wave). This paper discusses the analytical applicability and limitations of this system as an amperometric end-point detection system and describes the kinetic complications that arise in the titration of trace concentrations.

EXPERIMENTAL

Reagents and apparatus

Analytical-grade reagents were used without further purification. Diamino-

phenazine (daph) was prepared by the method of MAYER AND BERENDS⁴. The opda and daph solutions were prepared before each experiment with de-aerated water. A 10^{-2} *M* Au(III) stock solution was prepared from $\text{AuCl}_3 \cdot \text{HCl}_3 \cdot 3\text{H}_2\text{O}$ and was standardized electrogravimetrically⁵. Triple-distilled water was used for the preparation of all solutions. The nitrogen employed for de-aeration was purified by standard procedures.

A three-electrode polarograph, constructed essentially from the operational amplifiers circuits of DEFORD⁶, and an Electro Instrument recorder, Model 320, were used for recording polarographic data and the amperometric titration curves.

The dropping mercury electrode had a drop time of 4.30 sec and 1.84 mg/sec outflow of mercury at 52 cm column height in 1.0 *M* NaOAc, employing an applied potential of -0.8 V vs. Ag/AgOAc (in 1 *M* NaOAc).

The auxiliary platinum electrode and the reference electrode (Ag/AgOAc, 1.0 *M* NaOAc) were fitted into separate polyethylene tubes that were filled, respectively, with saturated KNO_3 solution and 1 *M* NaOAc solution. These two polyethylene tubes were inserted into the electrolysis cell and they made contact with the electrolysis solution through Vycor thirsty glass plugs.

The titrant (Au(III) solution) was added to the electrolysis cell by means of a 0.2-ml RG micrometer burette (Roger Gilmont).

RESULTS AND DISCUSSION

As has been previously shown⁸, NaOAc solution is a suitable supporting electrolyte for the analytical application of the Ni(II)-opda prewave. The titrant for opda must react rapidly and completely in this media. Two groups of titrants were investigated for the titration of opda. The first group, consisting of metals capable of complexing with this compound, was unsatisfactory. No suitable reaction system was found, as the values of the stability constants of the metal complexes (from the literature) were not sufficiently large to allow titration of solutions of 10^{-6} *M* opda. The second group consisted of species that were capable of oxidizing opda. The choice of a suitable oxidizing reagent depends on the oxidizing "power" as well as on the rate of the oxidation reaction, which is especially important in such dilute solutions. Quantitative data on the kinetics of opda oxidation reactions were not available in the literature and thus a trial-and-error testing of a large number of oxidants was undertaken to find a suitable system.

A large majority of the common oxidation reagents were found to react slowly [Fe(III), Sn(IV), Mn(VII), Cr(VI), Ti(IV), U(III), Hg(II), Ag(I), O_2]. Copper has been reported as a catalyst⁷ for the acceleration of some oxidation reactions of opda, but the oxidation rates were not sufficiently fast for a practical titration. Ce(IV) was somewhat faster, but again not sufficiently rapid. However, Au(III) was found to be an excellent oxidizing agent, as the rate of oxidation of opda was found to be very rapid even in dilute solutions.

The titration curve obtained with Au(III) was of unique shape having three well defined "end-point" inflections (Fig. 1). During the first portion of the titration (AB), the product of the oxidation reaction increased the rate of the catalytic electrode prewave reaction, as indicated by an increase in the limiting current of the prewave. The second portion (line BC) of the titration curve involved a reaction product that

decreased the limiting prewave current. Further addition of titrant beyond the second linear portion (line CD in Fig. 1) also decreased the limiting prewave current, but the rate of decrease diminished significantly. However, Fig. 1 shows that the overall catalytic effect on the limiting current of the last product of the reaction is still greater than that of the original opda.

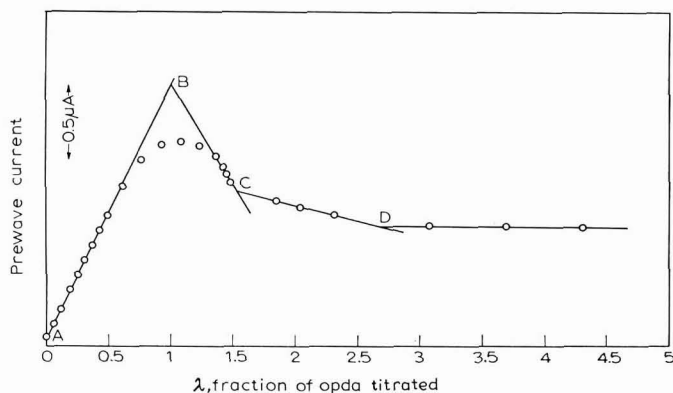


Fig. 1. Titration curve of opda with Au(III). λ -mole fraction of Au(III) and initial opda; [opda] = $1 \cdot 10^{-6}$ M, $[\text{Ni}(\text{OAc})_2] = 2.5 \times 10^{-3}$ M, $[\text{NaOAc}] = 4 \cdot 10^{-2}$ M.

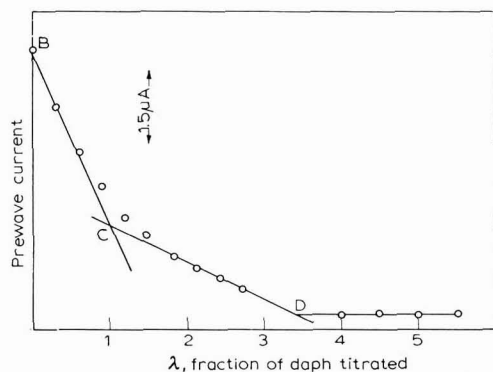


Fig. 2. Titration curve of daph with Au(III). λ -mole fraction of Au(III) and initial daph; [daph] = $4 \cdot 10^{-6}$ M, $[\text{Ni}(\text{OAc})_2] = 7.5 \times 10^{-3}$ M, $[\text{NaOAc}] = 1$ M.

The mechanism of the reactions involved in each portion of the titration curve are of considerable interest, as these characteristics were quite unexpected. The first portion (AB) of the titration curve corresponds to a 1:1 opda–Au(III) reaction ratio, as the end-point of the inflection occurs when one equivalent of Au(III) has been added to one equivalent of opda. Three electrons/molecule of opda are involved in this step, as one equivalent of Au(O) is precipitated.

The product of this step (diaminophenazine) was found to be the same as the well known product of the air oxidation of opda⁷. This was shown by comparing the behaviour of the product of this titration step with that of a pure daph solution. The two solutions had the same catalytic prewave effect, the same UV and visible spec-

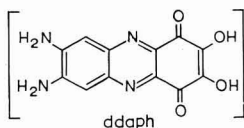
trum, and the amperometric titration curves were of the same shape, as shown in Fig. 2.

The second end-point of the titration curve corresponds, approximately, to the completion of a 1:1 daph-Au(III) reaction. No precipitate of Au(O) appears during this step (BC in Fig. 1 and Fig. 2). However, no attempt was made to determine if the product of this step is from (i) a complexation reaction between daph and Au(III), or (ii) a redox reaction in which gold is reduced to a +1 valence state.

The third step of the titration curve (CD in Fig. 1 and Fig. 2) involves the reduction of Au(III) to Au(O). The identification of the final product was carried out by determining the number of electrons involved in the overall reaction, and the elemental composition of the product. This was accomplished by dissolving 0.1000 g of opda in 20 ml water containing 2 g NaOAc. Then 30 ml of a $2.5 \times 10^{-2} M$ Au(III) solution was added slowly (over one hour), from a burette which had its tip immersed in the stirred solution. The precipitate formed, which contained the final product plus Au(O), was filtered from the solution (through a fine sintered-glass funnel, which had been previously weighed) and washed with hot dilute hydrochloric acid which dissolved the final product; the gold precipitate was thus isolated on the funnel. The Au(O) was then weighed and the number of electrons involved in the overall reaction calculated from the weight. Then NaOAc was added to the solution containing the final product and the reformed precipitate washed with cold water and dried at 130°. The product was dark red in colour and was not soluble in common organic solvents.

The number of electrons in the overall reaction for the oxidation of one molecule of opda was found to be 8 ± 0.2 . The first product of the oxidation is daph (as shown above). The oxidation of two molecules of opda yields one molecule of daph in a reaction which involves 3 electrons/molecule of opda. The further oxidation of one molecule of daph involves 10 electrons (or 8 electrons/molecule of opda to a half molecule of the final product).

From these results it is concluded that the final product is 2,3-dihydroxy-7,8-diaminophenazinchinon-(1,4) or ddaph, which is a 10-electron oxidation product of daph (16-electron oxidation product of 2 opda molecules).



The elemental composition of ddaph is: C, 52.94%; H, 2.94%; N, 20.6%. The elemental analysis of the final product was found to be: C, 53.24%; H, 3.16%; N, 20.75%, which is in fair agreement with the calculated values.

Recommended titration procedure

The opda (or daph in the mechanism study) solution is transferred into a 50-ml beaker and diluted with Ni(II) and NaOAc (as will be discussed below). Oxygen is then removed by nitrogen. An initial polarogram is run, and a voltage on the prewave plateau is chosen for the amperometric titration, or in cases where the concentration of opda is large, the peak potential of the prewave.

The titrant is added slowly, with the tip of the burette immersed in the solu-

tion; the solution is stirred thoroughly throughout the titration. If these precautions are not taken, a large localized concentration of oxidant can result in a complete conversion of opda to the final product, ddaph, in this localized volume. The first end-point will, therefore, be premature. During the rising portion of the amperometric titration curve (AB in Fig. 1), the rate of the oxidation reaction is fast and measurement of the currents are taken immediately after the solution is quiescent (a waiting period of 15 sec after stopping the stirring was found to be sufficient). Beyond the first end-point (BC in Fig. 1), the rate of the reaction decreases markedly and, in order to obtain constant current readings, the solution has to be stirred approximately 30 sec after each addition of titrant and then measured after a further 15-sec interval. After the second end-point (CD in Fig. 1), the rate of the reaction again increases and only a 15-sec period for quiescence is required. The overall time for one titration is approximately 35 min if a full curve is required or 25 min for determining the first end-point, which is used for calculating the concentration of opda as the second and the third end-points are not reproducible.

No temperature control is needed, provided no abrupt changes ($\pm 1^\circ$) in temperature occur during a particular titration.

Effect of composition of the supporting electrolyte

The composition and the nature of the supporting electrolyte strongly affect the behaviour of the prewave. As shown previously², the catalytic prewave arises from a rate-limiting surface reaction. Thus, the height of the catalytic prewave should decrease with increasing concentration of supporting electrolyte because of the ψ^2 -effect and the sensitivity of the proposed method can be increased by decreasing the concentration of the supporting electrolyte, NaOAc; $4 \cdot 10^{-2}$ M NaOAc solutions are most suitable for the concentrations of opda in the $1-2 \cdot 10^{-6}$ M range, and 1 M NaOAc for more concentrated solutions.

Effect of nickel ion concentration

As previously shown⁸, the prewave limiting current varies linearly with ligand concentrations (at constant Ni(II) concentration) when the ligand concentrations are small compared with the Ni(II) concentration. However, as the concentration of opda becomes comparable with the Ni(II) concentration, a limiting value of the prewave current is reached. The behavior of daph is the same, but the limiting current is reached at lower relative concentrations of ligand (Fig. 3).

When the Ni(II) concentration is increased, three effects are observed: (i) the plateau in Fig. 3 is reached at higher ligand concentrations, which means that the straight part of the curve in Fig. 3 is extended and the titration range of opda is thus extended to more concentrated solutions; (ii) the slope of the straight line portion of the curve in Fig. 3 increases which means that the sensitivity of the prewave (and of the titration) with respect to [opda] is increased; (iii) the overlapping of the prewave with the main wave is increased causing loss of sensitivity and precision.

Because two of these effects are advantageous in practical analyses, the optimum nickel concentration for the titration of different concentrations of opda must be determined as follows: the minimum concentration of nickel is determined by the basic requirement that a linear relationship between the prewave current and the concentrations of opda and daph must be attained, e.g., unless [Ni(II)] is such

that the opda concentrations to be determined, fall on the straight line portions of both curves in Fig. 3 large errors will occur. For example: when $1 \cdot 10^{-5} M$ opda is determined in $7.5 \times 10^{-3} M$ Ni^{2+} , $1 M$ NaOAc, the relative error is 1.2%. If $[Ni(II)]$ is decreased to $2.5 \times 10^{-3} M$, the relative error becomes 30%. The upper limit of $[Ni(II)]$ is determined by the overlapping or obscuring of the prewave by the initial

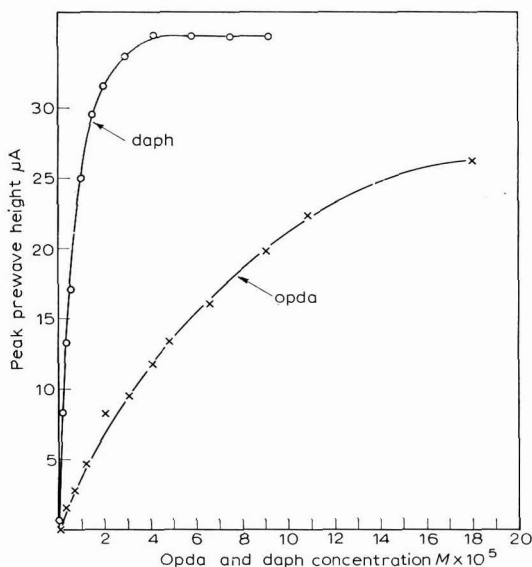


Fig. 3. Variation of peak prewave height with concn. of opda and daph. $[Ni(OAc)_2] = 7.5 \times 10^{-3} M$, $[NaOAc] = 1 M$.

rising portion (or foot) of the main wave as mentioned above. For example, in the titration of $10^{-6} M$ opda solution in $4 \cdot 10^{-2} M$ NaOAc, the $[Ni(II)]$ has to be decreased to a value of $2.5 \times 10^{-3} M$ in order to obtain a well defined prewave. On the basis of these considerations, the optimum composition of the titrated solution for different opda concentrations was experimentally determined as follows: for $2-10 \cdot 10^{-6} M$ opda a $7.5 \times 10^{-3} M$ $Ni(II)$, $1 M$ NaOAc solution should be used. For $1-2 \cdot 10^{-6} M$ opda, a $2.5 \times 10^{-3} M$ $Ni(II)$, $4 \cdot 10^{-2} M$ NaOAc solution should be used.

The upper limit of opda concentration that can be determined in a $7.5 \times 10^{-3} M$ $Ni(II)$, $1 M$ NaOAc solution is $10^{-5} M$ (see Fig. 3). For more concentrated solutions of opda, the concentration of $Ni(II)$ must be increased. However, it is impracticable to determine solutions of opda more concentrated than $5 \cdot 10^{-5} M$, as precipitation reactions of the products begin to take place during the titration and interfere with the polarographic waves.

Effects of a maxima suppressor

The prewave exhibits a peak⁸ in more concentrated solutions, but not a polarographic maximum. However, the $Ni(II)$ background wave does exhibit a sharp maximum. For the amperometric titration it was found that accurate results could be obtained without a maximum suppressor, but the titrations were usually carried

out in the presence of $4 \cdot 10^{-5} M$ CaOAc (as a maximum suppressor)⁸ which decreases the rate of rise and, hence, the overlap of the main Ni(II) wave with the prewave.

Sensitivity and accuracy of the method

The sensitivity of the method is limited by the degree of completeness of the oxidation reaction during the first two steps of the titration. The most dilute solution of opda that was determined experimentally was $1 \cdot 10^{-6} M$ (with a relative standard deviation of 4.6%). In the more concentrated ranges, the accuracy improves as expected ($1 \cdot 10^{-5} M$ solutions of opda were determined with 0.7% relative standard deviation). The quantitative results of typical determinations of various concentrations of opda are summarized in Table I.

TABLE I

AMPEROMETRIC TITRATION OF OPDA WITH Au(III)

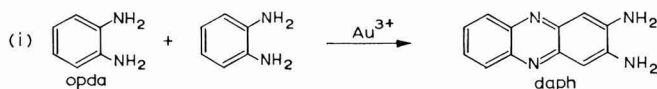
Concn. opda ($M \cdot 10^5$)	Relative standard deviation (%)	Medium composition (M)		
		Ni(OAc) ₂	NaOAc	Ca(OAc) ₂
1.0	0.7	7.5×10^{-3}	1	$4 \cdot 10^{-5}$
0.4	1.7	7.5×10^{-3}	1	$4 \cdot 10^{-5}$
0.3	2.3	2.5×10^{-3}	1	$4 \cdot 10^{-5}$
0.2	4.4	2.5×10^{-3}	$4 \cdot 10^{-2}$	0
0.1	4.6	2.5×10^{-3}	$4 \cdot 10^{-2}$	0

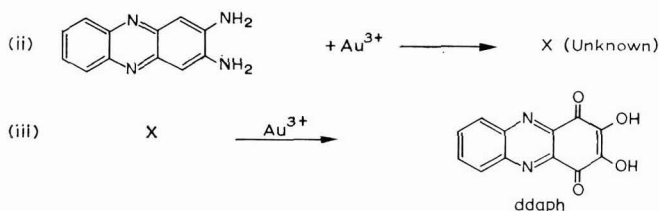
Determination of opda in the presence of other isomeric phenylenediamines

Although opda has been successfully determined polarographically in the presence of the other isomers⁹ (employing the Ni-opda prewave), the amperometric titration analysis failed when the other isomers were present. In the presence of either or both of the isomers, a very long time is necessary to reach a steady current after each addition of titrant. Slow and competitive side reactions seem to be taking place between the different isomers during the oxidation. Furthermore, the end-point is not the true opda equivalence point and is strongly influenced by the composition of the titrating solution and it is therefore impossible to carry out a titration of opda in isomeric mixtures. All other species that are readily oxidized by Au(III) also interfere in this titration.

SUMMARY

The catalytic prewave of the Ni-opda system has been used for a sensitive amperometric detection of the end-point of the opda titration. Au(III) was chosen as titrant from a large group of possible oxidants, because of its favourable equilibrium and kinetic properties. Three end-points are observed in the titration and the reactions involved were shown to be as follows:





The limiting sensitivity for the determination of opda was found to be $1 \cdot 10^{-6}$ M, with a standard deviation of 4.6%. The titration of opda was not feasible in the presence of the other phenylenediamines. The catalytic electrode reactions involving cyclic regeneration of the redox species, are applicable for end-point detection systems for the amperometric titrations of trace concentration of these species, provided titrants can be found that have suitable thermodynamic and kinetic properties in their reaction with the redox species.

ACKNOWLEDGEMENT

This research was supported in part by grants from the National Science Foundation (NSF GP-4620 and GP-6425) and the U.S. Army Research Office-Darham (contract No. DA 31124 ARO-D284).

REFERENCES

- 1 H. B. MARK, JR., *Rev. Polarog. (Kyoto)*, in press.
- 2 H. B. MARK, JR. AND L. R. MCCOY, *Rev. Polarog. (Kyoto)*, in press.
- 3 L. R. MCCOY, Ph.D. thesis, University of Michigan, 1967.
- 4 H. I. X. MAYER AND W. BERENDS, *Rec. Trav. Chim.*, 76 (1957) 28.
- 5 H. J. S. SAND, *Electrochemistry and Electrochemical Analysis*, Vol. 2, Blackie and Son, Ltd., London, 1940, p. 40.
- 6 D. DEFORD, Analytical Division, 133rd Meeting Am. Chem. Soc., San Francisco, 1958.
- 7 K. WUETHRICH AND S. FALLAB, *Helv. Chim. Acta*, 47 (1964) 1440.
- 8 H. B. MARK, JR., *J. Electroanal. Chem.*, 7 (1964) 276.
- 9 H. B. MARK, JR., *Anal. Chem.*, 36 (1964) 940.

J. Electroanal. Chem., 16 (1968) 397-404

POLAROGRAPHIC DIFFUSION COEFFICIENTS OF NITROAMMINECOBALT(III) COMPLEX IONS

HARUKO IKEUCHI

Faculty of Science and Technology, Sophia University, Chiyoda-ku, Tokyo (Japan)

(Received April 6th, 1967)

INTRODUCTION

The Ilkovič equation of the diffusion current in polarography¹, original or modified, has often been applied to the determination of the diffusion coefficients of depolarizers²⁻⁴. Because of the ease and rapidity of measurements, this method is expected to be particularly useful for the determination of the diffusion coefficients of relatively unstable species in supporting electrolyte solutions.

VON STACKELBERG and his co-workers determined the diffusion coefficients of some inorganic ions in supporting electrolyte solutions of various ionic strengths⁴; the diffusion coefficients were calculated from the mean diffusion currents by using the modified Ilkovič equation with the numerical factor of 17 in the correction term. The diffusion coefficients thus obtained were compared with the values determined by the Cottrell cell method under the same conditions. GOKHShteIN also developed similar studies³, where the polarographic diffusion coefficients were computed by means of HANS' equation⁵ as for the mean diffusion current, and the *D*-values were compared with the results obtained by micro-diffractometry with a solution of the same composition. According to their results, the diffusion coefficients, which were determined by different methods, generally showed very good agreement with each other. In order to clarify the physical meaning of the diffusion coefficient determined by the polarographic method, however, more accurate experimental studies are required. This work concerns the polarographic determination of the diffusion coefficients of nitroamminecobalt(III) complex ions, $[\text{Co}(\text{NH}_3)_6]^{3+}$, $[\text{Co}(\text{NH}_3)_5\text{NO}_2]^{2+}$, *cis*- $[\text{Co}(\text{NH}_3)_4(\text{NO}_2)_2]^+$, *trans*- $[\text{Co}(\text{NH}_3)_4(\text{NO}_2)_2]^+$, $[\text{Co}(\text{NH}_3)_3(\text{NO}_2)_3]$ and $[\text{Co}(\text{NH}_3)_2(\text{NO}_2)_4]^-$, in aqueous solutions of various ionic strengths. These ions are substitution-inert species and are theoretically interesting because they have nearly equal sizes but different charges.

EXPERIMENTAL

A potentiostat circuit⁶ with an operational amplifier and a high-speed recorder, as shown in Fig. 1, was used to measure the current-time curves during the life of a mercury drop. The instantaneous limiting current was measured by the following procedure: the electrode potential was adjusted to a given value on the limiting current plateau of the current-potential curve, and then the circuit was closed manually by the switch S in Fig. 1 at the moment when a mercury drop began to grow in the solu-

tion. The error due to possible fluctuations of time lag in the manual operation was negligible at the end of the life of a mercury drop, and the measured current was reproducible to $\pm 0.1\%$. The current-time curves thus recorded were corrected for residual currents which were measured by the same method with the supporting electrolyte solutions. The dropping mercury electrode (DME) used had a mean rate of mercury flow (\bar{m}) of 1.693 mg/sec and a drop time (t_d) of 5.05 sec, when measured in

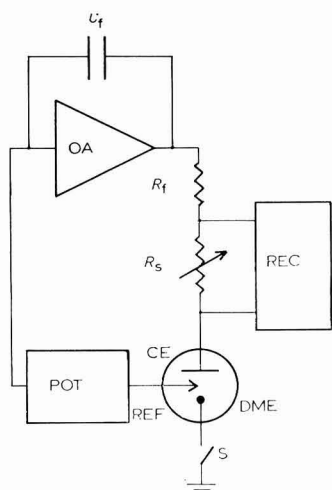


Fig. 1. Block diagram of the potentiostat circuit for the measurement of current-time curves; OA, operational amplifier (UPA-2, Philbrick Researches, Inc.); REC, high-speed recorder (Type D-5, Riken Denshi Co., Ltd.); POT, potentiometer; DME, dropping mercury electrode; CE, counter electrode (SCE); REF, reference electrode (SCE). $C_f = 0.5$ or $1 \mu\text{F}$; $R_f = 30$ or $60 \text{ k}\Omega$; $R_s = 0.5\text{--}5 \text{ k}\Omega$.

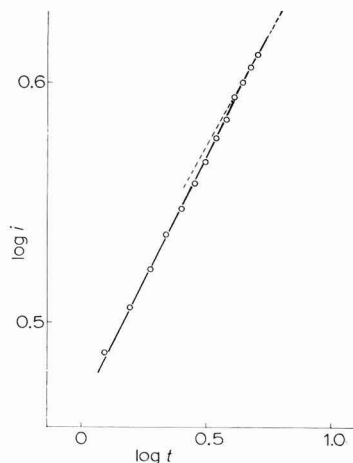


Fig. 2. Relation between $\log i$ and $\log t$ (i in μA , t in sec) of the first drop at the potential on the limiting current plateau, -0.7 V vs. SCE , and at a height of the mercury reservoir of 60 cm. Composition of soln.: $1 \text{ mM } [\text{Co}(\text{NH}_3)_6]\text{Cl}_3$, 0.1 M KNO_3 , 10 mM HNO_3 , $0.0005\% \text{ Triton X 100}$. The broken line corresponds to the line with a theoretical slope of 0.187 .

an air-free 0.1 M potassium nitrate solution at $-0.35 \text{ V vs. a saturated calomel electrode (SCE)}$ and at 60 cm of the height of a mercury reservoir. The values of t_d and \bar{m} were measured in each measurement of the diffusion current. The instantaneous rate of mercury flow (m) at the end of the life of a mercury drop was calculated from \bar{m} by considering the effect of back pressure. All measurements were carried out in a thermostatted bath of $25 \pm 0.1^\circ$.

Nitroaminocobalt(III) complexes ($[\text{Co}(\text{NH}_3)_6]\text{Cl}_3$, $[\text{Co}(\text{NH}_3)_5\text{NO}_2]\text{Cl}_2$, *cis*- $[\text{Co}(\text{NH}_3)_4(\text{NO}_2)_2]\text{Cl}$, *trans*- $[\text{Co}(\text{NH}_3)_4(\text{NO}_2)_2]\text{Cl}$, $[\text{Co}(\text{NH}_3)_3(\text{NO}_2)_3]$ and $\text{NH}_4[\text{Co}(\text{NH}_3)_2(\text{NO}_2)_4]$) of high purity were prepared and provided by Mr. T. ISOONO of the *Institute of Physical and Chemical Research, Tokyo**. All other chemicals were of analytical-reagent grade; redistilled water was used to prepare the solutions.

The composition of the cell solution was as follows: depolarizer, 1 mM nitroaminocobalt(III) complex; supporting electrolyte, $0\text{--}2 \text{ M KNO}_3 + 10 \text{ mM HNO}_3$;

* Chemical analysis data of the complexes are reported in ref. 9.

maximum suppressor, 0.0005% Triton X 100. Nitric acid was added in order to prevent the hydrolysis of cobalt(II) species at the DME.

Prior to each measurement, the cell solution was deoxygenated by bubbling oxygen-free nitrogen gas, saturated with water vapour at 25°, through the solution.

RESULTS AND DISCUSSION

All the nitroamminecobalt(III) complexes studied gave well-defined polarographic waves corresponding to the one-electron reduction of Co(III) to Co(II).

From the analysis of the relation between the maximum instantaneous limiting current (i_l) and the height of the mercury reservoir (h) corrected for back pressure, and also from the analysis of the current-time (i - t) curve, the limiting current of each complex was shown to be diffusion-controlled. The ratios of i_l to $h^{\frac{1}{2}}$, were almost independent of h as shown in Table 1. In each system, the log i -log t curve obtained with the first drop had a slope very close to that calculated by considering the correction term of Koutecký; the result obtained with a hexamminecobalt(III) ion is reproduced in Fig. 2 as an example. The value of i_l , measured in solutions of the same ionic strength, was proportional to the bulk concentration of each complex.

TABLE 1

RATIOS OF THE MAXIMUM INSTANTANEOUS LIMITING CURRENTS TO THE SQUARE-ROOTS OF THE HEIGHT OF THE MERCURY RESERVOIR CORRECTED FOR BACK PRESSURE, $i_l/h^{\frac{1}{2}}$ IN $\mu\text{A cm}^{-\frac{1}{2}}$, AT 25°.

Composition of the solutions: 1 mM nitroamminecobalt(III) complex, 0.1 M KNO₃, 10 mM HNO₃, 0.0005% Triton X 100.

Complex	h (cm)							
	38.5	43.5	48.5	53.5	58.5	63.5	68.5	73.5
[Co(NH ₃) ₆] ³⁺	—	—	1.32	1.31	1.31	1.31	1.30	1.30
[Co(NH ₃) ₅ NO ₂] ²⁺	1.41	1.39	1.38	1.37	1.37	1.35	—	—
<i>cis</i> -[Co(NH ₃) ₄ (NO ₂) ₂] ⁺	1.46	1.44	1.43	1.43	1.42	1.41	—	—
<i>trans</i> -[Co(NH ₃) ₄ (NO ₂) ₂] ⁺	1.39	1.37	1.37	1.36	1.36	1.36	—	—
[Co(NH ₃) ₃ (NO ₂) ₃]	1.38	1.36	1.34	1.32	1.32	1.31	—	—
[Co(NH ₃) ₂ (NO ₂) ₄] ⁻	1.52	1.51	1.50	1.49	1.49	1.48	—	—

The effect of the surface-active substance, Triton X 100, on the diffusion current, was examined with the reduction wave of hexamminecobalt(III) ions. In the absence of Triton X 100, the hexamminecobalt(III) ion in 0.1 M potassium nitrate solutions containing 10 mM nitric acid showed no maximum of the first kind and developed a well-defined diffusion current plateau. Although the half-wave potential became more negative with increasing concentration of Triton X 100, the shape of the i - t curve and the value of the maximum instantaneous diffusion current were not affected by the addition of up to 0.001% of Triton X 100. It was assumed, therefore, that the effect of 0.0005% Triton X 100 on the diffusion currents can also be neglected with the other nitroamminecobalt(III) complex ions studied.

The diffusion currents of the complex, except that of hexamminecobalt(III) ion, decreased linearly with the lapse of time after the preparation of the solution. Therefore, the diffusion currents at time zero, which were estimated by the method of extrapolation, were used for the determination of the diffusion coefficients.

TABLE 2
POLAROGRAPHIC DIFFUSION COEFFICIENTS OF NITROAMMINECOBALT(III) COMPLEX IONS IN AQUEOUS SOLUTIONS OF VARIOUS IONIC STRENGTHS AT 25°. Composition of the solution: 1 mM nitroamminecobalt(III) complex, 0.2 M KNO₃, 10 mM HNO₃, 0.0005% Triton X 100.

I	$D \cdot 10^6 \text{ (cm}^2/\text{sec)}$						
(M)	$[\text{Co}(\text{NH}_3)_6]^{3+}$	$[\text{Co}(\text{NH}_3)_5\text{NO}_2]^{2+}$	$\text{cis-}[\text{Co}(\text{NH}_3)_4(\text{NO}_2)_2]^{+}$	$\text{trans-}[\text{Co}(\text{NH}_3)_4(\text{NO}_2)_2]^{+}$	$[\text{Co}(\text{NH}_3)_3(\text{NO}_2)_3]$	$[\text{Co}(\text{NH}_3)_2(\text{NO}_2)_4]^{-}$	
0	(8.82)	(8.75)	(9.18)	(9.06)	8.99*	(8.80)	
0.01	7.60	7.71	8.36	8.03	9.09	9.99	
0.05	—	—	—	—	9.01	—	
0.06	7.69	8.03	8.66	8.35	—	9.53	
0.08	—	—	—	—	9.04	—	
0.11	7.70	8.20	8.68	8.41	—	9.63	
0.16	—	—	—	8.34	9.06	—	
0.21	7.70	8.24	8.62	8.28	—	9.59	
0.38	—	—	—	—	9.02	—	
0.41	—	—	—	8.33	—	9.67	
0.51	7.61	8.32	8.45	8.48	—	—	
1.01	7.57	8.06	8.39	8.34	8.98	9.31	
2.01	7.22	7.41	7.83	7.86	8.58	8.71	

* determined in nitric acid soln. of ionic strength 5 mM.

The diffusion coefficient (D) was calculated by the modified Ilkovič equation of Koutecký⁷:

$$i_d = k_1 n m^{\frac{2}{3}} t_d^{\frac{1}{3}} D^{\frac{1}{2}} C (1 + k_2 t_d^{\frac{1}{3}} m^{-\frac{1}{3}} D^{\frac{1}{2}}) \quad k_1 = 707.6 \quad k_2 = 39.7 \quad \text{at } 25^\circ$$

where i_d is the instantaneous diffusion current at the end of the life of a mercury drop, n , the number of electrons involved in the reduction process, and C , the bulk concentration of the depolarizer.

Table 2 and Fig. 3 represent the experimentally determined values of the diffusion coefficients of nitroamminecobalt(III) complexes in solutions of various ionic strengths. The reproducibility of D -values was about 1%. The diffusion coefficients at infinite dilution (D°) were calculated from the limiting ionic conductivities, λ° ^{8,9} according to the Nernst equation¹⁰. In solutions of high ionic strengths, the diffusion coefficients of the complex ions generally gave smaller values than those at infinite dilution. A similar decrease in the diffusion coefficient was also observed with an

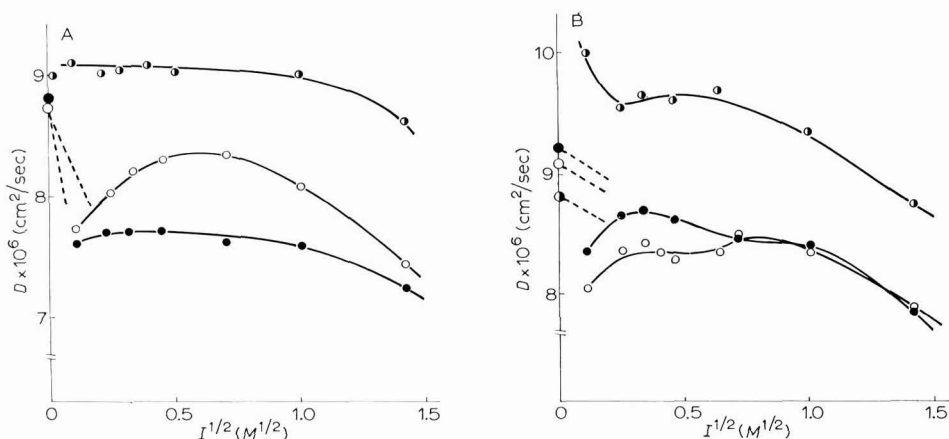


Fig. 3. Relation between the diffusion coefficients and the square-roots of ionic strength. Composition of solns.: 1 mM nitroamminecobalt(III) complex, 0.2 M KNO₃, 10 mM HNO₃, 0.0005% Triton X 100. The broken lines correspond to the theoretical Gosting-Harned lines.

(a) (●), [Co(NH₃)₆]³⁺; (○), [Co(NH₃)₅NO₂]²⁺; (●), [Co(NH₃)₃(NO₂)₃].

(b) (●), *cis*-[Co(NH₃)₄(NO₂)₂]⁺; (○), *trans*-[Co(NH₃)₄(NO₂)₂]⁺; (●), [Co(NH₃)₂(NO₂)₄]⁻.

electrically neutral complex, [Co(NH₃)₃(NO₂)₃]. The viscosity change of potassium nitrate solutions is relatively small in the concentration range studied; the viscosity decreases slightly with increasing concentration of potassium nitrate to about 1 M, after which it increases gradually and reaches a value almost equal to that of pure water at a concentration of 2 M¹¹. Therefore, the decrease in the diffusion coefficients cannot be explained solely by the viscosity effect.

The diffusion coefficients of [Co(NH₃)₂(NO₂)₄]⁻ showed a very different dependence on the ionic strength from those of the other complex ions, as shown in Fig. 3(b); in the range of ionic strength 0.01–1, the experimentally obtained D -values were much larger than those expected from the diffusion coefficient at infinite dilution.

The physical nature of the diffusion process under polarographic conditions is supposed to be similar to the so-called tracer-diffusion¹⁰. The diffusion coefficient,

D_j , of a tracer ion, j , in a solution of relatively low ionic strength is theoretically given by the equation of GOSTING AND HARNED¹²;

$$D_j = \frac{\lambda_j^\circ RT}{|Z_j| F^2} \times 10^{-7} - \frac{\lambda_j^\circ |Z_j| v^2 e}{3\epsilon} \times 10^{-9} \sqrt{\frac{4\pi}{1000 \epsilon RT}} \left[1 - \sqrt{d(\omega_j)} \right] \sqrt{T}$$

$$d(\omega_j) = \frac{1}{\Gamma} \sum_i \frac{C_i |Z_i| \lambda_i^\circ}{\lambda_j^\circ |Z_j| + \lambda_i^\circ |Z_i|} \quad \Gamma = \sum_i C_i Z_i^2$$

where λ° is the limiting ionic conductivity of the i th ion, C_i the ionic concentration in moles, T the absolute temperature, ϵ the dielectric constant of the solution, v the velocity of light, e the electric charge, R the gas constant, $|Z_j|$ the valence of the j th ion, and F the Faraday. The broken lines in Fig. 3 represent the theoretical curves calculated by means of the Gosting-Harned equation. The experimental values of nitroamminecobalt(III) complexes showed appreciable deviation from the theoretical lines both at high and very low ionic strengths. A more pronounced deviation was observed at high ionic strengths with ions of higher charges. Such a deviation would be due partly to the size-effect of ions in the solution and to the effect of possible ion-pair formation of the diffusing species. The relatively large deviation of the experimentally obtained D -values at very low ionic strengths from the theoretical values, cannot be explained by the migration effect; at present, no explanation is available for this rather peculiar behavior of the polarographic diffusion coefficients.

It can be concluded from the results that the polarographic diffusion coefficients generally show a relatively complicated dependence on the ionic strength of the solution, which cannot be explained by a limiting equation for tracer-diffusion such as that proposed by GOSTING AND HARNED. In order to understand the physical meaning of the polarographic diffusion coefficients, more information on the physicochemical properties of the diffusing species in the solution and more advanced theoretical treatments of the diffusion process would be required.

ACKNOWLEDGEMENT

The author wishes to thank Dr. R. TAMAMUSHI of the Institute of Physical and Chemical Research for his helpful discussion and generous support of this work, and also Dr. G. P. SATÔ for his valuable suggestions and discussion.

SUMMARY

The diffusion coefficients of nitroamminecobalt(III) complex ions, $[\text{Co}(\text{NH}_3)_6]^{3+}$, $[\text{Co}(\text{NH}_3)_5\text{NO}_2]^{2+}$, *cis*- $[\text{Co}(\text{NH}_3)_4(\text{NO}_2)_2]^+$, *trans*- $[\text{Co}(\text{NH}_3)_4(\text{NO}_2)_2]^+$, $[\text{Co}(\text{NH}_3)_3(\text{NO}_2)_3]$ and $[\text{Co}(\text{NH}_3)_2(\text{NO}_2)_4]^-$, were determined polarographically with a dropping mercury electrode in potassium nitrate solutions of various ionic strengths. In order to minimize the so called Verarmungs-Effekt, the current-time curve of the first mercury drop growing in the electrolyte solution was recorded at the potentials on the limiting current plateau. The properties of instantaneous limiting currents satisfied the conditions required for the diffusion-controlled limiting current. The diffusion coefficient was calculated from the maximum instantaneous current of the first drop according to the modified Ilkovič equation, with the correction term of Koutecký. The diffusion coefficients of the complex ions thus obtained were examined in terms of the Gosting-Harned equation for tracer diffusion.

REFERENCES

- 1 I. M. KOLTHOFF AND J. J. LINGANE, *Polarography*, Interscience Publishers, New York, London, 1952.
- 2 D. S. TURNHAM, *J. Electroanal. Chem.*, 9 (1965) 440; 10 (1965) 19.
- 3 YA. P. GOKHShteIN, *Zh. Fiz. Khim.*, 26 (1952) 224; 28 (1954) 1417; 30 (1956) 1584; 31 (1957) 403.
- 4 M. VON STACKELBERG, M. PILGRAM AND V. TOOME, *Z. Elektrochem.*, 57 (1953) 342.
- 5 W. HANS, W. HENNE AND E. MEURER, *Z. Elektrochem.*, 58 (1954) 836.
- 6 H. V. MALMSTADT, C. G. ENKE AND E. C. TOREN, JR., *Electronics for Scientists*, W. A. Benjamin, Inc., New York, 1963, p. 370.
- 7 J. KOUTECKÝ, *Czech. J. Phys.*, 2 (1953) 50.
- 8 S. KATAYAMA, *Rep. Inst. Phys. Chem. Res. Tokyo*, 42 (1966) 243.
- 9 R. TAMAMUSHI, T. ISONO AND S. KATAYAMA, *Bull. Chem. Soc. Japan*, 40 (1967) 334.
- 11 R. A. ROBINSON AND R. H. STOKES, *Electrolyte Solution*, Butterworths, London, 1959, p. 314.
- 11 *International Critical Tables*, 1929, V, p. 18.
- 12 L. J. GOSTING AND H. S. HARNED, *J. Am. Chem. Soc.*, 73 (1951) 159.

J. Electroanal. Chem., 16 (1968) 405-411

POLAROGRAPHY OF LEAD-TRIETHYLENETETRAMINE CHELATE

TSAI-TEH LAI AND JIA-YONG CHEN

Department of Chemical Engineering, Cheng Kung University, Tainan, Taiwan (China)

(Received May 2nd, 1967)

INTRODUCTION

In a polarographic study of the complexes of triethylenetetramine ("trien") with lead and other metals, JACOBSEN AND SCHRÖDER have shown that trien forms a stable complex with lead and that the reduction of the complex at the dropping mercury electrode is a reversible and diffusion-controlled process¹. PECOK *et al.*² have studied the Cr(II)-trien system by spectrophotometric and magnetic methods. SARGESON and co-workers have made an extensive study of the Co(III)-trien chelates and established their configuration^{3,4}.

In this paper we have made further investigations into the Pb-trien system to determine the composition and the instability constant of the Pb-trien chelate.

EXPERIMENTAL

Apparatus

Polarograms were recorded manually with a Sargent Model XII polarograph, equipped with a Leeds and Northrup Student potentiometer. Half-wave potentials were reproducible to ± 1 mV.

A modified H-cell, with a saturated calomel electrode (SCE) as a reference electrode, was employed. The dropping mercury electrode used had a mercury flow rate of 2.24 mg/sec and a drop time of 3.63 sec, which was measured in an air-free 0.2 M potassium nitrate solution at an applied potential of -0.200 V *vs.* SCE and at 70.3 cm of mercury height. The temperature of the cell was thermostatted at $25.0 \pm 0.1^\circ$.

The pH-values of the polarographic solutions were adjusted with nitric acid or potassium hydroxide and determined by a Toa Denpa Model HM-5A glass electrode pH-meter.

Chemicals

A stock solution of 0.01 M lead nitrate was prepared by dissolving 3.312 g of $\text{Pb}(\text{NO}_3)_2$ in distilled water and diluting to 1 l.

Extra pure trien (Kanto Chemical Co., Japan) was purified by the REILLEY AND SCHMID method⁵. Standard solutions of trien were prepared and standardized following the procedures given by REILLEY AND SHELDON⁶. The other chemicals were of reagent-grade and were used without further purification.

All the polarographic solutions contained 1.0 mM lead nitrate, and the ionic strength was adjusted to 1.0 with 2 M potassium nitrate solution. Maximum suppressors were not required.

RESULTS AND DISCUSSION

The conventional plots of $-\log i/(i_d - i)$ vs. $E_{d.e.}$ for all polarograms taken in the ligand concentration range, 0.0485–0.3416 M at pH 4.0–12.0 give straight lines with slopes falling in the range 0.028–0.034, indicating that the electrode reactions were reversible two-electron reduction processes.

The variation of the limiting current with the height of the mercury column was measured in a solution of 1.0×10^{-3} M lead nitrate, 0.0485 M trien, and 0.4 M potassium nitrate at pH 7.20. The current varied with the mercury height; the value, i_d/\sqrt{h} , where h is the column height after correction for the back pressure, was $0.728 \pm 0.006 \mu A \text{ cm}^{-\frac{1}{2}}$ for h -values of 49.6–84.3 cm, indicating that the electrode reactions are entirely diffusion-controlled.

Effect of pK on half-wave potential

Trien is a polyamine with $pK_1=3.37$, $pK_2=6.67$, $pK_3=9.20$ and $pK_4=9.92$, where the pK 's are the acid dissociation constants of the protonated trien^{2,7}. As trien is a tetradentate²⁻⁴ and lead invariably forms a dipositively-charged complex ion with trien (proved by zone electrophoresis, see below), it is evident that the ligand species is the neutral trien molecule rather than the protonated trien. The electrode reaction can, therefore, be represented as:



where A is the neutral trien molecule. The half-wave potential of the reaction is given by Nernst equation as

$$(E_{\frac{1}{2}})_c = (E_{\frac{1}{2}})_s + 0.030 \log K_c - 0.030 p \log [A] \quad (2)$$

where K_c is the instability constant of the $Pb(A)_p^{2+}$ complex. If $C_A = [A] + [HA^+] + [H_2A^{2+}] + [H_3A^{3+}] + [H_4A^{4+}]$, we have:

$$[A] = \frac{K_1 K_2 K_3 K_4 C_A}{[H^+]^4 + K_1 [H^+]^3 + K_1 K_2 [H^+]^2 + K_1 K_2 K_3 [H^+] + K_1 K_2 K_3 K_4} \quad (3)$$

Substitution of eqn. (3) into eqn. (2) gives:

$$(E_{\frac{1}{2}})_c = (E_{\frac{1}{2}})_s + 0.030 \log K_c - 0.030 p \log K_1 K_2 K_3 K_4 - 0.030 p \log C_A \\ + 0.030 p \log ([H^+]^4 + K_1 [H^+]^3 + K_1 K_2 [H^+]^2 + K_1 K_2 K_3 [H^+] + K_1 K_2 K_3 K_4) \quad (4)$$

Therefore, the half-wave potential depends on the acid dissociation constants of the chelating agent as well as the pH and the nominal concentration of the chelating agent.

Chelate species

At constant pH, eqn. (4) becomes

$$(E_{\frac{1}{2}})_c = C - 0.030 p \log C_A \quad (5)$$

where $C = (E_{\frac{1}{2}})_s + 0.030 \log K_e - 0.030 p \log K_1 K_2 K_3 K_4 + 0.030 p \log ([H^+]^4 + K_1[H^+]^3 + K_1 K_2[H^+]^2 + K_1 K_2 K_3[H^+] + K_1 K_2 K_3 K_4)$.

The half-wave potential is thus a function of the nominal concentration of the chelating agent only. Equation (5) suggests that a plot of $\log C_A$ vs. $-(E_{\frac{1}{2}})_e$ at a specified pH-value should give a straight line with reciprocal slope $0.030 p$. This deduction is supported by Fig. 1, in which the lines at different pH-values have reciprocal

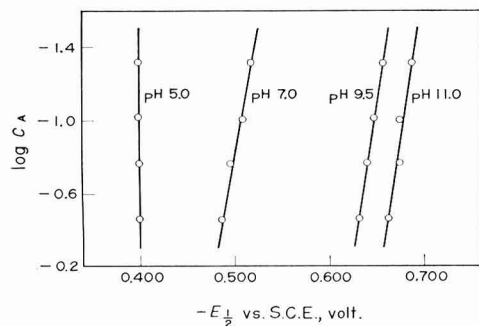


Fig. 1. Half-wave potential as a function of trien concn.

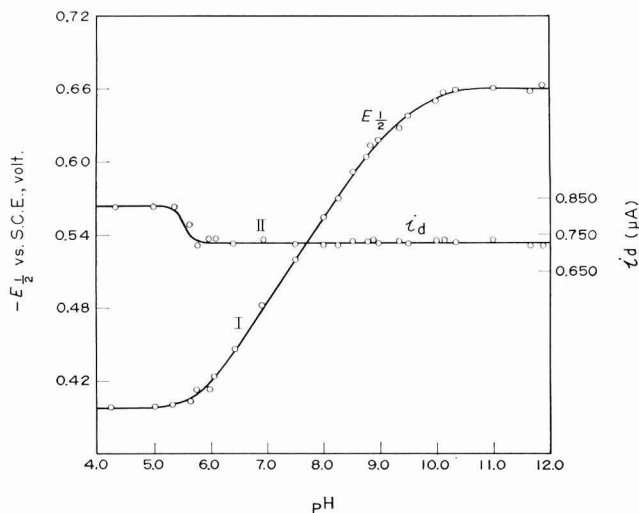


Fig. 2. Half-wave potential and diffusion current as a function of pH ($1.0 \text{ mM Pb(NO}_3)_2$, $4.85 \times 10^{-2} \text{ M trien}$).

slopes ranging from 0.027 to 0.032. Therefore, p , the ligand number, is 1 for the entire pH-range investigated except at pH-values below 5.4, where the concentration of the ligand species, $[A]$, is so low that no chelation occurs. This can be observed from Fig. 2, in which the half-wave potential of the complex is identical with that of the simple lead ion, -0.398 V , at pH-values below 5.4.

It is obvious from Table 1 that the diffusion current is independent of the ligand concentration but decreases from a constant value of 0.825 to $0.727 \mu\text{A}$ as the pH of the solution increases. Thus, the variation of current with pH suggests that

two complex species exist at different pH-ranges. The diffusion current *vs.* pH curve breaks at pH 5.4, which is in good agreement with that of the first breaking point of the $E_{\frac{1}{2}}$ -pH curve (see Fig. 2). It was verified, therefore, that below pH 5.4, lead exists as an *aquo* complex in trien solution, and at pH 5.4–12.0 forms with trien a 1:1 chelate which is a tetradentate.

Instability constant

Substituting $p=1$ in eqn. (4) and solving explicitly for $\log K_e$ we have:

$$\log K_e = \frac{(E_{\frac{1}{2}})_c - (E_{\frac{1}{2}})_s}{0.030} + \log K_1 K_2 K_3 K_4 + \log C_A - \log ([H^+]^4 + K_1[H^+]^3 + K_1 K_2[H^+]^2 + K_1 K_2 K_3[H^+] + K_1 K_2 K_3 K_4) \quad (6)$$

The instability constant of the complex is evaluated from eqn. (6) and the data are listed in Table 2. The pK_e -values calculated at different pH-values and various

TABLE 1

EFFECT OF pH AND LIGAND CONCENTRATION ON DIFFUSION CURRENT

<i>Trien</i> (M)	<i>i_d</i> (μA)				
	pH 4.25	pH 5.00	pH 7.50	pH 9.50	pH 11.00
0.0485	0.821	0.830	0.726	0.728	0.732
0.0970	0.830	0.824	0.738	0.730	0.726
0.1708	0.815	0.818	0.722	0.729	0.720
0.3416	0.828	0.832	0.735	0.724	0.728

TABLE 2

INSTABILITY CONSTANT CALCULATED AT VARIOUS pH VALUES AND LIGAND CONCENTRATIONS

C_A (M)	pH	$-(E_{\frac{1}{2}})_c$ (V)	$[A]$ (M)	pK_e
4.85×10^{-2}	6.00	0.418	6.50×10^{-10}	9.85
	7.00	0.488	2.50×10^{-7}	9.60
	8.00	0.558	3.32×10^{-5}	9.81
	9.00	0.618	2.15×10^{-3}	10.00
	10.00	0.646	2.46×10^{-2}	9.88
	11.00	0.663	4.49×10^{-2}	10.15
9.70×10^{-2}	6.00	0.427	1.30×10^{-9}	9.85
	7.00	0.495	5.00×10^{-7}	9.53
	8.00	0.556	6.64×10^{-5}	9.75
	9.00	0.626	4.30×10^{-3}	9.97
	10.00	0.654	4.92×10^{-2}	9.84
	11.00	0.670	8.98×10^{-2}	10.11
1.708×10^{-1}	6.00	0.440	2.29×10^{-9}	9.84
	7.00	0.508	8.80×10^{-7}	9.72
	8.00	0.576	1.17×10^{-4}	9.87
	9.00	0.635	7.56×10^{-3}	10.12
	10.00	0.662	8.67×10^{-2}	9.86
	11.00	0.677	1.58×10^{-1}	10.06
3.416×10^{-1}	6.00	0.450	4.58×10^{-9}	10.07
	7.00	0.518	1.76×10^{-6}	9.75
	8.00	0.585	2.34×10^{-4}	9.86
	9.00	0.645	1.51×10^{-2}	10.05
	10.00	0.672	1.73×10^{-1}	9.89
	11.00	0.685	3.16×10^{-1}	10.07
				Av. 9.86 ± 0.13

ligand concentrations are in good accord, and the average value is found to be 9.86 ± 0.13 at ionic strength 1.0.

The relation between the pK-values and the breaking points in $E_{\frac{1}{2}}$ -pH plots

We have shown previously, that the $E_{\frac{1}{2}}$ -pH curve always breaks into straight lines with slopes equal to a multiple of 0.030 or 0.060, and that the pH-values of the breaking points fall on the pK-values of the chelating agent⁸⁻¹¹. However, in the present study, as shown in curve 1 of Fig. 2, the pH of the breaking points (pH 5.4, 8.7 and 10.5) do not coincide with the pK-values of trien. This is deducible from eqn. (4) and it is obvious that for a chelating agent with four releasable protons, the half-wave potential of the chelate is dependent on the pH-value through the last term of the right-hand side of the equation, viz., $0.030 p \log ([H^+]^4 + K_1[H^+]^3 + K_1K_2[H^+]^2 + K_1K_2K_3[H^+] + K_1K_2K_3K_4)$. As the successive pK-values of trien are very close, it is only at limited ranges of pH that one term in parenthesis is predominant over the others. Therefore, the divergence from the deduction of our previous studies is to be expected for chelating agents such as trien.

Zone electrophoresis

In order to determine the charges of the complex species existing at different pH-ranges, zone electrophoresis was carried out using the method already described¹². In Fig. 3, the centre piece of A was impregnated with 2.0 mM $Pb(NO_3)_2$ and the

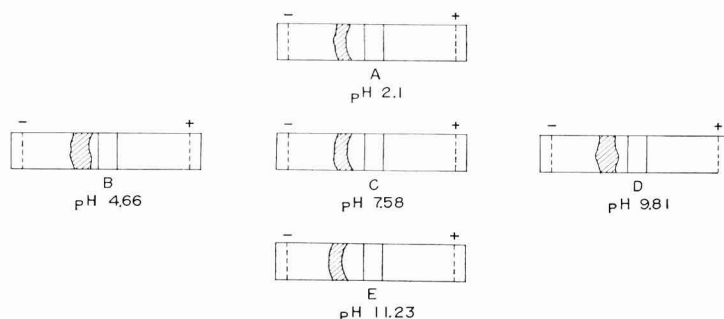


Fig. 3. Electrochromatograms of lead ion and lead-trien chelate at various pH-values. (A), lead ion; (B), (C), (D) and (E), lead-trien chelate.

end pieces with 0.15 M KNO_3 . For strips B, C, D and E, the centre piece was impregnated with 2.0 mM $Pb(NO_3)_2$ and 0.1 M trien, and the end pieces with 0.1 M trien. A 200 d.c. voltage was applied for 6 min. Ammonium sulfide was used as a developer. It is obvious from Fig. 3 that the lead-trien complexes formed are all dipositively charged above pH 5.4. Thus, the formation of only one kind of chelate species, $Pb(A)^{2+}$, was confirmed over the pH-range 5.4-12.0, where A denotes the neutral trien molecule.

ACKNOWLEDGEMENT

The authors thank the National Council of Science Development for their support of the work described.

SUMMARY

The formation of chelates between lead and triethylenetetramine has been studied by polarography and zone electrophoresis over the pH-range, 4.0–12.0 and the ligand concentration range, 0.0485–0.3416 *M*. Lead invariably forms with triethylenetetramine a 1:1 chelate, and only one kind of chelate species, Pb(A)^{2+} , (where A denotes the neutral triethylenetetramine molecule) exists in the pH-range 5.4–12.0. No chelate forms below pH 5.4. The logarithmic instability constant of the chelate obtained at 25° and ionic strength 1.0, is 9.86 ± 0.13 .

REFERENCES

- 1 E. JACOBSEN AND K. SCHRÖDER, *J. Phys. Chem.*, 66 (1962) 134.
- 2 R. L. PECSOK, R. A. GARBER AND L. D. SHIELD, *Inorg. Chem.*, 4 (1965) 447.
- 3 A. M. SARGESON AND G. H. SEARLE, *Inorg. Chem.*, 4 (1965) 45.
- 4 A. M. SARGESON, *Australian J. Chem.*, 17 (1964) 385.
- 5 C. N. REILLEY AND R. W. SCHMID, *J. Elisha Mitchell Sci. Soc.*, 73 (1957) 279.
- 6 C. N. REILLEY AND M. V. SHELDON, *Talanta*, 1 (1958) 127.
- 7 G. SCHWARZENBACH, *Helv. Chim. Acta*, 33 (1950) 974.
- 8 T.-T. LAI AND C.-K. WU, *J. Inorg. Nucl. Chem.*, 28 (1966) 869.
- 9 T.-T. LAI AND S.-J. WEY, *J. Electrochem. Soc.*, 111 (1964) 1283.
- 10 T.-T. LAI AND C.-C. HSIEH, *J. Inorg. Nucl. Chem.*, 26 (1964) 1215.
- 11 T.-T. LAI, S.-N. CHEN, B.-C. WANG AND C.-C. HSIEH, *Anal. Chem.*, 35 (1963) 1531.
- 12 T.-T. LAI AND H.-T. LIN, *J. Inorg. Nucl. Chem.*, 27 (1965) 173.

J. Electroanal. Chem., 16 (1968) 413–418

REVIEW

THE ELECTROCHEMICAL TRANSFER-COEFFICIENT

HENRY H. BAUER

Department of Chemistry, University of Kentucky, Lexington, Ky. 40506 (U.S.A.)

(Received January 27th, 1967; in revised form April 25th, 1967)

I. INTRODUCTION

The electrochemical literature pertaining to the “transfer coefficient” can readily confuse and frustrate those who seek the basis for this concept. Commonly^{1–8*}, it is stated that the kinetics of redox reactions at electrodes can be described by rate constants, k_f and k_b , respectively, for the forward and back reactions, with

$$k_f = k_f^0 \exp[-\alpha nF(E - E^0)/RT] \quad (1a)$$

and

$$k_b = k_b^0 \exp[(1 - \alpha)nF(E - E^0)/RT] \quad (1b)$$

where E is the electrode potential, α the transfer coefficient, E^0 a standard potential the choice of which fixes k_f^0 and k_b^0 , and n , F , R , and T have their usual significance.

A clear implication of eqn. (1) is that α is a parameter the value of which does not depend on the electrode potential, and on first confrontation with this formulation it is natural to ask what basis there might be for making such an assumption.

This question is not often discussed in the literature. Frequently^{1–3,5,7,9–21}, eqn. (1) is presented dogmatically, with α as a “constant”, and often without a reference; in those cases where references are given, it is quite common to find they refer to work the relevance of which is not immediately clear: *e.g.* to a discussion²² that is not nowadays accepted, or to a recapitulation²³ of the very earliest kinetic formulations; it is exceptional to find a source that even mentions “transfer coefficient”. To illustrate the possibilities for confusion, consider the proceedings²⁴ of a recent symposium on electrode processes: several authors use eqns. (1a) and (1b), with α called the transfer coefficient; one uses the equations with “ β , the transfer coefficient”; another writes $\beta = 1 - \alpha$ (*i.e.*, α for the cathodic and β for the anodic direction of the process); others reserve “ β , the symmetry factor” for the electron-transfer step itself (for which many use α , as in eqn. (1) above) and write α for the overall, or observed, or apparent value in systems where more is involved than the electron-transfer step alone.

The real point at issue is the dependence of the rate constants on the electrode

* Here, and similarly throughout this article, the references are intended to serve as examples and have been chosen from a larger number in the literature. No attempt has been made to quote exhaustively.

potential. This article traces the history of concepts relevant to this issue and seeks to make the following points:

1. There is no satisfactory theoretical basis for introducing, *a priori*, an implicitly potential-independent parameter such as α in relations such as (1) above.
2. Various workers use different physical models to provide a justification for eqn. (1), usually implicitly and without making clear that their interpretation differs from others in the contemporary literature.
3. Commonly in earlier work, but continuing to the present time, experimentally obtained values for α are suspect for one or both of two reasons: an unsound introduction of α into the theoretical treatment (*e.g.*, as potential-independent, followed by experiments at one potential only) or a failure to make adequate allowance for some parts of the overall reaction (mass transport, adsorption, double-layer effect). Suspect values of α are then sometimes used to draw inferences about the nature of the transfer coefficient in a more general context.
4. Over the last decade, discussions have been published that provide an approach to the dependence on potential of the rate constants of electron-transfer processes that does not suffer from the confusions prevalent in the earlier literature where eqn. (1) is introduced in an *a priori* fashion.

II. BASIC CONCEPTS AND SEMINAL STUDIES

The concept embodied in eqn. (1) is that the electrode potential affects the rate constants for the (reversible) electron-transfer step and that this effect can be calculated by apportioning one part of this potential, αE , as affecting the forward reaction and the other part, $(1-\alpha)E$, as affecting the backward reaction (most workers identify the forward reaction with reduction, but in the German literature αE is used to describe the fraction relevant for the oxidation). Thus, we wish to trace the history of the idea of apportioning the electrode potential between the forward and back reactions; and we shall be interested in views about the physical significance of α , about its dependence on—or independence of—electrode potential, and also in the question of terminology.

BUTLER^{25,26} appears to have been the first to treat electrochemical reactions from a kinetic viewpoint that is essentially the same as later views. He considered the work required to bring the electroactive species* to a "balance point" where the sum of the forces attracting the reactants to the electrode was equal to the sum of the forces attracting them into the solution. This work included electrical terms which were written by apportioning the electrode potential into two parts; the rates of the reactions were then written with the use of the Boltzmann distribution. Thus, the ideas that we associate with the rate theory and the concept of an activated state were presented in an *ad hoc* fashion. BUTLER was not explicit about the manner in which the potential should be apportioned, but his treatment does imply that it is the potential *vs.* distance relationship that is decisive. He showed that this kinetic point of view led to the reversible-electrode equation of Nernst and was therefore compatible with the thermodynamic view of redox reactions:

* BUTLER considered the deposition of metal ions on an electrode of the same material and also redox reactions at an inert electrode. The "balance point" was expressed for a metal ion in the first instance²⁵, for an electron in the second case²⁶.

At equilibrium, forward and back rates are equal; we have then

$$k_{\text{f}}C_{\text{ox}} = k_{\text{b}}C_{\text{r}} \quad (2)$$

where C_{ox} and C_{r} are concentrations of the oxidized and reduced species, respectively, at the electrode. From eqn. (1),

$$k_{\text{f}}^0 C_{\text{ox}} \exp[-\alpha nF(E - E^0)/RT] = k_{\text{b}}^0 C_{\text{r}} \exp[(1 - \alpha)nF(E - E^0)/RT] \quad (3)$$

or

$$E = E^0 + (RT/nF) (\ln [k_{\text{f}}^0/k_{\text{b}}^0]) + (RT/nF) (\ln [C_{\text{ox}}/C_{\text{r}}]) \quad (4)$$

In other words, the Nernst equation results. It is to be noted that this will ensue, irrespective of the value of α , or of whether α varies with potential.

BOWDEN²⁷ applied BUTLER's ideas to the evolution of hydrogen and oxygen. His physical model for the rate-determining step was a very special one and never gained acceptance; the importance of the work from the present viewpoint is that he wrote " αV " to describe the proportionality between electrode potential and activation energy, a formulation that implies $\alpha \neq f(V)$. BOWDEN applied the resulting equation to an irreversible process: If the back reaction can be neglected, then the net rate becomes equal to the rate of the forward process and the corresponding current-density can be written, using eqn. (1), as

$$i = nFk_{\text{f}}^0 C_{\text{ox}} \exp[-\alpha nF(E - E^0)/RT] \quad (5)$$

which gives, on rearrangement,

$$E - E^0 = (RT/\alpha nF) \ln (nFk_{\text{f}}^0 C_{\text{ox}}) - (RT/\alpha nF) \ln i \quad (6)$$

Equation (6) has the same form as the Tafel equation

$$\eta = a + b \log i \quad (7)$$

where η is the overvoltage and b is often called the "Tafel slope". If the identity of the theoretically derived eqn. (6) and the empirically based eqn. (7) is accepted, one has

$$b = 2.3 RT/\alpha nF \quad (8)$$

At the time of BOWDEN's work²⁷, most of the available experimental work was compatible with the Tafel equation (7) and the usual value of b for discharge of hydrogen ions was about 120 mV. BOWDEN pointed out that a value of $\alpha = 0.5$ satisfied these experimental findings.

The idea that the rate-determining step in hydrogen evolution is the discharge step itself was proposed by ERDEY-GRUZ AND VOLMER²⁸ in 1930. They considered that in the presence of a potential, E , the energy required for electron transfer was decreased by αFE , with $\alpha < 1$; they then proposed further that the electric field would affect the forward and backward electron-transfer rates to an equal and opposite extent, leading to the conclusion that $\alpha = 0.5$. Application to the irreversible case (appreciable over-potential, neglect of the backward reaction) then gave the Tafel equation with a slope that corresponded well with experiment (*cf.* BOWDEN²⁷, above). Since it was concluded that $\alpha = 0.5$, necessarily, no question of a dependence of α on potential arose in this work.

GURNEY²⁹ published in 1931 an article that ranks at least with those of

BUTLER, BOWDEN, and ERDEY-GRUZ AND VOLMER, in its effect on subsequent discussions of electrode processes. GURNEY proposed a theory of electron-transfer by quantum-mechanical tunnelling through an energy barrier, the effect of the electrode potential being to bring the energy levels on both sides of the barrier to equal values so that tunnelling could proceed with a maximum probability. For the irreversible case considered, the reaction rate was expressed by a distribution function that contained the exponential of the electrode potential; such a relationship would give a Tafel slope in which $\alpha=1$ rather than the accepted (experimental) value of close to 0.5. GURNEY introduced a factor that overcame this discrepancy by considering the electron transfer in terms of Morse curves: the stable hydrated ion (curve a, Fig. 1) would, upon neutralization, become an assembly (curve b) containing excess

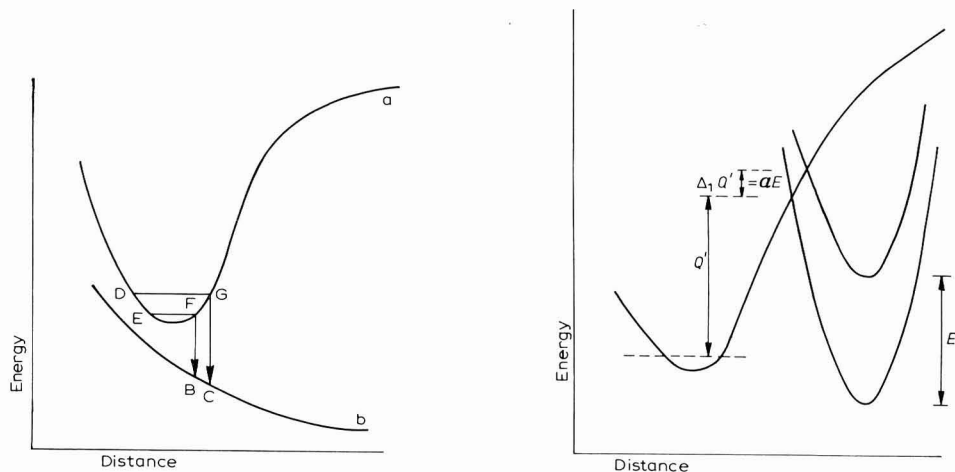


Fig. 1. Energy relations in reduction, after GURNEY²⁹. (a) the stable hydrated ion; (b) the products in an excited state.

Fig. 2. Reduction process according to HORIUTI AND POLANYI⁴⁴. The electrode potential raises the energy of the hydrogen ion but not of the reduced form. The change in activation energy is a fraction of the electrical energy and depends on the slopes of the curves in the region where they intersect.

energy which the products of the reaction would carry away. Therefore, the distribution function for the energy levels for which neutralization could occur (between levels EF and DG in Fig. 1) had to be modified to take into account that the energy required for neutralization was greater by the amount by which $(GC - FB)$ exceeds the difference between levels EF and DG. GURNEY wrote this difference as a factor γ (which in our notation corresponds to $1/\alpha$) and stated that, to a first approximation, γ would be constant and greater than 1, and that for $\gamma=2$, experimental results were in agreement with the theory.

The ideas of BUTLER, BOWDEN, ERDEY-GRUZ AND VOLMER, and GURNEY were adopted and adapted in all later work. One common thread in much of this later work is the explicit or implicit assumption³⁰⁻³³ that $\alpha=0.5$ (usually made because this value gave agreement with experimental results when used in the theories described). This assumption had a long reign despite the fact that it was

stated quite early by ERDEY-GRUZ AND WICK³⁴ and by FRUMKIN³⁵ that no satisfactory conceptual basis for this assumption existed.

ERDEY-GRUZ AND WICK³⁴ wrote eqn. (1b) in the form

$$k_b = k_b^0 \exp[\beta n F (E - E^0) / RT] \quad (9)$$

In order that eqns. (1a) and (9) should lead to the Nernst equation (*cf.* eqns. (2)–(4)), it was necessary that

$$\alpha + \beta = 1 \quad (10)$$

and this was pointed out by ERDEY-GRUZ AND WICK³⁴; $\alpha = \beta = 0.5$ corresponded in their view to a very special case only, *viz.*, to a situation where the energy barrier lies in the middle of the electrical field of the double layer. FRUMKIN³⁵ did not use a physical interpretation in his criticism and pointed out quite generally that no assumption beyond that represented by eqn. (10) was required to make this kinetic theory compatible with the Nernst equation.

Earlier, FRUMKIN³⁶ had indicated the formal similarity between eqn. (1) and the relationship found by BRØNSTED³⁷ between rates and equilibrium constants in acid–base reactions—in both cases, the activation energy is changed by a certain fraction of the overall energy (“Affinität”) change.

This work, all published before 1934, includes, explicitly or implicitly, all the ideas that have been formulated on the question of the transfer coefficient; in particular, the following had been suggested:

1. The transfer coefficient describes the symmetry of the energy barrier for the electron transfer. In its simplest form, this view apportions the electrode potential according to the relative positions of the initial, final, and activated states in the region where the potential drop at the electrode occurs; however, the “symmetry” idea has also been associated with quantum-mechanical formulations, and with the relative slopes of Morse curves. “Symmetry” views are discussed further in Section IV.

2. The transfer coefficient arises in the calculation of the relevant distribution functions in a quantum-mechanical treatment.

3. The transfer coefficient is a function of the relative slopes of Morse curves at the point(s) where transition from one curve to another occurs.

4. The transfer coefficient is one manifestation of a general relationship between free-energy difference (between reactants and products) and the corresponding activation energies.

During the remainder of the 1930's the ideas described above were re-formulated in various studies, without any essentially new ideas being introduced; in fact, as noted above, there was something of a regression in that often $\alpha = 0.5$ was accepted as a substantiated datum.

At this time, most of the articles on electrode kinetics dealt specifically or primarily with the problem of hydrogen overvoltage, and, in particular, with the question of what the rate-determining step might be in the overall reaction. These articles will not be quoted here because they are not relevant to our discussion, but one series of such papers must be mentioned because they are frequently and mistakenly referred to, even in comparatively recent years, as references for the source of eqn. (1):

EYRING and his colleagues discussed several aspects of the problem of hydrogen

discharge, and at the same time were developing the theory of absolute reaction rates. In the specific matter of electrochemical kinetics, the articles often quoted fall into two classes: those³⁸⁻⁴¹ that deal with rate theory in general but not with electron transfer in particular, and those^{22,42,43} that deal with charge transfer only for the particular case of hydrogen discharge and/or in terms of a model that was not accepted by other workers.

Other misleading quotations are also common in the relevant literature. More serious, however, is the cavalier manner in which potential-energy curves of various sorts have been used to illustrate the physical significance of the transfer coefficient. This is discussed in the following section.

III. ENERGY-CURVE REPRESENTATIONS

Potential-energy curves were, in the present context, first used by GURNEY²⁹ (see Fig. 1). The type of representation that is used most widely, however, is due to HORIUTI AND POLANYI⁴⁴ (see Fig. 2).

Considering the reaction to involve hydrogen atoms at the electrode and hydrogen ions on the solution side of the double layer, HORIUTI AND POLANYI represented the effect of the electrode potential by a vertical shift of the potential-energy curve of the hydrogen ion, noting that this involved neglecting small effects such as changes in the shape of the curve and in the position of the minimum. Further, it was assumed that the potential drop occurred entirely and only across the double layer and again the authors were careful to point out that this involved a simplification of the true situation. They made no unwarranted assumptions about the magnitude or constancy of α , stating merely that $\alpha=0.5$ indicated equality of the slopes of the curves at the crossing point.

A different type of energy curve (see Fig. 3) is given, *inter alia*, by PARSONS⁵⁹ (for the slow-discharge mechanism of hydrogen evolution), GERISCHER⁴⁶, and

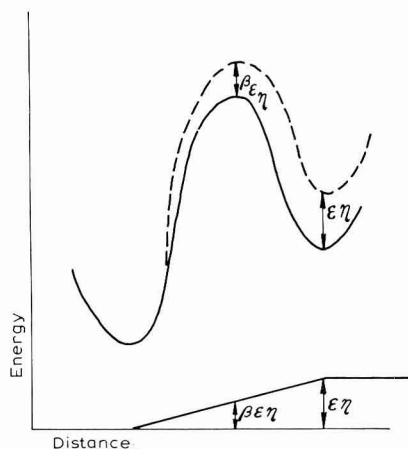


Fig. 3. Energy curve for reduction, after CHRISTOV⁴⁷.

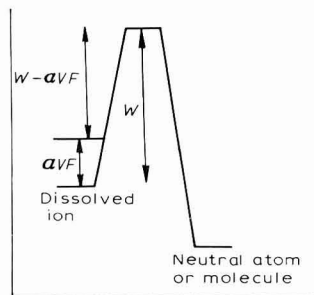


Fig. 4. Energy curve for reduction according to BOWDEN AND AGAR⁵⁰.

CHRISTOV⁴⁷. The effect of the potential is taken to be a change in energy by an amount that is determined by the potential-*vs.*-distance function, the latter generally being assumed to be linear or nearly so. The transfer coefficient is thus related to the position of the activated state in the double layer, an interpretation used by other workers also with explicit reference to distance from the surface^{7,34,42,43,48,49}. Here, then, the nature of α is bound more explicitly to a physical model than in the paper of HORIUTI AND POLANYI, but one can agree that the physical situation envisaged is not likely to be contrary to reality. Other workers, however, have given representations of the energetics of the reaction that are without apparent justification. Thus, BOWDEN AND AGAR⁵⁰ in a review article, presented the diagram shown in Fig. 4: it is not clear why the energy level of the ion was supposed to be shifted by the fraction αVF of the electrical energy involved, nor why the energy level of the activated state should remain the same; no references nor explanation were given. Similar diagrams (Fig. 5) in which the electrode potential is assumed to alter the energy levels of reactants and products in the proportions shown but to leave the energy level of the activated state unchanged, have also been given by other workers without explanation or justification^{7,13,42}.

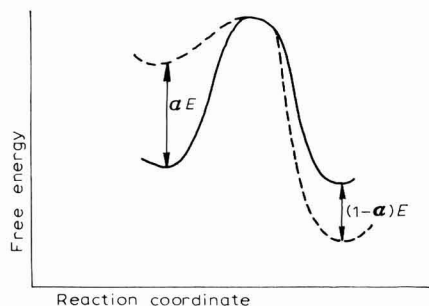


Fig. 5. Energy curve for reduction, after GARDNER AND LYONS¹³.

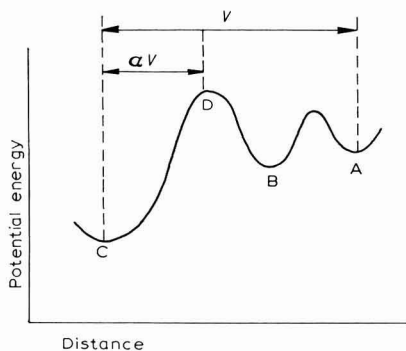


Fig. 6. Energy relation for reduction, after GLASSTONE, LAIDLER AND EYRING²².

Another type of energy curve in the literature^{6,42,46} shows the energy levels of the initial and final states as the same: sometimes for the situation where the potential is taken to be absent, at other times to describe the situation brought about when the potential is applied. In such diagrams, the energy difference between either stable state and the activated state is usually taken to represent activation energy; therefore, equality of the rate constants is implied in these cases and the diagram can refer only to one state of the system (in fact, to the standard state that is usually chosen), and not to any other situation; yet in the work quoted, no such restriction is apparently intended. This type of representation has been criticized also by CHRISTOV⁴⁷.

Finally, one²² of the references often quoted as a source for the modern view of electrochemical kinetics depicts the situation as shown in Fig. 6:

C represents the solvated ion in the bulk of the solution, B the probably

unsolvated ion adsorbed at the surface, A the atom in the electrode; α is defined, as usual, as the fraction of the potential that assists the forward reaction, but in this case the rate-determining step is seen to be the movement of the oxidized form to the electrode and not the discharge-step itself. This view is at variance with the generally accepted formulation in which α is defined in relation to the energy barrier between B and A, and the use of this work as a source reference is seriously misleading.

IV. SYMMETRY VIEWS

In eqn. (1), α has a value of between zero and unity; when it is one half, this represents some sort of symmetry. Descriptions or interpretations based on the concept of symmetry have been given by numerous authors, and some workers, in fact, use the term^{51,52} "symmetry factor", usually given the symbol β , rather than "transfer coefficient" (see Section VI for a fuller discussion of terminology). Often, unfortunately, it is not clear what it is that is being described as symmetrical:

For instance^{6,22,42,45,51,53-58}, the energy barrier, or the reaction itself, may be described as symmetrical. Now, this would normally be taken to mean that equal amounts of energy are required to surmount the barrier from either side;* but this is a situation that refers to the standard state where the rate constants are equal (*cf.* Section III) and says nothing about the parameter α . In fact, if one takes α as defined by eqn. (1), then it is apparent that it describes the way in which the energy barrier or curve changes with potential, and not the symmetry of the barrier itself.

In cases where the specific connotation of "symmetry" is made plain, the interpretation of $\alpha=0.5$ is, of course, merely a special case of the interpretation given for the parameter α in general; thus, we have the following opinions for $\alpha=0.5$:

1. Half the electrical energy represented by the potential adds to, and subtracts from, the activation energies for the back and forward reactions, respectively; *i.e.*, the situation is re-described rather than rationalized.

2. The Morse curves for the reactants have slopes of equal magnitudes at the point where they intersect.

3. The activated state lies midway between the initial and final states. Sometimes^{45,60} this is left in the general form of "along the reaction coordinate", at other times^{7,34,42,43,48,49} actual distances perpendicular to the electrode surface are implied (DESPIC AND BOCKRIS⁶¹ have shown that under certain conditions the "Morse curve" and "distance" interpretations are roughly equivalent).

V. SOME DISCREPANT VIEWS

A particular problem arises when kinetics are introduced *via* eqns. (1a) and (9), *i.e.*, when the only assumption made is that of an exponential variation of the

* A different connotation appears to be intended by some authors, at least; *e.g.*, "... β is a factor ... determined by the symmetry of the potential energy barrier ... and indicates approximately that fraction of ΔV through which the charge must be transferred to reach the transition state ..." ⁵⁷—in other words, a symmetrical barrier is one whose peak is in a symmetrical position (in the electrical field) with respect to the positions of the reactants and products (*cf.* 3. below).

rate constants with potential. In order to be consistent with the Nernst equation, $\alpha + \beta = 1$; but the question remains whether this is necessarily the case in irreversible processes also. Discussions showing $\alpha + \beta \neq 1$ on theoretical grounds have been given⁶²⁻⁶⁴ and criticized⁶⁵. The point is resolved if one considers sufficiently carefully the systems described: BONNEMAY⁶⁴ considered processes at heterogeneous surfaces and postulated that deposition and dissolution would occur at different types of sites; under these circumstances, there is no reason at all why $(\alpha + \beta)$ should be unity. For processes that take the same path in both directions, it is agreed⁶⁶ that $\alpha + \beta = 1$, necessarily.

The matter of transfer coefficients for different paths or processes arises also in a recent paper⁶⁷ where a value of $\alpha = 0.5$ is regarded as significant because it corresponds to minimum production of entropy in a cell with two identical electrodes. This is a point of view that does not lend itself to interpretation of the transfer coefficient in the usual situation where a single electrode process at one electrode is being considered.

Another discrepant view¹¹, related perhaps to loosely-worded "symmetry" explanations, is the implication that $\alpha = 0.5$ implies reversibility of the electrode reaction (or, in other words, absence of overvoltage; *e.g.*, "... dans le cas des faibles surtensions, β est peu différent de α ..."⁶⁸).

In some instances, the transfer coefficient is discussed as if its physical significance were established; *e.g.*, "... consideration of the structure of the electrical double-layer ... shows that α ... must decrease as the potential becomes more cathodic beyond the electrocapillary maximum ..."⁶⁹. Inferences of this sort are not uncommon in the literature; yet it should be evident that such statements assume, without justification, that the nature of α is already understood.

VI. TERMINOLOGY

The lack of consistency in the use of terms and symbols has already been alluded to. In this section, we shall make a chronological review in order to gain an insight into some reasons for the current state of affairs.

For a number of years, factors usually denoted by α , β , or γ were written in equations such as (1) and were referred to as proportionality constants, adjustable parameters, and so on. The first use of the term "transfer coefficient" appears in the work of AUDUBERT, and it is interesting that this term has found general acceptance although it was introduced in conjunction with a physical interpretation that is not generally accepted, *viz.*, that α represents that fraction of the kinetic energy of the reactant species (acquired as a result of the electrode potential) that is transmuted into energy of activation. Thus, in connection with equations (1a) and (9), AUDUBERT wrote: "Si l'on cherche à donner une signification physique aux termes α et β , on peut dire qu'ils représentent la fraction d'énergie cinétique qui, pour α est transférée à l'ion et lui permet de franchir la couche de barrage; pour β , celle qui est transférée au radical et s'oppose à la réaction inverse d'ionisation ... la fraction d'énergie cinétique transferable ..."⁶⁹. Again, "... lorsqu'un ion sous l'action de ce champ [électrique] arrive à l'électrode, l'énergie cinétique ... peut être, sinon totalement, au moins partiellement transférée à l'ion et se retrancher, de cette manière, de l'énergie d'activation ... α une constante que nous désignons sous le nom de facteur de transfert

de l'énergie cinétique ..."⁷⁰; and "... α et β les coefficients de transfert de l'énergie cinétique ..."⁶³.

This interpretation and terminology was adopted, for instance, by BONNEMAY^{64,71,72}; the idea of the transformation involving kinetic energy had also been used, albeit in a different manner, by GURNEY²⁹. However, it is not now a generally accepted view, and in fact has a certain similarity (see above⁶⁹) to the idea (Section III, Fig. 6) that α has to do with penetration into the double layer.

Nevertheless, this opinion has given the generally accepted name to the symbol. The first occurrence in English is in the Faraday Society Discussion of 1947, where a paper by AUDUBERT (translated from the French) reads "... activation energy must be diminished by a term ... where α is an energy transfer factor less than unity ... β the corresponding transfer coefficient ..."⁷³. The proceedings of this Faraday Society Discussion show that, at this time, the use of an " α -factor" in eqn. (1) was so universally accepted that frequently no reference for such formulations was considered necessary⁹; where reference was made, it was often^{19,74} to a source²² the inadequacy of which has been discussed. At the same time, FRUMKIN⁷⁵ pointed out that "... since the paper by HORIUTI AND POLANYI⁴⁴ no considerable progress ... in the interpretation of ... α " had been made. A review by BOCKRIS⁷⁶ in the following year also mentioned the lack of unanimity as to the significance of α .

During the next few years, an increasing number of authors^{11,77-79} began to use the term "transfer coefficient", while others^{12,20,76,80-84} continued to use the symbolic formulation without giving a name to α . At the same time, the use of β , the "symmetry factor", was introduced^{51,79,85,86}; in some cases^{52,85,86}, apparently as a synonym or substitute for α , the transfer coefficient, as used in eqn. (1); at other times^{51,87,88}, the distinction was made that β refers to the electron-transfer step itself, whereas α is the overall⁸⁹ or experimental value, the two being related, *e.g.* by the equation⁵¹ " $\alpha = \beta\lambda$... λ is the number of electrons necessary so that one act of the rate-determining step can occur" or by the relation⁸⁷ $\alpha = n(\beta + \gamma)/r$ where r is the stoichiometric number and γ is a factor referring to that part of the free energy that depends on the potential and not on the composition.

In recent years, some authors^{8,58,90,91} have assumed that the intended connotation of "transfer" in the term "transfer coefficient" was electron transfer or, more generally, charge transfer. This is, of course, a commendable usage since no physical significance is thereby attached to α : but it is as well to be aware that the term derives from AUDUBERT's concept of the transformation of kinetic energy into activation energy. In the German literature, α is usually called^{65,92} "Durchtrittsfaktor"; this term carries no implication beyond that of "passing through" in an unspecified sense, nor did it arise in connection with any particular assumption about the nature of the process.

VIII. THEORY AND EXPERIMENT

The views described in the previous sections were formed at a time when little quantitative and relevant experimental data was available. The thermodynamic description of reversible electrodes was well supported experimentally, but this lent no support to the kinetic formulation: it merely provided the corollary that if equations such as (1) and (9) were to be valid for reversible systems, then under conditions

of reversibility eqn. (10) must hold. The sole experimental support for eqn. (1) was its relation (eqns. (5) and (6)) to the empirically based Tafel relation. A reading of the literature gives the impression that the truth of eqn. (1) was rather uncritically accepted—in fact, as noted earlier, the assumption that $\alpha = \frac{1}{2}$ (precisely) under normal circumstances was frequently made because the Tafel slope was often approximately consistent with this value (see eqn. (8)).

It is now realised how inadequately the available evidence supported the weight of theoretical speculations on the nature of the transfer coefficient. Elucidation of the mechanisms of electrode processes was frequently inadequate, with the consequence that results were interpreted directly on the basis of an equation such as (6) when the data did not, in fact, refer to the charge-transfer step itself.

Much of the early work was concerned specifically with hydrogen discharge, and α was frequently obtained by applying eqn. (8) directly to experimental data. There exists a considerable number of articles in which α , calculated in this way, was found to be larger than unity and was rationalized in various ways that were often quite specific to the particular process studied. It is clear that a value of α greater than unity is incompatible with a definition based on eqn. (1), and a good deal of confusion was generated in work where eqn. (1) was used *a priori*, so that Tafel slopes were interpreted in terms of α -values, and the latter (as mentioned, on occasion greater than unity) used as a basis for speculation about the nature of the transfer coefficient.

Another example of α -values derived without adequate analysis of the applicability of theory to a particular physical situation, is to be found in the literature on polarography, of organic substances in particular. Until quite recently, it was not uncommon to find an indiscriminate use of polarographic log-plots to derive values for α by application of equations such as the following^{12,13,15,93}:

$$E = E_{\frac{1}{2}} + \{RT(1-\alpha)/\alpha nF\} \ln \{i/(i_d - i)\} \quad (11a)$$

$$E = E_{\frac{1}{2}} + (RT/\alpha nF) \ln \{i/(i_d - i)\} \quad (11b)$$

$$E = (\text{terms}) - (0.0542/\alpha n) \log \{i/(i_d - i)\} \quad (11c)$$

It was not realized how unreliable a criterion the log-plot is because of the enormous range of possible mechanisms that can give the same, or quite similar, slopes, and of the inherent inaccuracy in determination of the magnitude of the slope. A recent discussion bearing on this point has been given by MEITES⁹⁴.

It is now generally recognized that elucidation of the mechanism of a given process is essential if values are to be obtained for the kinetic parameters; however, at the present state of knowledge there are few systems the behaviour of which is sufficiently well understood that one would care to use the results as a basis for theorizing on the physical significance of the transfer coefficient. The absolute necessity for correcting for double-layer effects has been comparatively recently recognized and remains frequently neglected; the magnitude of errors possible through such neglect has been demonstrated by PARSONS⁸⁹.

Even beyond pitfalls such as these, in the application of theory to particular systems, there remain questions of a theoretical nature:

Can one legitimately use the same type of formulation (eqn. (1)) for all processes, when in some cases an electron is transferred, while in others an ion may be the charge carrier through the double layer? Usually, eqn. (1) is written in any

case and without discussion of this point.

How does one treat processes where charge transfer occurs in more than one step? What value does one use for n in eqn. (1)?

Discussion of these matters is lacking, as is experimental evidence that might guide such discussion or serve to test its validity.

During the last decade, systematic attempts have been made^{55,95-100} to formulate an "absolute" electron-transfer rate-theory. In such work, primary emphasis is on the characterization of the activated state, and the transfer coefficient is not introduced *a priori via* eqn. (1) or eqn. (8); it arises only at the end of the treatment, as whatever factor happens to modify the electrode-potential term(s) in the expression for the activation energy.

In the treatment by MARCUS⁹⁷, α is, in general, a function of several terms and not independent of the electrode potential, but becomes independent if the double-layer effects are small and for potentials not far removed (say ± 0.2 V) from the equilibrium potential; moreover, the value of α becomes 0.5 in the limiting case. Discussions by HUSH⁵⁵, MOTT AND WATTS-TOBIN⁵⁸, and DOGONADZE AND CHIZMADZHEV¹⁰⁰ lead to, at least qualitatively, similar conclusions.

Thus, these theories provide a rationalization for the frequent lack of dependence of α on potential and for the commonly found value of 0.5, and remove other cases from the category of anomalies for which *ad hoc* explanations have necessarily to be given as long as α is introduced arbitrarily as a constant through eqn. (1). In fact, PARSONS AND PASSERON¹⁰¹ have found quantitative agreement with MARCUS' theory in the experimentally determined dependence on potential of the transfer coefficient for the Cr(II)/Cr(III) system.

Modern quantum-mechanical treatments in which the calculation of distribution functions is the central issue (*cf.* GURNEY²⁹) also lead to the conclusion¹⁰² that α is not, in general, independent of potential, nor, for that matter, of the concentrations of the electroactive species.

A fuller discussion of this recent work is beyond the intended scope of this article, which seeks to make it possible to avoid or overcome confusion that can readily result from cursory expeditions into the earlier literature.

SUMMARY

In discussions of the kinetics of electrode reactions, the central issue is the manner in which the rate constants depend on the electrode potential. It is often stated *ex cathedra* that this dependence is exponential and that constant fractions of the electrode potential appear in the exponential terms; these fractions are characterized by the "transfer coefficient, α " or "symmetry factor, β ". The impression is thereby given that we understand the physical nature of the "transfer" or "symmetry" that determines the magnitude of α or β . In fact, the terminology "transfer coefficient" was introduced in connection with a model for the electron transfer that is not accepted; and the interpretation of β as describing the symmetry of the energy barrier is inadequate since, by definition, β describes the change in the barrier as the potential changes, and not any property of the barrier at a particular potential.

There is no adequate justification for an *a priori* introduction of the transfer coefficient as an implicitly potential-independent parameter.

REFERENCES

- 1 P. DELAHAY, *New Instrumental Methods in Electrochemistry*, Interscience Publishers Inc., New York, 1954.
- 2 P. DELAHAY, *Double Layer and Electrode Kinetics*, Interscience Publishers Inc., New York, 1965.
- 3 E. C. POTTER, *Electrochemistry*, Cleaver-Hume Press, London, 1956.
- 4 K. J. VETTER, *Elektrochemische Kinetik*, Springer, Berlin, 1961.
- 5 G. CHARLOT, J. BADOZ-LAMBLING AND B. TRÉMILLON, *Electrochemical Reactions*, Elsevier, Amsterdam, 1962.
- 6 C. N. REILLEY, *Treatise on Analytical Chemistry*, Part I, Vol. 4, Interscience Publishers Inc., New York, 1963, p. 2109.
- 7 B. BREYER AND H. H. BAUER, *Alternating Current Polarography and Tensammetry*, Interscience Publishers Inc., New York, 1963.
- 8 J. HEYROVSKÝ AND J. KŮTA, *Principles of Polarography*, Academic Press, New York, 1966.
- 9 J. N. AGAR, *Discussions Faraday Soc.*, 1 (1947) 81.
- 10 J. O'M. BOCKRIS AND B. E. CONWAY, *Record Chem. Progr.*, 25 (1964) 31.
- 11 J. VAN CAKENBERGHE, *Bull. Soc. Chim. Belges*, 60 (1951) 3.
- 12 H. EYRING, L. MARKER AND T. KWON, *J. Phys. Colloid Chem.*, 53 (1949) 1453.
- 13 H. J. GARDNER AND L. E. LYONS, *Rev. Pure Appl. Chem.*, 3 (1953) 134.
- 14 H. GERISCHER, *Z. Elektrochem.*, 57 (1953) 604.
- 15 R. GOTO AND I. TACHI, *Sb. Mezinarod. Polarog. Sjezdu Praze*, 1 (1951) 69.
- 16 T. HURLEN, *Tidsskr. Kjemi, Bergvesen Met.*, 24 (1964) 88.
- 17 M. KALOUSEK AND A. TOCKSTEIN, *Sb. Mezinarod. Polarog. Sjezdu Praze*, 1 (1951) 563.
- 18 G. E. KIMBALL, *J. Chem. Phys.*, 8 (1940) 199.
- 19 J. E. B. RANGLES, *Discussions Faraday Soc.*, 1 (1947) 11.
- 20 N. TANAKA AND R. TAMAMUSHI, *Bull. Chem. Soc. Japan*, 22 (1949) 187.
- 21 K. J. VETTER, *Z. Elektrochem.*, 55 (1951) 121.
- 22 S. GLASSTONE, K. J. LAIDLER AND H. EYRING, *The Theory of Rate Processes*, McGraw-Hill, New York, 1941, p. 575 *et seq.*
- 23 J. A. V. BUTLER, *Chemical Thermodynamics*, Macmillan, London, various editions.
- 24 *Trans. Symposium Electrode Processes, Philadelphia 1959*, John Wiley, New York, 1961.
- 25 J. A. V. BUTLER, *Trans. Faraday Soc.*, 19 (1924) 729.
- 26 J. A. V. BUTLER, *Trans. Faraday Soc.*, 19 (1924) 734.
- 27 F. P. BOWDEN, *Proc. Royal Soc. London*, A126 (1929) 107.
- 28 T. ERDEY-GRUZ AND M. VOLMER, *Z. Physik. Chem.*, A150 (1930) 203.
- 29 R. W. GURNEY, *Proc. Royal Soc. London*, A134 (1931) 137.
- 30 J. A. V. BUTLER, *Trans. Faraday Soc.*, 28 (1932) 379.
- 31 J. A. V. BUTLER, *Proc. Royal Soc. London*, A157 (1936) 423.
- 32 J. A. V. BUTLER, *Z. Elektrochem.*, 44 (1938) 55; and subsequent discussion.
- 33 L. P. HAMMETT, *Trans. Faraday Soc.*, 29 (1933) 770.
- 34 T. ERDEY-GRUZ AND H. WICK, *Z. Physik. Chem.*, A162 (1932) 53.
- 35 A. FRUMKIN, *Z. Physik. Chem.*, A164 (1933) 121.
- 36 A. FRUMKIN, *Z. Physik. Chem.*, A160 (1932) 116.
- 37 J. N. BRONSTED, *Chem. Rev.*, 5 (1928) 231.
- 38 B. TOPLEY AND H. EYRING, *J. Am. Chem. Soc.*, 55 (1933) 5058.
- 39 B. TOPLEY AND H. EYRING, *J. Chem. Phys.*, 2 (1934) 217.
- 40 H. EYRING, *J. Chem. Phys.*, 3 (1935) 107.
- 41 H. EYRING AND W. F. K. WYNNE-JONES, *J. Chem. Phys.*, 3 (1935) 492.
- 42 H. EYRING, S. GLASSTONE AND K. J. LAIDLER, *J. Chem. Phys.*, 7 (1939) 1053.
- 43 H. EYRING, S. GLASSTONE AND K. J. LAIDLER, *Trans. Electrochem. Soc.*, 76 (1939) 145.
- 44 J. HORIUTI AND M. POLANYI, *Acta Physicochim. URSS*, 2 (1935) 505.
- 45 R. PARSONS, *Trans. Faraday Soc.*, 47 (1951) 1332.
- 46 H. GERISCHER, *Angew. Chem.*, 68 (1956) 20.
- 47 S. G. CHRISTOV, *Z. Elektrochem.*, 62 (1958) 567.
- 48 M. VOLMER, *Physik. Z. Sowjetunion*, 4 (1933) 346.
- 49 M. VOLMER AND H. WICK, *Z. Physik. Chem.*, A172 (1935) 429.
- 50 F. P. BOWDEN AND J. N. AGAR, *Ann. Rep., Progr. Chem. (Chem. Soc. London)*, 35 (1938) 90.
- 51 J. O'M. BOCKRIS AND E. C. POTTER, *J. Electrochem. Soc.*, 99 (1952) 169.
- 52 J. O'M. BOCKRIS AND E. C. POTTER, *J. Chem. Phys.*, 20 (1952) 614.
- 53 T. P. HOAR, *Modern Aspects of Electrochemistry No. 2*, Butterworths, London, 1959, p. 262.
- 54 T. HURLEN, *Acta Chem. Scand.*, 14 (1960) 1564.
- 55 N. S. HUSH, *J. Chem. Phys.*, 28 (1958) 962.
- 56 J. V. PETROCELLI AND A. A. PAOLUCCI, *J. Electrochem. Soc.*, 98 (1951) 291.

- 57 B. E. CONWAY, *Trans. Roy. Soc. Can. Sect. III*, 54 (1960) 19.
58 N. F. MOTT AND R. J. WATTS-TOBIN, *Electrochim. Acta*, 4 (1961) 79.
59 R. PARSONS AND J. O'M. BOCKRIS, *Trans. Faraday Soc.*, 47 (1951) 914.
60 C. PERRIN, *Progr. Phys. Org. Chem.*, 3 (1965) 165.
61 A. R. DESPIC AND J. O'M. BOCKRIS, *J. Chem. Phys.*, 32 (1960) 389.
62 M. BONNEMAY, *J. Chim. Phys.*, 44 (1947) 187.
63 R. AUDUBERT AND M. QUINTIN, *J. Chim. Phys.*, 39 (1942) 92.
64 M. BONNEMAY, *Compt. Rend.*, 22 (1946) 1222.
65 K. J. VETTER, *Z. Elektrochem.*, 59 (1955) 596.
66 Discussion to ref. 65; pp. 603-604.
67 F. GUTMANN AND P. VAN RYSSELBERGHE, *Electrochim. Acta*, 10 (1965) 107.
68 R. AUDUBERT AND M. QUINTIN, *Electrochimie*, Presses Universitaires de France, Paris, 1942.
69 R. AUDUBERT AND S. CORNEVIN, *J. Chim. Phys.*, 38 (1941) 46.
70 R. AUDUBERT, *J. Phys. Radium*, 3 (1942) 81.
71 M. BONNEMAY, *J. Chim. Phys.*, 41 (1944) 218.
72 M. BONNEMAY, *Compt. Rend.*, 222 (1946) 793.
73 R. AUDUBERT, *Discussions Faraday Soc.*, 1 (1947) 72.
74 J. H. BAXENDALE, *Discussions Faraday Soc.*, 1 (1947) 46.
75 A. FRUMKIN, *Discussions Faraday Soc.*, 1 (1947) 57.
76 J. O'M. BOCKRIS, *Chem. Rev.*, 43 (1948) 525.
77 P. DELAHAY AND J. E. STRASSNER, *J. Am. Chem. Soc.*, 73 (1951) 5219.
78 P. VAN RYSSELBERGHE, *J. Chim. Phys.*, 49 (1952) C47.
79 E. C. POTTER, *J. Chim. Phys.*, 49 (1952) C103.
80 E. LANGE AND K. NADEL, *Z. Elektrochem.*, 53 (1949) 21.
81 H. GERISCHER, *Z. Elektrochem.*, 54 (1950) 362.
82 E. LEWARTOWICZ, *Compt. Rend.*, 232 (1951) 1207.
83 J. E. B. RANGLES, *Trans. Faraday Soc.*, 48 (1952) 828.
84 C. TANFORD AND S. WAWZONEK, *Ann. Rev. Phys. Chem.*, 3 (1952) 247.
85 R. PARSONS, *J. Chim. Phys.*, 49 (1952) C82.
86 J. O'M. BOCKRIS, *J. Chem. Phys.*, 24 (1956) 817.
87 J. O'M. BOCKRIS, *Modern Aspects of Electrochemistry*, No. 1, Butterworths, London, 1954, p. 180.
88 J. O'M. BOCKRIS, *Modern Aspects of Electrochemistry*, No. 3, Butterworths, London, 1964, p. 224.
89 R. PARSONS, *Advan. Electrochem. Electrochem. Eng.*, 1 (1961) 1.
90 K. J. VETTER, ref. 24, p. 47.
91 H. GERISCHER, *Advan. Electrochem. Electrochem. Eng.*, 1 (1961) 139.
92 K. J. VETTER, *Z. Naturforsch.*, 7a (1952) 328.
93 L. MEITES AND Y. ISRAEL, *J. Am. Chem. Soc.*, 83 (1961) 4903.
94 L. MEITES, *Treatise on Analytical Chemistry*, Part I, Vol. 4, Interscience Publishers Inc., New York, 1963, p. 2303.
95 N. S. HUSH, *Z. Elektrochem.*, 61 (1957) 734.
96 R. A. MARCUS, *Can. J. Chem.*, 37 (1959) 155.
97 R. A. MARCUS, *J. Phys. Chem.*, 67 (1963) 853.
98 R. A. MARCUS, *Ann. Rev. Phys. Chem.*, 15 (1964) 155.
99 R. R. DOGONADZE AND YU. A. CHIZMADZHEV, *Dokl. Akad. Nauk SSSR*, 144 (1962) 1077; English Transl., p. 463.
100 R. R. DOGONADZE AND YU. A. CHIZMADZHEV, *Dokl. Akad. Nauk SSSR*, 145 (1962) 848; English Transl., p. 563.
101 R. PARSONS AND E. PASSERON, *J. Electroanal. Chem.*, 12 (1966) 524.
102 H. GERISCHER, *Z. Physik. Chem. Frankfurt*, 26 (1960) 223, 325.

SHORT COMMUNICATIONS

Current-time dependence for charge transfer processes with reactant adsorption at a dropping electrode

In this communication the effect of reactant adsorption on the current-time dependence for a dropping electrode is examined and the diffusion problem solved on the basis of ideas recently suggested¹ and developed in this laboratory²⁻⁵. This problem has already been considered independently and from a classical point of view in this laboratory⁶ (at Louisiana State University) and by BUTLER AND MEEHAN⁷. A simple plot (in this treatment based on separation of faradaic and charging processes) allows the determination of the charge density on the electrode in presence of a faradaic process. This simple and useful method usually holds for limiting conditions, as will be shown. The mathematical treatment of the diffusion process for a pure metal electrode and its cation (no amalgam), which we consider here, is similar to that in a recent work⁸.

The problem is formulated for the following assumptions:

(i) Under potentiostatic conditions, the surface excess, Γ , of ions in the double layer is assumed to be a function of the concentration, c , of ions at the hypothetical boundary, $x=0$, of the diffuse double layer and the diffusion layer. We then have $\Gamma = \Gamma(c_{x=0})$. In order to simplify the treatment we assume the linear relationship

$$x=0: \quad \Gamma = Kc \quad (1)$$

and we implicitly assume that relaxation of double layer can be neglected and that the adsorption process is much faster than any other process in the system.

(ii) The rate of the electrode reaction at $x=0$ is

$$dc/dt = \sigma - \varrho Kc \quad (2)$$

where σ and ϱ are constants, and the faradaic current is

$$i_f = zF(\sigma - \varrho Kc_{x=0}) \quad (3)$$

(iii) The area A , of the drop is

$$A = A_0 t^{2/3} \quad (4)$$

(iv) Diffusion towards the drop is treated by

$$\frac{\partial c}{\partial t} = D \frac{\partial^2 c}{\partial x^2} + \frac{2x}{3t} \frac{\partial c}{\partial x} \quad (5)$$

The initial condition is

$$t=0, x>0: \quad c = c^s \quad (6)$$

and the boundary conditions are

$$t>0, x=0: \quad A\Gamma = D \int_0^t A(\partial c/\partial x) d\tau + \int_0^t A(\sigma - \varrho\Gamma) d\tau \quad (7)$$

$$t>0, x \rightarrow \infty: \quad c = c^s \quad (8)$$

The solution (Appendix) is given in the form of a convergent series by

$$\Phi(m, n, \chi) = \sum_{i=0}^{\infty} s_i \chi^i \quad (9)$$

where

$$\Phi(m, n, \chi) = (c/c^s)_{x=0} \quad (10)$$

$$m = \rho K^2/D, \quad n = K\sigma/(Dc^s) \quad (11)$$

$$\chi = (3Dt/7K^2)^{1/2} \quad (12)$$

The coefficients s_i are given by the recurrence formulae

$$s_0 = 0, \quad s_1 = 2/\sqrt{\pi}, \quad s_2 = 7n/5 - 2\Gamma(17/14)/(\sqrt{\pi}\Gamma(12/7)) \quad (13)$$

$$s_{i+2} = -\left(s_{i+1} \left\{ \Gamma\left(\frac{17+3i}{14}\right) / \Gamma\left(\frac{27+3i}{14}\right) \right\} + s_i \frac{14}{10+3i}\right). \quad (14)$$

The solution is also represented by the asymptotic series for sufficiently large values of the parameter, χ

$$\Phi(m, n, \chi) \approx \sum_{i=0} r_i \chi^{-i}, \quad \chi \gg 0 \quad (15)$$

where

$$r_0 = n/m, \quad r_1 = [1/(m\sqrt{\pi})] (1 - r_0), \quad (16)$$

$$r_{i+2} = \frac{3i-4}{14m} \left(r_i + r_{i+1} \left\{ \Gamma\left(\frac{11-3i}{14}\right) / \Gamma\left(\frac{18-3i}{14}\right) \right\} \right). \quad (17)$$

Plots of the function $\Phi(m, n, \chi)$ vs. χ for different values of the parameters m and n are shown in Fig. 1.

The faradaic current, making the assumptions (i)–(iv), is

$$i_f/(zF) = \sigma - \rho K c_{x=0} = (Dc^s/K) (n - m\Phi(m, n, \chi)) \quad (18)$$

Pseudo-equilibrium is reached when $i_f = 0$, i.e., when

$$(c_e)_{x=0} = \sigma/\rho K = c^s n/m \quad (19)$$

Therefore, the function $\Phi(m, n, \chi)$ should tend to n/m for large values of χ . This conclusion agrees with the asymptotic formula (15).

The total current for the drop is

$$i = Ai_r + \frac{d(Aq(c, E))}{dt} \quad (20)$$

where $q(c, E)$ is the charge density on the drop.

The solution thus obtained shows that for values of m and n that are not too different (small applied overvoltage), the pseudo-equilibrium concentration at the surface of the drop is obtained with an error smaller than 10% for $\chi > 10$. Also, for these values of χ , the transport process proceeds as if there were no accumulation of reactant at the interface. Moreover, q remains almost constant for $\chi > 10$ because pseudo-equilibrium is reached. Thus, it can be concluded on the basis of the model used here that the classical analysis⁷ applies for $m\chi \gg 1$ and for m not too different from n . Conversely, when $\chi < 2$ the concentration, $(c)_{x=0}$, changes markedly, and q

cannot generally be regarded as constant as in the analysis based on classical ideas. The range of χ for which the classical analysis applies with a good approximation, is valid for any values of m and n provided they are not very different. The approximation achieved by the classical analysis can be estimated more exactly from Fig. 1.

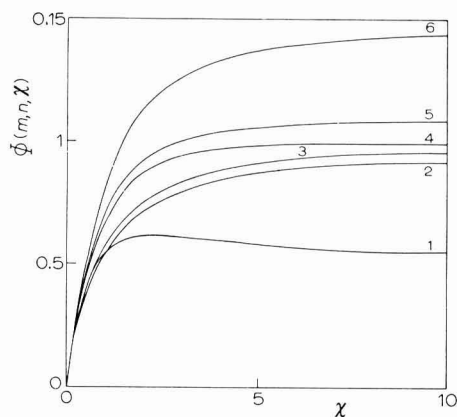


Fig. 1. Plot of the function $\Phi(m, n, \chi)$ vs. χ for different values of the parameters m and n . (1), $m = 0.5$, $n = 0.25$; (2), $m = n = 0.001747$; (3), $m = n = 0.07694$; (4), $m = n = 0.5$; (5), $m = 0.5$, $n = 0.55$; (6), $m = 0.5$, $n = 0.75$.

This diagram shows also that the value of χ for which the classical analysis is essentially valid decreases when m and n increase. Also, the classical treatment⁷ presupposes diffusion control, and consequently no further assumption is necessary about the reactant, provided the time is sufficiently long to correspond to a diffusion-controlled process.

Appendix

The solution was derived as follows. Equation (5) is reduced to the usual diffusion equation by introducing new variables⁸

$$Z = (x/K) (3Dt/7K^2)^{2/3}, \quad (21)$$

$$Y = (3Dt/7K^2)^{7/3} \quad (22)$$

From eqns. (5)–(8) we then obtain

$$\partial c / \partial Y = \partial^2 c / \partial Z^2, \quad (23)$$

$$Y = 0: \quad c = c^s \quad (24)$$

$$Y > 0: \quad \begin{cases} Z = 0: & cY^{2/7} = \int_0^Y (\partial c / \partial Z) dy - \int_0^Y (mc - nc^s)y^{-2/7} dy \\ Z \rightarrow \infty: & c = c^s \end{cases} \quad (25)$$

$$Z \rightarrow \infty: \quad c = c^s \quad (26)$$

where

$$m = \rho K^2/D, \quad n = K\sigma/(Dc^s). \quad (27)$$

The problem is now converted⁹ to the solution of an integral equation using

$$Z = 0: \quad \int_0^Y \frac{\partial c}{\partial Z} dy = - \int_0^Y \frac{c}{\sqrt{\pi(Y-y)}} dy + \frac{2c^s}{\sqrt{\pi}} Y^{1/2}. \quad (28)$$

The corresponding integral equation is

$$\Phi(m, n, Y) = (2/\sqrt{\pi}) Y^{3/4} + 7n Y^{3/7}/5 - \int_0^Y k(Y, y) \Phi(m, n, y) dy \quad (29)$$

where

$$\Phi(m, n, Y) = c_{Z=0}/c^s, \quad (30)$$

$$k(Y, y) = Y^{-2/7} [m y^{-2/7} + \pi^{-1/2} (Y - y)^{-1/2}] \quad (31)$$

The solution of integral eqn. (29) is found as in a previous paper⁸. Thus, the term $7n\chi^2/5$ is added to the right-hand side of eqn. (28) of that paper⁸, and we obtain directly either formulae (13) and (14) for the coefficients s_i in the power series (9) or formulae (16) and (17) for the coefficients r_i in the asymptotic expression (15) for the function $\Phi(m, n, \chi)$. The Viskovatov¹⁰ method for the conversion of the power series (9) into the corresponding continuous fraction was used in the numerical calculations. This method was also used in the previous paper⁸. Calculations were performed with a CDC 6600 digital computer.

Acknowledgement

This work was supported by the National Science Foundation. The author expresses his thanks to Professor DELAHAY for suggesting this work and for his kind interest in it.

Department of Chemistry,
New York University,
New York, N.Y. 10003 (U.S.A.)

K. HOLUB*

- 1 P. DELAHAY, *J. Phys. Chem.*, **70** (1966) 2067, 2373.
- 2 P. DELAHAY, K. HOLUB, G. G. SUSBIELLES AND G. TESSARI, *ibid.*, **71** (1967) 779.
- 3 K. HOLUB, G. TESSARI AND P. DELAHAY, *ibid.*, **71** (1967) 2612.
- 4 P. DELAHAY AND K. HOLUB, *J. Electroanal. Chem.*, **16** (1968) 131.
- 5 K. HOLUB, *J. Electroanal. Chem.*, submitted.
- 6 P. DELAHAY AND G. TESSARI, unpublished work.
- 7 J. N. BUTLER AND M. L. MEEHAN, *J. Phys. Chem.*, **69** (1965) 4051.
- 8 K. HOLUB, *Collection Czechoslov. Chem. Commun.*, **31** (1966) 1461.
- 9 M. SMUTEK, *ibid.*, **20** (1955) 247.
- 10 *Mathematical Analysis*, edited by L. A. LYUSTENIK AND A. R. YANPOL'SKII, translated by D. E. BROWN, Pergamon Press, Oxford, 1965, p. 257.

Received June 9th, 1967

* Present address: J. Heyrovský Polarographic Institute, Opletalova 25, Prague, Czechoslovakia.

On the applicability of the Heyrovský–Ilkovič equation to polarography in molten salts using a solid microelectrode

There is no uniformity in the literature regarding the equation to be used for expressing the current–voltage (C – V) curve in fused salt polarography at *solid* microelectrodes. If the activity of the deposited metal is taken as unity, the rising portion of the polarographic wave is expressed by the Kolthoff–Lingane equation:

$$E_{m.e.} = E_{\frac{1}{2}} + (2.303RT/nF) \log(i_d - i) \quad (1)$$

where i is the current at the applied potential $E_{m.e.}$, i_d the diffusion current and $E_{\frac{1}{2}}$ the half-wave potential which is *dependent* on the concentration of the depolarizer. The applicability of this equation has been confirmed by several workers^{1–5}. On the other hand, many, particularly DELIMARSKII *et al.*^{6–17}, have attempted to describe the polarographic wave, even on a *solid* microelectrode, by the Heyrovský–Ilkovič equation:

$$E_{m.e.} = E_{\frac{1}{2}} - (2.303 RT/nF) \log \{i/(i_d - i)\} \quad (2)$$

An essential feature in the derivation of this equation is that the activity of the metal deposited on the microelectrode is a function of the current strength and $E_{\frac{1}{2}}$ is *independent* of the depolarizer concentration. The present authors⁴ also found that eqn. (2) was obeyed in the polarographic reduction of Cd^{2+} and Pb^{2+} on a platinum microelectrode (PME) in molten chlorides. It was pointed out that at the working temperature (475°), both metals were deposited as liquid on the microelectrode and since in this state they are corrosive to platinum¹⁸, even at relatively lower temperatures, the current-dependent variable activity of the metal deposited on the PME was ascribed to “surface-alloy” formation.

Tungsten is known to be alloy-resistant¹⁸ to most molten metals. It was thus of interest to examine whether the polarographic wave with a tungsten microelectrode (WME) as the indicator electrode, in such a case would still be described by the Heyrovský–Ilkovič equation. In the present communication this point is considered from the data on the polarographic behaviour of Cd^{2+} in molten $MgCl_2$ – KCl eutectic (32.5:67.5 mole %) at 475° .

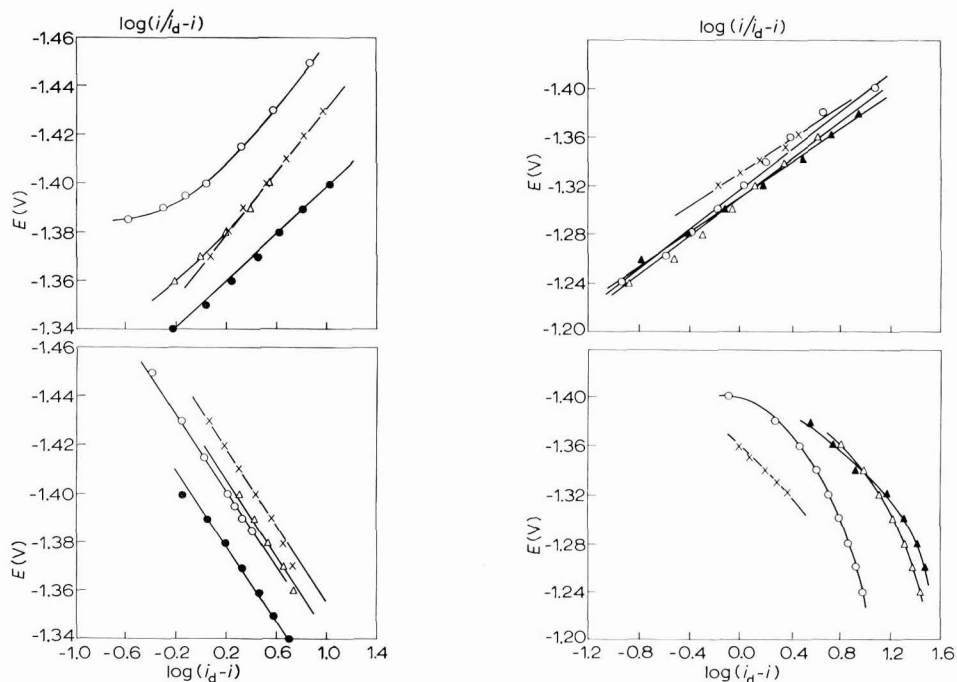
The preparation of the melt¹⁹, the general experimental techniques and the fused salt methodology²⁰ have been described elsewhere. An inert atmosphere was maintained over the melt surface by a flow of oxygen-free, dry nitrogen gas. The microelectrodes were fabricated by sealing suitable lengths of 0.25–30 mm diam. platinum wire in soda-lead glass (Corning 0120) and tungsten wire in Pyrex-glass through a C-9 (Corning 3320) graded seal. The sealed ends were ground flush to expose the cross-section of the wires, polished to a shining surface with a 0/3 emery paper and suitably²¹ pre-treated before use; the (projected) areas of the microelectrodes were determined. Polarograms were obtained with a Leeds and Northrup manual arrangement, the steady-state values of the electrolysis current having been recorded.

Polarograms for 6.67–36.04 mM $CdCl_2$ solutions in molten $MgCl_2$ – KCl were obtained using a WME (area 0.049 mm²) as indicator electrode; the system Pt/Pt(II) in the melt served as reference. The log-plots for these are presented in Fig. 1. The

$E_{m.e.}$ vs. $\log \{i/(i_d-i)\}$ plots were either curved or had slopes very different from the calculated value, indicating the inapplicability of the Heyrovský-Ilkovič equation. On the other hand, $E_{m.e.}$ vs. $\log (i_d-i)$ plots were rectilinear. The slopes of four typical plots were 0.076, 0.078, 0.078 and 0.080 V which may be compared with a calculated value of 0.074 for a two-electron process at 475°. Also, $E_{\frac{1}{2}}$ in this case shifted to more positive values with increasing concentration of Cd^{2+} , the magnitude of the shift being of the order of the calculated value. It is thus concluded that the $C-V$ characteristics of the polarographic wave in the reduction of Cd^{2+} on a WME are expressed by the Kolthoff-Lingane equation.

Polarograms for the same solution were also recorded with a PME (area 0.071 mm²) as indicator electrode. The corresponding log-plots are presented in Fig. 2. In this case, $E_{m.e.}$ vs. $\log \{i/(i_d-i)\}$ plots were rectilinear; the slopes for five such plots were 0.069, 0.072, 0.078, 0.079 and 0.080 (calcd: 0.074). The $E_{m.e.}$ vs. $\log (i_d-i)$ plots, however, are seen to be curved. Also $E_{\frac{1}{2}}$ was, within limits of experimental error, independent of Cd^{2+} concentration. The polarograms with a PME are thus described by the Heyrovský-Ilkovič equation; this is in accord with earlier findings⁴.

It is thus concluded that the nature of the microelectrode material plays an important role in deciding whether the Heyrovský-Ilkovič or the Kolthoff-Lingane equation expresses the current-voltage functions of a polarographic wave with a *solid* microelectrode in molten salt solutions.



Figs. 1-2. Log-plots for Cd^{2+} polarograms with: (1) a tungsten, (2) a platinum microelectrode as the indicator electrode.

Acknowledgement

The authors gratefully acknowledge the financial assistance provided by the Bhabha Atomic Research Centre Bombay, India.

*Department of Chemistry,
University of Delhi,
Delhi-7 (India)*

H. C. GAUR
H. L. JINDAL

- 1 D. L. MARICLE AND D. N. HUME, *Anal. Chem.*, **33** (1961) 1188.
- 2 E. D. BLACK AND T. DE VRIES, *Anal. Chem.*, **27** (1955) 906.
- 3 H. A. LAITINEN, C. H. LIU AND W. S. FERGUSON, *Anal. Chem.*, **30** (1958) 1266.
- 4 H. C. GAUR AND W. K. BEHL, *J. Electroanal. Chem.*, **5** (1963) 261.
- 5 D. L. MANNING, *Talanta*, **10** (1963) 255.
- 6 YU. K. DELIMARSKII, *Usp. Khim.*, **23** (1954) 766.
- 7 YU. K. DELIMARSKII AND O. V. GORODISKII, *Dopovidi Akad. Nauk Ukr.RSR*, (1955) 540.
- 8 YU. K. DELIMARSKII AND K. M. KALABALINA, *Ukr. Khim. Zh.*, **23** (1957) 584.
- 9 K. M. KALABALINA AND YU. K. DELIMARSKII, *Ukr. Khim. Zh.*, **24** (1958) 152.
- 10 YU. K. DELIMARSKII AND K. M. KALABALINA, *Ukr. Khim. Zh.*, **24** (1958) 435.
- 11 YU. K. DELIMARSKII AND V. V. KUZMOVICH, *Dopovidi Akad. Nauk Ukr.RSR*, (1959) 55.
- 12 YU. K. DELIMARSKII AND V. V. KUZMOVICH, *Zh. Neorgan. Khim.*, **4** (1959) 2732.
- 13 YU. K. DELIMARSKII AND O. V. GORODISKII, *Zh. Fiz. Khim.*, **35** (1961) 687.
- 14 YU. K. DELIMARSKII AND T. N. KAPTSOVA, *Ukr. Khim. Zh.*, **28** (1962) 802.
- 15 YU. K. DELIMARSKII AND N. KH. TUMANOVA, *Ukr. Khim. Zh.*, **29** (1963) 387.
- 16 T. N. KAPTSOVA AND YU. K. DELIMARSKII, *Ukr. Khim. Zh.*, **29** (1963) 714.
- 17 YU. K. DELIMARSKII AND N. KH. TUMANOVA, *Ukr. Khim. Zh.*, **30** (1964) 52.
- 18 E. C. MILLER, *Liquid Metals Handbook*, edited by R. N. LYONS, U.S. Atomic Energy Commission and Navy Department, Washington, D.C., 1952.
- 19 H. C. GAUR AND W. K. BEHL, *Electrochim. Acta*, **8** (1963) 107.
- 20 H. C. GAUR AND B. B. BHATIA, *J. Sci. Ind. Res. India*, **21A** (1962) 16.
- 21 W. K. BEHL, *Polarographic Studies and Standard Electrode Potential Measurements in Molten Magnesium Chloride-Sodium Chloride-Potassium Chloride Eutectic as Solvent*, University of Delhi, 1962, Ph. D. Thesis.

Received July 10th, 1967

J. Electroanal. Chem., **16** (1968) 437-439

Quantitative aspects of proton reduction in non-aqueous solvents

The electrochemical reduction of hydrogen ions in non-aqueous solvents is a well-known phenomenon. It has been amply demonstrated that various organic and inorganic acids exhibit reduction waves in solvents such as acetonitrile¹, N,N-dimethylformamide (DMF), dimethylsulfoxide (DMSO), etc.². The potential at which hydrogen ions are reduced is dependent upon the basicity of the non-aqueous solvent and the strength of the reducible acid. Generally, the stronger the acid (in a Brønsted sense) the more easily is it reduced in a particular aprotic solvent¹.

The presence of a proton reduction wave has also been used in the elucidation of organic electrode mechanisms employing chronopotentiometry³ and cyclic voltammetry⁴⁻⁶. The proton wave is usually indicative of a coupling reaction of some organic species where a dimer or polymer is formed *via* electrochemical oxidation.

In the course of investigating various organic oxidations in aprotic solvents, we have found this "proton wave" to be very helpful, both in a qualitative and quantitative sense. In many different types of systems where coupling is suspected,

J. Electroanal. Chem., **16** (1968) 439-442

this has been confirmed by the presence of hydrogen ion reductions, as shown previously^{4,5}. On a typical cyclic polarogram, the potential sweep is first carried out in an anodic-going direction and the organic species is electrochemically oxidized. When the potential is then scanned in the cathodic direction, a reduction wave will be observed in the vicinity of $+0.2$ to -0.4 V (*vs.* SCE) if protons were liberated in the oxidation step. It can be verified that this wave is due to proton reduction because the hydrogen couple is electrochemically irreversible in acetonitrile, but reversible in DMF and propylene carbonate (PC) (the criterion for electrochemical reversibility here is corresponding amounts of anodic and cathodic peak currents on a cyclic polarogram). Hence, if a cathodic wave is found in the vicinity of zero volts and it is suspected to be due to protons liberated in an electrode reaction, this can be confirmed by electrolyzing in acetonitrile and either DMF or PC.

Once it has been established that protons are being generated, it is of interest and importance to obtain a quantitative estimate of their numbers. In this way, the number of protons being released/parent molecule can be ascertained. This can be realized in the following manner. First, a calibration curve is necessary so that the experimental results can be compared with a known standard. Figure 1 shows the peak current (from linear scan polarograms) as a function of concentration at several potential scan rates. Picric acid was used because it is a strong acid in the aprotic solvents employed, accurate solutions can be prepared since it is a solid, and it seemed desirable to employ an organic acid bearing some structural similarity to the organic compounds being investigated. Linear behaviour is obtained up to acid concentrations of approximately 4.0×10^{-3} M. Above this concentration, the peak current drops and the linear relationship no longer holds but since organic systems are usually studied in the millimolar region, this was not considered significant.

The data are for acetonitrile, but similar behaviour is observed in the other aprotic solvents mentioned. For any particular solvent and a specific electrode one set of calibration curves must be constructed and used only in that system.

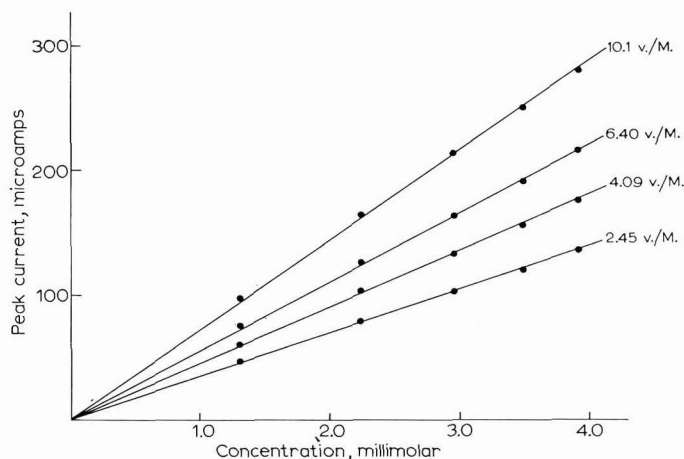


Fig. 1. Picric acid calibration curve. Scan rates are shown on the right.

TABLE 1

Compound	v^a	i_p^b	mMoles H^+
Triphenylamine (1.0×10^{-3} M soln.)	10.1	66.0	0.92
	6.40	52.0	0.93
	4.09	43.0	0.95
	2.45	33.0	0.93
4-Methyltriphenylamine (1.0×10^{-3} M soln.)	10.1	80.0	1.10
	6.40	62.0	1.10
	4.09	51.5	1.12
	2.45	40.0	1.12

^a Scan rate ($V \text{ min}^{-1}$). ^b Peak current (μA).

With the calibration curve for a reference, a controlled-potential exhaustive electrolysis of an approximately millimolar solution of the organic compound being studied is then carried out. A linear scan polarogram is run on the resulting solution at the same scan rates as those used on the calibration curves. The millimoles of protons liberated are compared with the millimoles of parent species and the number of protons involved in the electrode reaction ascertained. Table 1 shows some typical data for two aromatic amines the electrode reactions of which have been completely characterized^{4,7}. In both cases it was anticipated that one millimole of protons would be obtained/millimole of parent amine⁴. The agreement between theory and experiment is quite good.

These systems were chosen for illustration because their electrode reactions have been fully characterized. Proton waves have been observed in other organic systems in this laboratory, and it is anticipated that quantitative determination of the number of protons involved in the electrode reactions will aid in the elucidation of their mechanisms. This technique may possibly be of general utility in studies of organic anodic electrode processes in aprotic solvents.

Experimental

The electrochemical instrumentation used for cyclic voltammetry and linear sweep voltammetry has been described previously⁴. Solvent and supporting electrolyte purifications have also been reported^{4,8}. A Beckman platinum button⁴ was used in the linear sweep experiments, with a platinum foil auxiliary and SCE reference electrode.

For the controlled-potential coulometry, a Wenking model 61RS potentiostat with digital readout according to BARD^{9,10} was employed.

Picric acid was "Baker Analyzed" Reagent and was used without further purification.

This work was supported by The National Science Foundation through grant GP-5097X; this support is gratefully acknowledged.

Department of Chemistry,
University of Kansas,
Lawrence, Kan. 66044 (U.S.A.)

ROBERT C. NELSON*
R. N. ADAMS

* Present address: Dept. of Chemistry, Sacramento State College, Sacramento, California.

- 1 J. F. COETZEE AND I. M. KOLTHOFF, *J. Am. Chem. Soc.*, 79 (1957) 6110.
- 2 P. J. ELVING AND M. S. SPRITZER, *Talanta*, 12 (1965) 1243.
- 3 D. H. GESKE, *J. Am. Chem. Soc.*, 81 (1959) 4145.
- 4 E. T. SEO, R. F. NELSON, J. M. FRITSCH, L. S. MARCOUX, D. W. LEEDY AND R. N. ADAMS, *ibid.*, 88 (1966) 3498.
- 5 L. S. MARCOUX, Ph.D. Thesis, Kansas University, 1967.
- 6 R. F. NELSON, D. W. LEEDY, E. T. SEO AND R. N. ADAMS, *Z. Anal. Chem.*, 224 (1967) 184.
- 7 R. F. NELSON AND R. N. ADAMS, submitted for publication.
- 8 R. F. NELSON AND R. N. ADAMS, *J. Electroanal. Chem.*, 13 (1967) 184.
- 9 A. J. BARD, *Anal. Chem.*, 34 (1962) 1181.
- 10 A. J. BARD AND E. SOLON, *ibid.*, 35 (1963) 1125.

Received August 18th, 1967

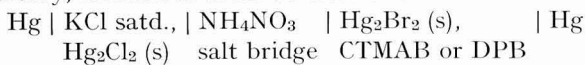
J. Electroanal. Chem., 16 (1968) 439-442

Determination of the critical micelle concentration of cationic surfactants from counter-ion activity measurements

In a recent communication¹ we have reported determinations of the critical micelle concentration (c.m.c.) values of potassium salts of the higher fatty acids by studying the variations of detergent anion activity, using cobalt-cobalt soap electrodes. In this communication an attempt has been made to determine the c.m.c. values of cetyltrimethylammonium bromide (CTMAB) and dodecylpyridinium bromide (DPB) by measuring the counter-ion (bromide) activity.

Experimental

DPB was prepared by the method described by ADDERSON AND TAYLOR². CTMAB was a B.D.H. product and was recrystallized from acetone. The solutions were prepared in doubly-distilled water. Mercurous bromide was prepared from $\text{Hg}_2(\text{NO}_3)_2$ and KBr (A.R.). Triple-distilled mercury was used for the preparation of the mercury, mercurous bromide electrode. E.m.f. measurements of the cell,



were carried out at $30 \pm 0.1^\circ$ in a water thermostat.

Results and discussion

The concentration ranges of DPB and CTMAB studied were $2 \cdot 10^{-3}$ – $66 \cdot 10^{-3}$ M and $1 \cdot 10^{-4}$ – $100 \cdot 10^{-4}$ M, respectively. Curves A and B (Fig. 1) are plots of the electrode potentials of the $\text{Hg}, \text{Hg}_2\text{Br}_2$ electrode vs. the logarithms of DPB and CTMAB concentrations.

Since the electrode potential is a measure of bromide ion activity, the first linear branch of the curves corresponds to the increase in bromide ion activity as the surfactant concentration is increased. This observation is in agreement with the accepted concept of a surfactant behaving as a moderately strong electrolyte below the c.m.c. However, above the c.m.c., the behaviour of surfactants is non-ideal owing to micellization.

According to HARTLEY^{3,4} the micelles contain, in addition to a large number of detergent ions, a considerable number of counter-ions which are bound to the

J. Electroanal. Chem., 16 (1968) 442-443

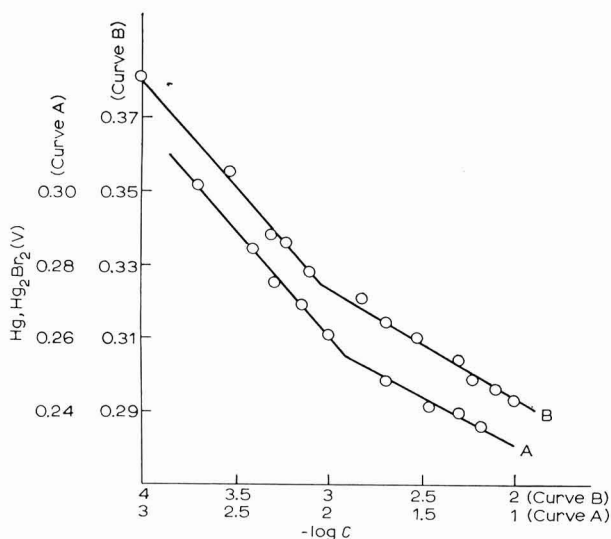


Fig. 1. Plots of $\text{Hg, Hg}_2\text{Br}_2$ electrode potential and log of the surfactant concn. (A) DPB; (B) CTMAB.

micelle surface and number at least one-half of the number of detergent ions in the micelle. The most concrete and clear evidence of the adhesion of counter-ions to the micelle is that the transport numbers^{5,6} of detergent ions exceed unity above the c.m.c. Therefore, above the c.m.c., the increase in concentration of surfactant will not cause the same increase in the concentration (activity) of free bromide ions (counter-ions) as it would have done had there been no counterion association with the micelles. Consequently, the $\text{Hg, Hg}_2\text{Br}_2$ electrode potential will show an abrupt change as the concentration of the surfactant exceeds the c.m.c. value. Obviously, the breaks in curves A and B must correspond to the c.m.c. values of cationic surfactants.

The c.m.c. values of DPB and CTMAB determined by this method are $1.23 \times 10^{-2} M$ and $9.12 \times 10^{-4} M$, respectively. These values are in close agreement with those reported in the literature^{2,7}.

Chemical Laboratories,
University of Roorkee,
Roorkee, India

WAHID U. MALIK
AJAY K. JAIN

- 1 W. U. MALIK AND A. K. JAIN, *J. Electroanal. Chem.*, **14** (1967) 37-41.
- 2 J. E. ADDERSON AND H. TAYLOR, *J. Colloid. Sci.*, **19** (1964) 495.
- 3 G. S. HARTLEY, *Kolloid Z.*, **88** (1939) 22.
- 4 G. S. HARTLEY, *Progress in the Chemistry of Fats and other Lipids*, Pergamon Press, London, 1955, chap. 2.
- 5 G. S. HARTLEY, B. COLLIE AND C. S. SAMIS, *Trans. Faraday Soc.*, **32** (1936) 795.
- 6 G. S. HARTLEY AND C. S. SAMIS, *Trans. Faraday Soc.*, **34** (1938) 1288.
- 7 W. D. HARKINS, *J. Am. Chem. Soc.*, **69** (1947) 1428.

Received May 31st, 1967; in revised form August 15th, 1967.

BOOK REVIEW

Catalytic and Kinetic Waves in Polarography, by S. G. MAIRANOVSKII (in Russian), "Nauka", Moscow, 1966, 288 pages, 1 Rbl. 29 kop.

As a rule, electrode processes in which organic substances participate involve the consumption (or evolution) of hydrogen ions, and under properly chosen conditions, the rate of the protonation reaction, usually preceding the electron transfer, may limit the rate of the total process. The currents observed in such cases are called kinetic currents. The electrode processes, both with and without the preceding chemical step, are greatly affected by the adsorption of the depolarizer and by the structure of the electric double layer at the electrode-solution interface. In the book under review, these effects are treated mainly on the basis of the experimental evidence obtained by the author and his co-workers, although the results of a large number of studies by other authors (871 references) are also used and critically discussed.

Kinetic currents can be used in the determination of the rate constants of fast chemical reactions, although, as is illustrated in the book by specific cases, in order to determine the true rate constants of these reactions, it is necessary to extrapolate the apparent (or observed) values of these constants to the conditions under which practically no adsorption of the reaction components would occur.

Much attention is given to the theory (developed by the author) of the catalytic hydrogen waves and to a detailed consideration of the effect of the composition of the binary systems, water-organic solvent, upon electrode processes of various types.

Among the drawbacks of the book should be mentioned the sometimes insufficiently systematic presentation of the subject matter. Too little attention is given to kinetic currents in the case of processes involving the participation of inorganic substances, and to the important analytical application of kinetic and, particularly, of catalytic currents. On the whole, the book is a valuable contribution to the development of the kinetics of electrode processes at the mercury electrode. The book has been prepared with some additions, for publication in English by the Consultants Bureau Plenum Press (New York).

A. FRUMKIN, Institute of Electrochemistry, Academy of Sciences of the U.S.S.R., Moscow

CONTENTS

Photocurrents at a metal-electrolyte interface V. P. SHARMA, P. DELAHAY, G. G. SUSBIELLES AND G. TESSARI (New York, N.Y., U.S.A.)	285
Potential-step electrolysis followed by linear-sweep voltammetry at a plane mercury-film electrode W. T. DE VRIES (Amsterdam, Netherlands)	295
Interaction of polyphosphate with the mercury electrode surface V. VETTERL AND J. BOHÁČEK (Brno, Czechoslovakia)	313
Undervoltage effects in the determination of silver by scanning coulometry R. C. PROPST (Aiken, S.C., U.S.A.)	319
Chronocoulometric measurement of indium(III) adsorption from thiocyanate medium G. W. O'DOM AND R. W. MURRAY (Chapel Hill, N.C., U.S.A.)	327
Chronopotentiometric determination of U(III), U(IV), UO ₂ (VI) and Np(IV) in molten LiCl-KCl eutectic F. CALIGARA, L. MARTINOT AND G. DUYCKAERTS (Liège, Belgium)	335
Polarography in the study of classical organic functional group reactions. I. Polarographic behaviour of <i>cis</i> - and <i>trans</i> -cinnamic acid and substituted cinnamic acids M. J. D. BRAND AND B. FLEET (London, Great Britain)	341
Electrochemical oxidation of formate in dimethylsulfoxide at gold and platinum electrodes E. JACOBSEN, J. L. ROBERTS JR. AND D. T. SAWYER (Riverside, Calif., U.S.A.)	351
Electrochemical oxidation of oxalate ion in dimethylsulfoxide at a gold electrode E. JACOBSEN AND D. T. SAWYER (Riverside, Calif., U.S.A.)	361
Biamperometric indication in chelometric titrations in acidic solutions F. VYDRA AND K. ŠTULÍK (Prague, Czechoslovakia)	375
The voltammetry of ethylenediaminetetraacetic acid (EDTA) and related compounds on a rotating platinum electrode K. ŠTULÍK AND F. VYDRA (Prague, Czechoslovakia)	385
Sensitive amperometric titration of <i>o</i> -phenylenediamine employing catalytic electrode reaction end-point detection E. KIROWA-EISNER AND H. B. MARK JR. (Ann Arbor, Mich., U.S.A.)	397
Polarographic diffusion coefficients of nitroamminecobalt(III) complex ions H. IKEUCHI (Tokyo, Japan)	405
Polarography of lead-triethylenetetramine chelate T.-T. LAI AND J.-Y. CHEN (Tainan, Taiwan, China)	413
<i>Review</i>	
The electrochemical transfer-coefficient H. H. BAUER (Lexington, Ky., U.S.A.)	419
<i>Short communications</i>	
Current-time dependence for charge transfer processes with reactant adsorption at a dropping electrode K. HOLUB (New York, N.Y., U.S.A.)	433
On the applicability of the Heyrovský-Ilkovič equation to polarography in molten salts using a solid microelectrode H. C. GAUR AND H. L. JINDAL (Delhi, India)	437
Quantitative aspects of proton reduction in non-aqueous solvents R. F. NELSON AND R. N. ADAMS (Lawrence, Kan., U.S.A.)	439
Determination of the critical micelle concentration of cationic surfactants from counter-ion activity measurements W. U. MALIK AND A. K. JAIN (Roorkee, India)	442
<i>Book review</i>	444

Countercurrent Separation Processes

by H. R. C. Pratt

Chief, Division of Chemical Engineering, C.S.I.R.O., Melbourne, Australia

6 x 9", xxii + 537 pages, 30 tables, 173 illus., 415 lit.refs., 1967, Dfl. 95.00, £11.0.0, US\$34.00

The countercurrent separation processes represent, in terms of invested capital, the most important single group of operations in the chemical and process industries. Such operations, which must be clearly distinguished from mechanical separations such as continuous countercurrent decantation and leaching, are normally restricted in the chemical engineering texts to distillation in its various forms (including azeotropic and extractive distillation), absorption and stripping, liquid-liquid extraction, and sometimes adsorption.

Since the 1940's, chemical engineers have become increasingly concerned with isotopic and other difficult separations. Furthermore, newer techniques, such as liquid thermal diffusion, etc. enable separations to be accomplished which are difficult or unobtainable by other means. It became evident therefore that a text should be available which generalises the treatment to cover all types of separation process, and this is in fact what the author hopes to have achieved here. The list of processes dealt with in the various chapters does not exhaust all possibilities. However, most of the remaining known processes are either of very limited application, or are as yet relatively undeveloped.

Although the book is fairly advanced in coverage, selected material can be used as the basis for a course for final year chemical engineering students. It should also be of particular interest to research workers, both in stimulating applications of the various processes to hitherto unachieved separations, and in development of entirely new types of separation process. Although not intended to be used as a design manual, it should prove of great value to practising chemical engineers and plant designers in providing a basic understanding of the principles involved in the design of equipment for these processes.

Contents: 1. Introduction and basic concepts. 2. Steady-state cascade theory: the ideal cascade. 3. Steady-state cascade theory: square and squared-off cascades. 4. Distillation. 5. Equilibrium processes employing a separating agent. 6. Other equilibrium processes. 7. Irreversible processes: gaseous diffusion. 8. Irreversible processes: mass and thermal diffusion. 9. Other irreversible processes. 10. Multicomponent separations. 11. The unsteady state. Appendix: Table of values of the separation potential. Subject index.



ELSEVIER PUBLISHING COMPANY

AMSTERDAM

LONDON

NEW YORK